

**Evaluating synergy between deregulation of the Wnt,
PI3-Kinase and MAP-Kinase pathways in prostate
tumourigenesis**



Matthew Thomas Jefferies

PhD

Cardiff University

2012 - 2015

Declarations

This work has not been submitted in substance for any other degree or award at this or any other university or place of learning, nor is being submitted concurrently in candidature for any degree or other award.

This thesis is being submitted in partial fulfillment of the requirements for the degree of PhD.

This thesis is the result of my own independent work/investigation, except where otherwise stated. Other sources are acknowledged by explicit references. The views expressed are my own.

I hereby give consent for my thesis, if accepted, to be available for photocopying and for inter-library loan, and for the title and summary to be made available to outside organisations.

Signed

Date

Acknowledgements

I would like to sincerely thank the late Professor Alan Clarke for his great enthusiasm and mentoring throughout this thesis. He will be deeply missed by our laboratory and the wider scientific community. I am also eternally grateful to Professor Howard Kynaston for his guidance and advice throughout my PhD and my career as a urologist.

I am greatly indebted to Mat Zverev and Elaine Taylor for carrying out genotyping, Mark Bishop for assistance with FACS, and Derek Scarborough for histology services. I wish to thank Dr David Griffiths (Consultant Histopathologist) for making the time to analyse and teach me through numerous histological slides. My sincerest thanks are also extended to Dr Valerie Meniel and Dr Boris Shorning for their assistance in overcoming the challenges and obstacles faced in the lab and my predecessor and great friend Adam Cox for setting the foundations for this thesis.

I am also grateful to the Welsh Cancer Bank for providing the human prostate cancer samples and The Urology Foundation and Prostate Cancer UK for the funding to make this research possible.

Finally, I would like to thank my wife, Vikki for her love and support and proofreading services, which have been second to none, and my sons Jack and Oliver for providing me with the joy and the escape that I have needed, from what have been the most challenging years of my life.

Contents

Abstract.....	1
Publications & Grants	2
Presentations & Awards.....	3
Abbreviations.....	4
1 General Introduction	6
1.1 The Human Prostate Gland	6
1.1.1 Gross anatomy of the prostate gland.....	6
1.1.2 Microscopic anatomy of the prostate gland	6
1.1.3 Histology of the prostate gland.....	7
1.1.4 Function of the prostate gland.....	8
1.1.5 Androgen synthesis and metabolism.....	9
1.2 The Murine Prostate Gland	10
1.2.1 Anatomy and histology of the murine prostate.....	10
1.3 Prostate Cancer	13
1.3.1 Epidemiology of prostate cancer.....	13
1.3.2 Risk factors.....	18
1.3.3 Prostate cancer detection.....	24
1.3.4 Grading and staging.....	28
1.3.5 Prognostic indicators and risk-stratification.....	31
1.3.6 Natural history of prostate cancer.....	33
1.3.7 Prostate cancer management.....	36
1.4 Prostate cancer biology.....	41
1.5 Prostate cancer genetics.....	42
1.5.1 PTEN and the PI3-Kinase pathway.....	45
1.5.2 β -catenin and the Wnt pathway.....	48
1.5.3 K-Ras and the MAP-Kinase pathway.....	52
1.6 Mouse models of prostate cancer	55
1.7 Tumour heterogeneity and Cancer stem cells (CSC).....	58
1.7.1 Technologies in Cancer Stem Cells research.....	61
1.7.2 Location and markers of prostate epithelial cancer stem cells.....	61
1.8 Current research strategies in prostate cancer	66
1.9 Hypothesis:.....	67
1.10 Aims:.....	67

2	Material and Methods	69
2.1	Human prostate samples.....	69
2.1.1	<i>Tissue Microarrays (TMA)</i>	69
2.1.2	<i>Targeted Next Generation Sequencing (NGS)</i>	71
2.2	Experimental animals.....	73
2.2.1	<i>Animal Husbandry</i>	73
2.2.2	<i>Breeding</i>	73
2.2.3	<i>Genetic Mouse Models</i>	73
2.2.4	<i>Polymerase Chain Reaction (PCR) Genotyping</i>	73
2.2.5	<i>Administration of 5'-Bromo-2-deoxyuridine</i>	76
2.2.6	<i>Mouse Tissue Preparation</i>	77
2.2.7	<i>Histological analysis of mouse specimens</i>	78
2.2.8	<i>Immunohistochemistry (IHC) of human and mouse specimens</i>	79
2.2.9	<i>Western blot analysis of mouse specimens</i>	83
2.2.10	<i>Mouse prostate organoid culture</i>	86
2.2.11	<i>Trypan blue cell viability counts</i>	86
2.3	Statistical analysis.....	90
3	Assessment of the Wnt, PI3-Kinase (PI3K) and MAP-Kinase (MAPK) cell signalling pathways in human prostate cancer	91
3.1	Introduction.....	91
3.2	Chapter aims.....	92
3.3	Results.....	94
3.3.1	<i>Tissue-Micro-Array (TMA) analysis</i>	94
3.3.2	<i>Next-generation sequencing (NGS) analysis</i>	116
3.4	Discussion.....	124
3.4.1	<i>Wnt Signalling Pathway</i>	124
3.4.2	<i>PI3K Signalling Pathway</i>	125
3.4.3	<i>MAPK Signalling Pathway</i>	126
3.4.4	<i>Cross-talk Between Signalling Pathways</i>	127
3.4.5	<i>Cell Signalling and DNA repair</i>	128
3.4.6	<i>Limitations</i>	129
3.4.7	<i>Summary and future directions</i>	130
4	The effect of Wnt, PI3-Kinase (PI3K) and MAP-Kinase (MAPK) signalling pathway deregulation on murine prostate tumourigenesis	132
4.1	Introduction.....	132

4.1.1	<i>Chapter aims</i>	132
4.2	<i>Results</i>	134
4.2.1	<i>Generation of prostate specific mouse models using the Probasin-Cre (Pb-Cre4) transgene</i>	134
4.2.2	<i>Pten loss and activation of K-Ras and β-catenin (triple mutants) cooperate to accelerate prostate tumourigenesis</i>	136
4.2.3	<i>Tumour progression occurs in a stepwise fashion from mouse PIN (mPIN) to invasive adenocarcinoma similar to that of human disease</i>	138
4.2.4	<i>Combinatorial pathway mutations shifts the spectrum of lesions to a more aggressive phenotype</i>	141
4.2.5	<i>Additional pathological phenotypes</i>	146
4.2.6	<i>Both K-Ras and β-catenin mutations drive metastatic spread in the context of loss of Pten</i> 147	
4.2.7	<i>Pathway signalling analysis</i>	149
4.2.8	<i>Summary of pathway readouts according to genotype</i>	163
4.3	<i>Discussion</i>	164
4.3.1	<i>Pten loss alone causes significant PI3K pathway up-regulation with further mild aberrant Wnt and MAPK signalling resulting in prostate tumourigenesis</i>	164
4.3.2	<i>Activation of β-catenin alone causes activation of the Wnt pathway resulting in prostate tumourigenesis with squamous metaplasia</i>	165
4.3.3	<i>Activation of K-Ras alone is insufficient to cause prostate tumourigenesis with elevated Pten levels</i>	165
4.3.4	<i>Double and triple mutant mice accelerate tumourigenesis through activation of multiple cell signalling pathways</i>	166
4.3.5	<i>Triple mutant mice display further aberrant mammalian target of rapamycin (mTOR) signalling</i>	167
4.3.6	<i>Single gene mutations are insufficient to cause metastases</i>	170
4.3.7	<i>Both K-Ras and β-catenin mutations drive metastatic spread in the context of loss of Pten</i> 170	
4.3.8	<i>Rate of proliferation correlates positively with stage of disease and number of mutations/activated pathways</i>	171
4.3.9	<i>Tumours show signs of EMT with Triple mutants displaying additional stromal Pten activity</i>	172
4.3.10	<i>Limitations</i>	172
4.3.11	<i>Summary and future direction</i>	173

5	Assessment of putative cancer stem cells (CSC) in human prostate cancer and optimisation of tumour organoid culture in the mouse effected by deregulation of the Wnt, PI3-Kinase (PI3K) and MAP-Kinase (MAPK) signalling pathways	174
5.1	Introduction	174
5.1.1	<i>Chapter Aims</i>	<i>175</i>
5.2	Results	176
5.2.1	<i>Evaluation of putative CSC markers in human PCa</i>	<i>176</i>
5.2.2	<i>Optimisation of prostate organoid culture assay in the mouse.....</i>	<i>178</i>
5.2.3	<i>The percentage of the stem-cell/CSC enriched population (Lin⁻Sca1⁺CD49⁺) increases as genetic mutations increased.....</i>	<i>184</i>
5.2.4	<i>WT enriched cells have the greatest organoid forming capacity with triple mutants demonstrating a greater OFC than single or double mutants</i>	<i>185</i>
5.2.5	<i>All organoids had a similar morphological phenotype.....</i>	<i>186</i>
5.3	Discussion.....	188
5.3.1	<i>Putative CSC markers that are associated with many signalling processes or cell types, are elevated in human prostate cancer – is there more than one CSC?.....</i>	<i>188</i>
5.3.2	<i>Increasing number of genetic mutations or pathway deregulation in the mouse causes expansion of the CSC population.....</i>	<i>189</i>
5.3.3	<i>Chapter Summary</i>	<i>191</i>
6	Final Discussion	192
7	References.....	195

Abstract

The Wnt, PI3-Kinase (PI3K) and MAP-Kinase (MAPK) cell signalling pathways play important roles in human prostate cancer (PCa). In this thesis, analysis of a human PCa tissue micro-array (TMA) constructed by the Welsh Cancer Bank demonstrated upregulation of markers associated with these pathways in PCa. There was also greater expression of these markers in high-risk tumours with some being predictive of biochemical recurrence following surgery. Furthermore, there is evidence to support cross talk between these pathways allowing clustering into low- and high-risk samples based on expression profiles. Targeted next generation sequencing (NGS) also demonstrated recurrent mutations of genes associated with these pathways in PCa.

Conditional transgenic mouse models were employed to explore the complex communication between these pathways. The loss of Pten was incorporated as a means of activating the PI3K pathway, and mutated β -catenin and K-Ras as means of aberrant Wnt and MAPK signalling. This study provides the first evidence of crosstalk and cooperation between these pathways, resulting in a significant effect on prostate tumourigenesis. Mice with loss of Pten in addition to activated mutations of β -catenin and K-Ras (Triple mutants) have significant upregulation of all three pathways resulting in a shorter survival compared to single and double mutants. The feasibility of these models allows further specific gene profiles to be induced in the mouse, providing a platform for pre-clinical testing of novel therapeutic agents.

The effect of deregulation of these pathways on the cancer stem cell (CSC) population was explored using fluorescence-activated cell sorting (FACS) and organoid culture. Compound mutant (doubles and triple) tumours have a greater number of CSC or enriched cells compared to single mutant or wildtype (WT) mice. Compound mutant tumours had greater organoid forming efficiency than single mutants however this was significantly inferior to WT cells. Overcoming the difficulty experienced in cultivating tumour organoids will help manufacture targeted drugs with the aim of forming a cryopreserved organoid library to facilitate precision medicine.

Publications

1. Submitted to Journal of Pathology: 20th January 2017

- Pten loss and activation of K-Ras and β -catenin cooperate to accelerate prostate tumorigenesis

Grants

1. **The Urology Foundation (TUF) Research Scholarship:** Exploring key mutations in molecular pathways associated with human prostate cancer. £48K
2. **Prostate Cancer UK:** Evaluating synergy between deregulation of the PI3-kinase, Wnt and Ras pathways in prostate neoplasia. £250K.

Presentations & Awards

1. **Welsh Urological Society** (November 2015). Oral presentation. Assessment of cell signalling pathways to help risk-stratify patients with Prostate Cancer.
 - **Awarded Huw Williams memorial prize for best paper presentation.**
2. **China-United Kingdom Cancer (CUKC) Conference: Fighting Cancer Together** (July 2015). Poster presentation. Assessment of PI3-Kinase, MAP-Kinase and WNT dependent pathways to help risk-stratify patients with prostate cancer.
 - **Nominated top 5 posters.**
3. **China-United Kingdom Cancer (CUKC) Conference: Fighting Cancer Together** (July 2015). Poster presentation. Expression analysis of putative stem cell markers in human prostate cancer.
4. **Royal Society of Medicine** (March 2015). Oral presentation. Assessment of PI3-Kinase, MAP-Kinase and Wnt dependent pathways to help risk-stratify patient with prostate cancer.
 - **Nominated for Malcolm Coptcoat spring short papers prize.**
5. **Academic Section of the British Association of Urological Surgeons (BAUS)** (Dec 2014). Oral presentation. Assessing synergy between Wnt, Pi3 Kinase and Ras pathways in human and murine prostate cancer.
 - **Nominated for BAUS Academic Research Prize.**
6. **10th National Cancer Research Institute (NCRI) Cancer Conference** (November 2014). Poster presentation. The effect of Wnt and PI3Kinase signalling on prostate cancer and the stem cell population.
7. **22nd Meeting of the European Association of Urology (EAU) Section of Urological Research** (October 2014). Poster presentation. Assessing synergy between Wnt, PI3Kinase and Ras pathways in human prostate cancer.
8. **22nd Meeting of the European Association of Urology (EAU) Section of Urological Research** (October 2014). Poster presentation. Expression analysis of putative stem cell markers in human prostate cancer.
9. **British Association of Surgical Oncology (BASO)** (June 2014). Poster presentation. Assessing Synergy between Wnt, PI3Kinase and Ras Pathways in Human Prostate Cancer. June 2014.
 - **Awarded best poster.**

Abbreviations

ADT	Androgen deprivation therapy
APC	Adenomatous polyposis coli gene product
AR	Androgen receptor
ATM	Ataxia telangiectasia mutated
BPH	Benign prostatic hyperplasia
CDH1	E-cadherin
CDKN2A	Cyclin-dependent kinase Inhibitor 2A
CHPv2	Cancer Hotspot Panel v2
CK	Cytokeratins
CNA's	Copy number alterations
COSMIC	Catalogue of somatic mutations in cancer from the Sanger institute)
CRPC	Castrate-resistant prostate cancer
CSC	Cancer stem cell
CTNNB1	β -catenin
CZ	Central zone
DAPI	4', 6-diamidino-2-phenylindole
DHT	5 α -dihydrotestosterone
DRE	Digital rectal examination
EBRT	External beam radiotherapy
ECM	Extracellular matrix
EGFR	Epidermal growth factor receptor
EMT	Epithelial-mesenchymal transition
FACS	Fluorescence-activated cell sorting
FFPE	Formalin-fixed paraffin embedded
GS	Gleason score
GWAS	Genome-wide association studies
H&E	Haematoxylin and Eosin
IHC	Immunohistochemistry
LH	Luteinizing hormone
LHRH	Luteinizing hormone releasing hormone
LHRH	Luteinizing hormone releasing hormone analogue
Lin ⁻	Linage negative

MAPK	MAP-Kinase-- Mitogen-activated protein kinase
MMP	Matrix metalloproteinase
mPIN	Mouse prostate intraepithelial neoplasia
mpMRI	Multi-parametric magnetic resonance imaging
mTOR	Mammalian target of rapamicin
NGS	Next generation sequencing
OFC	Organoid forming capacity
PAP	Prostatic acid phosphatase
PARPi	Poly(ADP-ribose) polymerase inhibitors
Pb	Probasin
PCa	Prostate cancer
PCA	Principle components analysis
PI3K	PI3-Kinase
PIK3CA	p110 α catalytic subunit of PI3K
PIN	Prostate intraepithelial neoplasm
PLL	Poly-L-lysine
PrEGM	Prostate Epithelial Growth Media
PSA	Prostate specific antigen
PTEN/Pten	Phosphatase and tensin homolog
PZ	Peripheral zone
RB1	Retinoblastoma
RFP	Red Fluorescent Protein
ROC	Receiver-operator characteristic
ROCK	Rho-associated kinase
RTK	Receptor tyrosine kinase
SNPs	Single nucleotide polymorphism
TMA	tissue micro-array
TP53	Tumour protein
TURP	Transurethral resection of the prostate
TZ	Transitional zone
WCB	Welsh Cancer Bank
WT	Wildtype

1 General Introduction

1.1 The Human Prostate Gland

1.1.1 Gross anatomy of the prostate gland

The human prostate is an exocrine gland that is slightly larger than a walnut, which increases with age under the influence of the male hormone, testosterone. It is located in the extraperitoneal space between the pelvic diaphragm and the peritoneal cavity. It is located posterior to the pubic symphysis, inferior to the urinary bladder and anterior to the rectum. It is separated from the rectum by Denonvilliers' fascia, a sheet of fused fibromuscular tissue. It is conical in shape surrounding the proximal urethra as it exits from the bladder, termed the prostatic urethra. The base of the gland is attached to the neck of the bladder with the apex resting on the superior surface of the urogenital diaphragm. It is supported anteriorly by the puboprostatic ligaments and inferiorly by the external urethral sphincter and perineal membrane. The seminal vesicles lie superior to the prostate under the base of the bladder and are approximately 6 cm in length. Each seminal vesicle joins its corresponding vas deferens to form the ejaculatory duct before entering the prostate at the verumontanum, just proximal to the striated external urinary sphincter. A capsule composed of collagen, elastin and large amounts of smooth muscle or stroma encloses the prostate forming a distinct layer separating the prostate from the periprostatic fat.

The prostate is covered by 3 distinct layers of fascia on the anterior, lateral, and posterior aspects. The anterior and anterolateral fascia is in direct continuity of the true capsule; this is the location of the deep dorsal vein of the penis and its tributaries. Laterally, the fascia fuses with the levator fascia. The outer longitudinal fibers of the detrusor muscle fuse and blend with the fibromuscular tissue of the capsule. The posterior aspect is covered by the rectovesical (Denonvilliers) fascia.

1.1.2 Microscopic anatomy of the prostate gland

The prostate can be divided in two ways: by lobe, or by zone. Traditionally lobes were used to describe the anatomy of the prostate dividing into: anterior, posterior, median and

two lateral lobes (left and right). This has however been superseded by zonal separation described by the pathologist McNeal. These are the anterior fibromuscular stroma, which is devoid of glandular components, the periurethral transitional zone (TZ), the peripheral zone (PZ), and the central zone (CZ) (McNeal 1981a; McNeal 1981b). The zonal separations accounts for distinct anatomical and histological features, which have predisposition to undergo benign or malignant change. The TZ surrounds the prostatic urethra and enlargement of the TZ; termed benign prostatic hyperplasia (BPH) can occur with increasing age resulting in symptoms of bladder outflow obstruction. The TZ accounts for 5-10% of the prostatic glandular tissue and 20% of the adenocarcinomas. The PZ constitutes 70% of the glandular tissue, which covers the posterior and lateral aspects of the prostate. The PZ is the area palpated when performing a digital rectal examination (DRE) and is where 70% of adenocarcinomas are found. The CZ surrounds the ejaculatory ducts and comprises of 25% of the glandular tissue and very few adenocarcinomas are found in this region (5%).

1.1.3 Histology of the prostate gland

The prostate consists of glandular epithelium embedded in a fibro-muscular stroma. The epithelium is composed of two-layers with three phenotypically distinct cell types: luminal, basal and rare, scattered neuroendocrine cells.

The secretory luminal epithelial cells are made up of tall columnar cells that are responsible for producing prostate specific antigen (PSA) and prostatic acid phosphatase (PAP) (McNeal 1988; Rittenhouse et al. 1998). The luminal cells are androgen-dependant that require androgens to survive and upon withdrawal undergo apoptosis and die. They express low-molecular-weight cytokeratins (CK) and are characterised most commonly by CK 8, CK18 and androgen receptor (AR) (Xue 1998). The basal epithelial cells form a layer of cuboidal cells, which in contrast to luminal cells stain positive for high molecular CK such as CK5 or the basal marker p63. Loss of the basal layer and subsequent p63 positivity on immunohistochemistry analysis is a hallmark of prostate cancer and commonly used in the clinical setting to aid diagnosis. The basal cell layer is in turn lined by a basement membrane consisting of extracellular matrix which forms a divide between the basal cells and the stroma (de Carvalho & Line 1996).

In addition to luminal, basal and neuroendocrine epithelial cells, there is emerging evidence for a fourth cell type in the prostate: the stem cell. Stem cells are defined as those cells able to proliferate and self-renew for an unlimited period of time, while generating diverse differentiated progeny specific to the given tissue (Potten & Loeffler 1990). In mammals there are two broad types of stem cells; the embryonic stem cells and the adult stem cells. The embryonic stem cells are derived from the inner cell mass (about 200-300 cells) of blastocysts in a developing embryo (Blair et al. 2011). The cells are pluripotent, that is, they can differentiate to develop all three germ cell layers (Ectoderm, mesoderm and endoderm). Adult stem cells are undifferentiated cells that can differentiate to multiple lineages and self-renew, a mechanism used for repairing damaged tissue (Wagers & Weissman 2004). Haematopoietic stem cells have been extensively researched leading to the subsequent development of the stem cell bone marrow transplantation, which has resulted in the successful treatment of certain types of leukaemias. Haematopoietic stem cells give rise to multiple downstream lineages, such as the myeloid and lymphoid lineage. The myeloid lineage differentiate into monocytes, macrophages, neutrophils and dendritic cells and the lymphoid lineage into T,B and NK cells (Weissman, 2000). Stem cells are present in many other tissues in the body such as intestinal, mammary, neural, bladder and prostate. Considering the central role the stem cells play in homeostasis, knowledge of stem cell function and regulation is crucial for our understanding of the normal and pathological processes in cancer. The cancer stem cell (CSC) theory is discussed in section 1.7.

1.1.4 Function of the prostate gland

The main function of the prostate gland is to liquefy the semen by producing a secretion containing strong proteolytic enzymes such as PSA and PAP.

PSA is an androgen-regulated glycoprotein belonging to the kallikrein family of serine proteases. It is produced primarily by prostate ductal and acinar epithelium and is secreted into the lumen, where its function is to cleave semenogelin I and II in the seminal coagulum (Lilja et al. 1987). As the coagulum dissolves, the sperm simultaneously become highly motile facilitating its journey from the vagina to the ova.

1.1.5 Androgen synthesis and metabolism

Androgens are sex hormones, which regulate the differentiation and maturation of male reproductive organs, as well as the development of male secondary sex characteristics (Dehm & Tindall 2006). The predominant androgen is testosterone, which is produced primarily by the testes (~90%) with a small contribution from the adrenal glands (~10%) (Basu & Tindall 2010). Testosterone is released following stimulation of the hypothalamus-pituitary-gonadal axis. In response to low levels of circulating testosterone, the hypothalamus releases Luteinizing hormone releasing hormone (LHRH). LHRH travels to the anterior pituitary gland where it binds to the LHRH receptor stimulating the release of luteinizing hormone (LH). LH then travels within the circulation to the testes where it stimulates the release of testosterone from the Leydig cells (Amory & Bremner 2003). When an increase in testosterone is detected by the hypothalamus and the pituitary gland, the release of LHRH and LH stops, via a negative feedback mechanism. The majority of testosterone is bound to serum proteins, such as sex hormone binding globulin or albumin, leaving only 1-2% unbound free testosterone (Hammond et al. 2003).

In the prostate, testosterone is converted to 5 α -dihydrotestosterone (DHT) by the cytochrome P450 enzymes, 5 α -reductase Type 1 and 2, which are highly expressed in prostate tissue (Wilson 2001). Both testosterone and DHT can bind to and activate the AR under physiological conditions, with DHT having a significantly greater affinity for the AR (~10 times, (Deslypere et al. 1992)). On binding to testosterone or DHT, the AR translocates into the nucleus, resulting in recruitment of co-factors, which ultimately results in regulation of gene expression such as PSA. Androgen signalling is fundamental in PCa development and progression. Treatments aimed at suppressing these signals will be discussed later in this chapter.

1.2 The Murine Prostate Gland

In order to model human prostate tumourigenesis in a mouse, a basic knowledge of the anatomical and histological similarities and differences between these two species (mouse and human) is necessary.

1.2.1 Anatomy and histology of the murine prostate

In contrast to the human, the murine prostate is divided into anatomically distinct lobes: the dorsal and lateral often grouped together as dorso-lateral, anterior and ventral lobes (Figure 1).

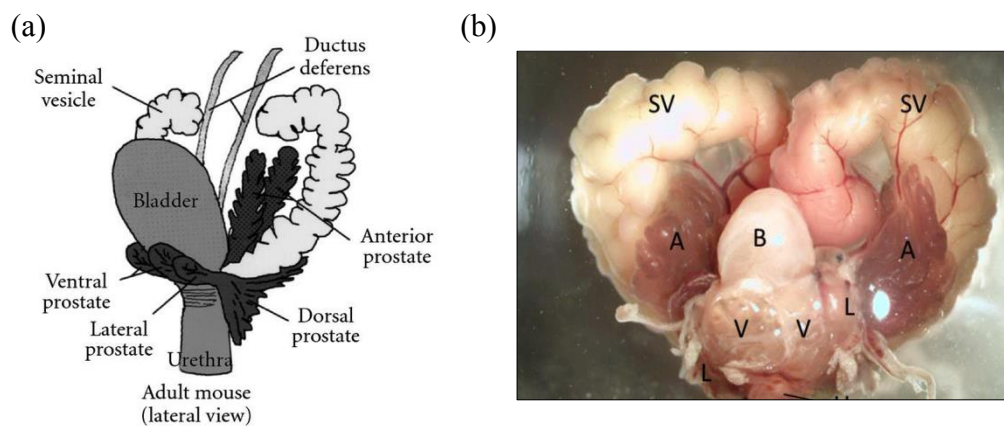


Figure 1: Gross anatomy of the mouse lower genitourinary tract. (a) Schematic diagram (adapted from (Valkenburg & B. O. Williams 2011)) and (b) photograph of a wildtype mouse prostate dissected en bloc: A: Anterior lobe, B: Bladder, L: Lateral lobe, U: Urethra, V: Ventral lobe, SV: Seminal Vesicles. Note, the Dorsal lobe is positioned posterior to the urethra and bladder neck so not visualized in this picture.

The lobes are separated by a thin mesothelial-lined capsule, often only appreciated microscopically, and composed of distinct glands of a series of blind ending branching ducts or tubules. The glandular prostate is surrounded by a thin layer of fibromuscular stroma that is composed of only a few layers of spindle cells that stain avidly for smooth muscle actin or mesenchymal vimentin. This is a fundamental difference to the human prostate, where there is an abundant amount of dense fibromuscular stroma surrounding the glands.

Each of the murine lobes has distinct morphological and cytological characteristics on histological sectioning as is demonstrated in Figure 2. The dorsal prostate is lined with simple columnar epithelium, with secretory cells with a lightly eosinophilic cytoplasm and a gland lumen containing homogenous eosinophilic staining. It has a moderate degree of in-folding in comparison to the anterior lobe that has a complex architecture with frequent mucosal folds protruding into the glands lumen. The anterior prostate abuts the seminal vesicles and histologically demonstrates a more papillary and cribriform growth pattern with cuboidal to columnar epithelium and eosinophilic cytoplasm. The lateral prostate has flatter luminal edges, with only sparse in-foldings, with an abundant luminal space containing eosinophilic secretions.

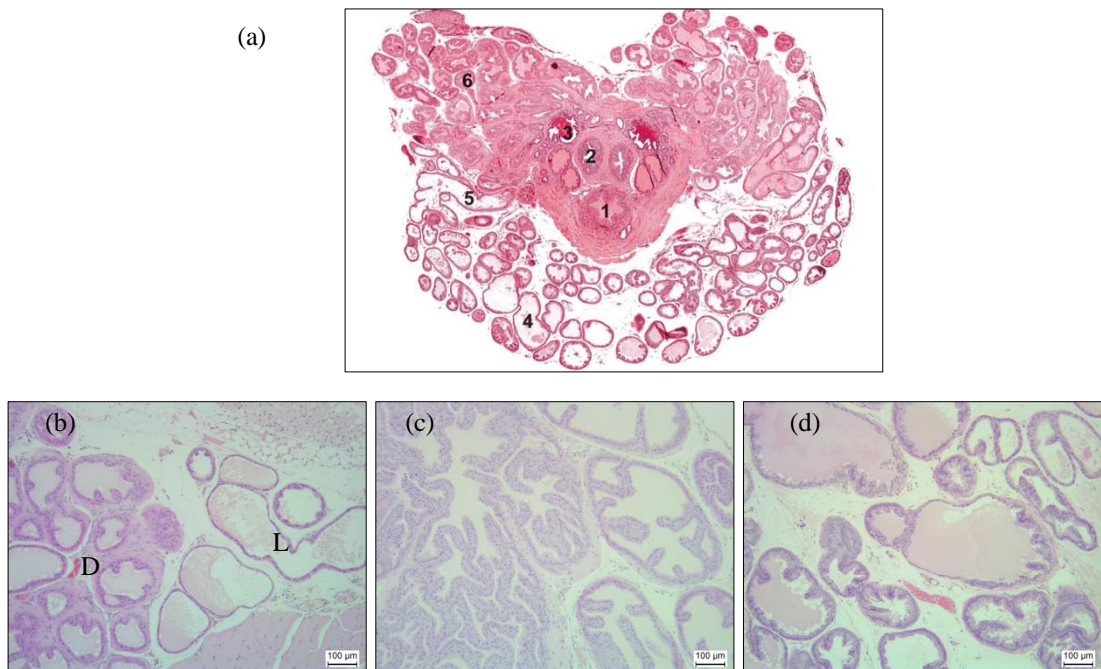


Figure 2: Histological characterisation of the wildtype mouse prostate gland. (a) gross microscopic illustration of mouse prostate 1: urethra, 2: paired vas deferens, 3: paired ampullary glands, 4: ventral lobe, 5: lateral lobe, 6: dorsal lobe (adopted from (Shappell et al. 2004)). Histological appearance of 10% formalin-fixed, paraffin-embedded sections stained with haematoxylin and eosin (H&E) of (b) Dorsal (D) and Lateral (L) (b) anterior and (c) ventral adult murine prostate lobes. Note the histological differences between each lobe of the prostate (see text for detail).

The epithelium of the lateral prostate is cuboidal, with a lighter granular cytoplasm and small uniform basally located nuclei. Lastly, the ventral prostate has flattened luminal edges with inly focal epithelial tufting or in-folds. The luminal space typically contains homogenous pale serous secretions.

The histological features of the mouse dorso-lateral prostate has long been compared to that of the human peripheral zone and thus thought to be homologous to the development of prostate cancer (PRICE 1963). More recently, the consensus opinion of the Bar Harbor Pathology Panel (three meetings and workshops attended by various members of the Prostate Pathology Committee of the Mouse Models of Human Cancer Consortium), has disputed this, concluding that there is no evidence to support direct similarities between specific mouse prostate lobes and specific zones in the human prostate (Shappell et al. 2004).

Similar to the human prostate, the cell populations of the mouse prostate are separated into luminal secretory cells, a basal cell layer and a minor population of neuroendocrine cells. These cells types have some cytological differences consistent with the human prostate, however it is often difficult to appreciate this on routine light microscopy. Comparable antibodies used in human disease can be used in the mouse. For example, CK5 and p63 stain the basal cell layer; CK8 and CK18 stain the luminal layer. The neuroendocrine cells appear to represent only 0.3% of the normal mouse prostate cell population and stain positive for chromogranin or synaptophysin (Shappell et al. 2004).

1.3 Prostate Cancer

1.3.1 Epidemiology of prostate cancer

1.3.1.1 Incidence

The lifetime risk of developing cancer in the United Kingdom (UK) is thought to be greater than one in three (Sasieni et al. 2011), with prostate cancer (PCa) affecting one in eight men (CRUK, 2012). PCa is therefore recognised as one of the most important health issues facing the male population. Approximately 40,000 men are diagnosed with PCa every year (CRUK, 2012: based on data obtained from the Office for National Statistics, Information Service Division Scotland and Welsh Cancer Intelligence and Surveillance Unit) in the UK. Since the mid-1970s there has been a steady increase in the incidence of PCa, with a particular rapid rise in the late 1980s and late 1990s (Figure 3). These periods correspond with the introduction of serum prostate specific antigen (PSA) testing from the late 1980s (Brewster et al. 2000; Pashayan et al. 2006) and the increase use of PSA testing around the late 1990s (Melia & Moss 2001). The data indicates that the incidence is now plateauing. However, with the worldwide trend towards an ageing population, the continued use of PSA testing and an increase in use of multiple-biopsy regimes the incidence is predicted to increase substantially over the next two decades. In fact, PCa is already the most common cancer in UK males, accounting for 25% of cancer diagnosis. It is also anticipated to overtake breast cancer and become the most commonly diagnosed cancer of all, (between both sexes) by 2030 (Mistry et al. 2011).

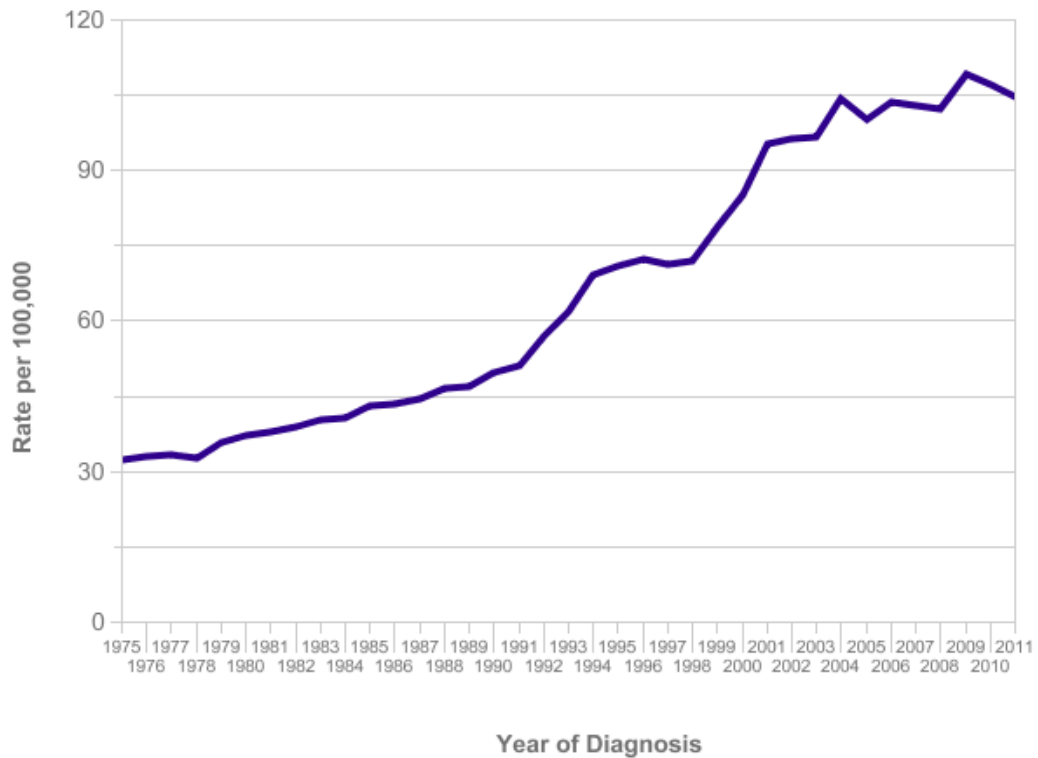


Figure 3: The incidence of prostate cancer in the UK from 1975 to 2011. A steady increase in incidence is noted largely as a result of the introduction and increased use of serum PSA testing. Graph obtained from the Cancer Research UK website (CRUK 2012) based on data obtained from the Office for National Statistics, Information Service Division Scotland and Welsh Cancer Intelligence and Surveillance Unit.

PCa incidence is strongly related to age, with a higher incidence in older men (Figure 4). It is rarely diagnosed in men younger than 50 years old, accounting for only 1% of all cases. At 85 years of age, the cumulative risk of clinically diagnosed prostate cancer ranges from 0.5% to 20% worldwide, despite autopsy evidence of microscopic lesions in approximately 30% of men in the fourth decade, 50% of men in the sixth decade, and more than 75% of men older than 85 years (Sakr et al. 1993; Grönberg 2003). In the UK between 2009 and 2011, an average of 9.9% of cases were in men aged between 50 and 59 years old, 33.7% between 60 and 69 years old, 36.4% between 70 and 79 year old and 18.9% in men over 80 year old (CR UK 2012).

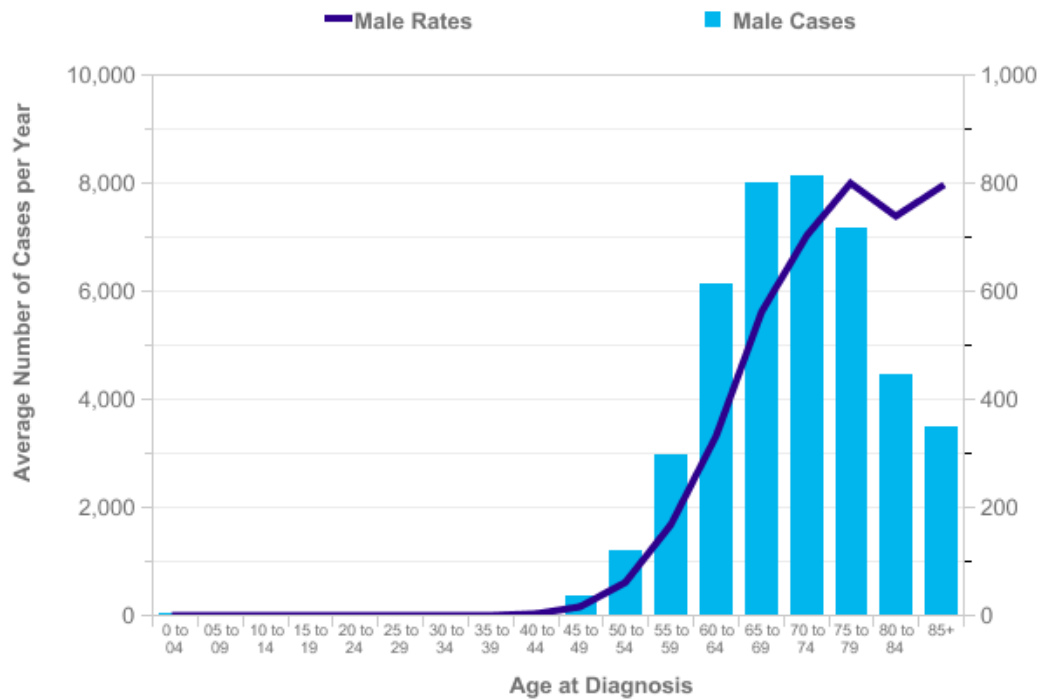


Figure 4: Prostate cancer incidence by age group. Age-specific incidence rates increase sharply from around age 50, peaking in men aged between 75 and 79 (CRUK 2012).

PCa incidence rates have increased for all of the broad age groups in the UK since the mid-1970s. The largest increase has been in younger men; with rates increasing almost nine-fold in men aged between 45 and 54 years, and six-fold in men aged between 55 and 64 years between 1975-1977 and 2009-2011 (Figure 5). Almost certainly the rapid rises from the late-1980s is secondary to the increased use of PSA testing. A more marked increase was seen in the United States (US) in the early 1990s following the introduction of PSA screening (SEER 1973-2011 n.d.).

The drop in incidence in men over the age of 85 years may reflect the reduced use of PSA testing in this age group (N. Williams et al. 2011). It has also been suggested that this reduction is due to an increase in early diagnosis in younger men through PSA testing, leaving fewer cases diagnosed when men reach their 80s (Bray et al. 2010).

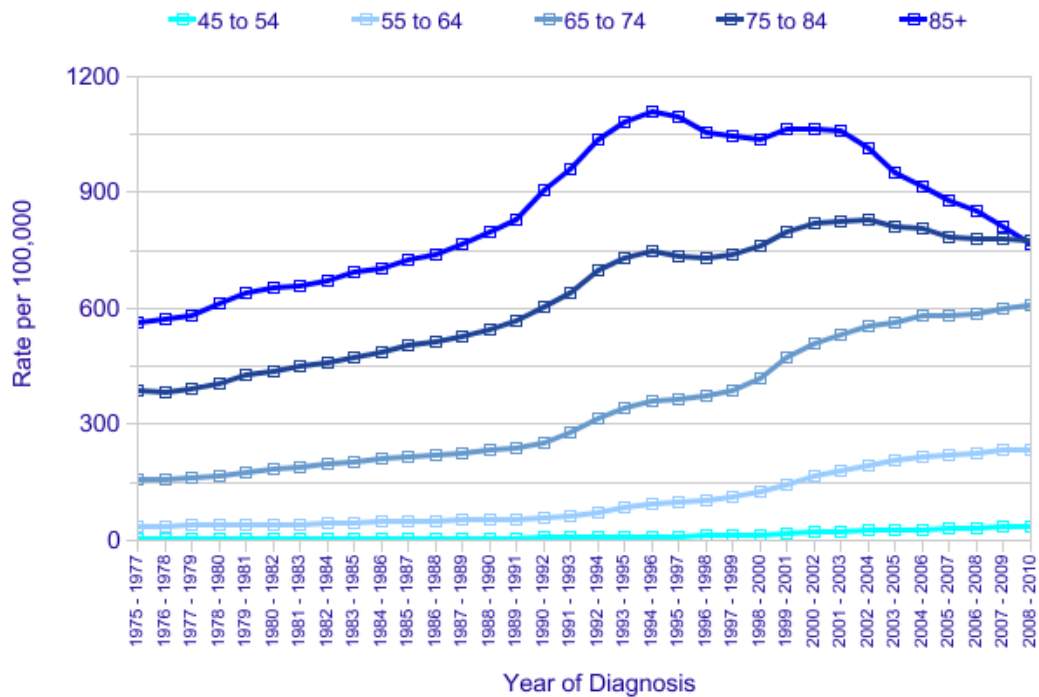


Figure 5: Prostate cancer incidence between 1975 and 2010 by age group. For men less than 65 years there is a steady increase in incidence with the most significant rise in the early 1990s. For men between 75 and 84 years and over 85 years there is a rise in incidence from 1975 to 2001 where the incidence begins to plateau or decrease following this, respectively (CRUK 2012).

1.3.1.2 Mortality & Survival

After lung cancer, PCa is the most common cause of cancer death in men in the UK, accounting for 13% of all cancer deaths in men, with an incidence of over 10,000 per annum. Like PCa incidence, the mortality is strongly related to age, with higher mortality rates in older men (Figure 6). In the UK between 2010 and 2012, an average of 74% of PCa deaths were in men aged 75 years and over, and more than 99% were in those aged 55 years and over (CRUK, 2012). Mortality from prostate cancer in the UK rose to a peak in 1993, reached a plateau, and has now started to decrease. The 1-, 5- and 10-year PCa-specific survivals between 2010 and 2011 were 94%, 85% and 84%, respectively. This is a marked improvement from those figures reported between 1971 and 1972 with 1-, 5- and 10-year PCa-specific survivals of 66%, 37% and 25%, respectively (CRUK, 2012). This improved survival is partly due to the increased detection of low-risk indolent tumours as a result of PSA testing, multi-biopsy regimes for diagnosis and via

transurethral resection of the prostate (TURP) to relieve bladder outflow obstruction as a result of benign enlargement (benign prostatic hyperplasia, BPH). But also due to improvement in detection resulting in earlier diagnosis and improvement in treatments such as surgery, radiotherapy, adjuvant hormone therapy and other systemic agents (Hanchanale et al. 2010; Etzioni et al. 2013; Kvåle et al. 2007).

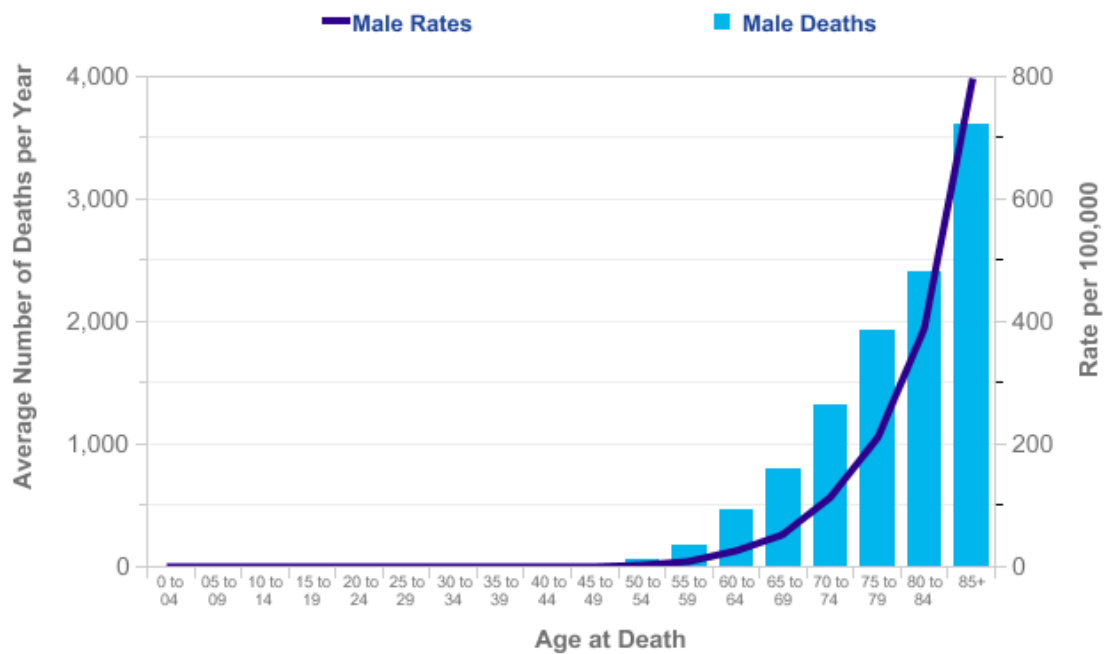


Figure 6: Prostate cancer related mortality by age group. Both the rate and number of deaths increases dramatically with increasing age with the greatest figures in men over the age of 85 years. (CRUK, 2012)

1.3.2 Risk factors

As previously discussed, age is the greatest factor influencing the development of PCa. Other risk factors include: race, familial and genetic influences, obesity, hormones, western-style diets and smoking.

1.3.2.1 Race

There is a marked geographical and ethnic variation in the incidence of clinical PCa, varying more than 25-fold worldwide. The incidence is highest in Australia/New Zealand (111.6 per 100,000), North America (97.2 per 100,000) and North/West Europe, and lowest in the Far East (for example, 10.5 and 4.5 per 100,000 in Eastern and South-Central Asia, Globcan, 2013).

Mortality rates are generally high in predominantly black populations (Caribbean, 29 per 100,000 and sub-Saharan Africa, 19-24 per 100,000), very low in Asia (2.9 per 100,000 in South-Central Asia for example) and intermediate in the Americas, Australia/New Zealand and Europe (Globocan, 2013). This ethnic variation is also evident within USA where there is a 1.6-fold increase in incidence in black men when compared to white men. Black men also appear to develop more aggressive disease with a 2.4-fold increase in mortality rate (SEER 1973-2011 n.d.).

The explanations for the large differences in incidence and mortality globally are currently unknown. Previous autopsy studies have shown that there is little variation in the prevalence of latent prostate tumours across countries (Breslow et al. 1977), so the large difference in clinical PCa rates across populations suggests a role for genetic and/or environmental factors in the progression from latent to clinically significant tumours.

1.3.2.2 Familial and Genetic influences

Evidence from epidemiological studies suggests that PCa has both a familial and genetic component. The first reports of familial clustering were published in the mid 20th century, demonstrating a greater risk of PCa in men with a first-degree relative. Subsequent results from meta-analyses support these findings, with an approximately 2.5-fold increase in developing PCa if a first-degree relative is affected. The relative risk increase according to the number of affected family members, their degree of relatedness and the age at which they were diagnosed are shown in Table 1 (Kiciński et al. 2011).

Family History	Relative Risk (95% CI)
None	1
First-degree relative	
All men	2.48 (2.25-2.74)
Diagnosed before 65 years	2.87 (2.21-3.74)
Diagnosed after 65 years	1.92 (1.49-2.47)
Father affected	2.35 (2.02-2.74)
Brother affected	3.14 (2.37-4.15)
2+ first-degree relatives	4.39 (2.61-7.39)
Second-degree relative (any age)	2.52 (0.99-6.46)

Table 1: Family history and risk of developing prostate cancer. Relative risk of developing PCa is increased according to the number of affected family members, their degree of relatedness and the age at which they were diagnosed. Data from meta-analysis (Kiciński et al. 2011).

It is estimated that 15% of PCa's are familial or hereditary, with the remaining 85% being sporadic (Carter et al. 1992). A number of linkage studies, which screen for genetic traits in high-risk groups, have identified many PCa susceptibility genes, including RNaseL (hereditary prostate cancer-1 [HPC1] region, 1q23-25) (Rökman et al. 2002) and ELAC2 (HPC2 region, 17p) (Tavtigian et al. 2001). However, due to the high incidence of sporadic PCa's, interpretations of these results can be difficult.

A number of studies have suggested a familial association between PCa and breast cancer through two susceptible genes: BRCA1 (17q21) and BRCA 2 (13q12). A germline mutation in BRCA1 has been shown to have a ~3.75-fold increase risk of developing PCa (Leongamornlert et al. 2012). Mutations in BRCA2 confers the highest genetic risk of PCa known to date, with an ~8.6-fold increase (Kote-Jarai et al. 2011). Castro et al. recently published data demonstrating that BRCA mutation carriers, in particular BRCA 2, have a more aggressive PCa phenotype with a higher probability of nodal and distant metastasis resulting in poor survival outcomes (Castro et al. 2013). Germline BRCA1 and BRCA2 mutations were also associated with higher incidence of Gleason score ≥ 8 and T3/T4 disease (Castro et al. 2013). Radical treatment should, therefore, be recommended immediately in these patients, rather than deferring treatment as part of an

active surveillance programme. Also, a lymph node clearance may be considered at the time of surgery even in those low-risk tumours to improve staging accuracy allowing for earlier adjuvant treatment. To date, the best form of radical therapy, whether surgery or radiotherapy, in men with BRCA 2 mutations is unknown. Given that the BRCA2 protein is involved in the repair of damaged DNA breaks, and that radiation induces double-strand breaks, it is possible that PCa patients with a BRCA2 mutation are more sensitive to radiotherapy than patients without a mutation (Narod et al. 2008). There are however no randomised studies comparing surgery and radiotherapy in BRCA mutation carriers.

Systemic treatments such as Poly(ADP-ribose) polymerase inhibitors (PARPi, e.g. olaparib) have shown significant survival benefit in a subset of patients with metastatic PCa with aberrations in one or more of the 12 DNA-repair gene that were tested, including as BRCA1/2 and ATM. 14 of the 16 (88%) men with a DNA-repair mutations responded to olaparib with a median survival of 9.8 months compared with 2.7 months for those without a mutation (Mateo et al. 2015). PARP is an enzyme that is important in repairing single-strand DNA breaks. If these single-stranded breaks fail to repair, subsequent cell division can result in double-strand breaks. PARPi thus result in multiple double-stranded DNA breaks, and in tumours with BRCA mutations, they are unable to be efficiently repaired, ultimately causing cell death. Knowledge of a man's BRCA status is, therefore, of prognostic value.

PCa has also been associated with Lynch syndrome. Lynch syndrome is caused by a germline mutation in one of the mismatch repair (MMR) genes, *MLH1*, *MSH2*, *MSH6*, or *PMS2* and is associated with several cancers: colorectal, endometrial, ovarian, gastric, small intestinal, pancreatic, ureteral, brain, and sebaceous gland adenocarcinoma (Aarnio et al. 1999). Haraldsdottir et al have reported an almost five-fold increase risk in PCa in the 188 men they identified with Lynch syndrome. This however was not associated with earlier onset or a more aggressive phenotype (Haraldsdottir et al. 2014).

Germline mutations are rare in PCa, unlike gene fusions. Gene fusions can occur as a result of chromosomal translocation and are the most common genetic alteration in human cancers (Futreal et al. 2004). These were initially thought to be mechanisms linked exclusively to haematological malignancies such as the BCR-ABL1 fusion gene resulting in the Philadelphia chromosome in chronic myeloid leukaemia (CML) (Faderl et al.

1999). In 2005 however, the TMPRSS2-ERG gene fusion was identified in PCa (Tomlins et al. 2005). Approximately 50% of PCa and 20% of PIN lesions are positive for the TMPRSS2-ERG gene fusion, and over 90% of PCas over-expressing ERG harbour this molecular abnormality (Tomlins et al. 2008). There has been great excitement following its discovery, especially knowing the success of the tyrosine kinase inhibitor Gleevec (Imatinib) in CML. It has been proposed that TMPRSS2-ERG fusion positive tumours are more resistant to taxanes (e.g. Docetaxel), a chemotherapy agent routinely used in the treatment of metastatic PCa (Galletti et al. 2014; Reig et al. 2016). It has also been shown to associated with increased risk of high Gleason score and progression during active surveillance (Berg et al. 2014; Hägglöf et al. 2014), with some reporting shorter survival in TMPRSS2-ERG positive patients (Hägglöf et al. 2014). The development of a urine TMPRSS-ERG assay has also been combined with other urinary markers such as PCA3 may help risk-stratify patients (Tomlins et al. 2015).

More recently, genome-wide association studies (GWAS) have emerged as a new approach to identifying somatic mutations and alleles associated with PCa. These will be discussed in detail later in this chapter.

1.3.2.3 Obesity

The suggested link between body mass index (BMI) and risk of PCa is weak and inconsistent. A meta-analysis by MacInnis et al reported a rate ratio or relative risk (RR: i.e. a rate ratio of 1 = no effect) of 1.05 (95% CI 1.01-1.08) per 5 kg/m² increments in BMI measurement. There was a marginally stronger association with higher stage of disease, with a RR of 1.12 per 5 kg/m² increments in BMI (95% CI 1.01-1.23) (MacInnis & English 2006). A more recent meta-analysis supports this finding, but interestingly, they also reported an inverse relationship with increasing BMI and localised disease, with a RR of 0.94 (95% CI 0.91-0.97), concluding that obesity may have a dual effect on PCa – a decreased risk for localised disease and an increased risk for advanced disease (Discacciati et al. 2011).

Despite only small trends associated with risk of PCa, increasing evidence suggests that higher BMI is associated with poorer outcomes i.e. higher PCa-specific mortality. A meta-analysis by Cao et al demonstrated that an increase in BMI of 5kg/m² was associated with a 21% increased risk of biochemical recurrence (RR 1.21, 95%CI 1.11–1.31 p<0.01) and a 15% (RR 1.15, 95%CI 1.06–1.25, p<0.01) higher risk of dying of PCa (Cao & Ma

2011). Several possible explanations for this have been proposed. Firstly, obesity could result in a delay in diagnosis resulting in a more advanced stage at diagnosis. Digital rectal examinations are less accurate and PSA values are often lower in obese patients. The lower values are thought to be due to a higher plasma volume resulting in an obesity-related dilution (Kvåle et al. 2007; Grubb et al. 2009). Secondly, there are difficulties associated with treatment, which could affect outcome. A higher positive margin rate has been reported following radical prostatectomy (Freedland et al. 2004) and there is an increased risk of suboptimal radiation delivery due to a greater day-to-day variation in prostate location (Millender et al. 2004). Lastly, biological mechanisms relating to adiposity and PCa progression have been proposed. Obesity is known to activate pro-carcinogenic pathways such as the insulin-like growth factor (IGF) axis which is related to greater risk of aggressive PCa in obese men (Weiss et al. 2007). Testosterone levels are also lower in obese men, which has been linked to the development of more aggressive higher-grade PCa (Severi et al. 2006).

1.3.2.4 Hormones

Testosterone and its potent metabolite DHT are essential for normal prostate growth and play a role in PCa development. The hallmark paper by Huggins and Hodges in 1941, highlighting that surgical castration causes a major regression of PCa, has initially led people to believe that high levels of testosterone are associated with higher risk of PCa. To support this argument, PCa almost never develops in the rare men castrate before puberty or in men deficient in 5 α -reductase; the enzyme responsible for converting testosterone to DHT. In addition, trials using inhibitors of 5 α -reductase, Finasteride and Dutasteride have also shown some reduction in risk of developing PCa (Andriole et al. 2010; Thompson et al. 2003), suggesting a key role for DHT.

It has long been hypothesised therefore that high serum androgen levels are a risk factor for PCa. A meta-analysis supports this, demonstrating that men with a total testosterone in the highest quartile of the population are 2.34 times more likely to develop PCa (Shaneyfelt et al. 2000). However, the incidence of PCa increases with age, while serum testosterone decreases. In fact, several epidemiological studies have shown that low serum testosterone levels have an adverse effect on men with newly diagnosed PCa. (Schatzl et al. 2003) suggested an enhanced malignant potential associated with low serum testosterone, describing higher AR density and a more aggressive tumour.

Messengill et al (2003) and also Imamoto et al (2005) show that a low pre-treatment total testosterone was an independent predictor of extra-prostatic disease (or non-organ confined) in patients with localised PCa undergoing radical prostatectomy (Massengill et al. 2003; Imamoto et al. 2005). Some case controlled studies have also shown that a low pre-treatment serum testosterone have a poorer response to endocrine therapy with earlier time to androgen-independence in metastatic disease (Furuya et al. 2002). Somewhat contradictory to this is a recent study by Klotz et al (Klotz, O'Callaghan, et al. 2015) reporting a higher PCa specific mortality in men with metastatic PCa who have a high nadir serum testosterone (i.e $>0.7\text{mmol/l}$) within the first year of androgen deprivation therapy. This observation might however highlight the PCa response to treatment and its sensitivity to hormone deprivation as oppose to initial risk of developing the disease. Some studies also report no difference in incidence of PCa in relation to testosterone level (Gill et al. 2010; C. Chen et al. 2003).

There remains controversy between the association of risk of developing PCa and the serum concentration of testosterone. Even so, there is little doubt that exposure of the prostate to androgens is important in prostate tumourigenesis. The duration and magnitude of exposure for this to occur is however unknown. Further detail on androgen-deprivation therapies will be discussed below.

1.3.2.5 Diet and lifestyle

Migration studies have highlighted the importance of diet and lifestyle on risk of PCa. Among migrants moving from a low risk country such as Japan to America, the incidence almost equalizes to that of white Americans within a generation. Furthermore, same ethnic group men raised in different environments have a risk of PCa comparable to the reported incidence of the country they live, not their country of origin (Wolk 2005; Kolonel et al. 2004). PCa incidence rates have been increasing in China, Korea, Japan, and Singapore during the last several decades (Zhang et al. 2012). This upward change has been primarily ascribed to the occurrence of nutrition transition in these countries during the same period of time. Nutrition transition is defined by a gradual change towards the Westernized diet characterized by high intake of energy, animal fat, and meats and low intake of fibre (Zhang et al. 2012). The potential mechanisms of action include increased IGF-1 levels as a result of excess dietary fat and thus energy levels, as

seen in the obese (see section 1.3.2.3), or possible induction of oxidative stress leading to genomic instability and cancer.

Several reports have found that diets high in saturated fat, meat, dairy foods and calcium have a positive association with risk of developing PCa (Aune et al. 2015; Chan et al. 2001), with a recent meta-analysis demonstrating some association of these dietary factors with advanced disease (Gathirua-Mwangi & Zhang 2014). Early animal experiments using the rat Dunning model further support a role of dietary fat in PCa progression, demonstrating that a fat-free diet can reduce the growth of androgen-dependent tumours (Clinton et al. 1988). The heterogeneity amongst studies in defining fat intake and subtypes and the severity of PCa makes interpreting the extent of this association difficult, with some studies demonstrating contrasting results: a large European multicentre cohort study demonstrates no association between dietary fat and PCa risk (Crowe et al. 2008).

1.3.2.6 Smoking

Despite demonstrating strong links with several other cancers, such as lung and bladder, the association of cigarette smoking and PCa remains a matter of debate. Both case-control and cohort studies have produced conflicting results and none have demonstrated a clear dose-response relationship, although some recent studies have suggested an association with more advanced stage at diagnosis and increased PCa-related mortality (Kenfield et al. 2011; Huncharek et al. 2010; Bostwick et al. 2004). Kenfield et al (2011) further show that men who have quit for at least 10 years have PCa-specific mortality risks similar to those who have never smoked. A direct effect of smoking on PCa progression is therefore biologically plausible. The main proposed hypotheses include: 1. Tumour initiation through carcinogens from cigarette smoke such as cadmium 2. By increasing circulating androgens, 3. Epigenetic effects, including aberrant methylation profiles among current smokers, which correlate with aggressive disease (Kenfield et al. 2011).

1.3.3 Prostate cancer detection

Most patients in whom PCa is suspected are identified on the basis of abnormal findings on digital rectal examination (DRE) or, more commonly, by raised levels of serum PSA. In current practice, a 10-12 needle biopsy is performed either transrectally or

transperineal under ultrasound guidance if PCa is suspected. More recently as a result of advancement in imaging, some centres in the UK perform a multi-parametric magnetic resonance imaging (mpMRI) prior to needle biopsy so that suspicious lesions can subsequently be targeted, increasing diagnostic yield.

1.3.3.1 Digital rectal examination (DRE)

As most (70%) of prostate tumours are detected in the peripheral zone, larger tumours can sometime be palpated on DRE. A DRE can also detect tumours when the PSA is within normal range. Underestimation is however common because small and anteriorly located tumours are generally impalpable. For this reason, the predictive diagnostic value and accuracy of staging is combined with PSA and imaging such as mpMRI and isotope bone scans.

1.3.3.2 Prostate Specific Antigen (PSA)

As previously alluded to, PSA is produced by the prostate and functions to liquefy the semen. Due to an alteration in the architecture of the prostate in PCa, the tissue barriers become compromised and PSA leaks out, leading to increased levels in the bloodstream. The PSA test has therefore revolutionised PCa detection. There are however concerns about its specificity; PSA is organ- but not tumour-specific (Hamdy 2001). Therefore, other conditions, such as benign prostate enlargement, prostatitis (inflammation of the prostate) and lower urinary tract infections, can also cause an elevated PSA.

The PSA test is currently the best method of identifying an increased risk of localised PCa, especially when symptoms are not apparent. Routine PSA testing or screening is however controversial. Although some asymptomatic PSA detected localised PCa will be clinically relevant and therefore be treated and cured earlier which could extend life, many will also be clinically insignificant which would not have become evident in a man's lifetime. PSA cannot therefore accurately differentiate between indolent and aggressive disease, resulting in risk of over-diagnosing and subsequently over-treating men. Patients should be counselled regarding these issues prior to having a PSA test in accordance with the Prostate Cancer Risk Management Programme (available at <https://www.gov.uk/guidance/prostate-cancer-risk-management-programme-overview>).

For these reasons PSA screening has been controversial. Any form of screening aims to reduce disease-specific and overall mortality, and to improve a person's future quality of life. A Cochrane review of 5 randomised controlled trials concluded that PCa screening did not significantly decrease PCa-specific mortality, with harms associated with diagnostic evaluations and over-treatment. They did further concluded that any reduction in PCa-specific mortality may take up to 10 years to accrue; therefore, men who have a life expectancy less than 10 to 15 years should be informed that screening for PCa is unlikely to be beneficial (Selley et al. 1997; Ilic et al. 2013). One trial in this Cochrane review (European Randomised Study of screening in Prostate Cancer [ERSPC]) has since updated their results, reporting a 21% significant reduction in PCa mortality in a subgroup of men aged 55 to 69 years, however. This trial with a 13 years follow-up, reiterated the risk of over-diagnosis and over-treatment, with the number needed to be screened of 781 and number needed to be diagnosed of 27, to avert one PCa related death (Schröder et al. 2014). PSA increases with age resulting in age-related reference values recommended by the Prostate Cancer Risk Management Programme (Table 2).

Age (years)	PSA referral value (ng/ml)
50-59	≥ 3.0
60-69	≥ 4.0
70+	> 5.0

Table 2: Age-related PSA reference values. (Prostate cancer risk management programme, 2010).

PSA levels above 20ng/ml are often indicative of tumour extension beyond the capsule (T3, see below), while levels above 40ng/ml suggest a high likelihood of bony or soft tissue metastases.

1.3.4 Grading and staging

1.3.4.1 Gleason grading system

Donald F. Gleason created a unique grading system for PCa in 1966, based solely on the architectural pattern of the tumour identified at relatively low magnification on microscopy (Gleason 1966). Despite production of the modified Gleason grading system in 2005, following the International Society of Urological Pathology (ISUP) conference in San Antonio (Texas, (Epstein et al. 2006), Gleason score remains one of the most powerful prognostic factors in PCa (Epstein 2010).

Specifically, the Gleason scoring system classifies prostate adenocarcinomas through its loss of normal glandular architecture (i.e. size, shape, relationship and differentiation of the glands). It is assigned a grade from 1 to 5, with 1 being the most differentiated and 5 being the least differentiated (Figure 7). Unlike in prostate intraepithelial neoplasm (PIN) cytological features play no role in grading the tumour. Since many PCa are multi-focal and heterogeneous, allowance is made by adding the two most dominant grades (primary -most prevalent and secondary -second most prevalent) or architectural patterns to give a Gleason score between 2 and 10 (e.g. 3+4=7). Since grades 1 and 2 are rarely if ever seen, only scores between 6 (3+3) and 10 (5+5) are observed. Cancers of the same Gleason score have a worse prognosis if the predominant primary grade is higher (e.g. 4+3 is worse than 3+4). For this reason, Epstein et al. have further updated the Gleason score, categorisation into 5 groups: Grade group 1: Gleason score =6, Grade group 2: Gleason score 3 + 4, Grade group 3: Gleason score 4 + 3, Grade group 4: Gleason score 8, and Grade group 5: Gleason score 9-10 (Epstein et al. 2016).

It is important to recognize Gleason pattern 4 tumours because tumours with this pattern have a significantly worse prognosis than those with pure Gleason pattern 3 (McNeal et al. 1990; Epstein et al. 1993). Gleason pattern 3 (3+3=6) tumours often behave in an indolent manner with a low risk of local and metastatic progression. Many patients will therefore embark upon a conservative management approach such as active surveillance (discussed in section 1.3.7.1), with long-term follow-up studies demonstrating feasibility and safety of this strategy with no effect on overall survival (Albertsen et al. 2005; Klotz, Vesprini, et al. 2015).

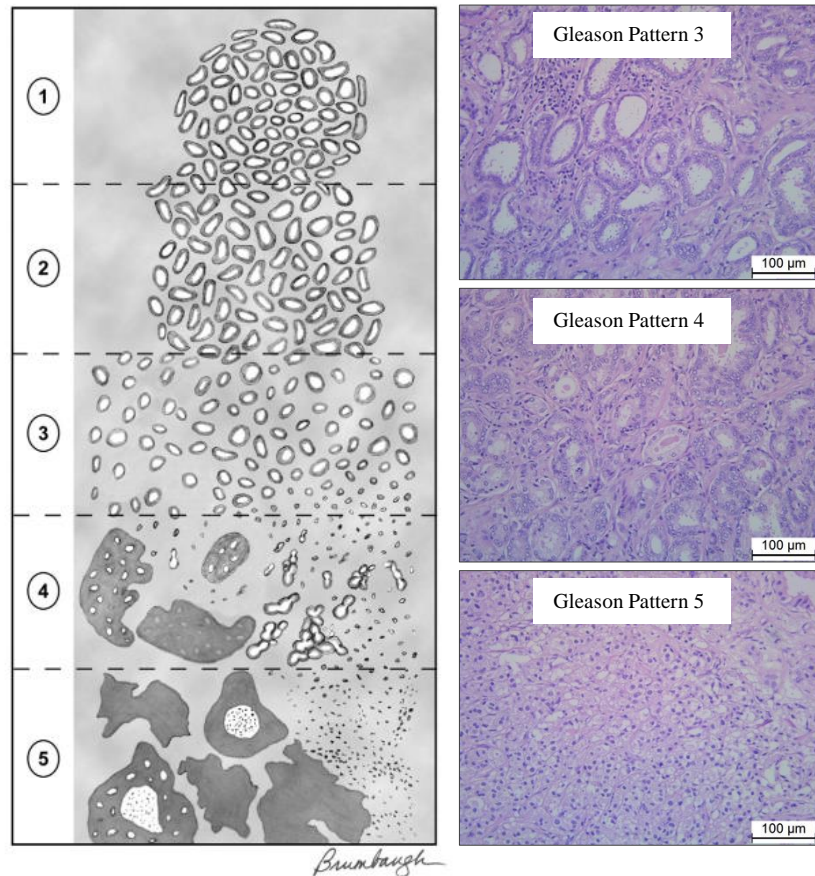


Figure 7: The Modified Gleason grading system. Schematic diagram of the Gleason grading system (Epstein 2010) and haematoxylin and eosin stained histological representation of each Gleason grade pattern (courtesy of Dr D Griffiths, Consultant Uro-pathologist, University Hospital of Wales, Cardiff).

1.3.4.2 TNM (Tumour, Nodal and Metastases) Staging

Prostate adenocarcinoma, like most other cancers, is staged using the TNM classification system as defined by the Union for International Cancer Control (UICC). This allows assessment of the tumour (T), lymph nodes (N) and metastases (M), which in turns affords accurate prognostic information and enables further treatment and/or follow-up to be planned (Table 3).

The T stage (T1-T4) describes the pathological development of the tumour. T1 represents ‘incidental’ status, in which the tumour is either discovered following transurethral resection of the prostate (TURP) surgery used to treat benign enlargement of the prostate and bladder outflow obstruction or, more commonly, by needle biopsy of the prostate following PSA testing which is impalpable. T2 represents a tumour that is palpable but still confined to the prostate. T3 tumours have breached the prostate capsule into the

surrounding fat or seminal vesicles. T4 tumours are advanced invading neighbouring organs. Metastases are most common in nodes (N1) and bone (M1). The lungs, liver and other soft tissue are less commonly involved.

TNM Classification of prostate cancer (7th Edition UICC, 2010)

Tumour Stage

- Tx** Primary tumour cannot be assessed
- T0** No evidence of primary tumour
- T1** Clinically inapparent tumour not palpable or visible by imaging
 - T1a:** ≤ 5% of TURP chips
 - T1b:** > 5% of TURP chips
 - T1c:** Identified by needle biopsy
- T2** Tumour confined to prostate (organ confined)
 - T2a:** Involves ≤ 50% of one lobe
 - T2b:** Involves > 50% of one lobe but not both lobes
 - T2c:** Involves both lobes
- T3** Tumour extends through the prostate capsule
 - T3a:** Extracapsular extension (unilateral or bilateral)
 - T3b:** Invades seminal vesicle(s)
- T4** Tumour is fixed or invades adjacent structures: bladder neck, external sphincter, rectum, levator muscles and/or pelvic wall.

Nodal Stage (regional)

- Nx** Cannot be assessed
- N0** No metastasis
- N1** Node metastasis

Metastasis Stage (Distant)

- Mx** Cannot be assessed
- M0** No metastasis
- M1** Metastasis
 - M1a: Non-regional lymph node(s)
 - M1b: Bone(s)
 - M1c: Other sites(s)

Table 3: TNM Classification of Prostate Cancer (7th Edition UICC, 2010)

1.3.5 Prognostic indicators and risk-stratification

Accurate grading and staging of PCa, particularly distinguishing between Gleason grades and between localised and more extensive disease is critical for selection of the optimum treatment option. Although developments in imaging techniques, especially multi-parametric MRI, have led to more accurate staging than can be achieved with digital rectal examination (DRE) or PSA testing alone, both under- and over-staging are still common clinical problems. Thus, a need remains not only for improving staging techniques, but also for better prognostic markers that will give an indication of future disease behaviour if left untreated.

1.3.5.1 D'Amico Risk Classification

First described in 1998, by D'Amico and colleagues, created a three-group risk-classification (low-, intermediate- and high-risk), to predict post-treatment biochemical failure (i.e. recurrence) following radical prostatectomy or external beam radiotherapy (D'Amico et al. 1998). Based on the individual prognostic powers of PSA, Gleason grade and Tumour stage, the D'Amico risk classification aids physicians in primary treatment decision for patients with non-metastatic disease as summarised by Table 4. To further help risk-stratify those patients with low risk disease, especially those considering deferred treatment or active surveillance, Epstein and colleagues have added a further very-low risk group (Kryvenko et al. 2014). In addition, the Epstein criteria also use the number and volume of cancer involved in needle core biopsies and PSA velocity: Very-low risk = <3 positive biopsy cores each $\leq 50\%$ cancer involvement and a PSA density ≤ 0.15 , in addition to a PSA ≤ 10 ng/mL, Gleason score ≤ 6 and T1c on clinical examination (Kryvenko et al. 2014).

Risk	PSA(ng/ml)		Gleason Score		Clinical stage
Low	<10	and	≤ 6	and	T1a-T2a
Intermediate	10-20	or	7	or	T2b
High	>20	or	8-10	or	$\geq T2c$

Table 4: D'Amico Risk Classification (D'Amico et al. 1998).

1.3.5.2 Multiparametric Magnetic Resonance Imaging (mpMRI)

mpMRI is increasing being used to identify areas of interest, so that biopsies can be better targeted, improving diagnostic yield and staging of PCa. For this reason, many centres across the UK are performing a mpMRI prior to biopsy. mpMRI uses anatomic T2-weighted imaging combined with two functional techniques: diffusion-weighted imaging (DWI) and dynamic contrast-enhance MRI. It is particularly sensitive at detecting higher-grade tumours. Bratan et al., for example, reported detection rates for tumours of <0.5 cc, 0.5-2 cc and >2 cc of 21-29%, 43-54% and 67-75%, respectively for Gleason ≤ 6 , 63%, 82-88% and 97 % for Gleason 7 and 80%, 93% and 100% for Gleason ≥ 8 cancers (Bratan et al. 2013). This data has been scrutinised further in the recent multicentre PROMIS trial, validating mpMRI and TRUS biopsy against a reference test (template prostate mapping biopsy). The authors conclude that mpMRI used as a triage test before first biopsy, could identify a quarter of men who might safely avoid unnecessary biopsy (Ahmed et al 2017). Although, these figures are encouraging, the accuracy of imaging and reporting remains magnet and reporter dependent.

1.3.5.3 Prostate Cancer gene 3 (PCA3)

PCA3 is a piece of non-coding RNA that is only present in the prostate. It is detectable in urine sediments obtained after three strokes of prostatic massage during DRE. It has value as a biomarker because levels in PCa are greatly increased. PCA3 is commercially available (ProgenSA, Hologic MA, USA) and is thought to be superior to PSA (Auprich et al. 2011). Some have demonstrated a correlation with higher risk disease prompting the notion that it can separate aggressive from indolent disease (Merola et al. 2015). It has also been included in biopsy-specific nomograms in order to improve diagnostic accuracy and help avoid unnecessary biopsies (Hansen et al. 2013). Controversy remains however, with regards to defining the cut off value for aggressive and indolent disease (NICE CG175, 2014).

1.3.6 Natural history of prostate cancer

The natural course of PCa can be very long and its often thought to progress in a step-wise fashion Figure 8. It is believed that the process begins with the development of the precursor lesion – prostatic intraepithelial neoplasm or PIN. PIN was previously classified into low- (mild) and high-grade (moderate) forms, but pathologists now only report high-grade PIN, since low-grade PIN reporting is very subjective and has no prognostic value (Clouston & Bolton 2012). The clinical significance of high-grade PIN is difficult to determine. The presence of high-grade PIN on prostate biopsy was previously thought to be a significant predictor for PCa (Clouston & Bolton 2012), but more recent evidence suggests this was due to sampling error (Lee et al. 2010; Merrimen et al. 2010). These more contemporary series, using multi-core needle biopsy regimes did conclude however that multi-focal (>2 cores) high-grade PIN was a predictor for PCa when compared to uni-focal high-grade PIN. Thus, the presence of multi-focal high-grade PIN often triggers a repeat prostate needle biopsy (Heidenreich et al. 2014).



Figure 8. Natural progression of prostate cancer. PIN = Prostatic intraepithelial neoplasm.

Although a step-wise process has been postulated, PCa remains very heterogeneous, with individual tumours behaving differently resulting in a diverse clinical course. For example, some tumours can behave indolently and never require active treatment, whilst others can present as an aggressive clinical entity resulting in progression and metastasis. In addition, men often present at different stages of their disease.

Indolent cancers, typically those well-differentiated tumours (Gleason 6), often have no effect on health or survival even without treatment. Consequently, more men are deferring radical treatment and avoiding its associated risks: incontinence and impotence, or radiation side effects, by enrolling into active surveillance schemes. A small minority of men will however develop high-grade tumours after several years, with some resulting in metastasis and mortality (Klotz, Vesprini, et al. 2015; Popiolek et al. 2013). The cause

for this progression is unclear. The residual low-grade cancer may require sufficient time to reach a certain size or for accumulation of critical mutations, in order to de-differentiate into a higher-risk lesion. Alternatively, due to the multifocal nature of PCa, a new higher-risk lesion may develop. Both of which would then pave the way for local progression and metastasis.

In men with high-risk poorly differentiated tumours (Gleason ≥ 8), whether it has de-differentiated or it is a separate entity, the outlook is far worse. Albertsen et al reported long-term follow-up (20 years) of men managed conservatively with localised disease. In men with low- and intermediate-grade PCa (Gleason 6 and 7), about 98 out of every 100 (98%) lived for more than 5 years. But in men with high-grade (Gleason 8-10) PCa, just over 2 out of 3 (67%) lived for more than 5 years (Albertsen et al. 2005). For high-grade or locally advanced disease radical treatment is recommended, as described in 1.4.7. Despite this recurrence rates in this group is far greater. Khan et al report a 62% and 97% 5-year biochemical recurrence free-survival in patients with Gleason 8-10 and Gleason 6 PCa following surgery, respectively (Khan et al. 2003). In those with lymph node involvement or with a pre-operative PSA between 20-50ng/ml, the outcome was worse with a 5-year biochemical recurrence free-survival of 37% and 50%, respectively. (Khan et al. 2003).

When metastases occur it almost always goes to lymph nodes or bone where it produces an osteoblastic response. The outlook for men presenting at the time of diagnosis with metastatic disease is poor. The main stay of treatment is androgen deprivation therapy (ADT), either medically using LHRHa or surgical with castration. However, virtually all men become hormone independent termed castrate-resistant within 18-24 months following diagnosis. Rapid progression results either locally, in lymph nodes, or in distant metastasis, subsequently resulting in death. The control arm (i.e. ADT only) of the STAMPEDE (Systemic Therapy in Advancing or Metastatic Prostate cancer: Evaluation of Drug Efficacy) trial recently reporting a median survival of 3.5 years in patients presenting with metastatic PCa (James et al. 2015).

In summary, men with well-differentiated tumours rarely die from their disease with many not requiring any treatment. Men with non-metastatic poorly differentiated tumours frequently die within 5 to 10 years of their diagnosis, often despite aggressive intervention (Albertsen et al. 2005; Popiolek et al. 2013). Finally, men presenting with

metastatic disease have a poor outlook, with a short survival with the majority of their remaining life in a state of castrate-resistance. The natural history of PCa is therefore complex often due to its heterogeneity or multi-focal nature. The ability of a tumour to de-differentiate from low- to high- risk, to progress locally or to metastases to lymph nodes or bone must however have a molecular or genetic correlate or understanding for them. This understanding will permit risk-stratification of patients and define future treatment strategies.

1.3.7 Prostate cancer management

1.3.7.1 Management of localised prostate cancer

Localised PCa is defined as those tumours that are confined to the capsule of the prostate ($T \leq 2$). The management of localised PCa is diverse ranging from conservative management such as active surveillance to more invasive treatments such as brachytherapy, external beam radiotherapy (EBRT), surgery and ADT.

Deferred treatment has evolved over the past few decades, from the traditional watchful waiting to the more contemporary active monitoring or surveillance protocols, with watchful waiting now reserved for those with a non-curative treatment approach. Those patients enrolling into an active surveillance protocol usually have close PSA surveillance with a repeat biopsy of the prostate typically around 12 to 18 months following diagnosis (NICE CG175, 2014). This is performed mainly in order to reduce sampling error and missing a higher-risk tumour that would require radical treatment. A systematic review of 7 active surveillance series reported up grading on repeat biopsy of between 2.5 and 28% (Dall'Era et al. 2012). Many patients embark on an active surveillance programme in order to avoid the potential side effects associated with radiotherapy and surgery, such as incontinence and impotence. Long term follow up of a large active surveillance series has shown comparable survival (98.1% and 94.3% 10- and 15- year disease-specific survival, respectively) with favourable-risk patients managed with initial definitive intervention (Klotz, Vesprini, et al. 2015).

The recent reported ProtecT (Prostate testing for cancer and Treatment) trial is the first of its kind to compare active monitoring, radical prostatectomy and radical radiotherapy in men with low-risk PCa. There was no cancer-specific survival benefit at 10 years between the three randomised cohorts, although there was a beneficial effect of treatment (radical prostatectomy or radiotherapy) over active monitoring in reducing time to metastasis (Hamdy et al. 2016). The PIVOT (Prostate cancer intervention versus observation trial) randomised men with localised PCa to surgery or observation (watchful waiting) (Wilt et al. 2012). 731 men were randomised with a median follow-up of 10 years. They concluded that there was no apparent difference between surgery and observation for men with low-risk PCa, whereas those with intermediate- and high-risk disease may have a better survival following surgery. A similar earlier study by the

Scandinavian Prostatic Cancer Group (SPCG-4), prior to widespread use of PSA testing concluded that radical prostatectomy was associated with a reduction in the rate of death from PCa (14.6% for surgery compared to 20.7% for observation), with a 12.8-year follow-up. Subgroup analysis further demonstrated additional benefit in men younger than 65 years of age. They reported a number needed to treat to avoid one death was 15 overall and 7 for men younger than 65 years of age (Bill-Axelsson et al. 2005). Caution must be taken interpreting the results from SPCG-4 however, as patients were enrolled between 1989 and 1999 when Gleason grading was different and the majority of patients had palpable disease, with only 12% having T1c cancers. This study has further been criticised for its under-recruitment and inclusion of men with significant comorbidities, leading to an excessive death from non-prostate-related cancer.

In summary, the best management for low-risk PCa remains unclear. For intermediate and high risk localised PCa, definitive treatment with surgery or EBRT are the mainstays of treatment.

1.3.7.2 Management of locally advanced prostate cancer

Locally advanced PCa is typically defined as tumours that breach the capsule ($T \geq 3a$). However, this definition often includes tumours with associated pelvic lymph node (N1) involvement. The management of men with localised PCa with a high-risk of extra capsular disease (i.e. Gleason score ≥ 8 , or PSA > 20) may also be considered under this heading.

EBRT in combination with neoadjuvant ADT is the gold standard treatment for locally advanced PCa. The ADT reduces the size of the PCa and appear to increase the sensitivity of cancer cells to death by irradiation. This approach has been validated by numerous randomised trials including Bolla et al, SPCG-7 and PRO7 (Widmark et al. 2009; Bolla et al. 2009; Warde et al. 2011). In particular evidence from the PRO7 trial co-ordinated by the UK Medical Research Council (MRC) have shown that combining EBRT with neo-adjuvant and continuous ADT improved the overall survival rate at 7 years ($p=0.03$) compared with ADT alone (Warde et al. 2011). Careful patient selection is therefore required especially in the elderly or those with medical comorbidity when their survival could be less than 10 years. Furthermore, Bolla et al have shown a survival benefit of

long term (3 years) versus short term (6 months) ADT in addition to EBRT in locally advanced PCa (Bolla et al. 2009). Further survival benefits are likely following the introduction of intense-modulated radiotherapy (IMRT), which allows very precise targeting of the prostate, with less radiation scatter to surrounding organs. As a consequence, higher doses can be given to men without significant increase in local toxicity. There is likely to be further benefit following the expansion of proton beam technology.

More recent practice has taken a multimodality surgical approach to managing locally advanced PCa, particularly in young fit patients where the cancer is thought to be fully excisable (T3a). Surgery is often considered as the primary treatment, accepting that there is a higher chance of adverse pathological features, such as upgrading or upstaging, positive margins or nodal disease where additional EBRT may be required. The role and timing of EBRT in this setting is controversial. The currently recruiting MRC RADICALS (Radiotherapy and Androgen Deprivation in Combination after Local Surgery) trial will evaluate the advantages of early (immediate) versus deferred (salvage) EBRT and short (6 months) versus long course (2 years) ADT in addition to EBRT versus EBRT alone (Parker et al. 2007).

1.3.7.3 Management of metastatic prostate cancer

Since the Nobel Prize winning research by Huggins and Hodges in 1941, surgical castration has been the main stay of treatment of metastatic PCa. Later work by Schally and colleagues developed medical castration through use of LHRHa. They showed that the testosterone level was reduced by 75% within 3 weeks (Tolis et al. 1982). Schally also received a Nobel Prize for his research in 1977. Due to the psychological issue and morbidity associated with surgery (sub-capsular orchidectomy) the majority of patients in current practice receive medical castration.

Medical castration, often referred to as androgen-deprivation therapy (ADT), involves blocking either the hypothalamus-pituitary-gonadal axis through the use of either LHRH analogues, such as leuprorelin, or gonadotropin-releasing hormone antagonists, such as Degorelix, or directly targeting the AR with anti-androgens, such as Bicalutamide. Most patients will initially respond to castration, but the majority will gradually develop

resistance typically after a median of 11 months (James et al. 2015). Typically the PSA will rise, indicating that AR activity has been restored and new metastases develop resulting in disease-related symptoms such as bone pain, spinal cord compression or ureteric obstruction. This androgen-independent disease often termed castrate-resistant prostate cancer (CRPC) or hormone-refractory PCa, where the outlook is poor with a median survival of 42 months (James et al. 2015).

When CRPC develops (following failure of first line hormone treatments), traditionally the second line treatment in fit men is Docetaxel-based chemotherapy. Newly released data from the STAMPEDE trial presented at American Society of Clinical Oncology Annual Meeting held in Chicago (31 May 2015) however, has shown that upfront Docetaxel in addition to hormones at the time of diagnosis of metastatic disease had an improved 10-month survival than hormones alone. This evidence has altered metastatic PCa treatment greatly, Docetaxel not only provides a vast survival benefit, but it is also relatively inexpensive (as it is off patent) and reasonably well tolerated. Service provision is the only limiting factor, as oncology units adapt to be able to accommodate the high volumes of men that are eligible for this treatment.

Over the past decades a number of third line treatment options have been developed for men with metastatic PCa. These include newer more specific hormonal agents such as Abiraterone and Enzalutamide, immunotherapies, bisphosphonates and novel targeted therapies. Many of these agents are only available in a trial setting.

Abiraterone works by irreversibly blocking cytochrome P17 (an enzyme involved in the production of testosterone), thereby stopping androgen synthesis in the adrenal glands, prostate tissue and the prostatic tumour. It has a 4.4 months survival benefit when compared to placebo (20.2 versus 15.8 months) in a post-Docetaxel setting (Fizazi et al. 2012). Currently, Abiraterone is only available on the NHS following Docetaxel chemotherapy (TA259 NICE, 2012). It has shown survival benefit pre-Docetaxel, but this has not been recommended by the National Institute of Clinical Excellence (NICE), so it is not currently available in the NHS. Enzalutamide (previously known as MDV 3100) is an anti-androgen with a higher affinity than Bicalutamide for the androgen receptor, which has also demonstrated survival benefit (Scher et al. 2012). Both Abiraterone and Enzalutamide have been added as an additional treatment arm in the STAMPEDE trial.

Since the pioneering work by Huggins and Schally, there was a period of over 20 years where advancements in treatments for metastatic PCa had stalled, with very few new drugs discoveries. Recently, however, there has been a surge in the development of new therapies, some using traditional methods targeting the androgen receptor and testosterone signalling such as Abiraterone and other more novel mechanisms like immunotherapy and alpha emitter Radium-223. Immunotherapies for PCa fall into 5 broad categories: therapeutic vaccines, oncolytic virus therapies, checkpoint inhibitors, adoptive cell therapies and adjuvant immunotherapies. All of which are in phase II or III trials (Cancer Research Institute). Radium-223 selectively targets bone metastases with alpha particles inducing double-stranded DNA breaks. It has been shown to have a modest improvement in survival over placebo in metastatic PCa: 14.9 months versus 11.3 months (Parker et al. 2013). Despite these, on the whole there remains a varied and mainly poor response to treatments in CRPC. This is thought to be due to the diverse genetic make-up displayed by the tumour cells in advanced disease. A better understanding of this concept as the driving force behind cancer evolution and progression should help yield new targeted therapies and prediction factors.

1.4 Prostate cancer biology

Our understanding of cancer has expanded greatly over the past decades and continues to do so. Cancer research has been the foundation of this expansion in knowledge, revealing that cancer is a disease caused by complex dynamic changes in the genome. The discovery of mutations that form oncogenes with dominant gain in function and tumour suppressor genes with recessive loss in function, in different cancers has been instrumental in the development of new genetic markers and treatments.

Cancer is caused by the stepwise accumulation of mutations of oncogenes and tumour-suppressor genes that affect growth, differentiation and survival causing transformation of normal human cells in highly malignant derivatives. This is thought to be an age-dependent process, resulting in four to seven rate-limiting, stochastic events (Renan 1993) resulting in malignancy. Pathological analysis of a number of organ sites has identified intermediate steps where normal cells progress to a pre-malignant state prior to invasive cancer (FOULDS 1954).

Hanahan and Weinberg propose in their sentinel article on ‘The Hallmarks of Cancer’, that tumours can possess six essential alterations in their cell physiology caused by genetic alteration that collectively dictate the malignant phenotype (Hanahan & Weinberg 2000). These cellular processes are self-sufficiency in growth signals (oncogene addiction), insensitivity to growth-inhibitory signals (loss of tumour suppressors), evading programmed cell death (anti-apoptosis), limitless replication potential (aberrant cell cycle), sustained angiogenesis, and invasion/metastasis (Hanahan & Weinberg 2000). Following the remarkable progress in cancer research, in their updated review, Hanahan and Weinberg have added two further ‘hallmarks of cancer’: reprogramming of energy metabolism and evading immune destruction (Hanahan & Weinberg 2011).

1.5 Prostate cancer genetics

Cancer genetics and DNA sequencing has expanded greatly over the past decade, particularly since the completion of the Human Genome Project in 2003. This 13-year venture was accomplished with first-generation sequencing, known as Sanger sequencing. Sanger sequencing also known as dideoxynucleotide sequencing, was first described by Edward Sanger in 1975 (Sanger 1975). Since completion of the human genome project, there has been a drive to devolve a faster and more importantly quicker sequencing method so that this technique could not only be used for research but also for diagnostics. This demand has driven the development of second-generation sequencing methods, or next-generation sequencing (NGS) (Grada & Weinbrecht 2013). Consequently, there has been a marked expansion in our knowledge of the somatic genetic basis of PCa.

Multiple studies have identified recurrent somatic mutations, copy number alterations, and oncogenic structural DNA rearrangements in primary PCa ((Barbieri et al. 2012; Taylor et al. 2010; Berger et al. 2011; Baca et al. 2013; Tomlins et al. 2005). These include TMPRSS2:ERG fusion (discussed in section 1.3.2.2); copy number alterations or loss of PTEN, RB1, MYC, NCOA2, NKX3-1 and CHD1; and point mutations in SPOP, FOXA1 and TP53, among other biological relevant genes. Further studies of metastatic prostate samples demonstrated additional alteration involving the androgen receptor (AR) and AR signalling; BRCA1 and BRCA2 (discussed in section 1.3.2.2); and Wnt signalling such as β -catenin (CTNNB1) and APC (Kumar et al. 2011; Grasso et al. 2012; Rajan et al. 2014; Beltran et al. 2013; Robinson et al. 2015).

These mutations, alone and in combination, cause activation and inhibition of different signalling pathways that promote the cellular processes described by Hanahan and Weinberg. For example, Ras pathway drives uncontrolled proliferation, the retinoblastoma (Rb) pathway alters cell-cycle control and the p53 pathway affects apoptosis (McCormick 1999). Genomic alteration in individual genes are not mutually exclusive implying that combination mutations have additive or synergistic effects, through their action on key signalling pathways that drives tumourigenesis.

Although data regarding mutational events underlying the development and progression of PCa has expanded greatly; few abnormalities in specific genes are highly recurrent, as highlighted by the rate of the 20 most common mutations reported by COSMIC (Catalogue of somatic mutations in cancer from the Sanger institute), a website designed to report somatic mutations reported from robust data sources from PubMed, is shown in Figure 9. Alterations in certain signaling pathways do predominate, however. These alterations include, for example, pathways known to affect tumorigenesis in a wide spectrum of cancers, such as the Pten-PI3-Kinase-AKT-mTOR pathway (discussed in section 1.5.1).

Mounting data suggests that PCa can be subdivided based on a molecular profile of genetic alteration known to affect certain pathways such as PI3-Kinase and Wnt pathway; or genes associated certain cellular mechanism such as DNA repair and cell cycle. Similar subdivision is reported in bladder cancer, where FGFR3 mutations predominate in superficial papillary tumours and p53 and/or Rb pathway alterations predominate in muscle-invasive lesions (Goebell & Knowles 2010). Importantly, these pathway or cellular mechanism can be targeted; with evidence from a multi-institute study (8 clinical sites) in PCa by Robinson et al (2015), concluding that 89% of 150 metastatic castrate resistant PCa harboured a clinical actionable aberration (Robinson et al. 2015). In addition to subdividing or stratifying on signalling pathway or cellular mechanism, a Cambridge group recently reported five distinct subgroups of PCa, termed "iClusters", based on a panel of 100 genes. These molecular profiles were correlated with risk of biochemical relapse following prostatectomy, with the authors concluding that they were able to outperform established clinical predictors of poor prognosis (e.g. PSA, Gleason score) (Ross-Adams et al. 2015).

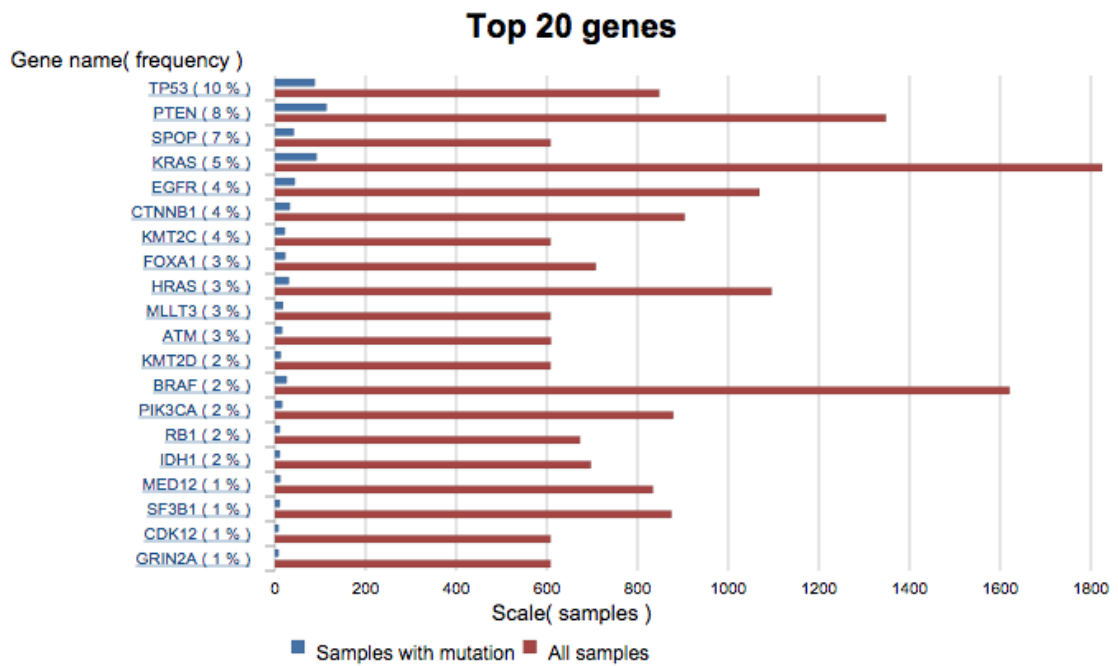


Figure 9: 20 most common somatic mutations in PCa. Data obtained from COSMIC (Catalogue of somatic mutations in cancer) website (www.cancer.sanger.ac.uk).

Although there has been a dramatic improvement in our understanding of genomic profiling in PCa, as yet, no ‘driver’ mutation has been identified or mutation that is effective in a clinical practice setting. The driver mutation is thought to promote and maintain the malignant phenotype even when in an advanced state, and targeting these genes has led to dramatic improvements in therapies in some cancers. For example, targeting EGFR with selective inhibitors in lung adenocarcinoma and targeting BRAF in malignant melanoma has revolutionised treatment (Ladanyi & Pao 2008; Flaherty et al. 2010; Chapman et al. 2011). K-Ras status in metastatic colorectal cancer is also an established predictive marker used in clinical practice to determine efficacy of anti-EGFR therapy. Specifically, patients with K-Ras mutations do not have a response to anti-EGFR therapy (Amado et al. 2008).

1.5.1 PTEN and the PI3-Kinase pathway

1.5.1.1 Structure and function

PTEN (phosphatase and tensin homolog) is a tumour suppressor gene located at the 10q23 locus of chromosome 10. The principal function of PTEN is to dephosphorylate phosphatidylinositol-3,4,5-trisphosphate (PIP3), opposing the action of phosphoinositide 3-kinase (PI3K). PIP3 is a potent activator of 3-phosphoinositide-dependent kinase 1 (PDK1) and AKT. Mutations in the PTEN gene cause its protein to become faulty resulting in loss of function. Consequently, this leads to increased levels of PIP3, PDK1 and AKT at the plasma membrane (Song et al. 2012). AKT is activated at two different phosphorylation sites: Thr308 and Ser473. Thr308 is phosphorylated by PDK1 and Ser473 by mammalian target of rapamycin complex 2 (mTORC2; composed of mTOR, DEP domain-containing mTOR-interacting protein (DEPTOR), mammalian lethal with SEC13 protein 8 (mLST8), stress-activated MAP kinase-interacting protein 1 (mSIN1; also known as MAPKAP1), Pro-rich protein 5 (PRR5; also known as PROTOR) and rapamycin insensitive companion of mTOR (RICTOR)) (Zoncu et al. 2011). Upon activation, AKT drives cell survival, cell proliferation and angiogenesis by further phosphorylating downstream proteins such as glycogen synthase kinase 3 (GSK3), forkhead box O (FOXO) B cell lymphoma 2 (BCL-2) antagonist of cell death (BAD), the E3 ubiquitin-protein ligase MDM2 and p27 (Manning & Cantley 2007). AKT can also directly phosphorylate tuberous sclerosis protein 2 (TSC2), which in a complex with TSC1 inhibits the Ras-related small GTPase Ras homologue enriched in brain (RHEB) (Song et al. 2012). Following phosphorylation of TSC2 by AKT, the TSC1/TSC2 complex is lost resulting in activation of RHEB, which then stimulates activity of mTOR. AKT can also activate mTORC1 (composed of mTOR, DEPTOR, mLST8, PRAS40 and regulatory associated protein of mTOR (RAPTOR)) directly, which further phosphorylates p70 ribosomal protein S6 kinase (S6K or RPS6K) that activates protein translation (Song et al. 2012).

This complex signaling pathway (Figure 10) is often referred to as the PTEN-PI3-Kinase-AKT-mammalian target of rapamycin (mTOR) pathway but will be referred to as PI3K pathway throughout this thesis. The PI3K pathway has a crucial role in cell growth, proliferation and survival (Cantley 2002). Mutations in genes associated with this pathway (most commonly PTEN) results in loss of control of normal cellular functions,

such as cell proliferation, which significantly contribute to the initiation and development of cancers.

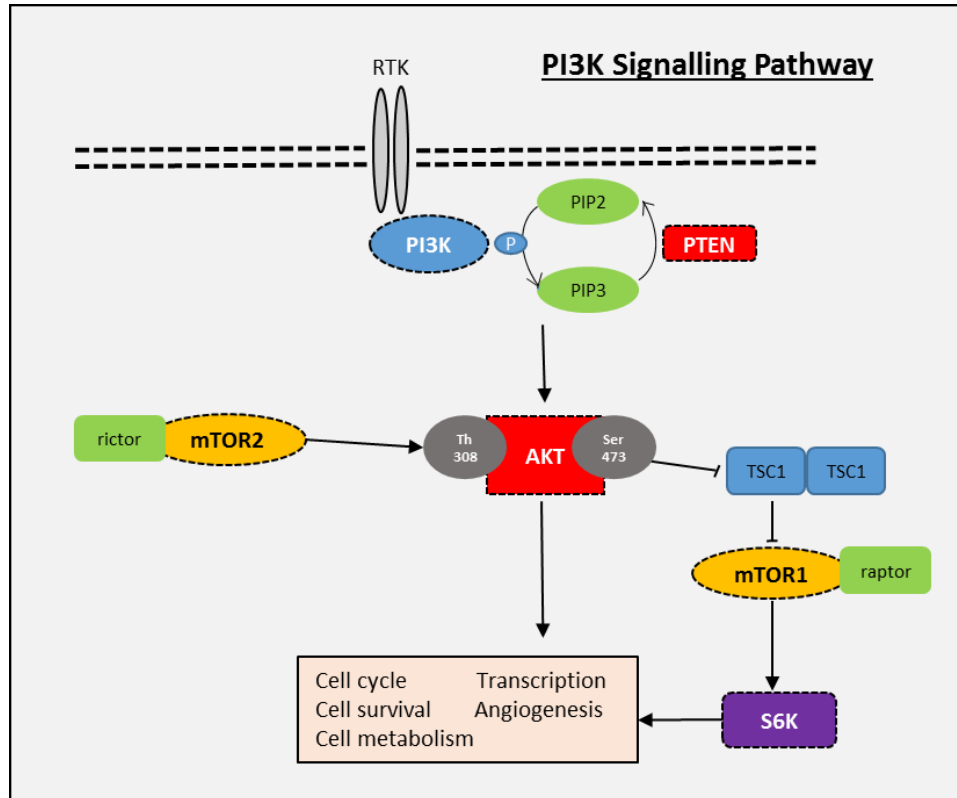


Figure 10: The PTEN-PI3-Kinase-AKT-mTOR pathway.

1.5.1.2 Role in prostate cancer

Although COSMIC only reports a PTEN mutational rate of 8% in PCa, this does not account for copy number alterations (CNAs), so in fact the overall somatic alteration is far greater. CNAs are somatic changes to chromosome structure that result in gain or loss in copies of sections of DNA. They have critical roles in activating oncogenes and in inactivating tumour suppressors (Zack et al. 2013), and are prevalent in many types of cancer (Beroukhim et al. 2010). PTEN commonly has loss of function, sometimes referred to as loss of heterozygosity or homozygosity. PTEN loss varies across studies especially when comparing samples obtained from primary and metastatic disease (Table 5). The reported incidence is approximately 7-18% in primary non-metastatic tumours (Taylor et al. 2010; Barbieri et al. 2012; Baca et al. 2013) and increases significantly to between 40-87% in metastatic samples (Taylor et al. 2010; Robinson et al. 2015; Grasso

et al. 2012; Friedlander et al. 2012). PTEN loss is also recognised to have prognostic significance with respect to earlier biochemical relapse (Barbieri et al. 2012) and PCa-specific death (Reid et al. 2010).

Incidence (mutation and deletion)				
N	Primary %	Metastatic %	Source of tissue	Reference
218*	14	42	Treatment-naïve prostatectomy Metastasis not declared	(Taylor et al. 2010)
189**	-	40	Fresh mCRPC	(Robinson et al. 2015)
61	-	51	Lethal mCRPC from rapid autopsy	(Grasso et al. 2012)
112	7	-	Treatment-naïve prostatectomy	(Barbieri et al. 2012)
57	18	-	Treatment-naïve prostatectomy	(Baca et al. 2013)
15	-	87	Lethal mCRPC from rapid autopsy	(Friedlander et al. 2012)

*181 primary, 37 metastatic. **lymph node=67, bone=76, liver=19, soft tissue 27. mCRPC: metastatic castrate resistant prostate cancer.

Table 5: Incidence of PTEN somatic alteration in primary and metastatic PCa.

The incidence of PI3-Kinase pathway deregulation; encompassing multiple somatic alterations; such as PTEN, PI3-Kinase and AKT, is far greater than when compared to individual mutations alone. For example, Taylor et al (2010) demonstrated up-regulation of the PI3-kinase pathway in 42% of primary tumours a 100% of metastatic tumours suggesting that this pathway plays a key role in the ability of the cancer cell to metastasise. Robinson et al (2015) reports somatic alterations associated with the PI3-Kinase pathway in 49% metastatic castrate resistant PCa affected individuals (Robinson et al. 2015). As previously alluded to, recent research has attempted to classify mutational profiles into signalling or cellular pathways. In doing so, there would be clinically actionable information available; permitting use of novel targeted therapies.

1.5.2 β -catenin and the Wnt pathway

1.5.2.1 Structure and function

β -catenin is a cytoplasmic protein that has two major functions. Firstly it is an essential component of cadherin cell adhesion complexes (Heuberger & Birchmeier 2010). β -catenin binds cadherin and other protein such as α -catenin which is thought to mediate the attachments to F-actin and other actin associated proteins (Huber & Weis 2001). These protein complexes or adherent junctions serve as a bridge connecting the actin cytoskeleton of neighbouring cells through direct interaction. This is important in growth of epithelial cell layers and important in signal transduction. Secondly, β -catenin is one of the key downstream effectors in the Wnt signalling pathway (Harada et al. 1999). The Wnt signalling pathway; often referred to as the canonical pathway (Logan & Nusse 2004), is formed by a series of protein on the cell surface, most importantly β -catenin, which acts as a transcription factor translocating signals into the cell nucleus regulating many genes implicated in cancer.

An overview of the Wnt pathway is shown in Figure 11. In the absence of Wnt (Figure 11A), cytoplasmic β -catenin is degraded by the Axin complex composed of Axin, the tumor suppressor adenomatous polyposis coli gene product (APC), casein kinase 1 (CK1), and glycogen synthase kinase 3 (GSK3). β -catenin is phosphorylated resulting in recognition by β -Trcp, an E3 ubiquitin ligase subunit, causing proteolytic degradation. β -catenin is not able to enter the nucleus to interact with DNA-bound T cell factor/lymphoid enhancer factor (TCF/LEF) family of proteins, and Wnt target genes are thereby suppressed. When the Wnt/ β -catenin pathway is activated (Figure 11 B) the Wnt ligand binds to a seven-pass transmembrane Frizzled (Fz) receptor and its co-receptor, low-density lipoprotein receptor related protein 5 or 6 (LRP5/6). A Wnt-Fz-LRP5/6 complex forms recruiting the scaffolding protein Dishevelled (Dvl) resulting in phosphorylation of LRP5/6 and recruitment of the axin complex to the receptors. This inhibits axin-mediated β -catenin phosphorylation preventing degradation of β -catenin. β -catenin accumulates in the cytoplasm and travels to the nucleus to form complexes with TCF/LEF and activates Wnt target gene expression such as c-MYC and MMP-7 (MacDonald et al. 2009).

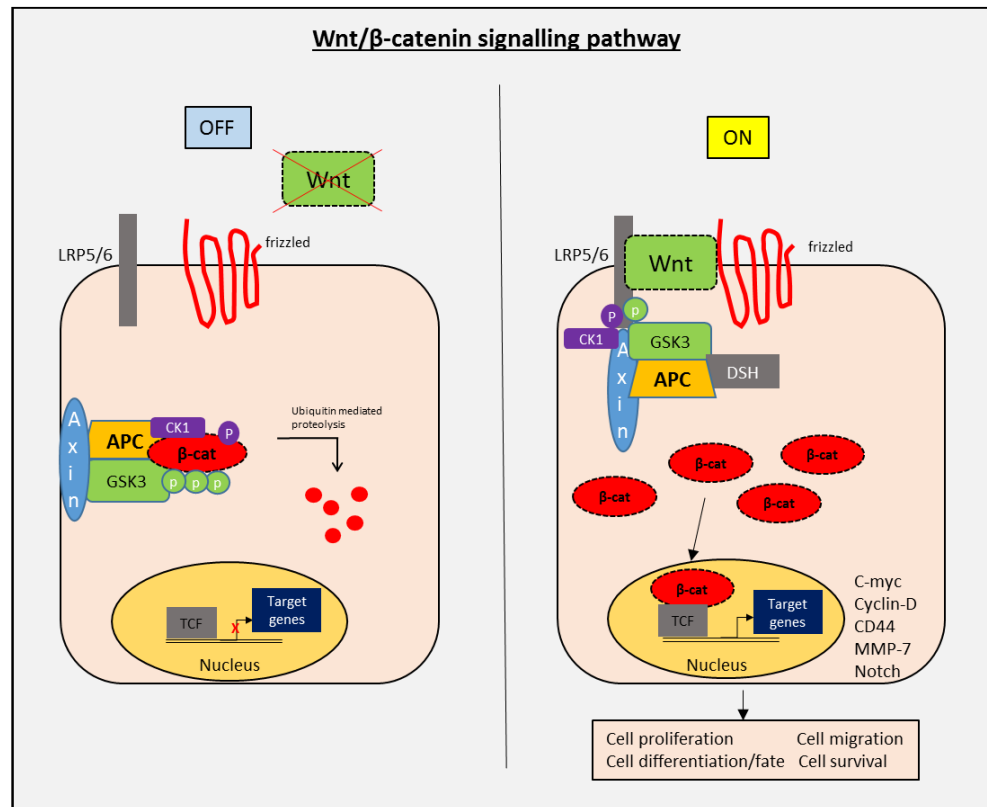


Figure 11: Overview of Wnt/ β-catenin signalling. From (MacDonald et al. 2009).

Wnt signalling has important roles in normal cells such as in the developing embryo and in tissue homeostasis/stem cell regulation in adults. In particular, it regulates proliferation, differentiation and the epithelial-mesenchymal transition (EMT), which is thought to regulate the invasive behaviour of tumour cells (Clevers 2006).

1.5.2.2 Role in prostate cancer

Deregulation of Wnt signalling is implicated in many types of cancers. The best known example is colorectal cancer, where greater than 90% have an activating mutation of the canonical Wnt signalling pathway. Mutations in APC are most common, occurring in 85% of colorectal cancers and are associated with Familial Adenomatous Polyposis (FAP), an inherited autosomal dominant condition leading to the development of multiple adenomas in the colon and rectum (Giles et al. 2003). APC mutations promote aberrant activation of Wnt signalling leading to adenomatous lesions due to increased cell proliferation. Mutations in the proto-oncogene β-catenin are reported in approximately 10% of colorectal carcinomas (Giles et al. 2003).

Genomic alteration of APC and β -catenin in PCa are far less, with reported incidence of 2.8-10.7% and 1.8-6.3% in primary tumours, respectively (Baca et al. 2013; Barbieri et al 2012; Taylor et al. 2010; Beltran et al. 2013). Similar to PTEN, the somatic alteration of APC and β -catenin are greater in metastatic disease, with an incidence of 8.7-19.7% and 4.9-12% respectively (Grasso et al. 2012; Robinson et al. 2015). Multiple other components of the Wnt signaling pathway have also been implicated in the progression of PCa (Grasso et al. 2012; Barbieri 2013) making it an attractive target for therapy. Wnt signaling has been also been implicated in the lethal phase of PCa, castrate resistant PCa (Kumar et al. 2011; Grasso et al. 2012). Mouse models have shown enhanced crosstalk between β -catenin and the androgen receptor (AR) causing resistance to androgen deprivation therapy (G. Wang et al. 2008). An alternative mechanism for androgen-resistance in advanced disease, is the effect β -catenin has on the cancer stem cell population (discussed in 1.7). Work on cell lines using a prostaspheres assay shows that Wnt signalling regulates self-renewal of PCa cancer cells with stem cell characteristics, independently of AR activity (Bisson & Prowse 2009). AR target genes are also elevated independent of androgen ligands following treatment of cells with Wnt3a-conditioned media (Verras et al. 2004). Taken together, this suggests that aberrant activation of Wnt signalling may regulate the prostate CSC population, with its ability to stimulate AR target genes regardless of androgen status. This in principle could explain the phenomenon of castrate resistance in advanced PCa and aid future treatment strategies.

Emerging evidence suggests that APC and β -catenin are mutually exclusive, consistent with the notion that mutations of either gene has more or less the same molecular defect: β -catenin stability and TCF transactivation within the nucleus (Giles et al. 2003). The presence of nuclear β -catenin on immunohistochemistry would therefore be a marker of Wnt activation. This idea is somewhat flawed however, by evidence suggesting no clear consensus on the significance of nuclear β -catenin expression in primary PCa on immunohistochemistry (Kypta & Waxman 2012). The inconsistency of β -catenin immunohistochemical reporting in summarised in table 6.

In summary, evidence from DNA sequencing demonstrates the importance of β -catenin and Wnt signalling in PCa particularly during the later stages of disease. No clear consensus however, explains the prevalence and inconsistency of nuclear localisation of β -catenin in PCa, or its clinical relevance.

N	Expression	Conclusions	Reference
132 (36 localised, 31 locally advanced, 65 metastatic)	Increased	Increased cytoplasmic staining 72% overall and 3% had nuclear staining. Increased expression correlated with: High GS, disease progression and increasing PSA.	(Jung et al. 2013)
225 (145 PCa, 80 BPH, 23 metastatic)	Increased	High staining intensity overall - 18% BPH, 15% GS<7, 22% GS=7, 44% GS>7. Nuclear alone: 37% BPH, 14% GS <7, 9% GS= 7, 5% GS >7.	(Whitaker et al. 2008)
67 (49 localised, 18 metastatic)	Increased	Increased cytoplasmic/nuclear staining in: 52% overall, 43% GS ≤7, 78% GS >7 and 85% metastatic.	(G. Chen et al. 2004)
212 (122 localised, 90 metastatic)	Increased	Increased cytoplasmic and nuclear expression in 29% overall: 21% GS<7, 26% GS 7, 37% GS >7, 38% metastatic.	(la Taille et al. 2003)
101 (73 localised, 25 locally advanced, 3 metastatic)	No change	Membrane staining in 88% and remaining 12% had no staining. No nuclear staining.	(Bismar et al. 2004)
252 (15 metastatic and 5 LNM)	Decreased	Decrease membranous and nuclear expression, but cytoplasmic expression unchanged. Expression significantly lower in metastatic PCa.	(Horvath et al. 2005)
112 (47 localised, 65 had locally advanced)	Decreased	Loss of overall expression in 5% of tumours + more frequent in tumours with GS ≥7	(Kallakury et al. 2001)

Table 6: Studies of β -catenin expression in PCa using immunohistochemistry. BPH – benign prostatic hyperplasia, GS – Gleason score, LNM – lymph node metastasis.

1.5.3 K-Ras and the MAP-Kinase pathway

1.5.3.1 Structure and function

Ras proteins are proto-oncogenes that are frequently mutated in human cancers. They are encoded by three ubiquitously expressed genes: H-Ras, K-Ras and N-Ras (Prior et al. 2012). Following extracellular stimulation, the Ras proteins deliver signals from the cell surface receptor such as growth factor receptors, receptor tyrosine kinases (RTKs) and integrins, into the cytoplasm where it sits at the center of a many-tiered cascade of molecular interactions. Ras proteins act as molecular switches that cycle between 2 conformational states: one when they are bound to GTP, the active or “on” form, and another one when bound to GDP, the inactive or “off” form. Guanine nucleotide exchange factors, or GEFs, promote formation of GTP-bound Ras whereas GTPase-activating proteins, or GAPs, stimulate the hydrolysis of GTP on Ras, returning them to their inactive state (Castellano & Downward 2011).

The active Ras-GTP regulates a complex signaling network that modulates cell behaviour by binding to and activating many distinct classes of effector molecules. Perhaps the best described of these is the Ras-Raf–MEK–ERK signalling pathway (also known as the Mitogen activated protein kinase (MAPK)). There are three Raf serine/threonine kinases (ARAF, BRAF and RAF1) that can activate MEK, which in turn activates ERK by phosphorylation (Figure 12). Ras is also known to interact with PI3K, typically through its p110-binding domain resulting in concurrent activation of the MAPK and PI3K pathway (Castellano & Downward 2011). Mutations in K-Ras favour GTP binding resulting in aberrant K-Ras activation and subsequent MAPK and PI3K pathway deregulation. Consequently, fundamental cellular processes such as growth, proliferation, cell survival and apoptosis are disrupted, permitting tumourigenesis.

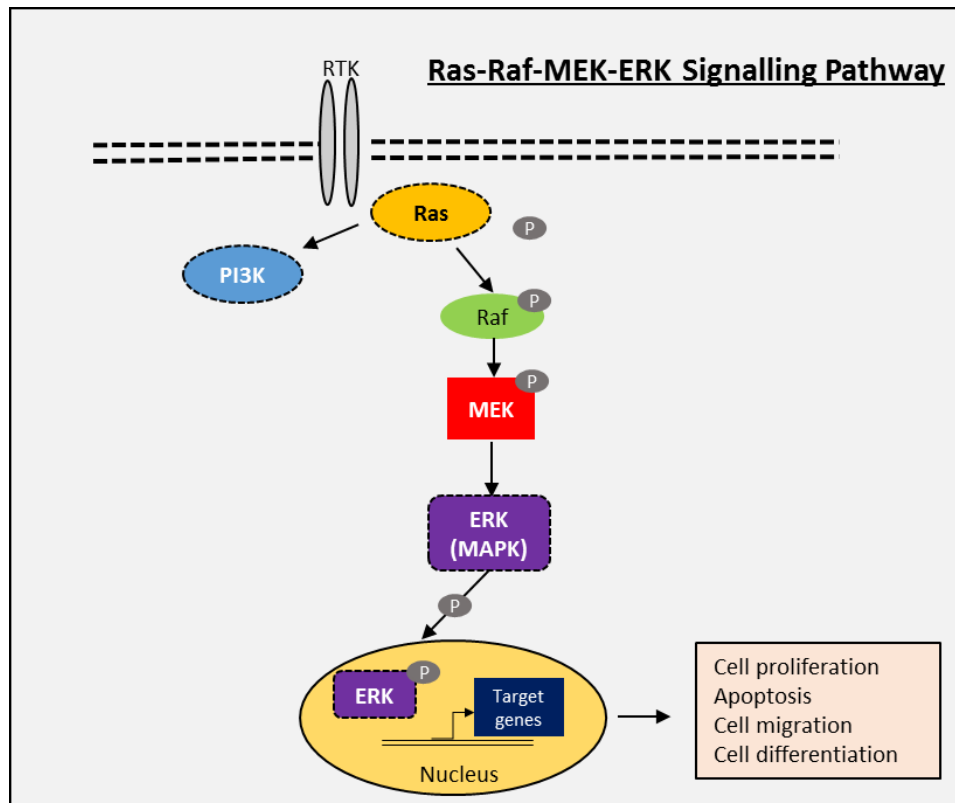


Figure 12: The Ras-Raf-MEK-ERK (MAPK) pathway.

1.5.3.2 Role in prostate cancer

According to the COSMIC dataset, approximately 30% of all human tumours screened are found to carry some mutation in one of the canonical Ras genes. These oncogenic mutations predominantly affect the K-Ras locus, present in 22% of samples analysed compared to 8% for N-Ras and 3% for H-Ras (Prior et al. 2012; Forbes et al. 2015). The incidence of mutations of K-Ras varies considerable between cancer types. An extreme example is found in pancreatic cancer; where the COSMIC dataset reports that 66% of tumours harboured a K-Ras mutation with some individual studies reporting an incidence as high as 90% (Biankin et al. 2012). Other cancers where K-Ras mutations are prevalent include the biliary tract, colon and lung with a reported incidence of 31%, 33% and 17%, respectively (Prior et al. 2012).

Ras mutations in PCa are rare however, with a reported incidence in K-Ras of 3-6% (Grasso et al. 2012; Baca et al. 2013; Taylor et al. 2010; Robinson et al. 2015). Paradoxically, aberrations that result in the upregulation of the MAPK pathway are

among the commonest seen in PCa, with Taylor et al (2010) reporting pathway alteration in 43% of primary tumours and 90% of metastasis. MAPK pathway has not only been implicated in the initial phase of metastasis but also is in the late transition to a castrate resistance state and time to death (Mukherjee et al. 2011). Multiple experiments have been undertaken to better understand how Ras and MAPK signalling grants cells with metastatic potential. Steps in postulated mechanisms include: weakening of cell-cell adhesion by destabilisation of and the nuclear translocation of β -catenin, and the upregulation of extracellular matrix (ECM) proteases (along with the downregulation of protease inhibitors) by Ras effectors to aid penetration of the ECM (Pylayeva-Gupta et al. 2011; Cox & Der 2003).

In PCa, it is unlikely that a solitary Ras mutation is sufficient for the development of metastatic disease; instead it contributes to the overall genetic events crucial to the metastatic phenotype in combination with mutation(s) of other key signalling pathways. Although, Ras mutations are rare in PCa, deregulation of its effectors such as the MAPK signaling pathway is very common. Taken together, the Ras effectors could represent a convergence point for numerous interconnecting cellular pathways and be instrumental in the ability of PCa cells to evade normal controlling mechanism and metastasise.

1.6 Mouse models of prostate cancer

Mouse models have been used over a number of decades to investigate the tumour genetics and complex gene environmental interactions in PCa. Although, mice are not prone to develop spontaneous benign or malignant prostate pathologies, it is possible to genetically manipulate the mouse genome with various technologies in an attempt to mimic PCa in humans. In doing so, the biology of the PCa can be studied in depth in its own microenvironment, one major advantage over using cell lines for example.

To date there are over 100 mouse models of PCa. The next section will thus summarise the important types and methods of mouse models used with particular emphasis on those affecting PI3K, Wnt and MAPK signalling pathways.

Early mouse models adopted constitutive or germline mutations, where the whole genome of the mouse was affected by loss or induced activation of a particular gene of interest. The major limitation precluding the widespread and continued use of this technique is embryonic lethality since many tumour suppressors play important roles in embryogenesis. For example, mice harboring a homozygous deletion of Pten ($Pten^{-/-}$) are incompatible with life, whereas those with heterozygotes ($Pten^{+/-}$) survived up to 1 year and resulted in broad-ranging phenotypes in various tissues including gonads, skin, uterus and endometrium, intestine, thyroid and adrenal glands. In the prostate, $Pten^{+/-}$ mice develop PIN (Podsypanina et al. 1999). Due to embryonic lethality and the varying degree of non-specific pathologies the majority of mouse models used to date are conditional knockouts adopting Cre-LoxP technology.

Cre-LoxP technology allows site or organ specific recombinase used to carry out deletions or insertions of specific genes. The system consists of a single enzyme, Cre recombinase, which causes recombination of a pair of short target sequences called the LoxP sites. The DNA between these LoxP sites is lost following recombination. LoxP-flanked alleles are therefore generated using gene targeting, allowing deletion of genes upon expression of Cre recombination. The most widely used 'prostate-specific' promoter of Cre recombination is the rat probasin (Pb). Several generations of the Pb promoter have been characterised, but the most commonly used is the Pb-Cre4. Pb-Cre4 has successfully facilitated recombination in all lobes of the murine prostate but not in the embryo; >95% of the lateral lobe of the prostate, 50% of the ventral lobe, and

approximately 10% and 5% of the epithelium of the dorsal and anterior lobes, respectively. Although Pb-Cre4 causes recombination in both basal and luminal cells, the luminal cell compartment does predominate (X. Wu et al. 2001). Consequently, many other promoters have been adopted, which have been used in cancer stem cell research to help identify the cell of origin of PCa. These include basal cell type specific promoters such as CK5-CreER (Rock et al. 2009) and p63 (Pignon et al. 2013), and luminal specific promoters such as PSA-CreER (Ratnacaram et al. 2008) or CK8-CreER (Van Keymeulen et al. 2011).

Many genes have been overexpressed or deleted alone and in combination using Cre-lox technology in the mouse. To date however, the only single gene knockout model to have recaptured all stages of PCa; PIN to adenocarcinoma to local invasion to metastatic disease (lung), is the Pb-Cre4 Pten^{fl/fl} mouse model (S. Wang et al. 2003). Pten loss is particularly prevalent in both localised and metastatic human PCa further enhancing the popularity of this model for researchers. A weakness of this model is that not all PCa have a reduction in Pten, and in reality multiple genetic ‘hits’ are required to progress to invasive tumour and metastasis in the human. Also, in humans it is well known that the majority of metastasis occurs in bone (Mundy 2002). Consequently, compound mutational models have been developed attempting to generate multiple ‘hits’ in an attempt to more accurately reflect human disease. For example, Pten^{fl/fl}K-Ras^{+V12} mice dramatically accelerate tumourigenesis when compared to their single mutant counterparts (Mulholland et al. 2012).

To date, few mouse models have incorporated more than two genetic mutations. This is somewhat surprising given that recent DNA sequencing by Robinson et al (2015) reported an average of 4.4 mutations per megabase (Mb); with four cases exhibiting a mutation rate of nearly 50 per Mb (Robinson et al. 2015). Although, studying the interactions between these genes becomes more complicated, this type of mouse model would more realistically reflect the complexity of PCa in the human, particularly in the metastatic setting.

The mouse is the most commonly used animal to model human biology and disease. The mouse offers particular advantages over other species because it is a mammal with similar behaviour and physiology to humans; almost all (99%) mouse genes have homologs in humans, the mouse genome supports targeted mutational manipulation analogous with

those in specific human diseases (Austin et al. 2004). Furthermore, mouse models offer advantage over in vitro studies (e.g. cell lines), in that the disease can be investigated in its own microenvironment including important epithelial-stromal interactions. The main disadvantages of mouse models are they are very expensive, they often do not represent the genetic diversity seen in human cancer and mouse tumours typically grow very fast relative to human tumours. Table 7 summarises the most relevant mouse models of PCa.

Mouse Model	Histology relevant to specific model	Reference
<u>Single genes</u>		
Pten (loss)	PIN, invasive adenocarcinoma, and metastasis	(S. Wang et al. 2003)
APC (loss)	Invasive adenocarcinoma	(Bruxvoort et al. 2007)
β -catenin (activation)	Invasive adenocarcinoma	(Pearson et al. 2009)
K-Ras (activation)	Focal PIN	(Scherl et al. 2004)
<u>Compound Mutations</u>		
Pten/K-Ras	Invasive adenocarcinoma with lung and liver metastasis	(Mulholland et al. 2012)
Pten/ β -catenin	Invasive adenocarcinoma with squamous metaplasia	(Francis et al. 2013)
β -catenin/K-Ras	Invasive adenocarcinoma with squamous metaplasia	(Pearson et al. 2009)
Pten/AKT	AKT loss inhibits development of PCa	(M.-L. Chen et al. 2006)

Table 7: Mouse models of Prostate cancer.

1.7 Tumour heterogeneity and Cancer stem cells (CSC)

Emerging evidence from both solid and haematological tumours (Nik-Zainal et al, 2012; Gerlinger et al, 2012; Anderson et al, 2011) have shown that cancer comprises a collection of related but subtly different clones (i.e. initiated from a single cell) termed intra-clonal heterogeneity. This intra-clonal heterogeneity not only occurs in different individuals tumours (inter-tumour heterogeneity) but also within the same tumour (intra-tumour heterogeneity). This so-called tumour heterogeneity poses an important challenge in order to predict how individual tumours will behave and interact leading to progression or recurrence of disease, and their impact on treatment (Brioli et al. 2014). The emergence of advanced molecular or genetic technologies, such as next-generation sequencing have enhanced our knowledge and began to pave the way for a number of cancers such as breast and brain, allowing their separation in to subtypes with markedly different molecular and clinical qualities (De Sousa E Melo et al. 2013).

PCa demonstrates great heterogeneity, with many patients presenting with different grades of tumour in a multifocal fashion. Indeed the behaviour of these individual tumours can act very differently. Although the higher-grade tumours are thought to be most aggressive with a greater metastatic potential, Haffner et al (2013) showed contrasting results by characterising the lethal clone in a patient who died from PCa. Surprisingly, they revealed that the lethal clone arose from a small, relatively low-grade cancer focus in the primary tumour, and not from the bulk, higher-grade primary cancer or from a lymph node metastasis resected at prostatectomy (Haffner et al. 2013). This data highlights the heterogeneity within PCa and the importance of developing other prognostic markers in PCa, such tumour suppressor genes or signalling pathways such as Pten or PI3-Kinase pathway, in order to augment the pathological evaluation currently available.

Despite advances in DNA sequencing, we are only beginning to understand the complexity of PCa tumours and our limited understanding of the molecular mechanisms (other than the role of testosterone) by which individual cancers are driven, precludes the development of future curative therapies. Recurrence following seemingly successful radical curative treatment such as EBRT for instance, is commonplace in high-risk tumours, often attributed to the presence of tumour heterogeneity. The link between this heterogeneity within a tumour and treatment failure or recurrence is thought to reside on

two conceptual mechanisms. The first theory is often compared to Darwinian classical evolution, stating that all organisms arise and develop through the natural selection of small, inherited variations that increase the individual's ability to compete, survive, and reproduce. In other words, selective pressure acting on tumour cells ultimately lead to genetically distinct, resistant clones (De Sousa E Melo et al. 2013). It is postulated that the primary treatment does not effectively eradicate these clones or as a result of treatment they undergo a process of adaption through inheriting further key mutations, resulting in recurrence or metastasis. The second, and more recent theory, describes a small sub-population of cells within the tumour that largely drives growth and metastasis. This sub-population of cells may possess unique properties, such as quiescence and self-renewal, that make them refractory to standard treatments, for example, those treatments that target actively proliferating cells. These so termed 'cancer stem cells' (CSC) have therefore been proposed to be a cause of resistance to conventional therapies and also to be instrumental in the ability of cancer cells to metastasise. This is particularly true for tumours that are composed of a heterogeneous population of cells such as PCa (Ni et al. 2014; Ni et al. 2012). In this scenario, tumours are perceived to have a hierarchy of cells, with a small population of CSC residing at the top and their more differentiated progeny (transit-amplifying or progenitor cells) below. The CSC is therefore not only thought to be important in recurrence and treatment failure, but also in the initiation of cancers: often referred to as the 'cell of origin' or 'tumour initiating cells'. This latter concept differs from the more traditional stochastic (clonal) model; which proposes that every transformed cell within a tumour has tumourigenic potential, which occurs as a result of extrinsic or intrinsic factors in a random or stochastic fashion (Figure 13). In theory, these two models do not need to be mutually exclusive; tumours that follow the CSC model could also undergo clonal evolution if more than one type of CSC coexists, or if the CSCs adapts under environmental selection or secondary to the changes in the complex microenvironment (Z. A. Wang & Shen 2011).

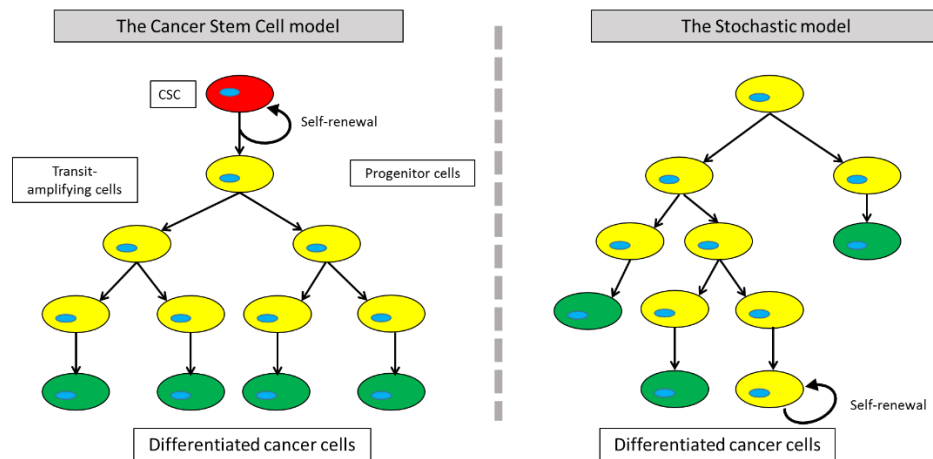


Figure 13: The cancer stem cell (CSC) theory suggests a clear hierarchy of cells within a tumour. The CSC can self-renew and produce more mature cells called transit-amplifying or progenitor cells. These cells can divide a certain number of times into specialised tumour or mature cells. These mature cells do not divide; therefore do not contribute to tumour growth. The stochastic model states that tumour growth is a random process where all cells are equal and can replicate or differentiate into mature cells. Adapted from (Welte et al. 2010).

The CSC concept has created great excitement in the research community over the last decade, being the focus of research in not only PCa but a range of tumour types, including other solid epithelial tumours such as breast (Dontu et al. 2003), colonic (Dalerba et al. 2007), and pancreatic (Li et al. 2007) and their role is well established in haematological cancer (Bonnet & Dick 1997). This promises the development of more effective treatments, aimed not at reducing tumor bulk as most conventional primary treatments do, but rather at targeting the ‘beating heart’ of the tumor, the CSC (Clevers 2011). A combined treatment approach must therefore be adopted targeting both the bulk of the tumour with conventional treatments and the CSC with novel targeting agents.

This area of research faces many challenges however, and many questions remain regarding the origins and markers of these specialised cells. Although some research groups have claimed markers for the CSC in certain tumour types; such as in Lgr5+ cells in the small intestine and colon (Barker et al. 2007), a reliable CSC marker has yet to be discovered in the majority of solid tumours, including PCa.

1.7.1 Technologies in Cancer Stem Cells research

As it is not experimentally feasible to investigate the existence of CSC in human solid tumours, a number of functional assays have been developed to help define the CSC concept. The most frequently used techniques include fluorescence-activated cells sorting (FACS) and xenotransplantation assays. The combined technology of FACS and specific monoclonal antibodies against cell surface antigens can be used to select a population of single cells with CSC properties. Defining these properties traditionally uses two assays, xenotransplantation or ex-vivo 3D organoid culture. In xenotransplantation assays, the CSCs are defined as a subpopulation of cells, usually selected using FACS that can initiate tumour formation when transplanted into immunodeficient (nude) mice (usually in the flank or renal sub-capsule), unlike the remaining tumour cells. This method has proven successful haematological malignancies, such as the CD34⁺CD38⁻ population in acute myeloid leukaemia (Bonnet & Dick 1997). When attempting to translate this early research into solid tumours such as PCa, although many candidate markers have been identified (discussed below), there remains scepticism that the complex endogenous microenvironment of the tumour cannot be modelled by xenotransplantation (Goldstein & Witte 2013). Ex-vivo organoid culture also adopts FACS sorting techniques or mouse models harbouring key mutations in tumourigenesis to isolate single cells that can be grown into a three-dimensional epithelial structure that aims to closely parallel the in vivo phenotype. These cells are grown in a matrix such as matrigel, which can be monitored in real time. The CSC model is assessed by the ability of these selected cells to differentiate into other cell types and/or their ability to serially-passage or self-renew, both key features defining the CSC.

1.7.2 Location and markers of prostate epithelial cancer stem cells

As the CSC may originate from oncogenic alteration of normal stem cells, many studies have focused on the identification of the normal stem cells in order to identify the cell of origin of PCa. The location of the prostate epithelial stem cell; whether basal or luminal has been a focus of great debate in PCa, with evidence supporting both locations.

1.7.2.1 Basal cells as the cell of origin

Although prostate tumours display a strongly luminal phenotype, in response to androgen deprivation, the majority of luminal cells undergo apoptosis (Evans & Chandler 1987), suggesting that the basal cell may be the cell of origin. New-born mice with deletion of the basal marker p63 (p63^{-/-}) do not develop a prostate gland (Signoretti et al. 2000), implying that basal cells are central to prostate development and may include the prostate stem cell. Further research has revealed several candidate basal cell subpopulations of CSCs. For example, Collins and Maitland's group have isolated enriched stem-cell populations using high levels of integrin $\alpha_2\beta_1$ selected from CD44⁺ basal cells ($\alpha_2\beta_1^{\text{hi}}\text{CD44}^+$) (Collins et al. 2001). This selected population accounted for approximately 1% of basal cells from human benign prostate tissue and are distinguished from other basal cells by their ability to generate prostate-like glands in vivo with morphologic and immuno-histochemical evidence of prostate-specific differentiation (Collins et al. 2001). Integrins are transmembrane receptors that are the bridges for cell-cell and cell-extracellular matrix (ECM) interactions. Integrin $\alpha_2\beta_1$ is expressed in both primary and metastatic PCa. It is thought to facilitate bone metastasis through selective adhesions between PCa cells and cells of the bone marrow (Lang et al. 1997). Further enrichment using addition of CD133 ($\alpha_2\beta_1^{\text{hi}}\text{CD133}^+\text{CD44}^+$), of human PCa samples has shown a cell population that is highly proliferative and can reconstitute prostate-like acini in immunocompromised male nude mice (Collins et al. 2005).

Research from the Witte laboratory has isolated prostate stem cells from wild-type mice using mouse Lin⁻Sca-1⁺CD49f^{hi} and mouse Lin⁻Sca-1⁺CD49f^{hi}Trop2^{hi} profiles. These correspond to a predominantly basal population, yet can differentiate into luminal cells both in ex-vivo 3D organoid culture and following xenotransplantation (Lawson et al. 2007; Goldstein et al. 2008). To facilitate tumour progression by recapitulating similar oncogenic signals that occur commonly in human PCa, the same group showed that lentivirus overexpression of ERG1, the fusion partner of TMPRSS2, in mouse Lin⁻Sca-1⁺CD49f^{hi} cells resulted in a PIN phenotype, while co-activation of AKT and AR signalling resulted in an aggressive adenocarcinoma with high expression of vimentin implying the basal/stem cells have progressed into a mesenchymal phenotype (Lawson et al. 2010). Sca-1 (stem cell antigen-1) is only expressed in the mouse; therefore similar studies have been conducted using FACS for cell the surface markers CD49f and Trop2 alone, in human benign prostate tissue. Using these two markers, they were able to

separate the cells into two predominant populations, basal (CD49^{hi}Trop2^{hi}) and luminal (CD49^{hi}Trop2^{lo}). Once again the basal/stem population (CD49^{hi}Trop2^{hi}) is able to regenerate benign prostate tissue following xenotransplantation into immunodeficient mice. Furthermore, following introduction of oncogenic signals using lentivirus induced activated AKT, ERG and AR to mimic human PCa, adenocarcinoma developed from the basal cells subpopulation but not from the luminal cells (Goldstein et al. 2010). Mulholland et al also explored the effect of deregulation of the AKT/PI3-Kinase pathway, through use of the Probasin induced Pten null mouse model. Again adopting the Lin⁻Sca-1⁺CD49^{hi} sub-population, mutant (Pten^{fl/fl}) mice have a greater stem cell population and sphere forming capacity. More importantly the spheres mimic the structural organisation of the epithelial compartment in the Pten null primary tumour. A further interesting finding was that castration both increased the number of stem cells and sphere forming capacity in Pten mutant mice, suggesting a possible role for Pten in castrate resistance (Mulholland et al. 2009). The same authors have since reported that Pten loss and Ras/MAP-Kinase activation cooperates to promote epithelial-to-mesenchymal transition (EMT) with significant expansion of the basal/stem Lin⁻Sca-1⁺CD49^{hi} population, with corresponding enhanced sphere forming capacity compared to single mutants (Mulholland et al. 2012).

Other combinatory antigen markers used to isolate the basal stem population include Epithelial Cell Adhesion Molecule (Epcam) or Trop-1, CD44 and CD49f. Using FACS for these markers, benign prostate cells could be separated into three distinct populations: (i) Epcam⁺CD44⁺CD49^{hi}: a putative prostate stem cell population that does not form spheres, but induces relatively robust tubule populations and induce differentiated ductal/acini structures, (ii) Epcam⁺CD44⁻CD49^{hi} progenitor cells possessing maximal sphere-forming ability and, (iii) Epcam⁺CD44⁻CD49^{lo} terminally differentiated luminal cells that lack both sphere-forming and tissue regeneration potential (Guo et al. 2012). Guo et al (2012) thus conclude that sphere-forming capacity is not necessary predictive of more complex tubule-formation.

1.7.2.2 Luminal cells as the cells of origin

By contrast, clinical observations suggest that luminal cells are the origin of PCa because it is histologically defined by basal cell loss and malignant luminal cell expansion. Although p63^{-/-} new-born mice fail to develop prostates (Signoretti et al. 2000), Kurita et al have shown that xenotransplanted p63^{-/-} embryos grafted into adult male nude mice, have the capability to form prostates in the absence of basal cells (Kurita et al. 2004). To further support the luminal cell as the cell of origin, Shen's group have shown that a rare population of luminal cells: castration-resistant Nkx3.1-expressing cells (CARNs) are bipotential and can self-renew following both xenotransplantation and in functional assays (X. Wang et al. 2009). Using luminal (PSA-CreER and CK8-CreER) and basal specific (CK5-CreER) Cre recombinase mouse models and lineage-marking, the same laboratory were able to track cells as they progress into PIN and adenocarcinoma. Using Nkx3.1^{+/-}Pten^{+/-}, Hi-myc and TRAMP mouse models and concluded that the luminal cells were consistently the favoured cell of origin (Z. A. Wang et al. 2014). Similarly, Korsten et al demonstrated in the Pten knockout mouse model using the PSA-Cre that hyperplastic cells were all luminal in origin (Korsten et al. 2009). Following successful growth of epithelial organoids from the small intestine (Sato et al. 2009), colon (Sato et al. 2011), stomach (Barker et al. 2010) and liver (Huch et al. 2013); Clevers laboratory have recently developed 3D culture conditions that allow long-term expansion of primary mouse and human normal prostate epithelial organoids (Karthaus et al. 2014). They demonstrated that a single liminal or basal cell could give rise to an organoid, yet the luminal-cell-derived organoid more closely resembled a prostate gland. Table 8 summarises commonly used basal and luminal stem cell markers.

Basal stem cell markers	Source of tissue	Research Group
$\alpha 2\beta 1^{hi}CD44^{+} +/- CD133^{+}$	Benign & malignant human tissue	Maitland & Collins
Lin⁻Sca-1⁺CD49f^{hi} +/- Trop2^{hi}	Normal & mutant mice	Witte /Goldstein/Garraway
Sca1⁺CD49f^{hi} Trop2^{hi}		Witte /Goldstein/Garraway
Sca1⁺CD44^{hi} Trop2^{hi}	Benign & malignant human tissue	Witte /Goldstein/Garraway
Epcam⁺CD44⁺CD49f^{hi}	Benign & malignant human tissue	Garraway/Witte
	Malignant human tissue	
Luminal marker	Source of tissue	Research Group
Castration-resistant Nkx3.1-expressing cells	Normal & mutant mice	Shen
CD26⁺	Normal murine & human tissue	Clevers

Table 8: Commonly used luminal and basal prostate stem cell markers.

Thus, there is evidence arguing for both basal and luminal cells as the cell of origin in PCa. Both arguments may well be true: could there be multiple cells of origin? Similar to that seen in breast cancer (Visvader 2009), different cells of origin could give rise to different sub-types of PCa, defined by specific gene expression profiles. Taylor et al. (2010) has helped initiate this idea in PCa, stratifying tumour by genetic profiles according to mutations affecting common signalling pathways, such as PI3-Kinase. Correlation of this type of data with the effects of oncological mutations on specific CSC markers in mouse models may help link the CSC theory and genetic profiles in human PCa. Our understanding of PCa initiation, progression and metastasis will continue to improve following the increased use of molecular profiling, particularly using next-generation sequencing and following further research seeking to identify robust candidate markers for the CSC. Importantly, the cell of origin/CSC and/or its associated molecular profile could have prognostic or treatment implications permitting risk-stratification and future targeted therapies.

1.8 Current research strategies in prostate cancer

Current research strategies or priorities in PCa adopted by different charities and organisations follow similar goals. For example, the British Association of Urological Surgeons prioritise their research into the identification of clinically-relevant PCa, new treatments for CRPC, best-treatment for high-risk PCa and focal therapy: safety, patient selection & “best” technology. The strategies for the research funded by the Prostate Cancer UK charity are similar but less specific: better diagnosis, better treatment and better prevention.

This thesis will frequently relate to these strategies attempting to answer key questions that will add to the plethora of past and current research, as outlined below.

1.9 Hypothesis:

It is important to understand the complex genetic landscape of prostate cancer in order to predict how individual genetic lesions will behave and interact leading to progression or recurrence of disease and their impact on treatment. Wnt, PI3-Kinase and MAP-Kinase signaling pathways are important in many epithelial cancers including prostate cancer. It is thought that these pathways interact, resulting in multiple ‘hits’ as prostate tumourigenesis adapts and progresses to a more aggressive phenotype.

Using pathway or mutational profiles it is hypothesized that patients can be risk-stratified, identifying those with more aggressive disease with a greater risk of recurrence and a reduced survival. In addition, targeted therapies can be developed with the ultimate goal of improving prostate cancer treatment and survival.

A postulated mechanism whereby these pathways may synergise is by altering or expanding the pool of ‘cells of origin’ or cancer stem cells, permitting self-renewal, survival and metastasis of the cancer.

1.10 Aims:

1. To determine the expression profile and any potential cross talk between Wnt, PI3-Kinase and MAP-Kinase pathways in human prostate tumourigenesis and to risk-stratify patients based on these:
 - a. Using a prostate cancer Tissue Micro-array (TMA) obtained from the Welsh Cancer Bank immunohistochemical analysis for markers of each of the pathways will be obtained;
 - b. Pathway expression profiles will be correlated with each other to assess any observational concurrency;
 - c. Immunohistochemical expressional profiles to be correlated with outcome data (tumour characteristics, biochemical recurrence and overall survival);
 - d. Targeted-next generation sequencing to be performed in University College London on the same human prostate samples based on genetic mutations associated with these pathways.

2. To study the interactions and biology of the Wnt, PI3-Kinase and MAP-Kinase signalling pathways using mouse models:
 - a. Using Cre-lox based mouse models to conditionally modify 3 genes associated with these pathways: β -catenin, PTEN, and K-Ras in the prostate;
 - b. To determine the extent of synergy in tumour formation between mutations in each of the pathways by generating and ageing cohorts of each combination of mutations;
 - c. To characterise the histological, expression profiles (using immunohistochemistry) and protein levels (using Western blot) of each of the single, double and triple mutants.

3. To evaluate the effect of Wnt, PI3-Kinase and MAP-Kinase deregulation on the stem cell population.
 - a. Using fluorescence-activated cell sorting (FACS) and a 3D organoid culture assay, mouse tumours driven by single, double and triple mutations will be investigated to determine:
 - i. Stem cell population
 - ii. Organoid forming capacity
 - iii. Self-renewal through serial passage

2 Material and Methods

2.1 Human prostate samples

Human prostate samples were obtained from the Welsh Cancer Bank (WCB, <http://www.walescancerbank.com>) based in the University Hospital of Wales. All ethical and consent issues were encompassed under those held by the WCB.

2.1.1 Tissue Microarrays (TMA)

The TMA was constructed using a semi-automated TMA Master (3DHistech, details at: http://www.3dhistech.com/tma_master) using 1 mm cores. The “recipient” paraffin block was first designed by drilling multiple holes using the TMA master drill, typically at 10 x10, allowing a total of 100 samples per TMA block. The recipient block was constructed to have non-experimental tissue (e.g. colorectal tissue) bordering the array, with a cross of the same non-experimental tissue to orientate the array (Figure 14).

	RWMBV000 0009PN 1A	RWMBV000 1153PT 1A		RT7AU0000 567PT 1A	RVFAR00001 64PT 1A	RWMBV000 0331PT 2A	RWMBV000 0031PN 1A	RWMBV000 1168PT 1A	
	RT7AU0000 602PT 1A	RVFAR00002 94PT 1A		RWMBV000 0465PT 1A	RWMBV000 0085PN 1A	RWMBV000 1375PT 2A	RT7AU0000 610PT 1A	RVFAR00003 25PT 1A	
	RWMBV000 0944PT 1A	RT7AU0000 088PN 1A		RWMBV000 1632PT 1A	RT7AU0000 611PT 1A	RVFAR00003 50PT 1A	RWMBV000 1611PT 1A	RT7AU0000 154PN 1A	
	RWMBV000 1635PT 1A	RWMBV000 0043PT 1A		RVFAR00004 56PT 1A	RT7AU0000 417PT 1A	RT7AU0000 158PN 1A	RT7AU0000 440PT 1A	RWMBV000 0045PT 1A	
	RVFAR00004 68PT 1A	RT7AU0000 461PT 1A		RT7AU0000 045PN 1A	RT7AU0000 524PT 1A	RWMBV000 0096PT 2A	RVFAR00004 69PT 1A	RVFAR00001 58PT 1A	
	RT7AU0000 048PN 1A	RT7AU0000 531PT 1A		RWMBV000 0706PT 1A	RVFAR00004 74PT 1A	RVFAR00002 93PT 1A	RT7AU0000 077PN 1A	RWMBV000 0095PT 1A	
	RWMBV000 0707PT 1A	RVFAR00005 16PT 1A		RVFAR00003 03PT 1A	RWMBV000 0095PN 1A	RWMBV000 0116PT 1A	RWMBV000 0717PT 1A	RVFAR00005 22PT 1A	


 Non-experimental tissue

Figure 14: TMA design: non-experimental tissue around the perimeter of the block to protect the experimental tissue within. In addition, further non-experimental tissue was used to make a cross in order to orientate the block. Each sample was given a unique WCB ID code.

Paraffin blocks of formalin-fixed surgical prostatectomy specimens and needle core-biopsies were obtained from the archives of the WCB. A core tissue biopsy was carefully selected, morphologically representative of areas of the original paraffin blocks ('donor' blocks) by comparing to the area of tumour marked on the original H&E slide.

This was then arrayed into the recipient paraffin block. Once the block was full it was placed in-between two glass slide and placed on a hot plate for 30 seconds to ensure the cores in the recipient block bond to the surrounding wax. The block and glass slides were then incubated at 37°C for 24hrs.

The TMA block was sectioned with 4µm sections on SuperFrost Plus slides for experimental IHC and H&E staining. Each tissue sample was assigned a unique WCB ID number and TMA location number, which have been subsequently linked to a database containing demographic and clinico-pathological data. The Gleason score of each core was quality assured by Dr David Griffiths (Consultant Uro-Histopathologist, University Hospital of Wales), in accordance with 2005 International Society of Urological Pathology (ISUP) Consensus Conference on Gleason Grading of prostate carcinoma (Epstein et al, 2005).

Following H&E or IHC staining each slide was scanned using the Zeiss Axio Scan.Z1 and analysed using the Zen image analysis.

2.1.1.1 Immunohistochemistry (IHC)

IHC was performed using the same methods as that used in the mouse, as described below.

2.1.1.2 TMA scoring

There are several scoring methods used for semi-quantitative evaluation of IHC staining of paraffin embedded tissue. Some of the most widely used are the Quick score, the H score and the Allred score (Detre et al. 1995; Miller et al. 1985; Allred et al. 1998). All methods rely on proportion and intensity of staining. In this study the Quick score was used. The proportion of immune-positive (stained) nuclei within the tissue section is scored in the range 1–6, corresponding to proportions of 0–4%, 5–19%, 20–39%, 40–59%, 60–79%, and 80–100%, respectively. The average intensity of staining is scored in the range 0–3: negative (no staining) = 0, weak = 1, intermediate = 2, and strong staining = 3. An overall score was then calculated multiplying proportion and intensity staining, ranging from 0-18. All samples were evaluated blinded from clinical details. Representative staining was agreed with Dr David Griffiths (Consultant Uro-Histopathologist, University Hospital of Wales).

2.1.2 Targeted Next Generation Sequencing (NGS)

DNA extraction was performed in Velindre Hospital, Cardiff. The FFPE prostate blocks from the TMA were used to extract the DNA using standard extraction kits. A minimum concentration of 50ng extracted with the percentage of tumour noted. Tumour percentage or cellularity was estimated from the original H&E slide with following categories: 0-20% (n=8), 21-40% (n=8), 41-60% (n=35), 61-80% (n=64), and 81-100% (n=73). A low percentage of tumour can increase the false negative mutation rate. All DNA samples were quantified using both NanoDrop (ThermoScientific) and QuBit (ThermoScientific) technology. The ratio of absorbance at 260 nm and 280 nm was used to assess the purity of DNA. A ratio of ~1.8 was accepted as “pure” for DNA.

Targeted NGS was performed in Imperial College London. The Life Technologies Ion Torrent: Ion AmpliSeq Cancer Hotspot Panel v2 and the Ion Personal Genome Machine (PGM) sequencer was used. The hotspot panel covers ~2800 COSMIC mutations of 50 oncogenes and tumour suppressor genes, with wide coverage of K-Ras, BRAF and EGFR (Table 9). The Ion AmpliSeq Cancer Hotspot Panel v2 (CHPv2) brochure is available at <https://tools.thermofisher.com/content/sfs/brochures/Ion-AmpliSeq-Cancer-Hotspot-Panel-Flyer.pdf>.

Ion Ampliseq Cancer Hotspot Panel v2 targets 50 genes				
ABL1	EGFR	GNAS	KRAS	PTPN11
AKT1	ERBB2	GNAQ	MET	RB1
ALK	ERBB4	HNF1A	MLH1	RET
APC	EZH2	HRAS	MPL	SMAD4
ATM	FBXW7	IDH1	NOTCH1	SMARCB1
BRAF	FGFR1	JAK2	NPM1	SMO
CDH1	FGFR2	JAK3	NRAS	SRC
CDKN2A	FGFR3	IDH2	PDGFRA	STK11
CSF1R	FLT3	KDR	PIK3CA	TP53
CTNNB1	GNA11	KIT	PTEN	VHL

Table 9: Ion Ampliseq Cancer Hotspot Panel v2 targets 50 genes.

Following DNA extraction the library is constructed using a library kit. Each individual sample is provided with a bar code and mixed with the primer pool. The individual DNA samples are then amplified using PCR. The samples are then mixed (usually 16) and

placed onto the chip ready for sequencing. Following sequencing the samples are then analysed using life technology software, where filters are applied to remove single nucleotide polymorphism (SNPs), for example.

2.2 Experimental animals

2.2.1 Animal Husbandry

All animal experiments were carried out in accordance with UK Home Office regulations, under valid personal and project licenses. Mice were given access to the Harlan standard diet (Special Diets Service UK, expanded diet) and water.

2.2.2 Breeding

Adult mice of known genotypes were caged in trios consisting of one male and 2 females. Pups were weaned at approximately 4 weeks when independently feeding.

2.2.3 Genetic Mouse Models

Mice bearing a Probasin Cre4 (PB-Cre4) recombinase transgene were crossed with mice bearing one or more loxP targeted alleles, including β -catenin, Pten and K-Ras. The conditional, constitutively active β -catenin mutant strain was created by Makoto M. Taketo (Harada et al. 1999). Mice with the conditional activating mutation of K-ras were derived by Mariano Barbacid (Guerra et al. 2003). Pten was highlighted for LoxP-targeted homozygous deletion (Suzuki et al. 2001). The creation of these transgenic mice is depicted in Figure 15. The PB-Cre4 transgene was incorporated into the cohort using male mice as PBCre⁺ females have been shown to recombine in the ovaries resulting in a mosaic phenotype (Wu et al, 2001).

2.2.4 Polymerase Chain Reaction (PCR) Genotyping

At the time of weaning mice were sexed and separated. Ear clippings were taken for identification and DNA genotyping using a 2mm ear punch (Harvard Apparatus). Matthew Zverev (lab technician) provided assistance in performing routine PCR genotyping of mice. Mice were genotyped at time of weaning and confirmed at death. PCR was also used to assess re-combination of each gene mutation within the prostate tissue. The primer sequences used for genotyping is summarised in Table 10.

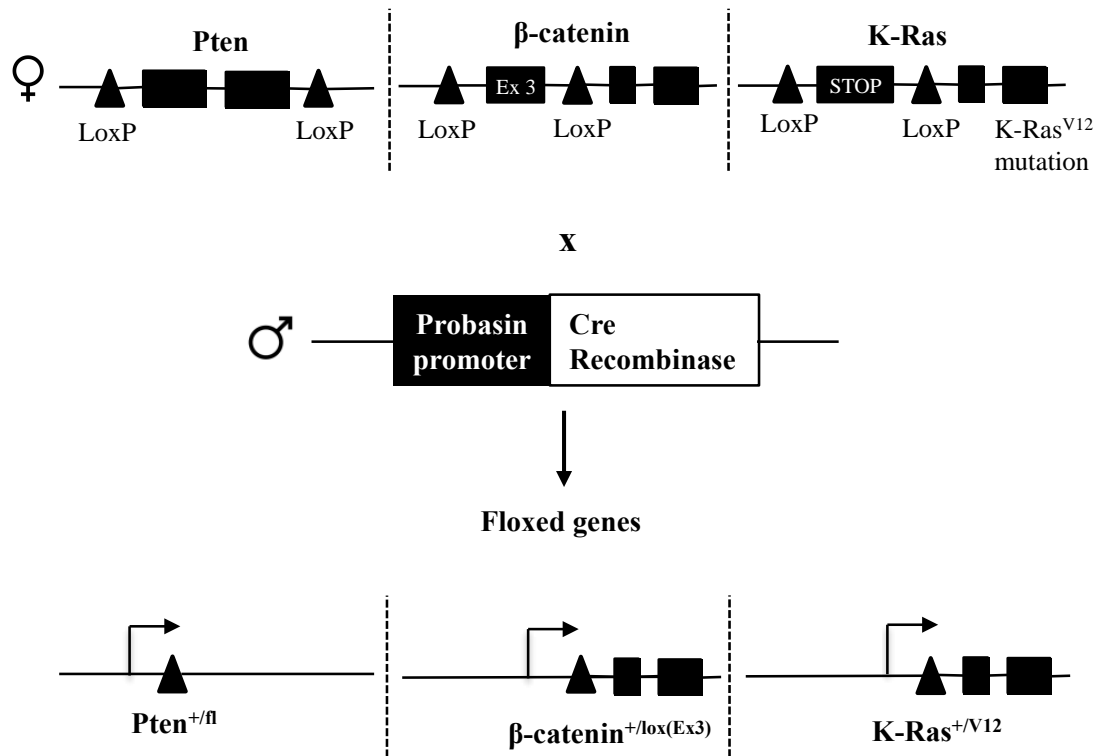


Figure 15: Cre-Lox technology used to generate prostate specific (conditional) gene knockouts. Pten is flanked by LoxP sites. Upon Cre recombination promoted by the prostate specific enzyme Probasin, the LoxP sites are cleaved resulting in Pten gene knockout. Critical phosphorylation sites on exon 3 of β-catenin have been deleted, which in transcription of a mutated form. Similarly the excision of the ‘STOP’ codon upstream of exon 1 results in oncogenic K-Ras (V12).

2.2.4.1 DNA purification (Puregene method)

Ear biopsies were stored at 20°C until the DNA was extracted. Tissue was digested in 250µl lysis buffer (Puregene) containing 5µl of 20mg/ml Proteinase K (Roche), overnight at 37°C with agitation. Protein was precipitated by adding 100µl of protein precipitation solution (Puregene) and mixed by inversion. Protein and any insoluble debris was pelleted by centrifugation at 14000 rpm for 10mins. The supernatant was recovered and mixed with 250µl of isopropanol in a fresh 1.5 ml eppendorf tube and centrifuged at 14000 rpm for 15 min. The supernatant was carefully discarded, and the tubes were left to air-dry for 1 hour. The DNA was then dissolved in 250µl of PCR-grade water (Sigma) and 2.5µl of the resulting solution was used in PCR reactions.

Gene	Primer Sequence (5'-3')	Product size
Cre Specific (general)	TGACCGTACACCAAATTTG ATTGCCCTGTTTCACTATC	1000-bp
ROSA26:LacZ	CTGGCGTTACCCAACCTTAAT ATAACTGCCGTCCTCAAC	500-bp
Pten-loxP (Suzuki et al. 2001)	CTCCTCTACTCCATTCCTCCC ACTCCCACCAATGAACAAAC	Wt = 228-bp Targeted = 335-bp
K-Ras-loxP (Guerra et al. 2003)	AGG GTA GGT GTT GGG ATA GC CTC AGT CAT TTT CAG CAG GC CTG CTC TTT ACT GAA GGC TC	Wt = 403bp Targeted = 621bp
β -catenin-loxP (Harada et al. 1999)	CTGCGTGGACAATGGCTACT TCCATCAGGTCAGCTGTAAAAA	Wt = 324-bp Targeted = 500bp
Recombined Pten	GGC CTA GGA CTC ACT AGA TAG C CTC CCA CCA ATG AAC AAA CAGT GTGAAA GTG CCC CAA CAT AAGG	Targeted: 514bp Recombined: 705bp
Recombined K-Ras	AGG GTA GGT GTT GGG ATA GC CTC AGT CAT TTT CAG CAG GC CTG CTC TTT ACT GAA GGC TC	Wt band: 403bp Targeted stop cassette: 621bp Recombined: 669bp
Recombined β -catenin	GGT AGG AGC TCA GCG CAG AGC ACG TGT GGC AAG TTC CGC GTC ATC C	Wt band: 900bp Recombined: 700bp

Table 10: Primer sequences used for each gene specific and recombined PCR.

2.2.4.2 Generic protocol for PCR genotyping

PCR reactions were carried out in thin-wall 96-well plates or in thin-wall 0.2 ml strip tubes (Greiner Bio-One) and run using either PTC-100 Peltier (MJ Research), Techne Flexigene (Krackeler Scientific) or GS1 (G-Storm) thermal cycler. Pipetting of the reagents and DNA samples was carried out using filtered pipette tips to avoid aerosol contamination. 2.5 μ l of crude genomic DNA extract was loaded into wells using multi-channel pipette. The master-mix containing the remaining components of the reaction; distilled water, GOTaq 5X PCR buffer (Promega), 25 mM Magnesium Chloride (Promega), 25mM dNTPs (Bioline), Primers (Sigma-Genosys) and either GOTaq (Promega) or Dream-Taq (Fermentas) DNA polymerase, was prepared according to table 2.2. 47.5 μ l of the appropriate master-mix were added to each well to make a final volume of 50 μ l. 96-well plates were sealed with aluminium foil tape, while strip-tubes were closed with appropriate caps (Greiner Bio-One). The tubes were gently tapped to dislodge air bubbles and ensure the mixture was at the bottom of the well. The PCR reaction was

then run using a GS4 thermocycler (G storm). The primer sequences used for genotyping of the particular transgenes and the size of respective products are provided in table 10.

2.2.4.3 Visualisation of PCR products

After completion of PCR reactions the products were visualised by agarose gel electrophoresis. 2% agarose gels were made by dissolving agarose (Eurogentech) 2% (w/v) in 1x Tris-Borate-EDTA (TBE) buffer (Sigma) and heated in a microwave until boiling. Once boiled the gel was cooled rapidly under cold running water and 14µl of Safe View (NBS Biologicals) was added per 400ml of gel. Safe view is a nucleic acid stain that binds to DNA and fluoresces under Ultraviolet light allowing visualisation of DNA. The gel was then poured into moulds (Bio-Rad) and combs inserted to create wells. When set the gels were placed in a gel electrophoresis tank and covered with 1 x TBE (Sigma). Safe view was also added to the buffer.

PCR product samples were prepared by adding 5 µl of loading dye (50% glycerol(Sigma), 50% distilled water, 0.1% (w/v) bromophenol blue (Sigma)). PCR samples (20µl) were added to the wells and a molecular marker (e.g. 100bp ladder) was added to one well in order to assess PCR product size. The gel was then run in 1 x TBE (sigma) containing Safe View at 120V for approximately 30mins. Products were visualised in UV light using GelDoc apparatus (BioRad).

2.2.5 Administration of 5'-Bromo-2-deoxyuridine

Where specified, animals were administered 0.25 ml of 10 mg/ml 5'-Bromo-2-deoxyuridine (BrdU, Amersham Biosciences) either 2 or 24 hours prior to dissection in order to label cells in S-phase of the cell cycle. This was administered as a single intraperitoneal injection.

2.2.6 Mouse Tissue Preparation

2.2.6.1 Tissue Dissection, Fixation and Sectioning

Following a schedule 1 approved method of culling, animals were dissected using a micro-dissection kit. The fur was sprayed with 70% (vol/vol) ethanol and an incision made along the mid-line of the abdomen. The urogenital system (bladder, testes, prostate, urethra, ureters and seminal vesicles) were excised and dissected. The mouse urogenital system was further dissected to isolate the prostate using a microscope. Using two fine forceps the anterior lobes of the prostate were separated from the seminal vesicles by dividing any connective tissue. The seminal vesicles including any strands of fat were removed. The bladder was removed by gently placing one pair of forceps near the bladder neck adjacent to the prostate, and pulling the bladder away leaving behind the prostate and the urethra. The two ureters were peeled away with the bladder. The remaining urethra has a deeper red colour and protrudes anteriorly when the prostate is lying flat. This was removed by gently retracting the surrounding prostatic tissue with one pair of forceps and pulling the urethra away from the prostate with the other pair of forceps. The kidneys, spleen, liver, lungs and any lymph nodes were also removed and fixed together.

Once collected, tissue samples were immersed in ice-cold formalin (10% neutral buffered formaldehyde in saline, Sigma) and incubated for 12-24 hours at 4° C. After initial fixation, samples were either processed straight away as described below or transferred into ice cold 70% (vol/vol) ethanol and stored at 4°C until processing.

Tissue samples were arranged in histocassettes and processed using an automatic processor (Leica TP1050). Samples were dehydrated in increasing concentrations of ethanol (70% for 1 hour, 95% for 1 hour, 100% 2 x 1 hour 30 min, 100% for 2 hours), Xylene 2 x 1 hour and paraffin 1 x 1 hour and 2 x 2 hours. After dehydration, samples were embedded in paraffin wax. A microtome (Leica RM2135) was used to cut 5µm thick sections from paraffin blocks. Sections were then floated onto slides coated with poly-L-lysine (PLL) and baked at 58°C for 24 hours.

Paraffin embedding and sectioning was performed by Derek Scarborough and Mark Isaac.

2.2.6.2 Snap freezing tissue

Several sections of normal prostate and prostate tumour tissue (approximately 2 mm × 2 mm) were placed in lockable microtubes and placed in liquid nitrogen and stored at -80°C until required.

2.2.7 Histological analysis of mouse specimens

2.2.7.1 Haematoxylin and Eosin (H&E) staining

In order to visualise tissue sections for histological analysis, tissue sections were stained with Haematoxylin and Eosin (H&E). Haematoxylin stains the cell nuclei blue, whereas Eosin stains protein red. Poly-L-lysine (PLL) sections were de-waxed and rehydrated and were stained by immersing in a bath of Mayer's Haemalum (R. A. Lamb) for 45 seconds. The slides were washed in running tap water for 5 minutes and then placed in a bath of Eosin (R.A. Lamb). The slides were further washed to remove any excess Eosin, prior to being dehydrated and mounted.

2.2.7.2 Pathological analysis

Histological analysis of the prostate gland was performed in accordance with the consensus report from the Bar Harbour meeting of the mouse models of human cancer consortium prostate pathology committee (Shappell et al. 2004). The histological subtypes used, include mouse prostate intraepithelial neoplasia (mPIN), microinvasive adenocarcinoma and invasive adenocarcinoma.

mPIN is the neoplastic proliferation of epithelial cells within preexisting or normal basement membrane confined gland spaces. mPIN presumably shares some of the molecular alterations characteristic of carcinoma; however, the neoplastic cells have not invaded through the basement membrane into surrounding stroma (Shappell et al. 2004).

Microinvasive adenocarcinoma is the earliest recognisable form of invasive carcinoma, with penetration of malignant cells through the basement membrane of PIN-involved glands into the surrounding stroma. It is distinguished from invasive carcinoma by the greater extent of the invasive focus of carcinoma in the latter. Microinvasion is defined by a focus size of less than 1mm (Shappell et al. 2004).

Invasive carcinoma is a malignant epithelial neoplasm that exhibits destructive growth in prostate parenchyma and stroma. In contrast to microinvasion it has a focus size of greater than 1mm and extension into a widened (potentially desmoplastic) stroma or into the loose connective tissue and periprostatic fat surrounding the contractile fibromuscular stroma (Shappell et al. 2004).

To assess the severity or aggressiveness of the tumour histologically, the percentage of invasion was estimated at 100 days and end point (death or 500 days).

Dr David Griffiths (Consultant Histopathologist, University Hospital of Wales, Cardiff) provided assistance with histopathological analysis.

2.2.8 Immunohistochemistry (IHC) of human and mouse specimens

2.2.8.1 De-waxing and Rehydrating PLLs

Formalin-fixed, paraffin-embedded sections were de-waxed by soaking slides in xylene (2 x 5mins). The slides were then rehydrated using decreasing concentrations of ethanol (2 x 2mins cycles of 100%, 95% and 70% ethanol) followed by a wash with dH₂O.

2.2.8.2 Antigen retrieval and blocking endogenous peroxidases

Following de-waxing and rehydration, antigen retrieval was performed. Slides were incubated in 1× citrate buffer (pH 6.0) solution in a pressure cooker and microwaved for 15 min. Antigen retrieval was carried out in order to break cross-linking bonds formed during fixation, and therefore unmasking the antigens. The slides were allowed to cool at room temperature in the citrate buffer solution for 30 minutes. A border was drawn around the prostate tissue with a DAKO pen (hydrophobic barrier pen) and slides were then covered for 20mins with a hydrogen peroxidase blocking solutions (Envision plus Kit, DAKO) to inhibit endogenous peroxidase activity. Slides were washed for 3 x 5mins in 1X TBS/T.

2.2.8.3 Blocking of non-specific antibody binding

Non-specific binding of antibodies was blocked by incubation tissue sections with serum obtained from an animal that is different to the animal in which the primary antibody was raised. For example normal goat serum could be used to block tissue sections that will

be incubated with antibodies raised from a rabbit. The serum was diluted in wash buffer to a concentration that adequately blocks non-specific binding, typically 10-20%.

2.2.8.4 Primary antibody incubation

Following removal of the serum block, the tissue sections were incubated with the primary antibody, without performing any washes. The antibodies and concentrations used are summarised in Table 11. Antibodies were generally incubated overnight in a humidified chamber at 4°C. Slides were then washed for 3 x 5mins in 1X TBS/T.

2.2.8.5 Secondary antibody incubation

For mouse and rabbit primary antibodies, the Envision plus kit (DAKO) anti-mouse and anti-rabbit secondary antibody were used. These pre-diluted secondary antibodies are conjugated to horseradish peroxidase (HRP), which amplifies the signal. For non-mouse or -rabbit primary antibodies, a suitable biotinylated secondary antibody against the host was used. These were used at a concentration of 1/200 (diluted in TBS/T). Tissue sections were incubated with the secondary antibody for 1 hour in a humidified chamber. The slides were then washed for 3 x 5mins in 1X TBS/T.

When biotinylated secondary antibodies were used, a signal amplification step was performed. This involved the formation of a complex between the biotin bound to the secondary antibody and a protein called avidin, which is bound to HRP. The Vectastain Avidin-Biotin Complex (ABC) kit (Vector labs) was used according to manufactures protocols. HRP enzyme was now bound to secondary antibodies that remained bound to primary antibodies, so the antigen could be visualised. Slides were then washed for 3 x 5mins in 1X TBS/T.

2.2.8.6 Detection of signal

Detection and visualization of the antigen was carried out using the 3,3'-diaminobenzidine (DAB) chromagen (DAKO) according to the manufacturer's protocol. DAB is a substrate for HRP, and when catalyzed results in a brown coloured stain.

2.2.8.7 Counterstaining and slide mounting

Slides were then washed for 3 x 5 minutes in dH2O before counterstaining in Meyer's haematoxylin for 30-60secs, rinsing in running tap water for 5 minutes. The slides were

dehydrated in increasing concentrations of alcohol and then cleared in 2 x 5 minutes xylene. Slides were then removed from xylene, mounted in DPX mounting medium (R.A. Lamb) and glass cover slips and left to air-dry in a fume hood.

2.2.8.8 Ki67 and BRDU scoring

Proliferation markers, Ki67 and BRDU were scored by dividing the number of positively stained cells by the total number of cells counted (positive and negatively stained cells). Photographs were taken using the Motic Images Plus 2.0 software at 40x magnification, and a minimum of 5 different field views or 1000 cells were counted. This was performed on n=4 in each mouse cohort.

Antibody	Host	Manufacturer	Dilution
Characterisation markers			
Androgen Receptor	Rabbit	Labvision Neomarkers 1358	1/100
β -actin	Mouse	Sigma A5316	1/5000
BRDU	Mouse	BD Bioscience 347580	1/150
Cleaved Caspase-3	Rabbit	CST 9661	1/200
Keratin 5	Rabbit	Covance PRB-160p	1/2000
Keratin 18	Mouse	Progen 61528	1/50
Ki67	Mouse	Vector Labs VP-K452	1/100
Pan-Cytokeratin	Mouse	CST 4545	1/500
p63	Mouse	Neomarkers MS-1081-P1	1/100
Vimentin	Rabbit	CST 5741	1/100
Signalling pathway markers			
p-AKT 308	Rabbit	CST 50561	1/100
p-AKT 473	Rabbit	CST 3787s	1/100
Pan-AKT	Rabbit	CST 4685s	1/100
β -catenin	Mouse	BD Transduction labs 610154	1/200
CD44	Mouse	Pharmingen 550392	1/50
Cyclin D1	Rabbit	CST 2978s	1/100
MMP-7	Goat	Santa-cruz 12346 G022)	1/100
p-ERK (p44/42)	Rabbit	CST 4376s	1/100
p70 S6K	Rabbit	CST 2708	1/100
P90 RSK	Rabbit	CST 9346p	1/100
p-MEK (Ser221)	Rabbit	CST 2338	1/75
p-MTOR (Ser 2448) XP	Rabbit	CST 5536	1/100
p-S6K (S240/244)	Rabbit	CST 5364s	1/100
Pten	Rabbit	CST 95591	1/100
Stem cell markers			
Trop2	Goat	R&D systems AF1122	1/400
Notch 1	Rabbit	Abcam 8925	1/300
Notch 4	Rabbit	Santa-cruz 5594	1/200
CD49f	Rat	eBioscience, cat. no. 12-0495-83: clone eBioGoH3	1/500

Table 11: Primary antibodies used in IHC and Western blot analysis. CST: Cell Signalling Technology.

2.2.9 Western blot analysis of mouse specimens

Western blot analysis was performed with the help of Boris Shorning (Post-doctoral scientist).

2.2.9.1 Protein extraction

Protein was extracted from prostates of 100-day-old mice from each cohort (n=3). Frozen tissue was removed from storage and placed on ice. 200µl of chilled Radioimmunoprecipitation assay (RIPA) lysis buffer (5ml 1M Tris pH7.4, 10ml 10% Non-idet-p40 (IGEPAL), 3ml 5M Sodium Chloride, 400µl 0.25M EDTA pH8, 250mg C₂₃H₃₉NaO₄ and made up to 100ml with dH₂O) with protease inhibitor (Complete protease cocktail mini tablets (Roche), 1 tablet per 5 ml RIPA buffer). Samples were transferred into Precellys® beaded microtubes and homogenised on the Precellys®24 homogeniser for 2 x 45 seconds and then placed on ice. This was repeated until the sample was completely homogenised. Samples were then centrifuged at 13000 rpm for 10 minutes at 4°C and the supernatant containing the protein was aliquoted into 50µl aliquots and stored at -80°C until use.

2.2.9.2 Protein sample preparation

Samples were defrosted on ice and 30 µg of protein was re-suspended in 25µl of Laemmli buffer (0.125M Tris-HCL pH6.8, 4% w/v Sodium Dodecylsulphate (SDS), 40% v/v Glycerol, 0.1% w/v bromophenol blue, 6% v/v β-mercaptoethanol in ultrapure H₂O (Sigma)). Samples were heated to 95°C for 5 minutes and quenched on ice before loading into gels.

2.2.9.3 Gel formation and protein loading

The Mini-Protean III (Bio-Rad) gel casting apparatus was used to prepare polyacrylamide gels. 5% stacking gels and 10% resolving gels were made (Table 12). The gel casting apparatus was assembled and TEMED was added to the 10% gel solution, which was then mixed and poured between the two glass plates, to 2 cm below the top of the glass plates. Once set (45 mins), TEMED was added to the 5% stacking gel and poured on top of the resolving gel to the edge of the glass plates and well comb was inserted. The gels were placed in the SDS-polyacrylamide gel electrophoresis apparatus with running buffer (Table 12) and 10µl of prepared protein samples were added to individual wells and 5µl

of pre-stained full-range 100bp Rainbow molecular weight ladder (GE Healthcare) was added at one end. The gels were then run at 120-200V until the dye reached the end of the gel.

2.2.9.4 Protein transfer

Following separation of the proteins in the polyacrylamide gel, the gels were removed and placed in transfer buffer (Table 12). Amersham Hybond- ECL nitrocellulose filter (GE Healthcare) was then cut to size and placed on top of the gels before being sandwiched between two sheets of 3MM blotting paper (Whatman) and sponge, each pre-soaked in transfer buffer. The 'sandwich' was then placed into a plastic transfer support and placed in a transfer tank, orientated so that the nitrocellulose filter was between the gel and the positive electrode. This allowed transfer of the negatively charged proteins to the nitrocellulose filter. Transfer buffer was then added to the tank, and it was run at 100V for 1 hour. The filter was then washed 3 x 10 minutes in TBS/T prior to signal detection.

2.2.9.5 Primary and secondary antibody probing

The nitrocellulose filter was blocked for 1 hour in 5% [w/v] skimmed milk powder diluted in TBS/T with agitation. Following 3 x 5 minute washes with TBS/T; the primary antibody was added at a concentration of 1 in 1000 (1 in 5000 for β -actin) diluted in 5% [w/v] skimmed milk powder. This was incubated overnight at 4°C with agitation. The filter was then washed 3x 5 minutes in TBS/T and incubated with HRP-linked secondary antibody (1 in 2000 diluted in 5% [w/v] skimmed milk powder, according to host) for 1 hour at RT with agitation. The filter was washed for 3 x 10 minutes in in TBS/T prior to signal detection.

2.2.9.6 Signal detection

The electrochemiluminescence (ECL) reagent kit (GE Healthcare) was used according to manufacturers instructions for detection of antibody signal. The ECL reagent utilises a chemifluorescent reaction catalysed by HRP to expose X-ray film. The filter was then taken to a dark room under safelight conditions, and X-ray film (Fujifilm Super RX, blue background) was exposed, and the film processed using an automatic processor (Xograph Compact X4 automatic X-ray film processor). The molecular weight ladder was superimposed onto the image in order to confirm the correct protein bands. To confirm

that the loading concentration of each sample was equal, the filters were re-probed with β -actin antibody.

5% Stacking gel (2 Gels)	10% Resolving gel (2 Gels)
6.9ml ddH ₂ O 1.7ml 30% acrylamide (Sigma) 1.3ml 1M Tris-HCl pH 6.8 100 μ l 10% SDS (Sigma) 66 μ l 25% Ammonium Persulphate (Sigma) 13.2 μ l TEMED (Sigma)	6.8ml ddH ₂ O 8.4ml 30% acrylamide (Sigma) 9.4 1M Tris-HCl pH 6.8 250 μ l 10% SDS (Sigma) 72 μ l 25% Ammonium Persulphate (Sigma) 13.2 μ l TEMED (Sigma)
5 x Running Buffer (1L)	1 x Transfer Buffer (1L)
950ml ddH ₂ O 15.1g Tris base (Sigma) 94g Glycine (Sigma) 50ml SDS (Sigma)	800ml ddH ₂ O 200ml Methanol (Fisher) 2.9g Tris base (Sigma) 14.5g Glycine (Sigma)

Table 12: Recipes for polyacrylamide gels and buffers.

2.2.10 Mouse prostate organoid culture

2.2.10.1 Digestion of prostate cells

The prostate gland was harvested as described above using sterile instruments and placed in a 10ml falcon tube containing dissection media (DMEM supplemented with 10% (vol/vol) FBS, 1% (vol/vol) 100x glutamine and 1% (vol/vol) 100x penicillin/streptomycin solution). Ear clipping was sent for confirmation of genotype. The mouse prostate was transferred into a new 10cm petri dish containing fresh dissecting media using sterile conditions within a tissue culture hood. Using a No. 21 sterile scalpel blade the mouse prostate was minced. The minced prostate was placed in a 15ml falcon tube and 10mls of dissecting media containing collagenase solution (1mg/ml) was added ensuring to wash all cells from the petri dish. The prostate tissue was incubated on a shaker at 37°C for 2 hours.

Prostate spheres were cultured as previously described (Lukacs et al. 2010). In summary, following collagenase digestion the tissue was spun down at 1300rpm for 5 minutes at room temperature; the supernatant was discarded before the pellet was re-suspended in 5mls of warm trypsin/0.05% EDTA and incubated at 37°C for 5 minutes. The cell suspension was mixed with 3ml of dissecting media containing 500U (25µl of 10mg/ml) DNase I added to inactivate the trypsin and break up any DNA released from dead cells. The suspension was then *gently* passed through an 18-G needle 5 times. To improve cellular yield the trypsin/EDTA step was repeated. The mixture was then filtered through a 40µm nylon mesh filter and pelleted. The supernatant was removed and the pellet was re-suspended in a known volume of dissection media prior to calculating the viable count and concentration.

2.2.11 Trypan blue cell viability counts

10µl of suspended cells in a known volume of media was mixed with 10µl trypan blue and placed in a 1.5ml Eppendorf tube. 10µl of sample was placed on a Neubauer Counting Chamber and only viable cells excluding the blue dye were counted. The average number of cells per 1mm² was multiplied by 1 x 10⁴ to determine the number of viable cells per ml of suspension.

2.2.11.1 Fluorescence-activated cell sorting (FACS) and analysis

FACS was facilitated and supervised by Mark Bishop, Laboratory manager and FACS lead. The Lin⁻Sca-1⁺CD49f⁺ stem cell enrichment assay was used as previously described (Lawson et al. 2007). Following digestion the single cell suspension was separated into compensation tubes (50,000 cells in 500µl dissection media) where individual antibodies were added at a concentration shown in Table 13. This step allows compensation on the FACS machine prior to sample analysis. The remaining sample was separated into 3 x 10⁶ cells suspended in 1 ml of dissection medial. All antibodies were then added to the samples at the concentrations shown in Table 13. All tubes were wrapped in aluminum foil and placed on a shaker at 4°C for 30 minutes. Media was then aspirated off and the cells re-suspended in 500µl fresh dissecting medium for the compensation tubes and 1ml for the sorting sample. The cells were placed on ice prior to analysis using the BD FACS vantage (BD Biosciences).

FACS Antibody	Concentration
Compensation tubes	
CD31-FITC (eBioscience 11-0311-85)	1µl
CD45-FITC (eBioscience 11-0451-85)	1µl
Ter119-FITC (eBioscience 11-5921-85)	1µl
Sca-1-PE-Cy7 (BioLegend 122514)	1µl
CD49f-PE (eBiocience 12-04595-83)	1µl
DAPI-Violet	1µl
Sample tubes	
CD31-FITC (eBioscience 11-0311-85)	4µl
CD45-FITC (eBioscience 11-0451-85)	4µl
Ter119-FITC (eBioscience 11-5921-85)	4µl
Sca-1-PE-Cy7 (BioLegend 122514)	2µl
CD49f-PE (eBiocience 12-04595-83)	3µl
DAPI-Violet	2µl

Table 13: FACs antibodies and concentrations.

2.2.11.2 Plating prostate cells

Using a 12-well plate, a calculated number of cells were placed into each well. Concentrations of cells were suspended in 20µl of dissection media. Each sample was mixed with 40 µl of cold Matrigel (BD Biociences) and pipetted around the well. The plate was swirled so that the mixture was evenly distributed around the rim. The samples were incubated for 30 minutes at 37°C to allow the Matrigel to solidify. 1ml of Prostate Epithelial Growth Media (PrEGM, Table 14) was added to the centre of each well as not to disturb the matrigel. The cells were incubated at 37° C and 5% CO₂. Half media changes were made every 3 days. A flow-diagram summary of the prostate epithelial culture is illustrated in Figure 16.

PrEGM Growth Media (Lonza Bullet-Kit)	
Serum free basal media	Insulin
Epidermal growth factor	Retinoic acid
Hydrocortisone	Triiodothyrodine
Epinephrine	Antibiotics
Transferin	Bovine pituitary extract

Table 14: Content of the Prostate Epithelial Growth Media (PrEGM) Bullet Kit by Lonza.

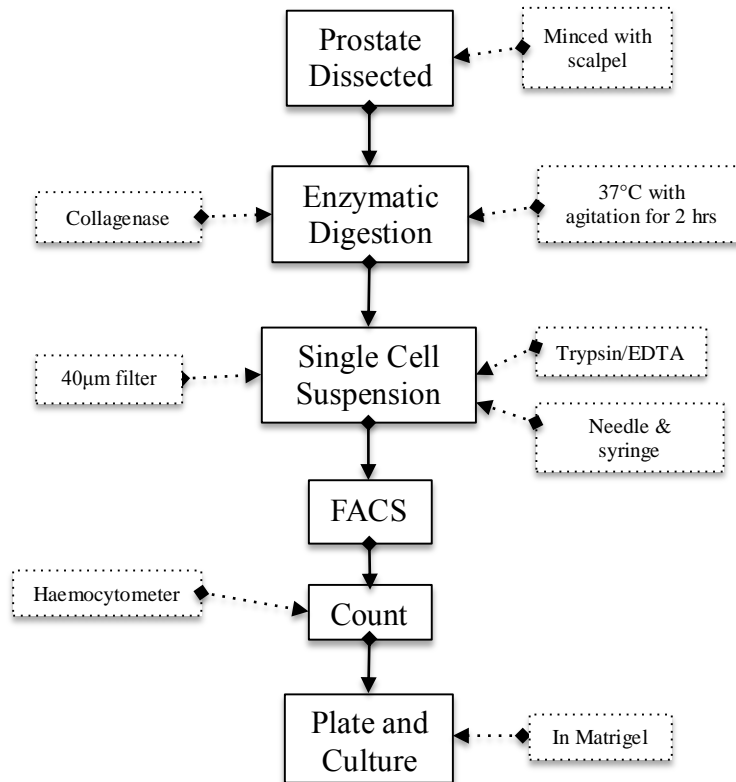


Figure 16: Flow diagram of prostate epithelial culture.

2.2.11.3 Counting Prostate Organoids

The prostate spheres were counted manually on day 7. Spheres $\geq 40\mu\text{m}$ were considered true organoids. Spheres less $\leq 40\mu\text{m}$ at 7 days tended not to formulate any sizeable structure (Mulholland et al. 2009).

2.3 Statistical analysis

Statistical analysis was carried out using SPSS 20 and GraphPad Prism Version 5.0b for both human and mouse data. The distribution of the data was checked visually using frequency distribution graphs (histograms). The Mann-Whitney U test was used to compare data between each test group for non-parametric data and t-test for continuous parametric or normally distributed data. A p value of <0.05 was considered significant.

The overall survival of human prostate samples was defined as that from the date of the operation to the date of death. Cancer specific survival was defined as mortality directly caused by the cancer. The overall survival in the mouse was defined as date of birth to date of death. Kaplan- Meier curves were used to determine the probability survival and the data was analysed using the log-rank test.

Spearman's rank correlation was used to assess correlation between groups of markers and clinical outcome. Principle components analysis (PCA) was used for the human IHC TMA data. This statistical test transforms the data from multiple variables (expression level of each marker in this case) and converts them into a new coordinate system with each coordinate called a principle component. The greatest variance of the data lies on the first coordinate (first principle component) and the second variance on the second coordinate, and so on. This reduces the amount of data so that typical 2 or 3 principle components are used to place the expression profile of each sample in a unique linear space. This attempts to predict areas where certain types or features of tumours may cluster, usually represented by a scatter plot.

3 Assessment of the Wnt, PI3-Kinase (PI3K) and MAP-Kinase (MAPK) cell signalling pathways in human prostate cancer

3.1 Introduction

The natural history of prostate cancer (PCa) is diverse with individual tumours behaving in very different ways. Men with well-differentiated tumours rarely die from their disease with many not requiring any treatment. In contrast, men with non-metastatic but poorly differentiated tumours frequently die within 5 to 10 years of their diagnosis, often despite aggressive intervention (Albertsen et al. 2005; Popiolek et al. 2013). For those presenting with metastatic disease, the outlook is significantly poorer, with a median survival of just 3.5 years (James et al. 2015), with the majority of this time spent in a state of castrate-resistance. This diversity in disease phenotype will be driven by molecular and genetic aberrations and understanding this will permit risk stratification and define future treatment strategies.

The emergence of advanced molecular and genetic technologies, such as next-generation sequencing (NGS) has enhanced our knowledge and began to pave the way for future research and therapies. Multiple studies have identified a vast number of somatic mutations, copy number alterations, and oncogenic structural DNA rearrangements in both primary (Taylor et al. 2010; Berger et al. 2011; Barbieri et al. 2012; Baca et al. 2013; Tomlins et al. 2005) and metastatic PCa (Kumar et al. 2011; Grasso et al. 2012; Rajan et al. 2014; Beltran et al. 2013; Robinson et al. 2015). What is evident from these studies and further highlighted by COSMIC (Catalogue of somatic mutations in cancer from the Sanger institute), is that there are few abnormalities in specific genes that are highly recurrent. Consequently, somatic mutations can be allied into those effecting cell signalling pathways or processes that can be clinically actionable or targeted by emerging therapies. These cell signalling pathways include Wnt, PI3K and MAPK.

Deregulation of Wnt signalling is implicated in many types of cancers. The best known example is colorectal cancer, where greater than 90% have an activating mutation of the canonical Wnt signalling pathway (Giles et al. 2003). The incidence of Wnt signalling

deregulation in PCa is far greater in metastatic disease than when compared to primary disease, with somatic alteration of APC and β -catenin reported between 8.7-19.7% and 4.9-12% in the metastatic setting, respectively (Grasso et al. 2012; Robinson et al. 2015). Wnt signalling has also been implicated in the lethal phase of PCa, castrate resistant prostate cancer (CRPC), independent of androgen signalling (Kumar et al. 2011; Grasso et al. 2012). The incidence of PI3K pathway deregulation, encompassing multiple somatic alterations, such as PTEN, PI3K and AKT, is far greater than when compared to individual mutations alone. For example, Taylor et al (2010) demonstrated up-regulation of the PI3K pathway in 42% of primary tumours and 100% of metastatic tumours suggesting that this pathway plays a key role in the ability of the cancer cell to metastasise. Lastly, aberrations that result in the upregulation of the MAPK pathway are among the commonest seen in PCa, with Taylor et al (2010) reporting pathway alteration in 43% of primary tumours and 90% of metastasis. Furthermore, the MAPK signalling pathway has not only been implicated in the initial phase of metastasis but also is in the late transition to CRPC (Mukherjee et al. 2011).

The available evidence is expanding; correlating dysfunction of the Wnt, PI3K and MAPK pathways with PCa. It is widely accepted that multiple signals or mutations are required for PCa to initiate and progress; however the evidence supporting communication between these signals in human disease is limited. Specifically, there is a lack of data correlating genetic or expressional profiles (such as Wnt, PI3K and MAPK signalling) to outcome data such as recurrence and survival.

3.2 Chapter aims

To determine the expression profile and potential cross talk between the Wnt, PI3K and MAPK cell signalling pathways in human PCa and to risk-stratify patients based on these.

- a. Using a prostate cancer Tissue Micro-array (TMA) obtained from the Welsh Cancer Bank immunohistochemical analysis for markers of each of the pathways will be obtained.
- b. Pathway expression profiles will be correlated with each other to assess any observational concurrency.

- c. Immunohistochemical expressional profiles to be correlated with tumour characteristics and outcome data (biochemical recurrence and overall survival).
- d. Targeted-next generation sequencing to be performed in University College London based on genetic mutations associated with these pathways.

3.3 Results

3.3.1 Tissue-Micro-Array (TMA) analysis

3.3.1.1 TMA samples and characteristics

The Welsh Cancer Bank (WCB) (described in section 2.1.1) constructed the PCa TMA. TMA technology facilitates high-throughput analysis of tissue specimens stained for one or more biological markers (Allred et al., 1998). Figure 17 illustrates an example of one cover-slip slide with the multi-core prostate samples (a) and an individual core (b). There are a number of methods used to score IHC staining of TMA tissue. The most widely used method, as adopted here, is the ‘quickscore’ which is an adaption of the Histo or H-score (Amaral et al. 2013). This uses estimation of intensity and estimation of proportion of staining, with a score between 0 and 18, as described in section 2.1.1.2.

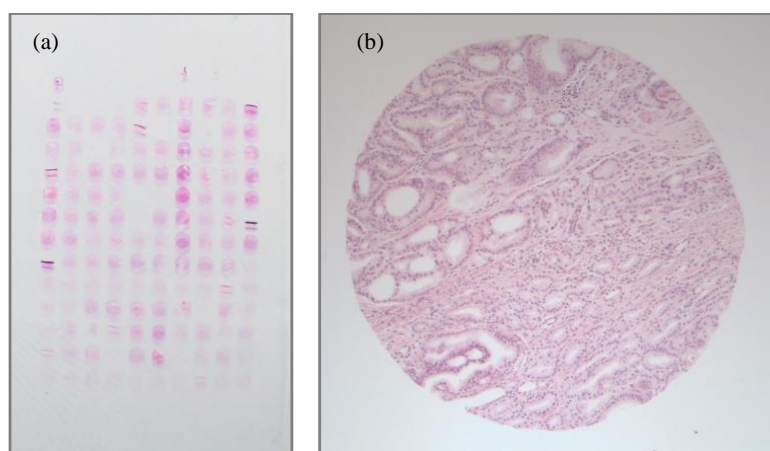


Figure 17. (a) Prostate TMA slide and (b) an individual core.

There were 317 prostate samples from 245 patients. The mean patient age was 65.5 years (range 40-86 years) with a median follow-up of 5.3 years (Range 0.8-9.5 years). 220 samples were obtained from radical prostatectomy samples, 95 from core biopsy samples and 2 from transurethral resection of prostate (TURP) samples.

The median PSA level at diagnosis was 9.1 ng/ml (range 0.5-165 ng/ml). 56.1% had a PSA less than 10 ng/ml, 26.2% had a PSA between 10 and 20 ng/ml and 17.7% had a PSA greater than 20 ng/ml. There were 123 Gleason score (GS) 6 (3+3) samples, 69 GS 7 (47 GS 3+4 and 22 Gleason 4+3), 43 GS 8 (40 GS 4+4 and 3 GS 3+5), 5 GS 9 (4 GS 4+5 and 1 GS 5+4) and 4 GS 10 (5+5). Based on D'Amico Risk Classification but using GS alone, there were 123 low-risk (GS 6), 69 Intermediate risk (GS 7) and 52 high-risk (GS \geq 8) samples. In addition, there were 73 normal samples controls, which were histologically normal prostate tissue adjacent to tumour. In other words these were histological normal prostate samples from a patient with PCa. This may not be a true negative control as there may be a degree of pathway deregulation even in normal tissue in these patients. Unfortunately, the WCB can only store tissue on those patients consented that have cancer. A summary of the patient and demographics and clinicopathological characteristics is shown in Table 15.

At the time of analysis there were 13 deaths, 6 as a result of PCa. 24 patients had biochemical recurrence following surgery. 4 men developed metastasis following surgery with 2 subsequently dying from their disease.

TMA Characteristic	Number
Number of samples	317
Number of patients	245
Mean Age (range)	65.5 years (40-86)
Normal	73
Cancer	244
Low-risk (GS 6)	123 (50.4%)
Intermediate Risk (GS 7)	69 (28.3%)
High Risk (GS \geq 8)	52 (21.3%)
PSA <10 ng/ml (%)	136 (56.1%)
PSA 10-20 ng/ml (%)	65 (26.2%)
PSA >20 ng/ml (%)	43 (17.7%)

Table 15. TMA demographics and clinicopathological characteristics.

3.3.1.2 Association of Wnt pathway markers with pathological characteristics and clinical outcomes

To characterise the Wnt signalling pathway in PCa, the following markers were used using IHC: total β -catenin levels and the Wnt target genes matrix metalloproteinase-7 (MMP-7), Cyclin D1, C-myc and CD44. Figure 18 illustrates representative intensity staining of β -catenin and MMP-7. β -catenin stains the membrane of wildtype cells, which is considered normal. Aberrant β -catenin and thus Wnt signalling is evident on nuclear and cytoplasmic staining for β -catenin. Although nuclear staining is most suggestive of β -catenin activation, the presence of cytoplasmic staining is thought to occur as the abnormal β -catenin signals leave or enter the nucleus. The location of β -catenin staining, whether nuclear or cytoplasmic, is often influenced by the method and durations of formalin fixation. MMP-7 positivity is also apparent in the cytoplasm and nucleus of the cell.

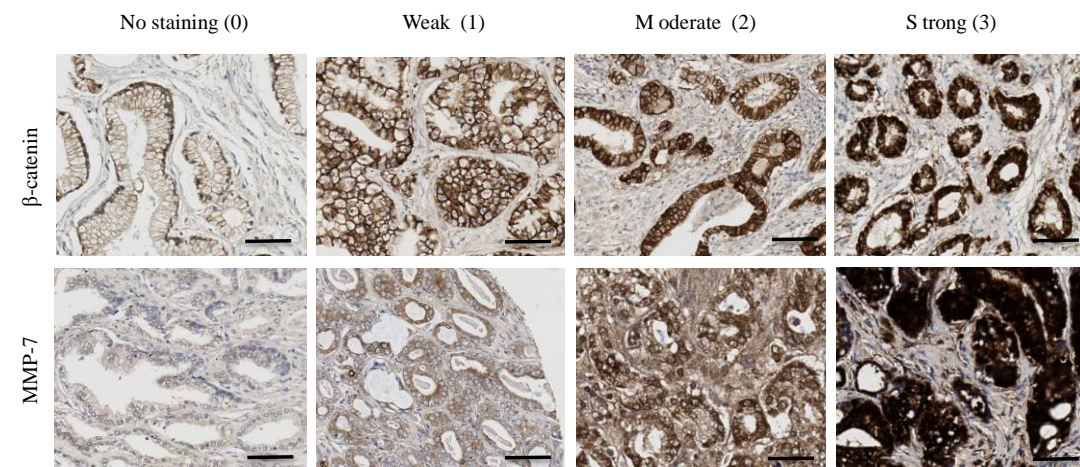


Figure 18: Examples of representative immunohistochemistry staining for Wnt pathway markers: β -catenin and MMP-7. Error bars = 100 μ m. Intensity scoring: No staining = 0, Weak = 1, Moderate = 2, Strong = 3. Proportion was also calculated formulating an overall quickscore (described in main text and methods section). MMP-7 = matrix metalloproteinase-7.

The protein expression (mean quickscore) of β -catenin, MMP-7, Cyclin D1 and C-myc was increased by between 1.5 and 4.4 fold (Table 16) in malignant samples compared to benign prostate tissue ($p < 0.0001$). The greatest increase was in the expression of C-myc (4.4-fold increase in mean quickscore, $p < 0.0001$, Table 16), a key target of β -catenin transcription. There was only a mild increase in membranous CD44 staining (1.1 fold) in malignant samples, which was not statistically significant ($p = 0.420$). Figure 19 further illustrates these findings.

Marker	Benign vs malignant	P-value	Mean Quickscore (95% CI)	Fold increase
β-catenin	Benign	$p < 0.0001$	6.4 (5.4-7.5)	1.5
	Malignant		9.8 (9.1-10.5)	
MMP-7	Benign	$p < 0.0001$	3.0 (1.8-4.2)	2.9
	Malignant		8.6 (7.7-9.4)	
Cyclin D1	Benign	$p < 0.0001$	0.9 (0.4-1.4)	2.3
	Malignant		2.1 (1.7-2.5)	
C-myc	Benign	$p < 0.0001$	0.5 (0.2-0.8)	4.4
	Malignant		2.2 (1.8-2.7)	
CD44	Benign	$p = 0.420$	6.1 (5.0-7.3)	1.1
	Malignant		6.8 (6.2-7.5)	

Table 16: Summary of Wnt markers expression (mean quickscore) between benign and malignant prostate samples. MMP-7 = matrix metalloproteinase-7.

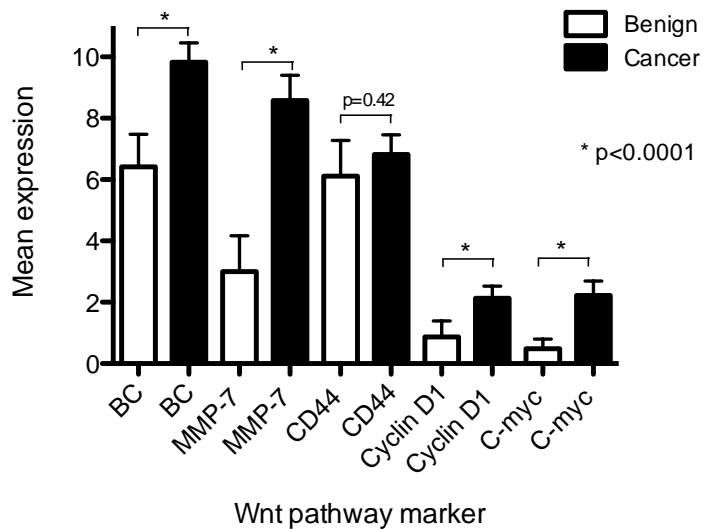


Figure 19: Summary of Wnt pathway marker expression (mean quickscore) between benign and cancer prostate samples. Error bars = 95% CI. There is a significantly greater expression of all markers, other than CD44, in prostate cancer samples when comparing to benign samples. BC = β -catenin, MMP-7 = matrix metalloproteinase-7.

The expression profiles were further correlated with the GS of the sample on the TMA. This confirmed a generalised trend of increasing Wnt marker expression with increasing GS (Figure 20). As previously demonstrated (Table 16 & Figure 19), there was a significant increase in expression of all markers, other than CD44, in malignant tissue samples when compared to benign samples. This was also apparent when comparing benign samples to low risk samples (D'Amico 1, GS 6). On further examination of the data, there was a significant increase in expression between low-risk and high-risk samples (D'Amico 3, GS ≥ 8) for β -catenin, MMP-7, and Cyclin D1 ($p < 0.01$). This was also observed when comparing expression of β -catenin for low-risk with intermediate risk samples (D'Amico 2, GS 7) ($p < 0.01$). Comparison of expression levels of markers with all other combinations (e.g. comparing intermediate- and high-risk samples) demonstrated no significant difference. Finally, there was no significant difference in CD44 expression when compared between all GS of disease.

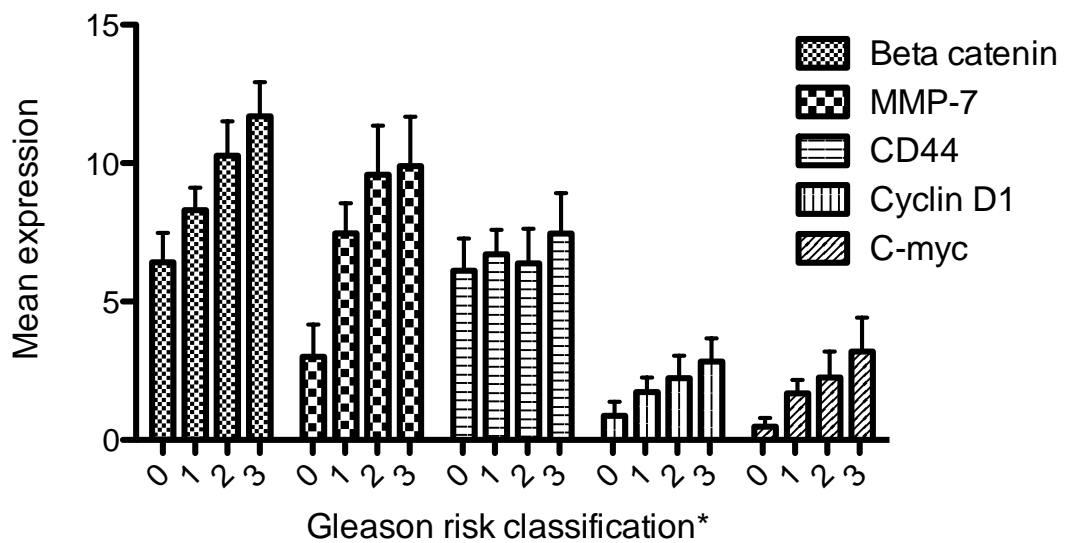


Figure 20: Summary of Wnt marker expression (mean quickscore) categorised according to Gleason score (GS) risk classification as defined by D’Amico (*0 = normal, 1 = low-risk (GS=6), 2 = intermediate-risk (GS=7), 3 = high-risk (GS≥8)). There is a general trend for all Wnt markers, with increasing expression with increasing GS. Error bars = 95% CI. MMP-7 = matrix metalloproteinase-7.

Although overall and cancer-specific outcome would have been the best clinical outcome to measure against, there were only 13 deaths in total and 6 from PCa in this cohort, therefore no robust conclusions could be made using these. Alternatively, biochemical-free survival using PSA was used. This surrogate was only used for samples from radical prostatectomy specimens and defined as a PSA rise of greater than 0.2ng/ml following surgery. Of the 220 samples from prostatectomy specimens, 160 demonstrated cancer and 60 was adjacent normal tissue. Only the cancer samples were used for biochemical-free survival analysis.

The threshold used to determine abnormal from normal expression of a marker is often difficult to define. This is particularly difficult when trying to correlate to biochemical recurrence. One method is to use a specific quickscore value; an alternative is to define a value based on the clinical outcome. This can be obtained by using a Receiver-operator characteristic (ROC) curve. This assesses the accuracy of a test typically used for defining threshold laboratory values for diagnostic tests. The accuracy of the test depends on how well the test separates the groups into those with and without the disease in question (i.e. biochemical relapse), based on sensitivity and specificity. Sensitivity is the

ability of a test to correctly identify those with the disease (true positive rate), whereas specificity is the ability of the test to correctly identify those without the disease (true negative rate). ROC curves are often used to assess the accuracy and reliability of biomarkers.

Figure 21 illustrates a ROC curve of all Wnt markers. The area under the curve is calculated. An area of 1 is a perfect test and an area of 0.5 represents a worthless test. A rough guide used is 0.9-1.0 = excellent, 0.8-0.9 = good, 0.7-0.8 = fair, 0.6-0.7 = poor, 0.5-0.6 fail. The dotted black line in figure 21 represents an excellent test with the solid reference line representing 0.5. This demonstrates that MMP-7 is a fair test and C-myc a poor test with an area under the curve of 0.721 and 0.623, respectively. All other markers were a fail. When comparing the areas under the curve to the reference line (0.5) there was a significant difference for both MMP-7 ($p < 0.001$) and C-myc ($p = 0.044$).

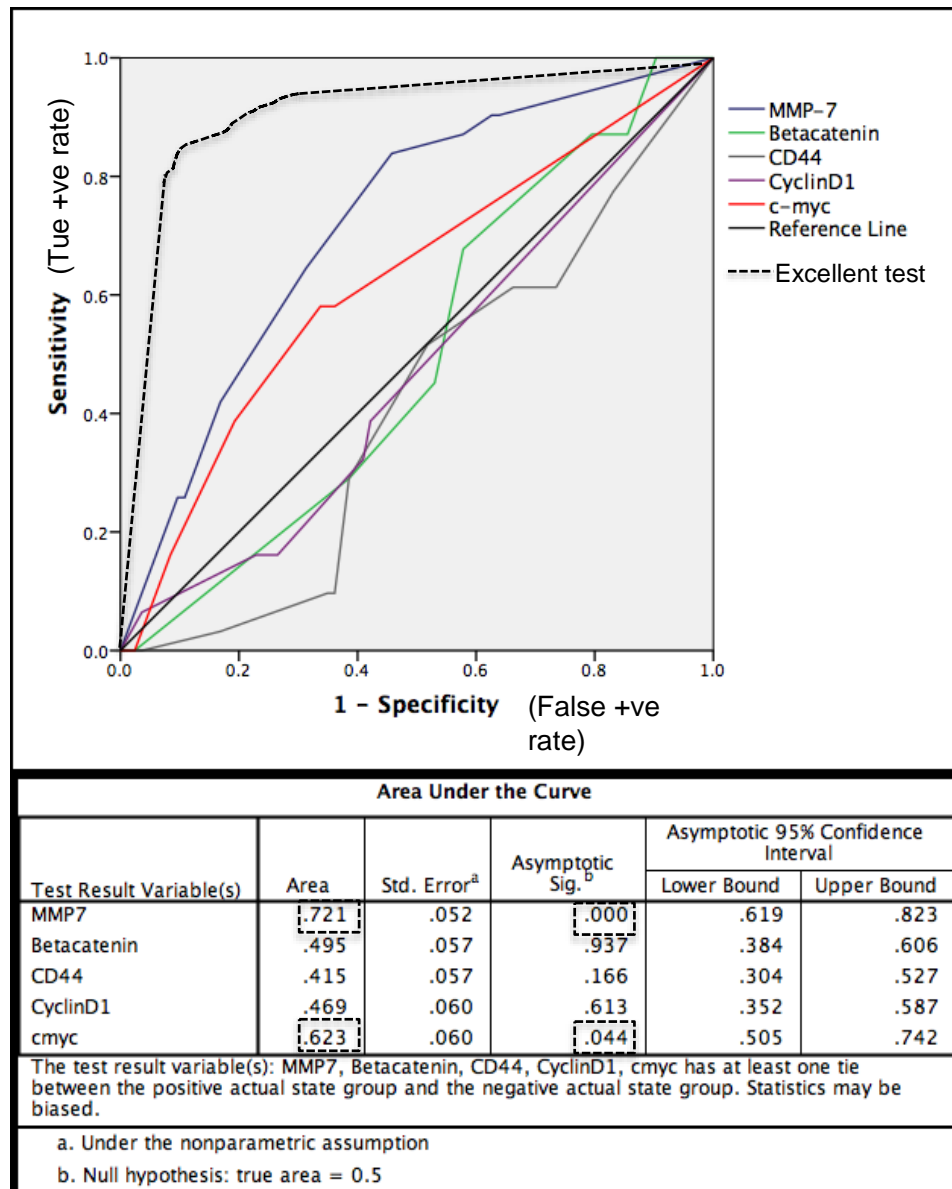


Figure 21: ROC curve of Wnt markers. The reference line represents an area under the curve of 0.5, whereas the broken black line represents a value closer to 1.0, and deemed an excellent test. MMP-7 and C-myc have values greater than 0.5 and represent a fair (0.721) and poor (0.623) test, respectively. Comparison of these curves and the reference curves is significant for both MMP-7 and C-myc, $p < 0.001$ and $p = 0.044$ respectively. MMP-7 = matrix metalloproteinase-7.

Using the ROC curve for MMP-7, a value can be obtained for abnormal expression. The aim is to pick a value, which yields the highest sum of sensitivity and specificity. Figure 22 demonstrates that a threshold value of 5.5 offers a sensitivity of 71.9% and a specificity of 53.7% ($1 - 0.463$). If a greater value is used; although the specificity will increase the sensitivity will fall. Using a value of 5.5, with all samples with a quickscore of 6 or more defined as abnormal MMP-7 expression, there is a significant difference in predicting time to biochemical relapse (Figure 22, $p < 0.05$).

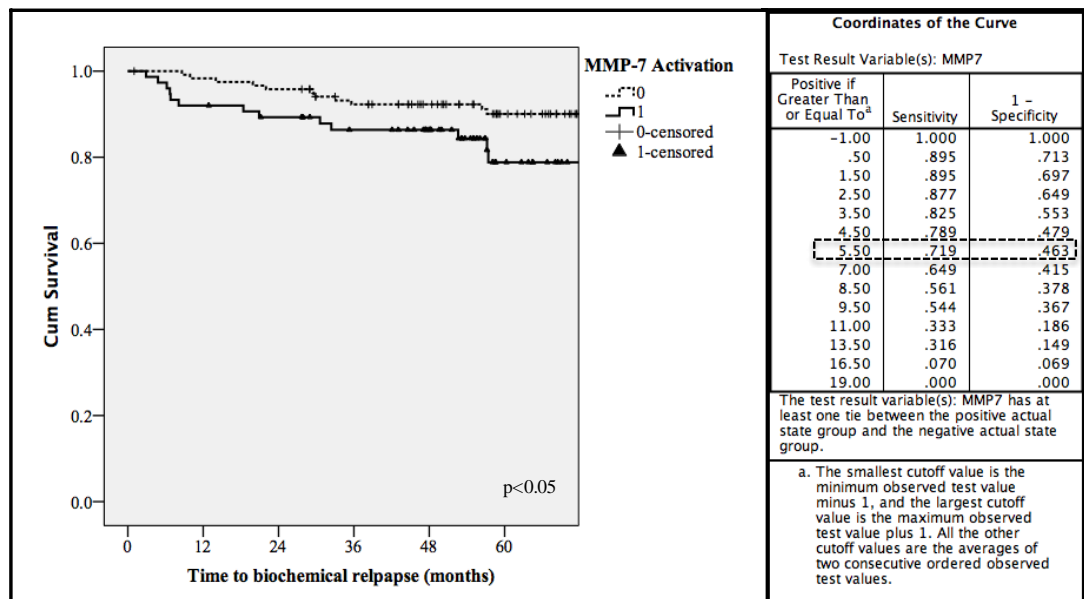


Figure 22: Kaplan-Meier curve of time to biochemical relapse as a function of MMP-7 expression using ROC curve calculated threshold values. A quickscore above 5.5 (i.e. ≥ 6) represents MMP-7 activation and less than 5.5 (i.e. ≤ 5) represents no activation. Log rank $p < 0.05$. $N=24$.

An alternative method of separating the data into normal and abnormal is using the quickscore values. A value of 0 = no staining, 1-6 = mild staining, 7-12 = moderate staining, 13-18 = strong staining. No and mild staining can then be compared to moderate and strong staining using a Kaplan-Meier curve and log-rank analysis (Figure 23). This confirms a greater incidence of biochemical recurrence when there is a moderate/strong expression of MMP-7, based on the quickscore. In this instance, this method confirms a similar finding to that obtained using the ROC curve calculations. However, when the quickscore expression levels are low, as for Cyclin D1 and C-myc (mean values in malignancy of 2.1 and 2.2, respectively), this method may not be suitable and lower values for abnormal expression are required in order to depict trends.

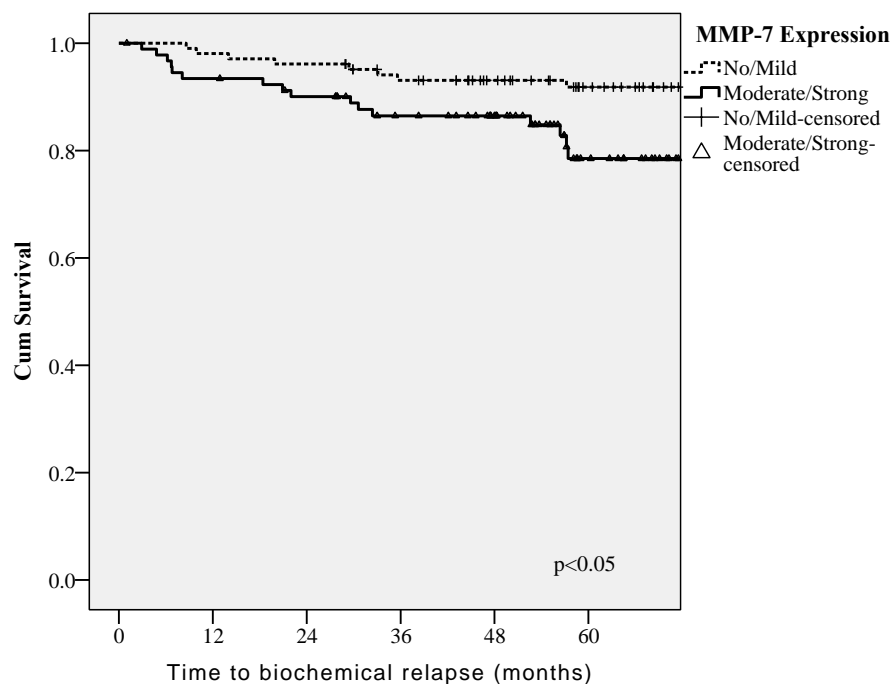


Figure 23: Kaplan-Meier curve of time to biochemical relapse as a function of MMP-7 expression using degree of staining using quickscore values. No/mild staining = 0-6, moderate/strong = 7-18. Log rank $p < 0.05$. $N = 24$. MMP-7 = matrix metalloproteinase-7.

One of the best prognostic markers for biochemical recurrence and subsequent survival is the GS. When the times to biochemical relapse following radical prostatectomy are plotted using a Kaplan-Meier curve as a function of GS (Figure 24), clear patterns emerge; the higher the GS the greater the rate of biochemical relapse. So, could MMP-7 expression, for example, be a marker of Gleason score as oppose to a true independent marker for biochemical relapse? To attempt to answer this question, the data for each cohort of GS (based on D'Amico: low-, intermediate- and high-risk) were investigated separately.

Of the 24 patients who had biochemical relapse following surgery; 1 had low-risk Gleason score based on D'Amico, 4 had intermediate-risk and 19 had high-risk disease. Consequently, very few conclusions could be drawn from the low- and intermediate-risk groups. Sub-group analysis of the high-risk prostate samples demonstrated no correlation with activation or abnormal MMP-7 signalling and time to biochemical relapse (Figure 25, $p=0.22$, log-rank).

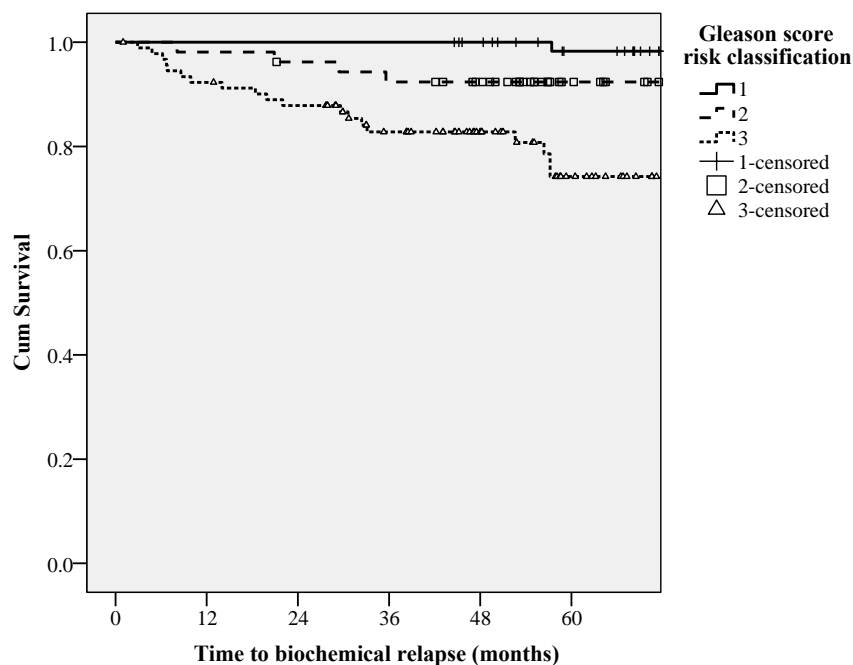


Figure 24: Kaplan-Meier curve of time to biochemical relapse as function of Gleason score (GS) based on D'Amico risk classification. 1 = low-risk (GS 6), 2 = intermediate-risk (GS 7), 3 =high-risk (GS \geq 8). High-risk disease has a greater risk of biochemical relapse following surgery. N=24.

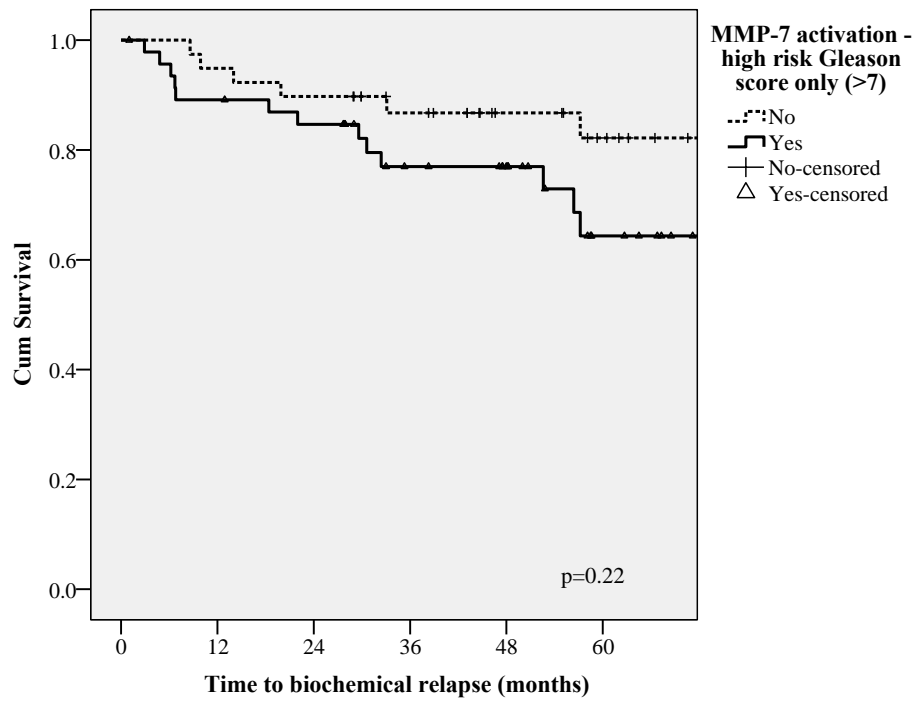


Figure 25: Kaplan-Meier curve of MMP-7 expression for high-risk prostate samples ($GS \geq 8$) demonstrating no significant difference in rate of biochemical relapse. Log rank $p=0.22$. $N=19$. MMP-7 = matrix metalloproteinase-7.

3.3.1.3 Association of PI3K pathway markers with pathological characteristics and clinical outcomes

To characterise the PI3K pathway the following markers were used using immunohistochemistry: PTEN, p-AKT, p-MTOR and p-S6. Figure 26 illustrates examples of representative intensity staining for p-AKT and p-S6. Although, each marker stains at a different intensity, they both demonstrate predominately cytoplasmic with occasional nuclear positive staining. Staining can be homogenous with staining throughout individual glands and tumours, but also more heterogeneous with focal positivity within single glands (Figure 26). p-MTOR also exhibits cytoplasmic positivity with occasional nuclear staining. For PTEN, a loss of cytoplasmic and/or nuclear staining suggested abnormal expression (data not shown).

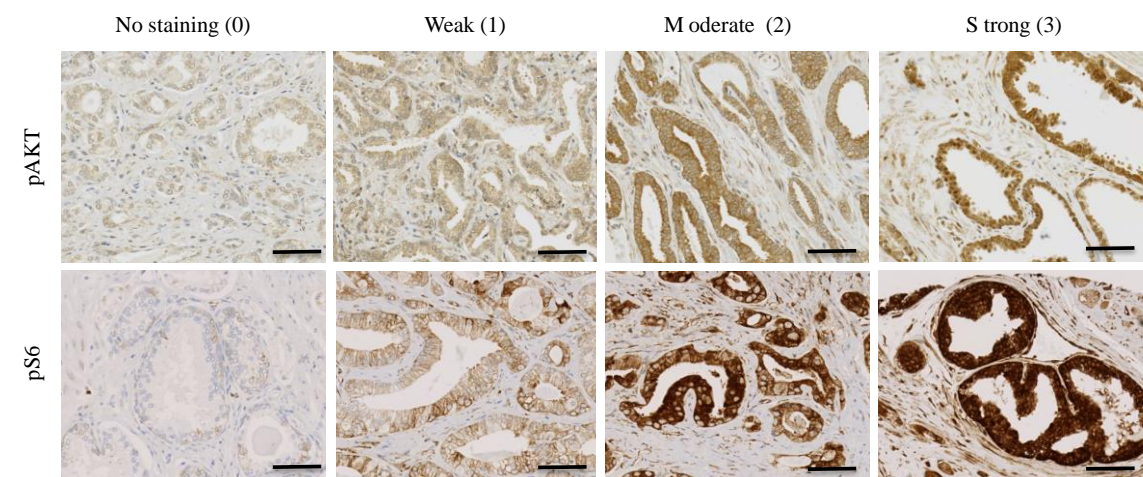


Figure 26: Examples of representative immunohistochemistry staining of the PI3K markers: p-AKT and p-S6. Error bars = 100µm. Intensity scoring: No staining = 0, Weak = 1, Moderate = 2, Strong = 3. Proportion was also calculated formulating an overall quickscore (described in main text and methods section).

The protein expression (mean quickscore) of PTEN was marginally reduced in malignant compared to benign prostate samples; with a 0.9 fold increase ($p=0.160$). There was a significant increase in the mean expression of p-AKT, p-MTOR and p-S6; with an increase of between 1.3 and 2.4 fold in malignant compared to benign prostate tissue samples ($p<0.001$) (Table 17). This data is further demonstrated in figure 27. A further observation was the elevated expression of p-AKT in benign tissue (Mean expression

8.2), which did not necessary result in increased expression of down stream markers: p-MTOR and p-S6.

Marker	Benign vs malignant	P-value	Mean Quickscore (95% CI)	Fold increase
PTEN	Benign	p=0.160	10.5 (9.5-11.4)	0.9
	Malignant		9.5 (8.9-10.2)	
p-AKT	Benign	p<0.001	8.2 (6.9-9.5)	1.3
	Malignant		10.4 (9.7-11.0)	
p-MTOR	Benign	p<0.001	1.0 (0.3-1.7)	2.4
	Malignant		2.4 (1.8-3.0)	
p-S6	Benign	p<0.0001	4.3 (3.1-5.6)	2.1
	Malignant		8.8 (8.0-9.6)	

Table 17: Summary of PI3K pathway markers expression (mean quickscore) between benign and malignant prostate samples.

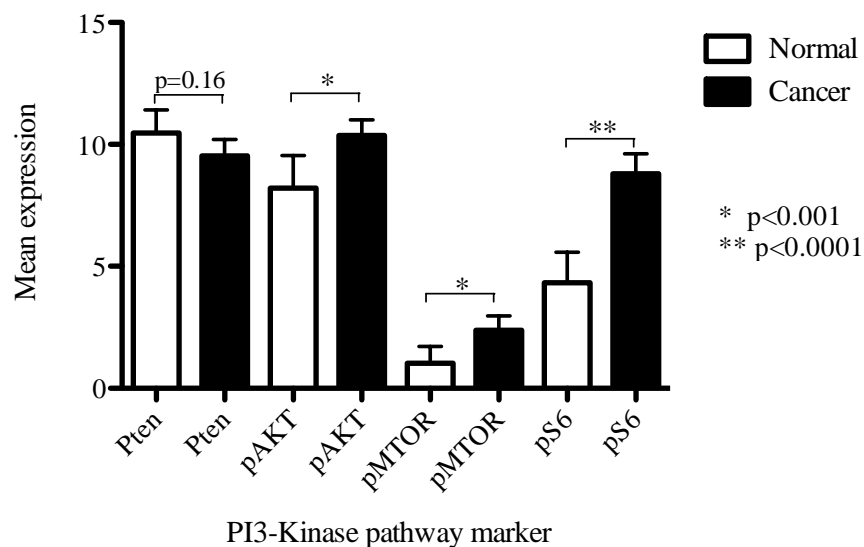


Figure 27: Summary of PI3K pathway marker expression (mean quickscore) between benign and cancer prostate samples. Error bars = 95% CI.

When correlating the mean expression of the PI3K pathway markers with GS, similar trends were seen as for that of the Wnt pathway markers, with greater expression in higher-risk disease (Figure 28). This was evident for p-mTOR and p-S6, with increasing expression from normal to low-risk (D'Amico 1, GS 6), to intermediate-risk (D'Amico 2, GS 7) to high-risk (D'Amico 3, GS ≥ 8). These rises were statistically significant for p-S6 ($p < 0.05$) but not for p-MTOR. These observations were not apparent for PTEN or p-AKT staining.

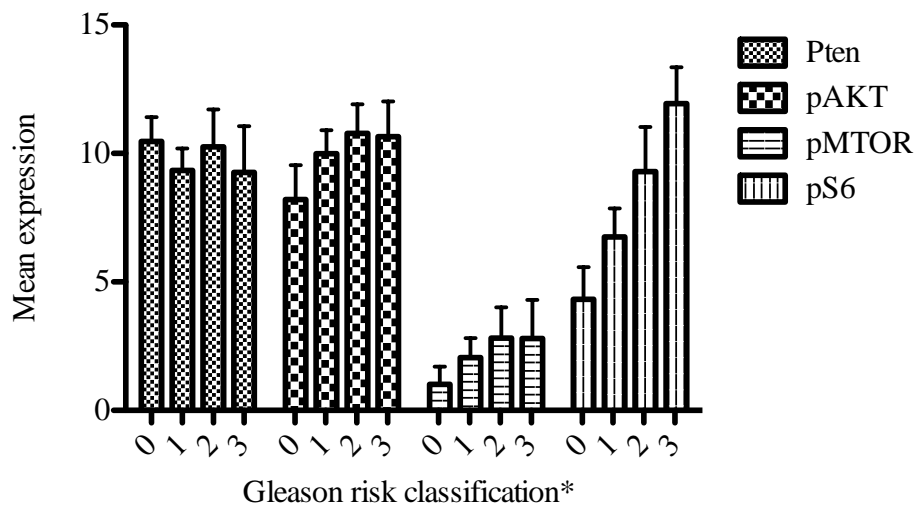


Figure 28: Summary of PI3K pathway marker expression (mean quickscore) categorised according to Gleason score risk classification as defined by D'Amico (*0 = normal, 1 = low-risk, 2 = intermediate-risk, 3 = high-risk). Error bars = 95% CI.

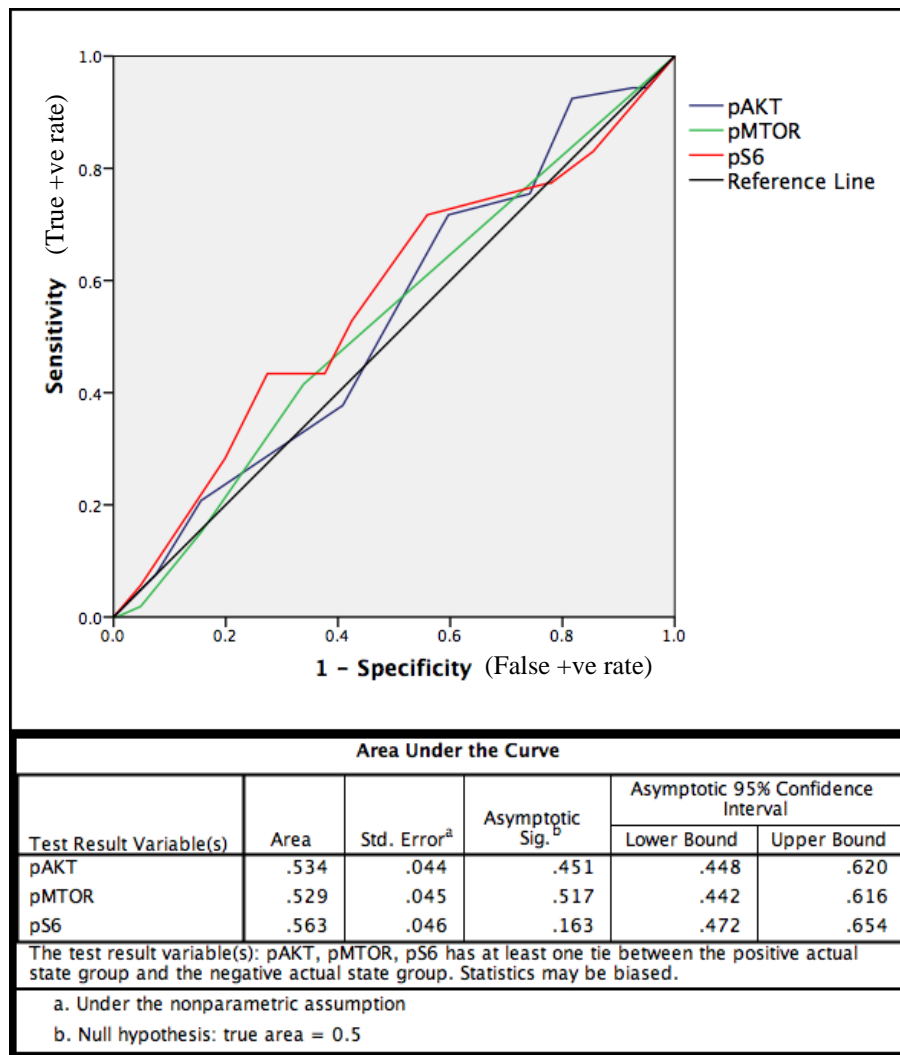


Figure 29: ROC curve of PI3K markers. The reference line represents an area under the curve of 0.5. All markers have an area under the curve close to 0.5 (0.534, 0.529 and 0.563) and are deemed a very poor test for identifying those that develop biochemical relapse following surgery.

When ascertaining if a cut of value for activation or aberrant signalling of each marker could correlate with biochemical relapse, the ROC curve failed to identify any significant marker (Figure 29). A comparison of no/mild to moderate/strong staining of pS6 did not demonstrate any differences in biochemical relapse (Figure 30, $p=0.373$, log-rank). Further analysis of the high-risk group ($GS \geq 8$), where the majority of biochemical relapses following surgery occurred, failed to show any difference in time to biochemical relapse when comparing moderate/strong to no/low staining for pS6 (Figure 31, $p=0.337$, log-rank).

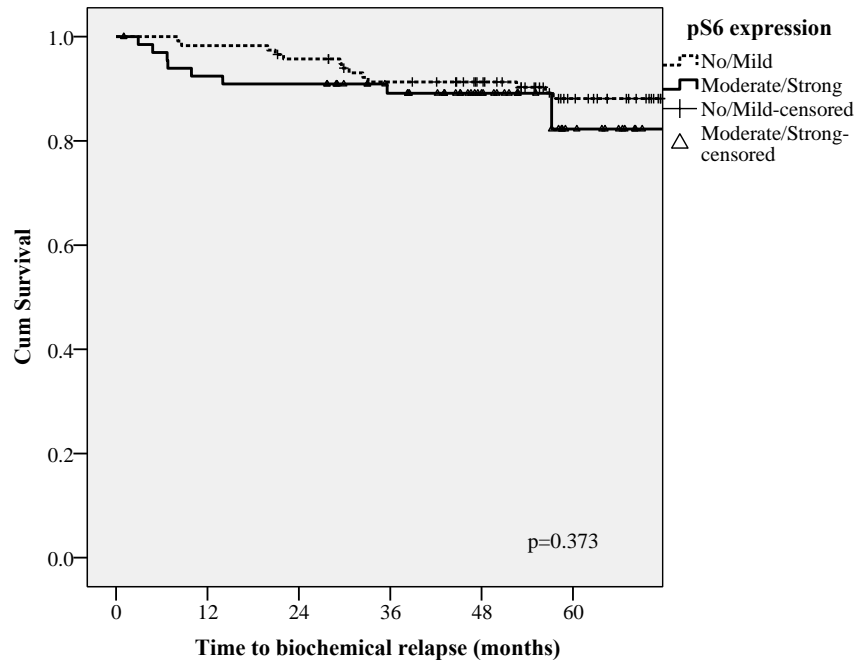


Figure 30: Kaplan-Meier curve of time to biochemical relapse as a function of pS6 expression using degree of staining using quickscore values. No/mild staining = 0-6, moderate/strong = 7-18. Log rank $p < 0.373$. N=22.

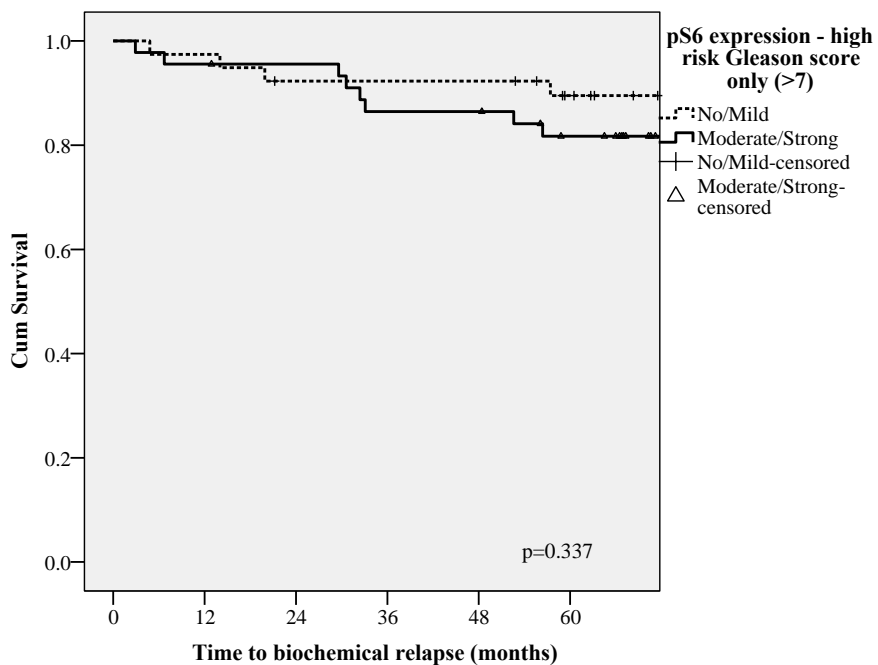


Figure 31: Kaplan-Meier curve of pS6 expression for high-risk prostate samples (GS>7) demonstrating significant difference in rate of biochemical relapse. Log rank $p < 0.337$. N=17.

3.3.1.4 Association of MAPK pathway markers with pathological characteristics and clinical outcomes

To characterise the MAPK signalling pathway, the downstream markers p-ERK and p-MEK were used. p-ERK and p-MEK demonstrated nuclear and cytoplasmic staining, respectively (Figure 32).

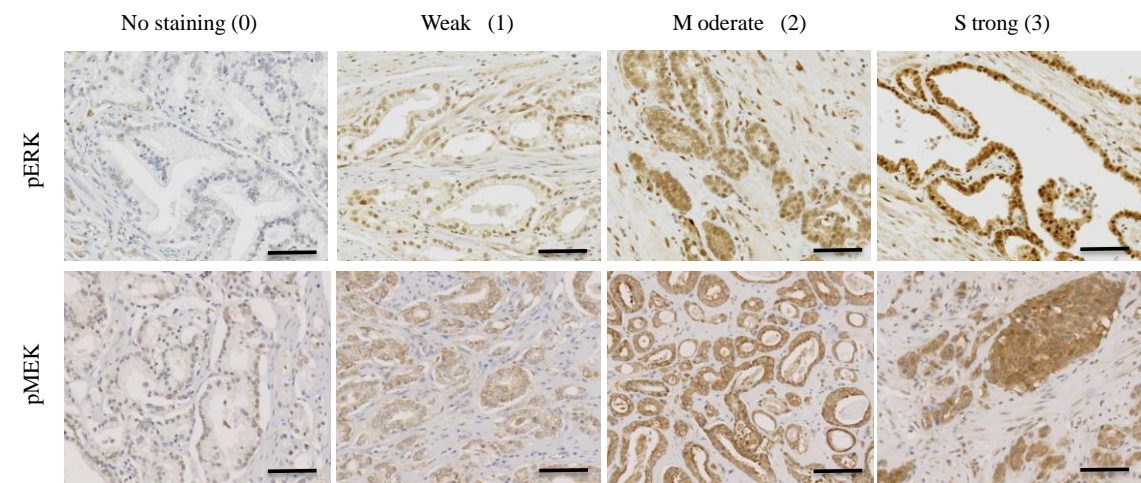


Figure 32: Examples of representative immunohistochemistry staining of the MAPK markers: p-ERK and p-MEK. Error bars = 100 μ m. Intensity scoring: No staining = 0, Weak = 1, Moderate =2, Strong = 3. Proportion was also calculated formulating an overall quickscore (described in main text and methods section).

There was a higher expression of both p-MEK and p-ERK in PCa samples when compared to normal tissue, this was only significant for p-MEK however (Figure 33A). When assessing expression levels as a function of GS, there was no trend towards increased expression in higher-risk disease for p-ERK unlike that for p-MEK (Figure 33B). Expression of p-MEK was significantly higher in all cancer grades when compared to normal ($p < 0.0001$). However when comparing low- (D'Amico 1, GS 6) to intermediate-risk (D'Amico 2, GS 7) and intermediate- to high-risk (D'Amico 3, GS ≥ 8) samples no significance was demonstrated, although an upward trend with increasing expression with GS was observed (Figure 33B, $p = 0.06$).

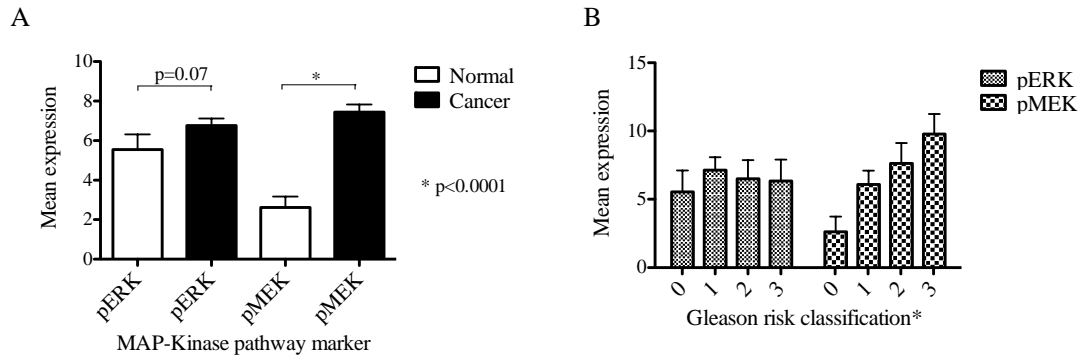


Figure 33: Summary of MAP-Kinase pathway marker expression (mean quickscore) between: A: Normal and cancer samples and B: categorised according to Gleason score risk classification as defined by D’Amico (*0 = normal, 1 = low-risk, 2 = intermediate-risk, 3 = high-risk). Error bars = 95% CI.

ROC curve analysis failed to demonstrate any significant difference for p-ERK and p-MEK expression when correlating with risk of biochemical relapse following surgery (data not shown). However, when using quickscore estimations, no/mild versus moderate/strong expression, p-MEK was statistically predictive of time to biochemical relapse after surgery (Figure 34, $p < 0.01$, log-rank). Similar to that of p-S6, p-MEK failed to predict risk of biochemical relapse independently of GS (Figure 35). Those high-risk cancers with moderate/strong expression of p-MEK had a shorter time to biochemical relapse than PCa samples with no/mild staining, however this was not statistically significant ($p = 0.117$, log-rank).

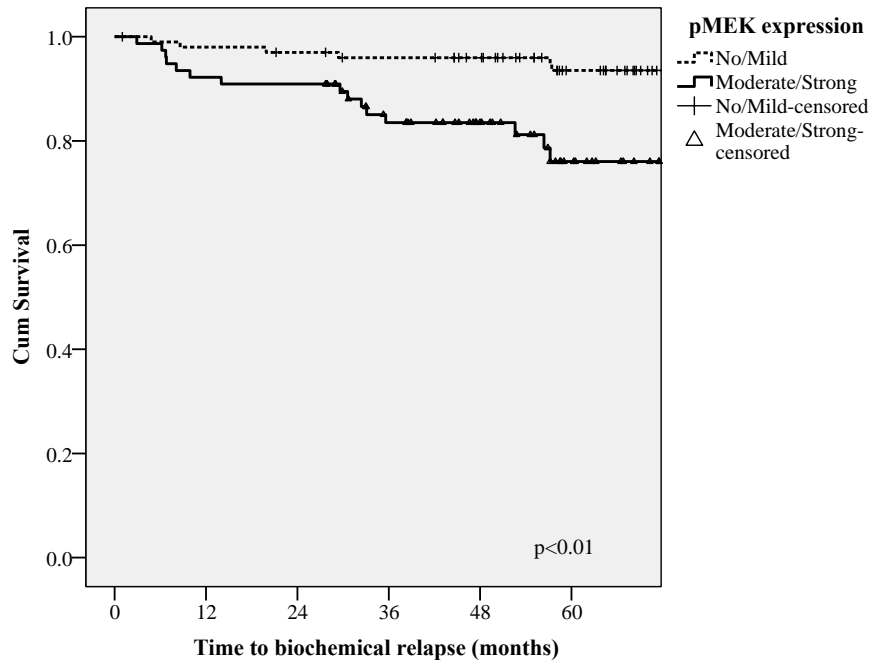


Figure 34: Kaplan-Meier curve of time to biochemical relapse as a function of p-MEK expression using degree of staining using quickscore values. No/mild staining = 0-6, moderate/strong = 7-18. Log rank $p < 0.01$. N=24.

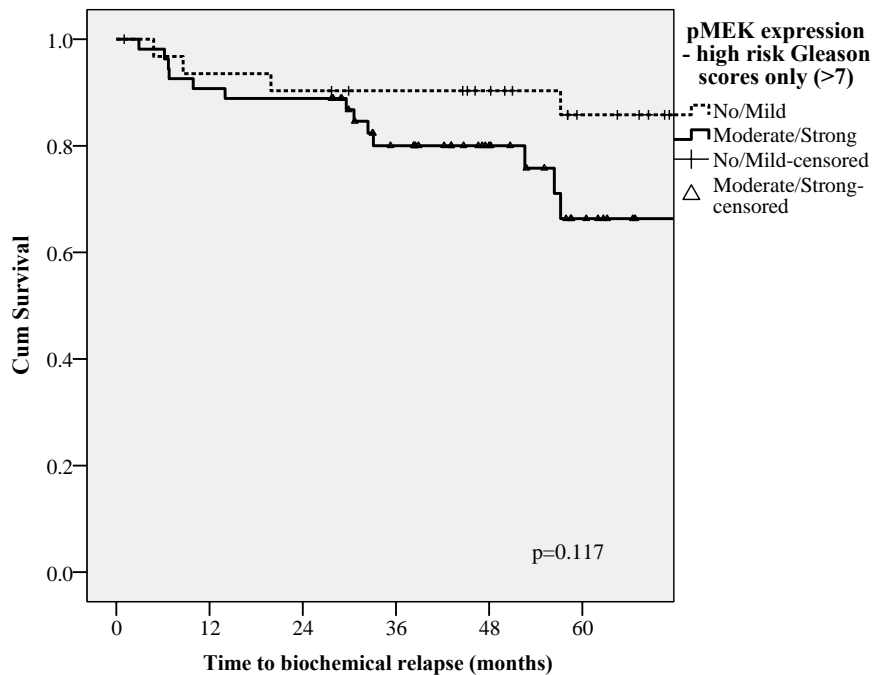


Figure 35: Kaplan-Meier curve of p-MEK expression for high-risk prostate samples (GS>7) demonstrating a significant difference in rate of biochemical relapse. N=19. Log rank $p < 0.117$.

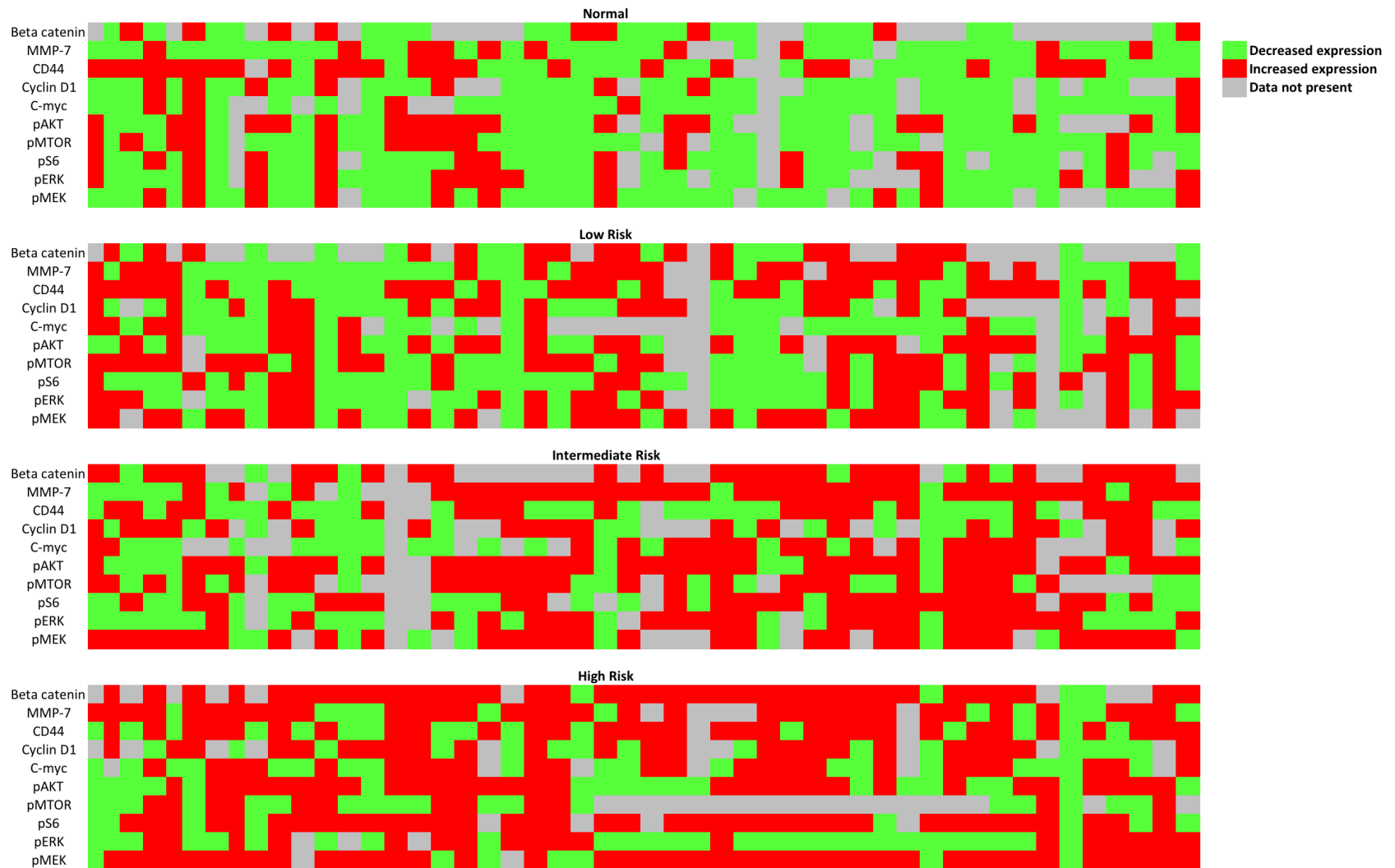


Figure 36: Heat map of Wnt, PI3-Kinase and MAP-Kinase markers for 50 samples of each grade of tumour (normal, low-risk (GS 6), intermediate-risk (GS 7) and high-risk (GS \geq 8)). Decreased expression = no/low expression (quickscore 0-6), Increased expression = moderate/high expression (quickscore 7-18).

3.3.1.5 Expression of Wnt, PI3K and MAPK signalling pathways markers are greater in higher risk disease

The heatmap in Figure 36 illustrate the trends found in expression levels of markers associated with all three pathways when separated into GS risk group. There is a clear trend, with more samples displaying upregulation of pathway markers as the GS increases.

3.3.1.6 Some Wnt, PI3K and MAPK signalling pathways markers are positively correlated

To assess correlation between different markers and pathways, a Pearson correlation coefficient was measured. This statistical test is a measure of the linear correlation between two variables X and Y, giving a value between +1 and -1 inclusive, where 1 is total positive correlation, 0 is no correlation, and -1 is total negative correlation.

Adopting this statistical method, table 18 summarises the correlation of the best or most reliable markers in each pathway. Any correlation between single pathways was assessed first. Wnt pathway, analysed using β -catenin, MMP-7 and C-myc were all positively correlated, with a Pearson correlation coefficient of between .150 and .265. PI3K pathway markers: p-AKT, p-MTOR and p-S6 (Pearson correlation coefficient between .125 and .270) and MAPK markers: p-ERK and p-MEK (Pearson correlation coefficient .226) were also positively correlated. Although single pathway analysis showed only modest correlations, assessing interplay of the different pathways demonstrated greater correlations. For example, the strongest correlations were those between the PI3K and MAPK pathway, in particular: p-ERK and p-AKT, p-MEK and p-S6 and p-MEK and p-AKT, with a Pearson coefficient of .534, .461 and .440, respectively. There was also positive correlation between the Wnt pathway and PI3K and MAPK pathways, but to a lesser degree. This observation suggests possible crosstalk between the signals produced from each of these cancer pathways.

Marker	β -cat	MMP-7	C-myc	pAKT	pMTOR	pS6	pERK	pMEK
β -catenin	1							
MMP-7	.150*	1						
C-myc	.173*	.265**	1					
pAKT	.306**	.366**	.266**	1				
pMTOR	.075	.190**	.326**	.270**	1			
pS6	.394**	.208**	.374**	.252**	.125*	1		
pERK	.090	.293**	.370**	.534**	.357**	.254**	1	
pMEK	.411**	.134*	.432**	.440**	.026	.461**	.226**	1

Table 18: Pearson correlation coefficient of Wnt, PI3-Kinase and MAP-Kinase signalling pathways. * p=0.05, ** p=0.01

An alternative way to correlate all these markers is to use principle components analysis (PCA, Figure 37). This statistical test transforms the data from multiple variables (expression level of each marker in this case) and converts them into a new coordinate system with each coordinate called a principle component. The greatest variance of the data lies on the first coordinate (first principle component) and the second variance on the second coordinate, and so on. This reduces the amount of data so that typical 2 or 3 principle components are used to place the expression profile of each sample in a unique linear space. This attempts to predict areas where certain types or features of tumours may cluster, usually represented by a scatter plot.

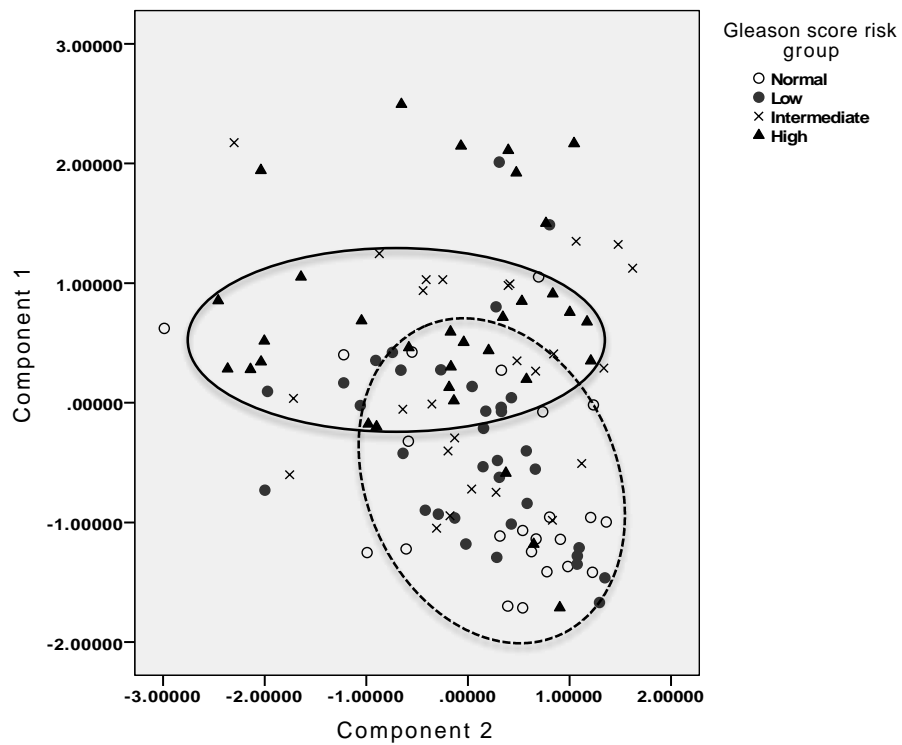


Figure 37: Principle components analysis (PCA) using all Wnt, PI3K and MAPK markers demonstrating some molecular correlation categorised by Gleason score (GS) risk group (Low-risk=GS 6, Intermediate-risk=GS 7, High-risk=GS>7). Oval shape (solid line) representing the majority of high-risk samples and oval shape (broken-line) representing the majority of low-risk or normal samples.

Although there is a lot of crossover between the samples, the normal and low-risk samples appear to cluster to the middle/lower right area of the graph with the majority having negative values for component 1 and positive values for component 2 (Oval shape broken line, Figure 37). Intermediate-risk samples do not demonstrate any clustering. Whereas high risk samples predominately populate the centre of the graph (Oval shape solid line, Figure 37) and many are positive for components 1 and 2.

3.3.2 Next-generation sequencing (NGS) analysis

3.3.2.1 NGS samples and characteristics

200 prostate DNA samples were extracted from formalin-fixed paraffin embedded (FFPE) prostate samples and analysed using the Ion Torrent platform, with the 50-gene Ampliseq Cancer Hotspot Panel v2 (CHPv2), as discussed in section 2.1.2. Unfortunately, despite careful DNA extraction and quantification only 61 samples had sufficient coverage in order to report accurate data. The remaining samples either displayed very poor coverage or high background levels, features that can be problematic in FFPE samples.

Although the tissue morphology is preserved in FFPE samples, nucleic acid damage occurs caused by the fixation and embedding conditions, and due to long-term storage of samples. The most common nucleic acid artefact is C>T base substitution caused by deamination of cytosine bases to deoxyuracil. This results in DNA damage and strand-breaks affecting the quality and number of amplifiable copies of DNA. Deaminated cytosine residues can be removed by the enzyme Uracil-N-Glycosylase (UNG) overcoming this problem and improving the DNA quality. Future DNA extractions could adopt this extra step in order to improve NGS run success. Alternatively, fresh-frozen tumour tissue should have even better results as the nucleic acids are of high quality.

Of the 61 successfully sequenced prostate samples, 58 were from radical prostatectomy specimens and 3 were from transurethral resection of prostate (TURP) gland sections. The median age was 63 year (Range 43-85 years). The median PSA at diagnosis was 9.9 ng/ml (Range 3-64 ng/ml). 4 had pathological (p) T1 disease, 19 pT2 and 35 pT3 and the 3 TURP's were clinical stage T3. Histologically 10 had a low-risk GS (GS=6), 16 had intermediate-risk GS (GS=7: 13 GS 3+4 and 3 GS 4+3) and 35 had high-risk (GS>7: 4 GS 3+5, 6 GS 4+4, 16 GS 4+5, 2 GS 5+3, 5 GS 5+4 and 2 GS 5+5). Of the 58 radical prostatectomy samples, 8 had biochemical relapse.

3.3.2.2 Types of genetic mutations

A brief description of the types of mutations detected using the Ion Torrent CHPv2 panel is shown in Table 19.

Mutation	Description
Synonymous	Substitution of one base for another in an exon, such that the produced amino acid is not modified
Missense	Point mutation in which a single nucleotide change results in a codon that codes for a different amino acid. It results in a slightly altered protein.
Nonsense	Point mutation that results in premature stop codon usually resulting in a non-functioning protein. i.e. it blocks protein production.
Frameshift	Mutation caused by an insertion or deletion of a number of nucleotides, which causes a shift in the translational reading frame. This has a more dramatic effect as causes a change in all amino acids. The resulting protein is usually non-functional.

Table 19: Types of genetic mutations

3.3.2.3 Spectrum of mutations from Ion Torrent CHPv2 panel in primary prostate malignancy

Cellularity scoring showed that 1 sample had 0-20% tumour, 2 samples had 21-40% tumour, 12 samples 41-60% tumour, 26 samples had 61-80% tumour and 20 samples had 81-100% tumour content.

Of the 61 samples analysed, 22 (36.1%) showed no potentially pathogenic variants (single nucleotide variants flagged as common by UCSC Genome Browser, University of California, Santa Cruz; <http://www.genome.ucsc.edu> only). Of these, 2 had a cellularity scoring of less than 40% tumour. Therefore, it is not possible to draw any firm conclusions in these samples, as there is a high false negative rate, being contaminated with more than 60% of normal tissue.

Of the remaining 39 samples, there were 20 different gene mutations detected from the CHPv2 panel.

3.3.2.3.1 Wnt pathway genes

The genes associated with the Wnt pathway on the CHPv2 panel included Adenomatous polyposis coli (APC), β -catenin (CTNNB1) and E-cadherin (CDH1). Both mutations in APC and CTNNB1 results in Wnt pathway deregulation and activation of Wnt target genes such as c-MYC and MMP-7. CTNNB1 is also important in adherent junctions between epithelial cells where it binds and forms a complex with CDH1. Mutations in either of these genes are associated with cancer progression and metastasis.

10/61 (16.5%) of samples harboured a mutation in a gene associated with the Wnt pathway (figure 41). There were 7 (11.5%) APC mutations; 1 occurring in a sample with a low-risk GS, 2 with an intermediate-risk GS and 4 with a high-risk GS. There was only 1 (1.6%) CTNNB1 mutation, which occurred in a high-risk GS sample. There were 2 (3.3%) CDH1 mutations both in high-risk GS samples, with 1 also harbouring a CTNNB1 mutation.

3.3.2.3.2 PI3K pathway genes

The genes associated with the PI3K pathway on the CHPv2 panel included Phosphatase and tensin homolog (PTEN), AKT1 (also know as Protein Kinase B), p110 α catalytic subunit of PI3K (PIK3CA) and the Receptor tyrosine kinases (RTK's): epidermal growth factor receptor (EGFR also called ERBB1 or HER1) and erb-b2 receptor tyrosine kinase 2 (ERBB2) or human epidermal growth factor receptor 2 (HER2). PTEN is a tumour suppressor gene located at the 10q23 locus of chromosome 10, which is a potent activator of downstream AKT, in particular, the AKT1 isoform. PI3K is composed of an 85 kDa regulatory subunit and a p110 α kDa catalytic subunit. PI3K is activated upon ligand binding to a receptor tyrosine kinase (RTK), which then activates the regulatory subunit (85 kDa) to bind to the catalytic p110 α subunit. Both activation of AKT and PI3K triggers various downstream signalling cascades resulting in cell survival, apoptosis, transformation, cell migrations and metastasis (Karakas et al. 2006). RTK's such as EGFR and ERBB2/HER2 can activate both the PI3K and MAPK pathway.

14/61 (23.0%) of samples analysed had a mutation in a gene commonly associated with the PI3K pathway (Figure 39). There were 7 (11.5%) mutations in the PTEN gene, 1 in a low-risk GS sample, 1 in an intermediate-risk GS and 5 in high-risk GS. There were 3

(4.9%) mutations in AKT1, 2 in a low-risk GS and 1 in high-risk GS samples. There were 4 RTKs (2 EGFR and 2 ERBB2) mutations, 1 intermediate-risk sample having a mutation in both and 2 other mutations (1 EGFR and 1 ERBB2) both in high-risk GS samples. Only 1 (1.6%) sample, with a high-risk GS, harboured a PIK3CA mutation.

3.3.2.3.3 MAPK pathway genes

The genes associated with the MAPK pathway on the CHPv2 panel included the three RAS (rat sarcoma viral oncogene homolog) genes (KRAS, HRAS and NRAS), BRAF and the two RTKs: EGFR and ERBB2/HER2. RAS acts as a molecular “on/off” switch; when mutated it remains in the “on” state activating the MAPK pathway. BRAF is a Raf Kinase that can activate MEK (downstream of RAS), which in turn activates ERK by phosphorylation. Consequently, fundamental cellular processes such as growth, proliferation, cell survival and apoptosis are disrupted, permitting tumourigenesis. As discussed above, RTK’s upstream of the MAPK pathway, such as EGFR and ERBB2/HER2 can also cause aberrant signalling of this pathway.

The incidence of mutations in genes associated with the MAPK pathway was 8.2% (n=5) (Figure 39); with 1 (1.6%) intermediate-risk GS sample harbouring a KRAS mutation, 1 (1.6%) low-risk GS sample harbouring a HRAS mutation and there were no mutations identified in the BRAF gene. There 4 mutations in the RTK’s (EGFR and ERBB2/HER2) occurring in 3 samples as discussed above.

3.3.2.3.4 Cell cycle and DNA repair genes

Other cellular processes or pathways whereby gene mutations can be grouped include cell cycle and DNA repair genes. The genes on the CHPv2 panel associated with this process include Tumour protein p53 (TP53), Retinoblastoma (RB1), Cyclin-dependent kinase Inhibitor 2A (CDKN2A) and Ataxia telangiectasia mutated (ATM). TP53 is a tumour suppressor gene located on chromosome 17 and has several anti-cancer roles. It can activate DNA repair pathways and proteins, regulate the cell cycle at the G1/S check-point and can initiate apoptosis (Sidransky & Hollstein 1996). RB1 is a tumour suppressor gene located on chromosome 13. When bound to the transcription factor E2F,

RB1 prevents cell cycle progression and DNA replication (Indovina et al. 2015). CDKN2A is located on chromosome 9 and codes the cell-cycle inhibitor protein p16. p16 controls abnormal cell growth and proliferation by binding to complexes of cyclin-dependent kinases (CDK) such as CDK 4 and 6 and Cyclin D. This binding inhibits the kinase activity of the enzyme, which arrests the cell cycle in the G1 phase (Foulkes et al. 1997). ATM is located on chromosome 11 and is recruited and activated following DNA double-strand breaks. It results in cell cycle arrest, DNA repair and apoptosis through activation of key targets such as p53 and BRCA1 (Ahmed & Rahman 2006).

21/61 (34.4%) samples harboured a mutation in a cell cycle pathway gene and 3/61 (4.9%) in a DNA repair gene (Figure 39). 19 had 1 mutation and 2 samples had 2 mutations. 17 (27.9%) samples had a TP53 variant, the majority (n=12) being missense. Interestingly, there were no TP53 mutations in low-risk GS samples, with 7 (43.8%) in intermediate-risk GS and 10 (32.2%) in high-risk GS samples. There were 2 (3.3%) mutations in the RB1 gene. There were 2 (3.3%) mutations in CDKN2A and 3 (4.9%) mutations in the DNA repair gene, ATM.

3.3.2.3.5 Other gene mutations

In addition there was 2 in FGFR3, 1 in MET, 2 in ALK, 1 in SRC, 1 in RET and 1 in HNF1A.

Table 20 and Figure 38 shows a summary of all mutations.

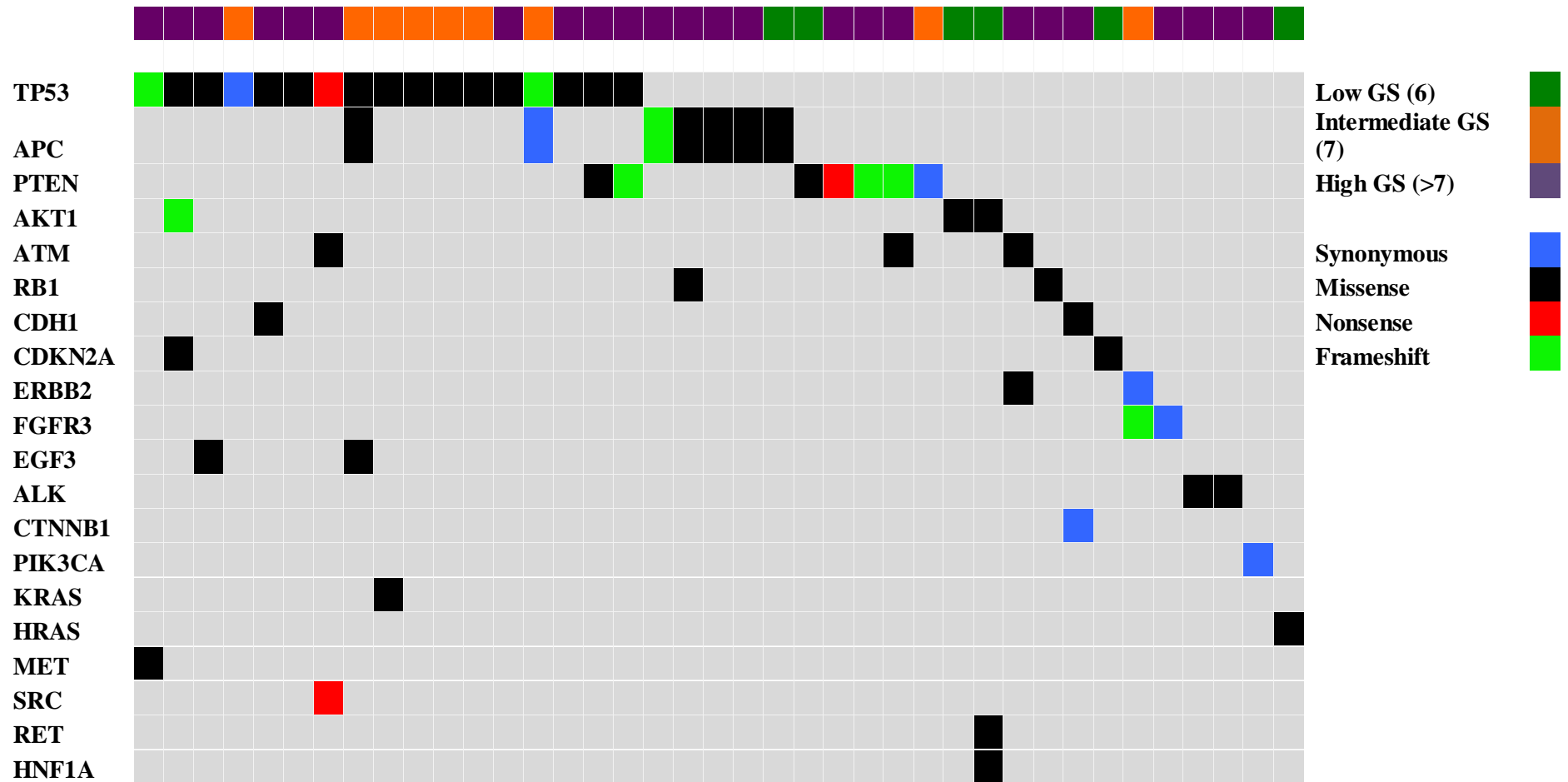


Figure 38: Distribution of mutations identified. Genes are ordered by their mutational frequency within the cohort. Mutations are labelled according to GS risk group and type of mutation (Synonymous, missense, nonsense, frameshift)

Gene	Cases	
	N	%
TP53	17	27.9%
APC	7	11.5%
PTEN	7	11.5%
AKT1	3	4.9%
ATM	3	4.9%
RB1	2	3.6%
CDH1	2	3.3%
CDKN2A	2	3.3%
ERBB2	2	3.3%
FGFR3	2	3.3%
EGFR	2	3.3%
ALK	2	3.3%
CTNNB1	1	1.6%
PIK3CA	1	1.6%
KRAS	1	1.6%
HRAS	1	1.6%
MET	1	1.6%
SRC	1	1.6%
RET	1	1.6%
HNF1A	1	1.6%

Table 20: Number of mutated cases for each gene

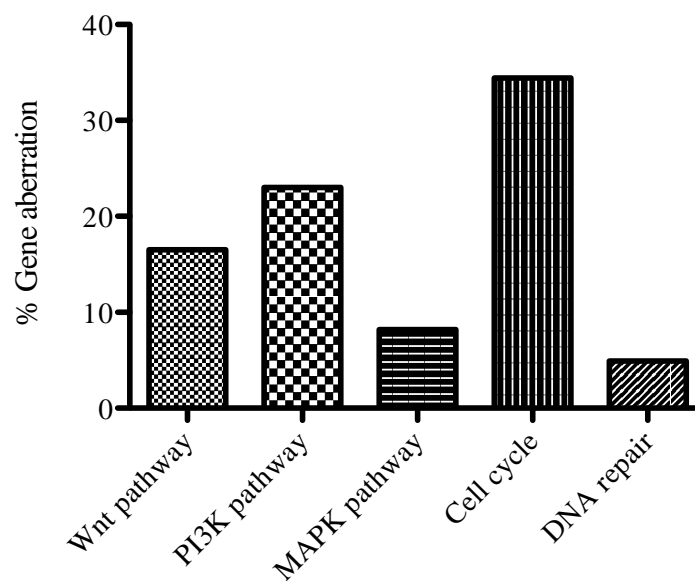


Figure 39: Percentage of gene aberrations separated into molecular or pathway processes.

3.3.2.4 Patient follow-up data

The median follow-up time was 4.4 years (Range 2.1-9.5 years). Of the 61 patients, 2 have died during this follow-up period with 1 as a result of PCa. This was a TURP sample from a patient with high-grade (GS 4+5=9) PCa and harboured a single mutation from the CHPv2 panel: TP53. 8 patients had biochemical failure all having high-risk disease according to D'Amico criteria (GS 8-10 or \geq T2c or PSA.20 ng/ml). 2 had GS 7 (1 GS 3+4=7 and 1 GS 4+3=7) and 6 had GS8-9 (4 GS 4+5, 1 GS 5+3, 1 GS 5+4). 7 patients had pT3 disease and 1 had pT2 disease. 3 had a PSA <10ng/ml and 5 had a PSA>20ng/ml. 2 of these patients had mutations in Wnt pathway associated genes, 1 having mutations in both CTNNB1 and CDH1 and the other having a mutation in APC. There was 1 PI3K associated gene mutation: PTEN and 4 patients had a TP53 mutation. A summary of all mutations present in these samples is shown in Table 21.

Patient	Gleason score	PSA (ng/l)	pT-stage	Gene Mutations
1	4+5	23.1	3	MET, TP53
2	5+4	8.0	3	PTEN
3	4+5	4.5	2	CTNNB1,CDH1
4	4+5	25.0	3	PTEN
5	5+3	9.1	3	NIL
6	4+4	5.5	3	ATM,TP53,SRC
7	4+3	23.0	3	NIL
8	3+4	5.7	3	APC, TP53

Table 21: Tumour characteristics and mutational profiles of the 8 samples that had biochemical relapse following radical prostatectomy.

3.4 Discussion

This chapter reports the expressional profile of a large cohort of primary PCa samples as part of a TMA and demonstrates the feasibility of performing targeted sequencing using primary PCa tumour FFPE samples using the Ion Torrent and CHPv2 gene panel.

3.4.1 Wnt Signalling Pathway

This study demonstrates upregulation of the Wnt pathway in PCa, particularly as the GS increases, with elevated expression of β -catenin and Wnt target genes: MMP-7, Cyclin D1 and C-myc using IHC. In the literature there remains inconsistency of β -catenin staining using IHC with reports favouring both an increased and decreased expression (Kypta & Waxman 2012). β -catenin staining was considered positive if there was cytoplasmic or nuclear staining consistent with the theory that cytoplasmic staining is as a result of β -catenin entering or leaving the nucleus.

The incidence of β -catenin mutations in primary PCa samples is low (1/61, 1.6%), similar to that reported by others (Baca et al. 2013; Barbieri et al. 2012; Taylor et al. 2010; Beltran et al. 2013). Emerging evidence suggests that β -catenin and APC are mutually exclusive, consistent with the notion that mutations of either gene has more or less the same molecular defect: β -catenin stability and TCF transactivation within the nucleus (Giles et al. 2003). Therefore, when both β -catenin and APC mutational profiles are combined the rate of Wnt pathway alteration increases to 8/61 (13.1%). The incidence is increased further to 10/61 (16.4%) when CDH1, which is important in adherent junctions by binding to β -catenin, is added.

Recent studies have further demonstrated that the somatic alteration of APC and β -catenin are greater in metastatic disease, with an incidence of 8.7-19.7% and 4.9-12% respectively (Grasso et al. 2012; Robinson et al. 2015). Although, metastatic PCa samples have not been examined, there is an upward trend with greater expression of Wnt associated markers in higher GS samples and in those with biochemical relapse. The Wnt pathway has been linked to the progression of PCa (Grasso et al. 2012; Barbieri 2013) and has been implicated in the lethal phase of PCa, castrate resistant PCa (Kumar et al. 2011; Grasso et al. 2012).

Given the importance of the Wnt signalling in all stages of PCa, particularly those with high-risk and metastatic disease, targeting this pathway is an attractive therapeutic approach. However, success has been limited because of the lack of effective therapeutic agents for targets in the Wnt pathway and the lack of a defined patient population that would be sensitive to a Wnt inhibitor. Promising work by Liu et al (2013) has shown that a drug that targets Porcupine (LGK974), a Wnt-specific acyltransferase, potently inhibits Wnt signaling and has strong efficacy in rodent tumour models, and is well-tolerated (J. Liu et al. 2013). Novel agents like this in combination with techniques such as targeted NGS, as displayed by this study, would maximise future success.

3.4.2 PI3K Signalling Pathway

In the present study, the PI3K pathway was commonly altered, with elevation of downstream markers (p-AKT, p-MTOR and p-S6), particularly in patients with high-risk disease, where positive association with biochemical recurrence was demonstrated. Using targeted NGS, the Ion Torrent platform and CHPv2 gene panel, 9.8% of primary prostatectomy samples had a PTEN mutational. This is similar to that reported by the COSMIC database (8%) and others who report an incidence between 7-18% in non-metastatic tumours (Taylor et al. 2010; Barbieri et al 2012; Baca et al. 2013). This increases significantly to between 40-87% in metastatic samples (Taylor et al. 2010; Robinson et al. 2015; Grasso et al. 2012; Friedlander et al. 2012). PTEN loss has also been associated with biochemical recurrence after radical prostatectomy (Bedolla et al. 2007) and resistance to radiation (Skvortsova et al. 2008) and chemotherapy (Grünwald et al. 2002). In addition, PTEN loss has also been shown to predict for shorter time to metastasis (Lotan et al. 2011) and PTEN null prostate cancer cells demonstrate castration resistant growth (Mulholland et al. 2011). There was a low AKT1 and PIK3CA mutation rate consistent with other reports (Sun et al. 2009; Robinson et al. 2015). Like PTEN loss, AKT1 activation has also been associated with poor clinical outcome such as biochemical relapse following radical prostatectomy (Ayala et al. 2004) and resistance to radiation (Skvortsova et al. 2008).

Overexpression ERBB2/HER2 is well established in breast cancer occurring in ~15% cases and defines one of the unique subtypes, which responds to different treatment (Burstein 2005). Trastuzumab (Herceptin) is a monoclonal antibody that interferes with

the HER2 receptor and is used in the management of HER2-positive breast cancer following surgery and/or radiotherapy and in advanced metastatic disease alone or in combination with chemotherapy (Figueroa-Magalhães et al. 2014). Expression of ERBB2 (HER2) in PCa has been inconsistent with some reporting greater expression (Morote et al. 1999) and others reporting low expression (Savinainen et al. 2002). A phase II UK trial using Pertuzumab single-agent in castrate chemotherapy-naive patients with hormone-refractory PCa demonstrated no clinical benefit, with the authors concluding that failure was likely secondary to the continued presence of significant levels of intraprostatic androgen driving androgen receptor signaling (de Bono et al. 2007). EGFR (ERBB1/HER1) overexpression has been observed in more than 40% of CRPC patients, but similar to ERBB2 the use of specific inhibitors (Gefitinib) in clinical trials has failed to provide survival benefits (Canil et al. 2005).

When combining somatic mutations (PTEN, AKT1, PIK3CA, ERBB2/HER2 and EGFR) the incidence increases to 21.3% (13/61). The expression of PI3K markers is also higher in high-risk PCa. Alterations of components of the PI3K pathway, including mutation, altered expression, and copy number alterations, have been reported by others, with 42% occurring in primary prostate tumours and 100% occurring in metastatic tumours (Taylor et al. 2010). Furthermore, Robinson et al (2015) reports somatic alterations associated with the PI3-Kinase pathway in 49% of metastatic castrate resistant PCa affected individuals (Robinson et al. 2015).

Given the high prevalence of PI3K pathway activation demonstrated in this study of primary PCa and by others in metastatic PCa (Robinson et al. 2015; Taylor et al. 2010), inhibitors of this pathway have great potential to deliver clinical benefit. There are a number of agents under investigation, which inhibit various components of the pathway including mTOR inhibitors, PI3K inhibitors and AKT inhibitors. These agents have been mostly used in the metastatic setting and the results to date have been poor (Bitting & Armstrong 2013)

3.4.3 MAPK Signalling Pathway

This study shows a low mutational rate in genes associated with the MAPK pathway with only 2 mutations in RAS genes. This is similar to others with a reported incidence in

KRAS of 3-6% (Grasso et al. 2012; Baca et al. 2013; Taylor et al. 2010; Robinson et al. 2015). Despite this, there was a high expression level of the downstream markers p-ERK and p-MEK in this cohort of primary prostate cancers implying aberrant MAPK signalling. This is in accordance with work by Taylor et al (2010), reporting MAPK pathway alteration in 43% of primary tumours and 90% of metastasis.

We further show that p-MEK expression can predict risk of biochemical relapse independent of GS (Figure 37). In the clinical setting this finding could be useful in predicting biochemical relapse in those with intermediate and high-risk disease. These patients could then be offered additional treatment; whether adjuvant hormones or radiotherapy, or novel targeted agents.

Although RAS mutations are rare in PCa, deregulation of its effectors such as the MAPK signaling pathway is very common. MAPK signaling has been implicated in both initiation of metastatic disease and in the late transition into CRCP (Mukherjee et al. 2011). It is thought to represent a convergence point for numerous interconnecting cellular pathways. It is hypothesized that this complex combination of signals grant cells the ability to evade normal controlling mechanism and to permit metastasis. (Pylayeva-Gupta et al. 2011; Cox & Der 2003).

3.4.4 Cross-talk Between Signalling Pathways

Cell signaling pathways are complex with many interactions between one another, resulting in both activation and inhibitory cross-talk. These cross-talk signals are important in targeted therapies and important in treatment failure, particularly when using single agents. To attempt to capture the cross talk between the Wnt, PI3K and MAPK pathway a heat map and Pearson correlation coefficient was performed on pathway marker expression from each pathway. The heat map displayed greater activity of all pathways, as the GS increased. When analysing individual markers the greatest correlation was seen between the PI3K and MAPK markers. In particular there was strong correlation between the downstream PI3K/mTOR marker p-S6 and the downstream MAPK marker p-MEK, both of which have shown to predict risk of biochemical relapse independent of GS. There was also positive correlation between the Wnt pathway and PI3K and MAPK pathways, however to a lesser degree. This

observation suggests possible crosstalk between the signals produced from each of these cancer pathways.

The PCA analysis in this study displays clustering of low-risk GS and high-risk GS. Each individual samples was put into a space based on expressional profile using IHC for all markers (PCA discussed in section 2.3). This finding strengthens the theory that different grades of cancer have different molecular or genetic profiles resulting in some behaving indolently and some behaving aggressively.

Cross talk and the combinatory effect of deregulating these pathways will be examined in the next chapter using mouse models.

3.4.5 Cell Signalling and DNA repair

Although this thesis did not aim to evaluate cell signalling or DNA repair genes, it was difficult to ignore them, given the high incidence of detected mutations using targeted NGS. 20/61 (32.8%) samples had a mutation in one of these genes. TP53 was the commonest occurring in 16 (26.2%) of samples. TP53 is the most commonly mutated gene in PCa and all human cancer. Recent data show mutations in over 50% of samples with metastatic CRPC (Robinson et al. 2015). This data and that of others (Barbieri et al 2012), suggests that these alterations are not exclusively late events, with localised PCa also harbouring lesions in TP53. This study does however only display mutations in TP53 in intermediate- and high-risk disease where they have a greater metastatic ability. Consistent with others (COSMIC), the mutational rate of the tumour suppressor gene, RB was low (3.6%). In contrast, RB is important in CRPC and is commonly inactivated with recent data showing RB1 loss in 21% cases. RB is thought to offer its protective role by modulating AR signalling and inhibits progression to castrate resistance (Aparicio et al. 2011).

There were 3 (4.9%) mutations in the DNA repair gene, ATM, in our cohort, slightly lower than that reported in a cohort of metastatic CRPC samples (7.3%) (Robinson et al. 2015). Similar to BRCA1/2, ATM is recruited and activated following DNA double-strand breaks. Encouragingly, following success of poly(-ADP-ribose) polymerase (PARP) inhibition (i) in selective breast cancer, similar benefits have been seen in patients with metastatic CRPC. Patients who were treated with the PARPi Olaparib, lived nearly

three times longer without their cancer worsening if their tumors had mutations in at least one of 12 DNA repair genes (Mateo et al. 2015).

3.4.6 Limitations

There are limitations in both types of experiments used in this chapter: IHC and targeted NGS. IHC is an observational analysis and although scoring methods (e.g. H score in this study) help with the consistency in reporting there are many other confounding factors. Type and duration of tissue fixation, for example, is known to affect IHC staining, and accuracy of staining is only as good as the antibodies used. PCa is often multifocal and it is difficult to account for this using IHC of a TMA. Although, in this thesis IHC scores have been correlated to outcome data such as biochemical relapse, it is hard to prove that the area examined on the TMA was directly the cause of this. Nevertheless, clear trends have been identified.

Tissue fixation and processing has also likely played a part in the targeted NGS. Only 61/200 (30.5%) DNA samples were successfully sequenced using the CHPv2 gene panel and Ion Torrent platform, consistent with the success rate from others (Hedegaard et al. 2014). Extracting DNA from FFPE samples is fraught with difficulty. The main reason for the failure is the non-efficient DNA amplification of the libraries, most probably as a result of DNA modifications caused by the fixation and subsequent storage. As discussed above, future DNA extractions could adopt a UNG step in order to improve DNA quality and NGS run success. Alternatively, fresh samples could be used. In fact, our research unit is currently making enquiries into the use of a twin core biopsy gun, whereby one sample is sent for histological analysis and the second adjacent sample is used for research.

In addition to problems associated with DNA extraction, errors can occur within the NGS platform, with reported error rates of between 0.1% and 1.0% (Shendure & Ji 2008). These can occur during DNA amplification; such as polymerase mistakes resulting in incorrect variant calls, or during the sequencing cycles or image analysis (Fox et al. 2014).

The CHPv2 gene panel is only a hotspot panel. All genes within the panel have been collaborated and matched to the COSMIC database. Although, the panel includes 50 genes, it only sequences commonly reported hotspots and not the whole gene. Some

genes like KRAS, which is short, are well covered but larger genes, such as PTEN, are not. Thus, this data is likely to represent an under estimate of the true mutational rate of each gene. The overriding advantages of using this hotspot panel however, are the ease of use, time and cost, in comparison to whole genome sequencing. This method is likely to represent a more cost-effective method that can be adopted in everyday clinical practice.

The median follow-up time was 5.3 years; therefore few men have died from their cancer. Future analysis in 5 or 10 years time, using overall survival and disease specific survival, will truly see the effect of deregulation of these pathways on PCa outcome.

3.4.7 Summary and future directions

In summary, this study highlights the importance of the Wnt, PI3K and MAPK signalling pathways in PCa. These results offer a glimpse into the molecular signature of individual PCa samples. This opens exciting future prospects, with the development of targeted assays or biomarker/genetic panels permitting personalised molecular profiles, thereby directing future therapies.

The results of targeted therapies in PCa clinical trials have on the whole been poor. The majority of these studies have been in the metastatic setting where there is a complex genetic profile making single agent targeted therapies ineffective. Historically, new treatments are tested first in the metastatic disease and then evaluated in the preoperative (or neoadjuvant) setting, however is this too late? Future trials could aim to use drugs in a neo-adjuvant or adjuvant setting in primary cancer treatment (prostatectomy or radiotherapy) as oppose to waiting for the onset of metastatic disease where the molecular signature is more complicated.

Until recently, there has been no selection criteria or personalisation of trial agent used, possibly contributing to the poor reported results. As discussed above, a recent study by Mateo et al (2015) has shown a three fold survival benefit by stratifying patients with a mutation in one or more DNA repair gene to the PARPi, Olaparib (Mateo et al. 2015). The incorporation of tumour molecular profiles (using both NGS and IHC) in future clinical trials is key for the success of these drugs. This study using IHC and the CHPv2

gene panel has shown the feasibility of obtaining molecular profiles for the Wnt, PI3K and MAPK pathways. Future studies could stratify their targeted agents based on these profiles. The recently designed molecular stratified randomised control trial, FOCUS4 in metastatic colorectal cancer has adopted these ideas. Here, four molecular cohorts are identified: BRAF mutant tumours, PI3K mutant tumours, KRAS or NRAS mutant tumours and EGFR dependent tumours. Each cohort is given a specific agent, for example, dual pathway inhibition using an AKT inhibitor and MEK inhibitor in KRAS or NRAS mutant tumours. The primary outcome is effect on progression free survival (further information is available at www.focus4trial.org).

A further hypothesis for targeted or selective treatment failure is the complex interactions between cancer pathways, resulting in both activation and inhibitory cross-talk. This chapter has highlighted some potential communications between pathways, in particular the PI3K and MAPK pathways. The next chapter will explore these further using mouse models. Deregulation of the Wnt, PI3K and MAPK pathways through specific gene loss or activated mutation will be investigated alone and in combination, assessing their effects on PCa initiation, progression and metastasise.

4 The effect of Wnt, PI3-Kinase (PI3K) and MAP-Kinase (MAPK) signalling pathway deregulation on murine prostate tumourigenesis

4.1 Introduction

The previous chapter has highlighted the importance of the Wnt, PI3K and MAPK signalling pathways in human PCa. In particular some markers of these pathways are expressed more commonly in higher risk disease and associated with biochemical relapse following surgery. Furthermore, it introduces the possibility of crosstalk or co-operation between these pathways.

To investigate this further, mouse models of PCa will be explored using Cre-lox technology and the probasin promoter. In particular, three oncogenic mutations will be used: the loss of Pten, mutation of β -catenin and K-Ras, as a means to activate the PI3K, Wnt and MAPK signalling pathways, respectively.

Our laboratory has previously shown in the mouse that the Wnt and MAPK pathway synergise to accelerate prostate tumourigenesis (Pearson et al. 2009). Others have also demonstrated crosstalk between the Wnt and PI3K pathways (Francis et al. 2013) and the PI3K and MAPK pathways (Mulholland et al. 2012) in mouse models. This chapter explores the effect of deregulation of all three pathways in a mouse model.

4.1.1 Chapter aims

To study the interactions and biology of the Wnt, PI3K and MAPK signalling pathways using mouse models as follows:

- a. Using Cre-lox based mouse models to conditionally modify 3 genes associated with these pathways: β -catenin, Pten, and K-Ras;
- b. To determine the extent of synergy of tumour formation between mutations in each of the pathways by generating and ageing cohorts of each combination of mutations;

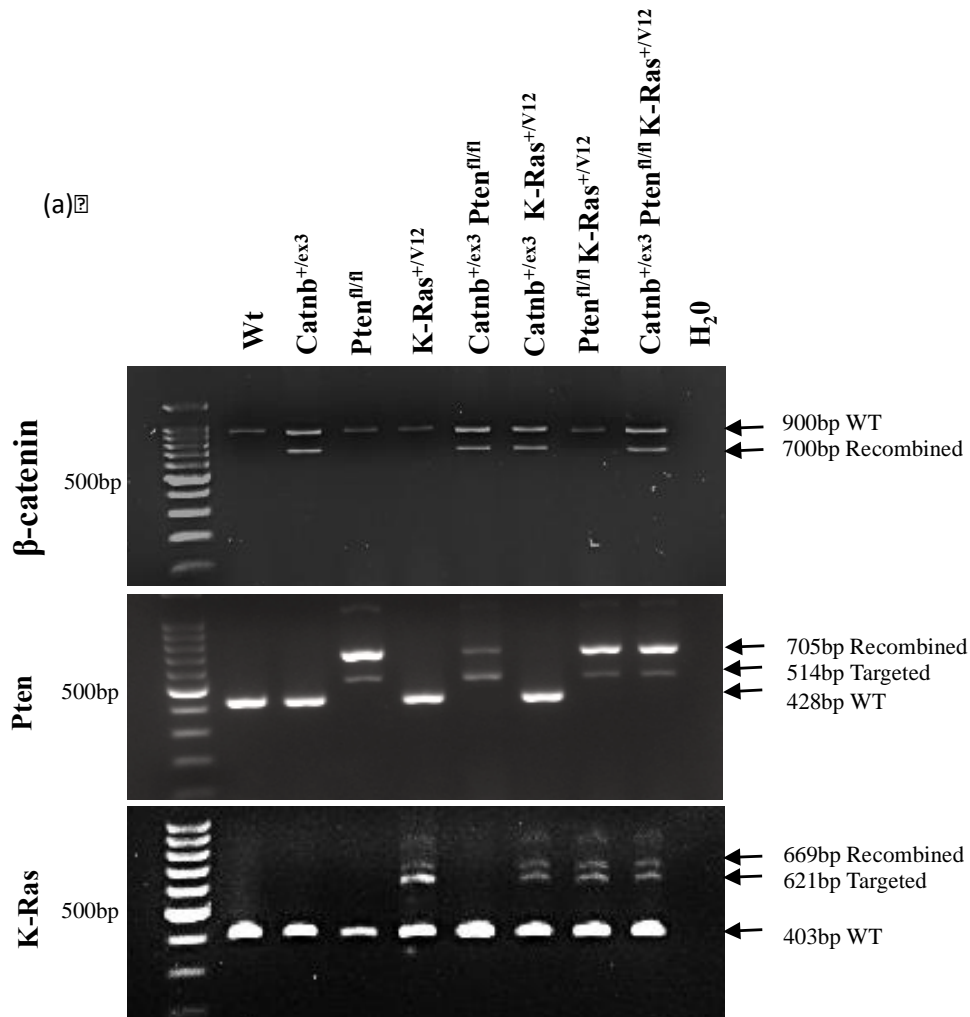
- c. To characterise the histological expression profiles (using immunohistochemistry) and protein levels (using Western blot) of each of the single, double and triple mutants;
- d. To assess the effect of pathway deregulation on lymph node metastasis.

4.2 Results

4.2.1 Generation of prostate specific mouse models using the Probasin-Cre (Pb-Cre4) transgene

In order to investigate the effects of Pten loss and activation of β -catenin and K-Ras in prostate epithelium, Cre-LoxP technology was adopted using the Pb-Cre4 promotor (X. Wu et al. 2001). For successful recombination of targeted genes in murine prostate epithelium, the Pb-Cre4 transgene must be transmitted paternally. If transmitted maternally a mosaic recombination results, producing an inconsistent prostate phenotype with male mice developing mammary tumours for example. Accurate genotyping and breeding plans were therefore adopted as discussed in chapter 2. Cohorts of male mice were generated (n=15) including wild-type (WT, Pb-Cre4⁺ Catnb^{+/+}Pten^{+/+}K-Ras^{+/+}), single mutants (Pb-Cre4⁺: Catnb^{+/ex3}, Pten^{fl/fl}, K-Ras^{+/V12}), double mutants (Pb-Cre4⁺: Catnb^{+/ex3}Pten^{fl/fl}, Catnb^{+/ex3}K-Ras^{+/V12}, Pten^{fl/fl}K-Ras^{+/V12}) and triple mutant (Pb-Cre4⁺ Catnb^{+/ex3}Pten^{fl/fl}K-Ras^{+/V12}). Animals were then monitored for signs of illness and sacrificed if found to display signs of ill health or at termination of the experiment (500 days). In order to monitor disease progression, an early time point was also assessed, with an additional 6 mice harvested from each cohort at day 100.

To confirm deletion of Pten and activation of the β -catenin and K-Ras alleles upon activation of the Pb-Cre4 recombinase, two methods were adopted. Firstly, DNA of 100-day-old prostate tissue (n=3) of Pb-Cre4⁺ and Pb-Cre4⁻ mice were assessed for targeted alleles for recombined Pten, β -catenin and K-Ras using PCR. Recombination of each target gene was present in all combinations of gene mutations (Figure 40a). Secondly, the LacZ reporter gene was used to confirm recombination. Upon recombination, the LacZ gene expresses β -galactosidase, which stains blue following X-gal staining. Positive staining was present in all four lobes of the prostate in Pb-Cre4⁺LacZ⁺ 100 day old mice with greatest staining in the anterior and dorso-lateral lobes. Minimal staining was present in Pb-Cre4⁻LacZ⁺ age matched controls (Figure 40b). Further staining, was also evident to a lesser degree in the testis, urethra and epididymis of Pb-Cre4⁺LacZ⁺ mice consistent with previous reports (X. Wu et al. 2001).



(b)

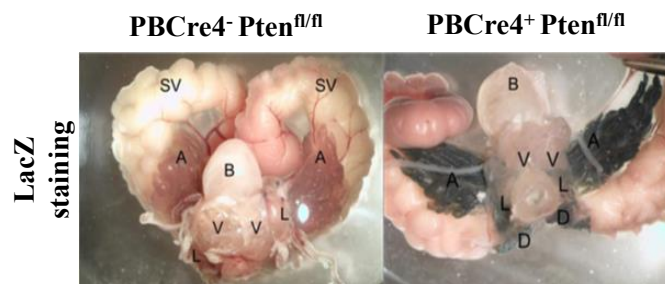


Figure 40: Recombined PCR and LacZ staining of murine prostates. (a) Recombined PCR performed on DNA harvested from mouse prostate tissue at 100 days, demonstrating successful recombination of each gene (β -catenin, Pten and K-Ras) within each combinations of mutations. (b) **LacZ staining:** Cre-mediated recombination is further shown by β -galactosidase reporter gene (LacZ) expression in the prostate using Pten-deficient (Pten^{fl/fl}) mice at 100 days of age. When cleaved by β -galactosidase X-gal turns blue. Pb-Cre4⁺ prostate tissue demonstrates extensive recombination within all lobes (A= anterior lobes, B= bladder, D = dorsal lobes, L = lateral lobes, SV = seminal vesicles) of the prostate (to a lesser degree in the ventral lobes) compared to Pb-Cre4⁻ prostate tissue.

4.2.2 Pten loss and activation of K-Ras and β -catenin (triple mutants) cooperate to accelerate prostate tumourigenesis

All WT and K-Ras single mutant mice survived until the end of the experiment. As previously reported (Pearson et al. 2009), K-Ras single mutant mice (Pb-Cre4⁺ K-Ras^{+V12}) did not produce PCa. All other mouse models developed extensive locally advanced adenocarcinoma of the prostate (100% incidence) resulting in mortality. The cause of death was ureteric or bladder outflow obstruction secondary to the local effects of the primary tumour (Figure 41A-B).

Macroscopic phenotype



Figure 41: Macroscopic tumour phenotype. (A) Large bilateral locally invasive prostate tumour (red arrowhead) causing bladder outflow obstruction. Black arrow demonstrating enlarged bladder with turbid infected urine. (B) Left kidney demonstrating dilatation (hydronephrosis/hydroureter) of the renal pelvis and proximal ureter (*) caused by compression secondary to the prostate tumour. (C) Significant retroperitoneal/para-aortic lymphadenopathy (red arrow).

Consistent with reports from others (S. Wang et al. 2003; Pearson et al. 2009), homozygous deletion of Pten (Pb-Cre4⁺Pten^{fl/fl}) and activation of β -catenin (Pb-Cre4⁺Catnb^{+ex3}) alone resulted in a reduced median survival of 407 days and 383 days, respectively. All double mutant mice had reduced survival when compared to single mutants ($p < 0.0001$, Log-Rank) (Figure 42). Mice with activation of both β -catenin and K-Ras (Pb-Cre4⁺ Catnb^{+ex3}K-Ras^{+V12}) had a reduced median survival of 182 days, as

reported previously (Pearson et al. 2009). Mice with loss of Pten and activation of β -catenin (Pb-Cre4⁺ Catnb^{+/ex3}Pten^{fl/fl}) also had a reduced median survival of 140 days. Consistent with work from others (Mulholland et al. 2012), mice with both Pten loss and activation of K-Ras (Pb-Cre4⁺ Pten^{fl/fl}K-Ras^{+V12}) had a reduced median survival of 238 days (p<0.0001, Log-Rank). A novel mouse model was to study Pten loss in addition to activation of β -catenin and K-Ras (Pb-Cre4⁺ Catnb^{+/ex3}Pten^{fl/fl} K-Ras^{+V12}, triple mutants). Triple mutant mice demonstrated significantly earlier morbidity and mortality compared to double mutant mice (n=15). All triple mutant mice succumbed to their disease by 130 days (median 96 days p<0.0001, Log-Rank) (Figure 42).

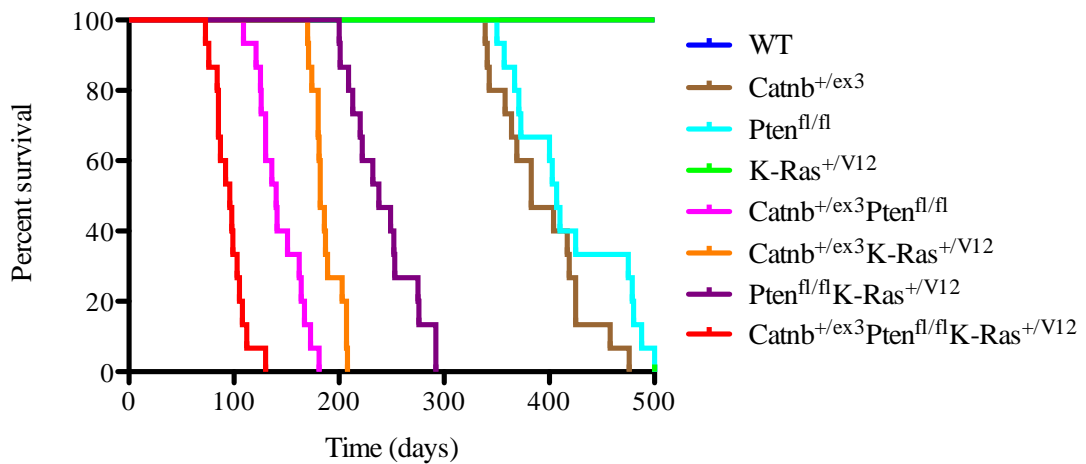


Figure 42: Kaplan-Meier survival curve. The median survival for triple mutant (Pb-Cre4⁺ Catnb^{+/ex3}Pten^{fl/fl} K-Ras^{+V12}) mice was significantly lower than double mutants (p<0.0001, Log-Rank): 96 days (range = 76-130), compared to 238 days (range 200-292), 182 days (range 170-208) and 140 days (range 109-181) for the double mutants: Pb-Cre4⁺ Pten^{fl/fl} K-Ras^{+V12}, Pb-Cre4⁺ Catnb^{+/ex3} K-Ras^{+V12} and Pb-Cre4⁺ Catnb^{+/ex3}Pten^{fl/fl}, respectively. All double mutant combinations had a significantly shorter survival when compared to single mutants (p<0.0001, Log-Rank). The survival of Pb-Cre4⁺ Catnb^{+/ex3} and Pb-Cre4⁺ Pten^{fl/fl} was 383 days (range 339-476) and 373 (range 350-479), respectively. Pb-Cre4⁺ K-Ras^{+V12} and wild-type mice all survived to the end-point of the experiment (500 days). Wild-type (WT), Catnb^{+/ex3} (β -catenin).

4.2.3 Tumour progression occurs in a stepwise fashion from mouse PIN (mPIN) to invasive adenocarcinoma similar to that of human disease

mPIN is characterised by increased cell proliferation within the glands with frequent cellular atypia (Figure 43D). There is positive nuclear AR staining (Figure 43E) of the luminal cells and positive membranous CK5 staining of the basal layer (Figure 43F) in mPIN lesions. Microinvasive adenocarcinoma occurs when the normal glandular structure begins to get distorted with some epithelial cells invading into the surrounding stroma (typically <1mm). At the site of invasion there is a breach in the basal layer with loss of CK5 and positive AR staining of the cells, which invade the stroma (Figure 43G-D). In invasive adenocarcinoma the whole basal layer is breached with loss of CK5 positivity (Figure 43L), allowing invasion of epithelial cells into the stroma. Loss of staining of basal cell markers (e.g CK5 or p63) is a hallmark of human PCa, and is used routinely in clinical practice to evaluate problematic or suspicious lesions. As the prostate tumours progress, the prostate glandular architecture becomes increasingly distorted as glands fuse together and areas of cribriform pattern form, pathognomonic of Gleason pattern 4 (Figure 43J & 44C). Furthermore, features of Gleason pattern 5 develop; with single PCa cells appearing in the stroma (Figure 44B). Tumours are rapidly proliferating with frequent mitosis and occasional apoptotic bodies (Figure 44A&C).

WT mice had histologically normal prostates (Figure 43A) with an intact basal layer confirmed by positive CK5 staining (Figure 43C). Although androgen receptor (AR) staining can cause some stromal activity, the luminal epithelial cells stain more avidly (Figure 43B). All tumour models examined demonstrated a stepwise progression from mouse prostate intraepithelial neoplasia (mPIN) to microinvasive and invasive adenocarcinoma, with each having histological, cytological and immunohistochemical characteristics as illustrated in Figure 43.

Histological Characterisation

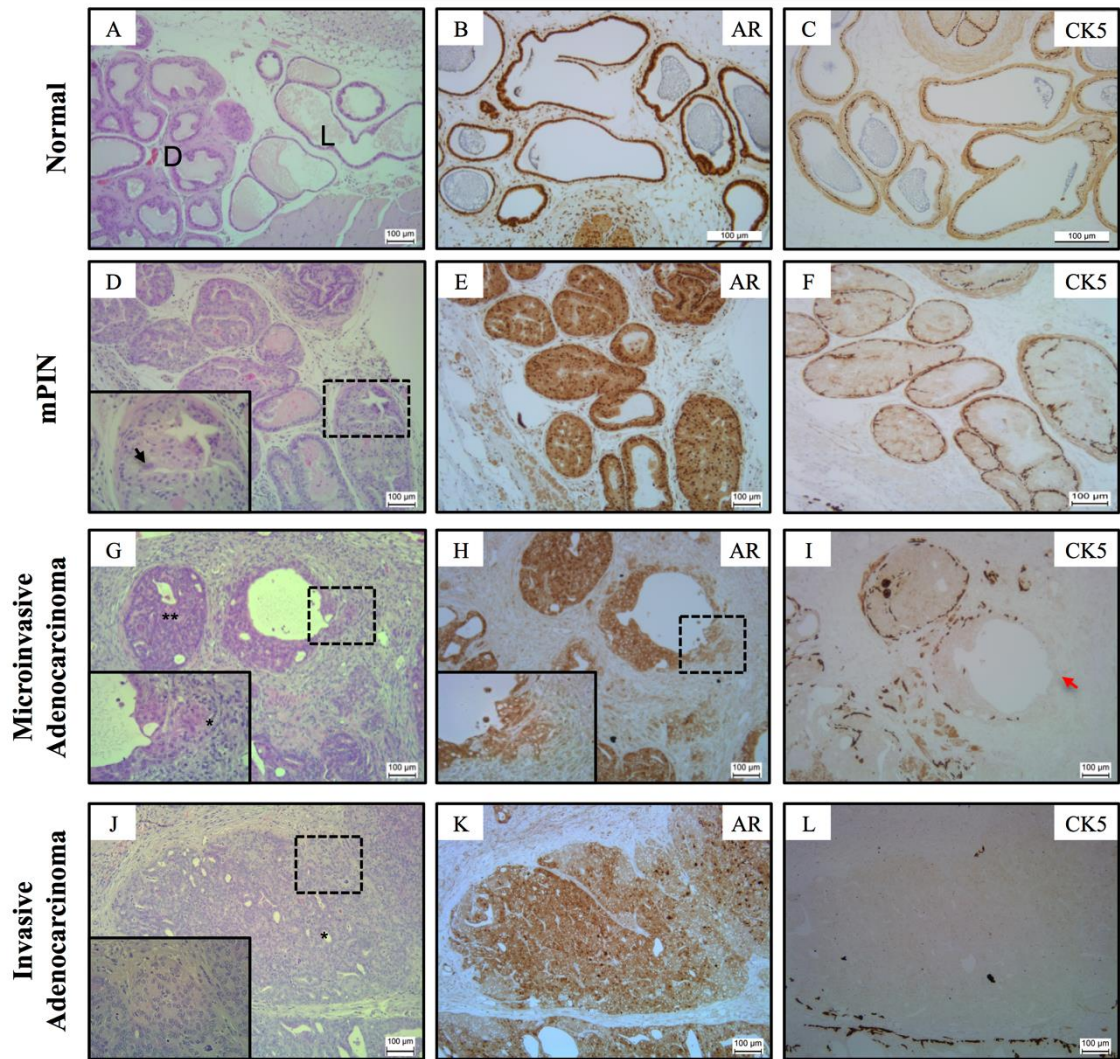


Figure 43: Histological characterisation of normal, mouse prostate intraepithelial neoplasia (mPIN), microinvasive adenocarcinoma and diffuse adenocarcinoma of the mouse prostate. (A-C) The histologically normal prostate has different glandular patterns dependent on lobe; the dorsal (D) lobe has glands with frequent mucosal folds protruding into the lumen when compared the lateral (L) lobe, which has larger glands with fewer mucosal folds. Androgen receptor (AR) immunohistochemistry demonstrates avid staining of the luminal cells with cytokeratin (CK) 5 staining the membrane of the basal layer abutting the basement membrane in a continuous fashion. (D-F) mPIN has a characteristic appearance with increased cell proliferation within the glands with frequent cellular atypia (arrow). The CK5 staining once again remains continuous. (G-I) The glandular structure begins to get distorted with focal areas of microinvasion (*) of epithelial cells into the surrounding stroma (microinvasive adenocarcinoma) staining positive for AR. The continuous CK5 staining basal layer is lost at the site of invasion. Note the adjacent area of mPIN (**), where the gland is packed with cells with a normal intact basal layer. (J) Hematoxylin and eosin staining of prostate adenocarcinoma sections demonstrate diffuse invasion of epithelial cells into the stroma, with fusion of glands and areas of cribriform pattern, which is pathognomonic of Gleason pattern 4. (K) AR staining demonstrates more intensely epithelial cells invading the stroma with loss of the basal marker CK5 (L).

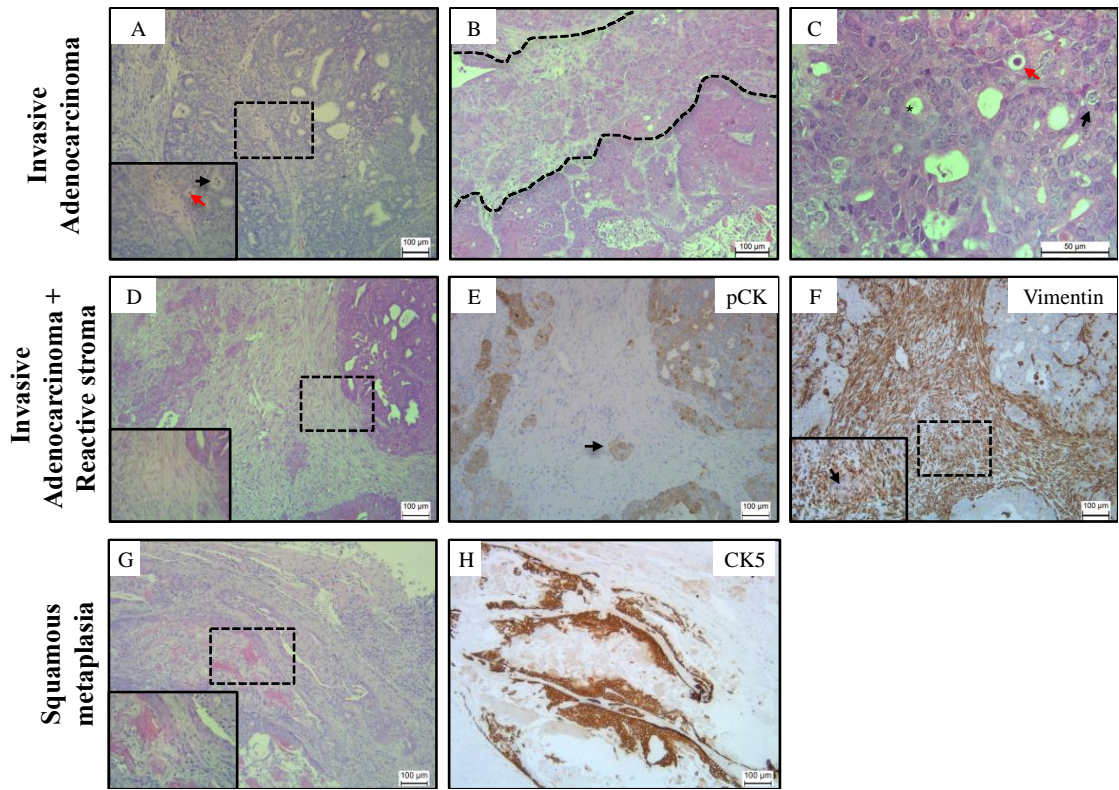


Figure 44: Histological characterisation. (A) Tumours contain frequent mitosis (black arrow), and occasional apoptotic bodies (red arrow). When mice succumb to disease (B), diffuse invasion of epithelial cells into the stroma is seen (between dotted lines). Higher power magnification of hematoxylin and eosin stained tumours with widespread cribriform pattern (C) (*), frequent mitosis (black arrow), and occasional apoptotic bodies (red arrow). (D) Invasive adenocarcinoma with spindle mesenchymal cells in the stroma (inset). (E) Pan-cytokeratin (pCK) IHC staining positive for epithelial cells in glands within the stroma (arrow). (F) Mesenchymal marker vimentin staining displaying positive staining of invasive glands within the stroma (inset arrow) a characteristic of EMT. (G) Diffuse adenocarcinoma with areas of keratin formation adjacent to flattened nuclei (inset) at areas of squamous metaplasia. (H) Areas of squamous metaplasia stain avidly for basal marker CK5.

4.2.4 Combinatorial pathway mutations shifts the spectrum of lesions to a more aggressive phenotype

It is often difficult to compare progression of disease between different mouse models, as most cases studied develop locally advanced tumours, with few having significant metastatic disease to cause death. Consequently, the percentage of invasive adenocarcinoma (as defined by the consensus report from the Bar Harbour meeting (Shappell et al. 2004)), between each mouse cohort at 100 days and at death was estimated. WT and single K-Ras mutant mice had histologically normal prostate at both time points. Single β -catenin or Pten mutant mice displayed predominately mPIN with occasional foci of microinvasion adenocarcinoma but no diffuse invasion at 100 days. At death (endpoint) single β -catenin or Pten mutant mice displayed invasive adenocarcinoma, with a mean percentage of 16.7% (95% CI: 8.1-25.2) and 50.0% (95% CI: 40.6-59.4), respectively. At 100 days β -catenin/K-Ras double mutant mice had no areas of invasive adenocarcinoma but displayed mPIN with widespread microinvasive disease. Upon aging, 23.3% (mean, 95% CI: 10.6-36.0) of these mice displayed invasive adenocarcinoma. β -catenin/Pten double mutants had a mean invasive adenocarcinoma rate of 60% (95% CI: 35.2-84.8) at 100 days and 83.3% (95% CI: 69.0-97.7) at death. Pten/K-Ras double mutant mice had small areas of invasion (mean 10%) at 100 days, which increased to a mean of 61.7% (95% CI: 53.8-69.6) at death. Finally, triple mutants had the most aggressive histological characterisation with a mean of 100% (95% CI: 91.1-102.1) invasive adenocarcinoma at 100 days or death (maximum 130 days) (Figure 45).

In summary, triple mutant mice have a more aggressive phenotype with more rapid progression to invasive adenocarcinoma resulting in a significantly reduced survival when compared to double and single mutant mice.

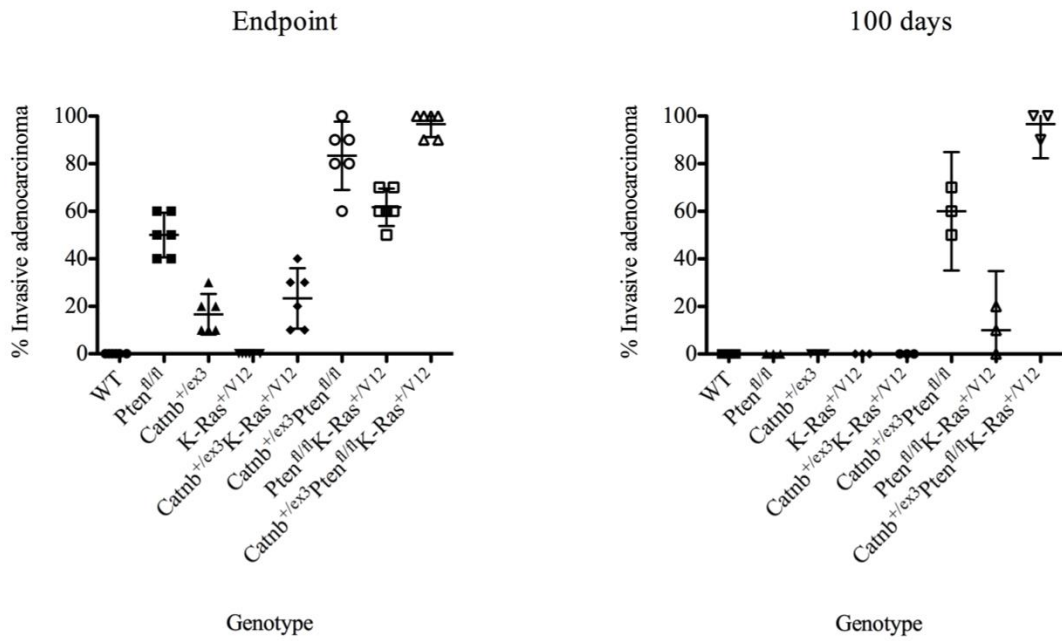


Figure 45: Percentage invasive adenocarcinoma at endpoint (n=6) and 100 days (n=3) as function of genotype. Compound (double and triple) mutant mice have a greater percentage of invasive adenocarcinoma at 100 days and endpoint (death or 500 days) compared to single and WT mice. Mean with error bars = 95% CI.

In human disease, prostate specific antigen (PSA) is not only used in early detection of PCa but also used to monitor disease progression and response to treatment. Typically, more aggressive tumours have a shorter doubling-time. Unfortunately there is no surrogate marker for PCa in the mouse. To attempt to capture the rate of progression of tumours, tumour burden was estimated by weighing the prostates at serial time points (Figure 46). In all combinations of mutations diffuse invasive adenocarcinoma was observed at death other than in K-Ras single mutant mice, which interestingly were histologically normal as described above. Each tumour reached a similar size at death across all genotypes, however triple mutants had a significantly greater rate of growth compared to double and single mutant mice (Figure 46).

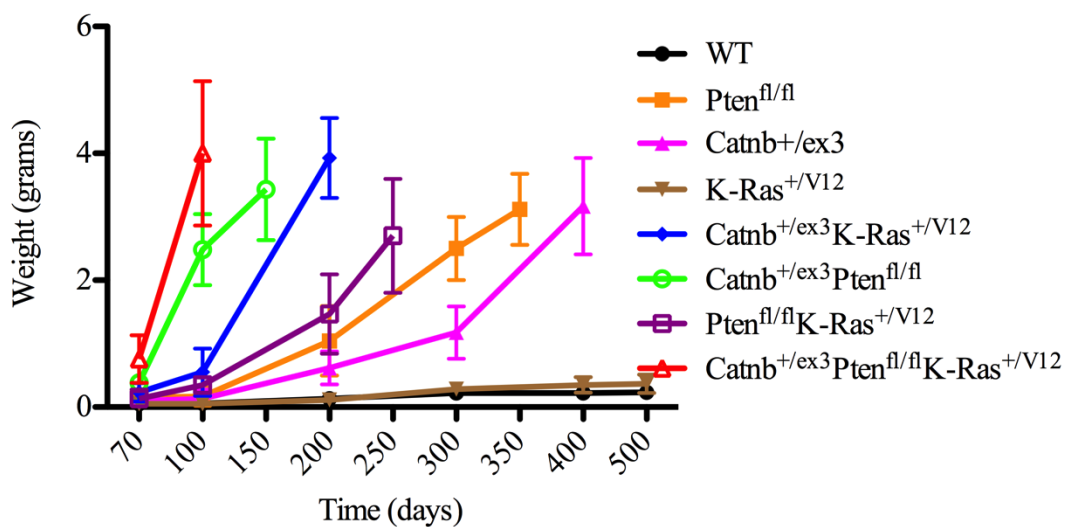
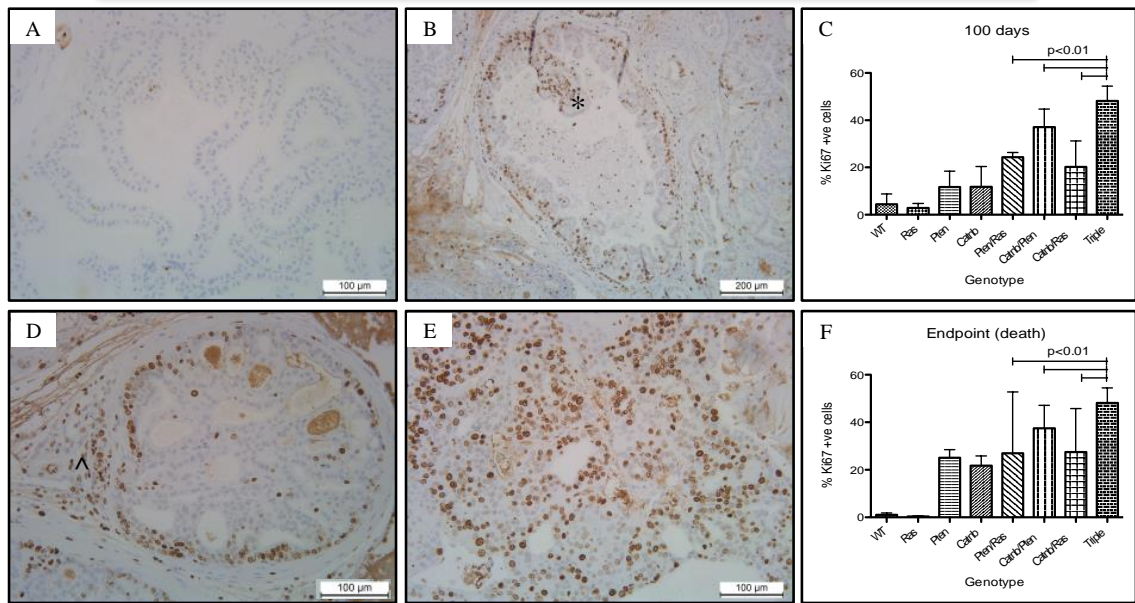


Figure 46: Rate of growth of prostate tumours (mean + error bars = 95% CI). Dry prostate gland weights (n=3) were recorded and plotted against time so as to assess the rate of growth of tumours. $Pb-Cre^+ Catnb^{+/ex3} Pten^{fl/fl} K-Ras^{+/V12}$ prostate tumours have a significantly faster rate of growth compared with double mutants ($Pb-Cre^+; Pten^{fl/fl} K-Ras^{+/V12}$, $Catnb^{+/ex3} K-Ras^{+/V12}$, $Catnb^{+/ex3} Pten^{fl/fl}$) and single mutants ($Pb-Cre^+; Catnb^{+/ex3}$, $Pten^{fl/fl}$, $K-Ras^{+/V12}$).

This is further shown using immunohistochemistry for the proliferation markers Ki67 and BRDU (Figure 47). The level of Ki67 positive cells in wild-type mice is low (Figure 47). Expression level increased progressively from mPIN (Figure 47B) through microinvasion (Figure 47D) to diffusely invasive adenocarcinoma (Figure 47E). Proliferation rate not only correlates with progression of disease but also with the number of induced mutations. Triple mutant mice have a greater percentage positivity of Ki67 at 100 days and at experimental endpoint (500 days or earlier if sick) compared to double and single mutants ($p < 0.01$, Figure 47C & 47F).

In summary, using prostate weight as a surrogate marker to assess tumour burden, and Ki67 and BRDU to assess proliferation rate, this study demonstrates a more aggressive phenotype in triple mutant mice compared to single/double mutant mice. These findings outbalance the rate of apoptosis, which is low (<1%) across all tumours with no significant difference between genotypes.

Ki67 Expression



BRDU Expression

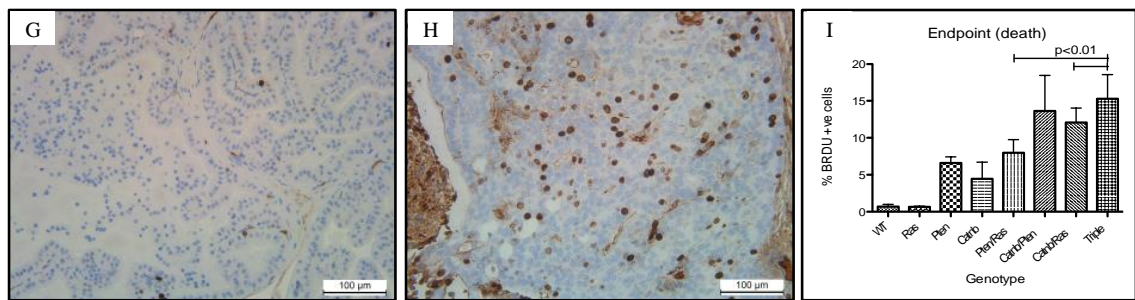


Figure 47: Proliferation of prostatic lesions using Ki67 and BRDU. (A) Wild-type prostatic epithelium demonstrates minimal proliferation. (B) Areas of mPIN have tufting of epithelium into gland (*), which is avidly stained nuclear staining for ki67. (D) Similarly, areas of focal invasion display strong staining at the basement membrane and particularly at the site of invasion into the stroma (^). (E) Diffuse invasive adenocarcinoma has widespread staining, as the normal glandular architecture is lost. (C+F) Mean %Ki67 staining according to genotype at 100 days and endpoint, error bars represent 95% confidence interval (CI). Triple mutants have significantly greater Ki67 staining compared with all double mutant combinations ($p < 0.01$). Furthermore, double mutants have a greater % Ki67 staining than single mutants at 100 days ($p < 0.01$). BRDU staining in wild-type prostate epithelium (G) and diffuse adenocarcinoma of the prostate (H). (I) Triple mutants have significantly greater BRDU nuclear staining compared with $Pb-Cre4^+; Pten^{fl/fl}; Ras^{+/V12}$ and $Catnb^{+/ex3}; K-Ras^{+/V12}$ but not $Pb-Cre4^+; Catnb^{+/ex3}; Pten^{fl/fl}$ double mutants ($p < 0.01$).

4.2.5 Additional pathological phenotypes

4.2.5.1 Tumours across all genotypes demonstrated reactive desmoplastic stroma, with evidence of epithelial-mesenchymal transition (EMT)

All tumour models investigated displayed reactive desmoplastic stroma, however this was more apparent in models where there was loss of Pten. This occurred in the stroma adjacent to mPIN and invasive adenocarcinoma (Figure 44D). Interestingly, some reported aggressive mouse models, such as Pten and p53 deletion (Martin et al. 2011), develop sarcomatoid areas in the stroma, which can have a similar appearance to the reactive stroma seen here. Sarcomatoid lesions typically have spindle shape cells in the stroma, which co-stain for both epithelial (e.g. pan cytokeratin, pCK) and mesenchymal (e.g. vimentin) IHC markers. Although there were isolated glands in the stroma with staining for both pCK and vimentin (Figure 44E & 44F), in contrast to sarcomatoid lesions, the spindle shaped stromal cells only stained positive for vimentin.

Areas of tumour staining positive for both pCK and vimentin in the epithelium in this study are suggestive of an epithelial-mesenchymal transition (EMT), which is thought to be important in progression of disease and evident in most mouse PCa models.

4.2.5.2 Mice harbouring a mutation of β -catenin demonstrate adenocarcinoma with squamous metaplasia

Squamous metaplasia occurs when normal epithelial cells develop a squamous morphology becoming flattened and release keratin before being shed into the lumen. When exposed to additional stress such as carcinogens or chronic inflammation, dysplasia can occur resulting in squamous cell carcinomas. Squamous metaplasia with keratin formation (Figure 44G) is characterised by positive staining for CK5 (Figure 44H), unlike that seen in prostate adenocarcinoma. Squamous metaplasia was evident in all models investigated where a mutated β -catenin allele was present, an observation also noted by others (Pearson et al. 2009; Francis et al. 2013).

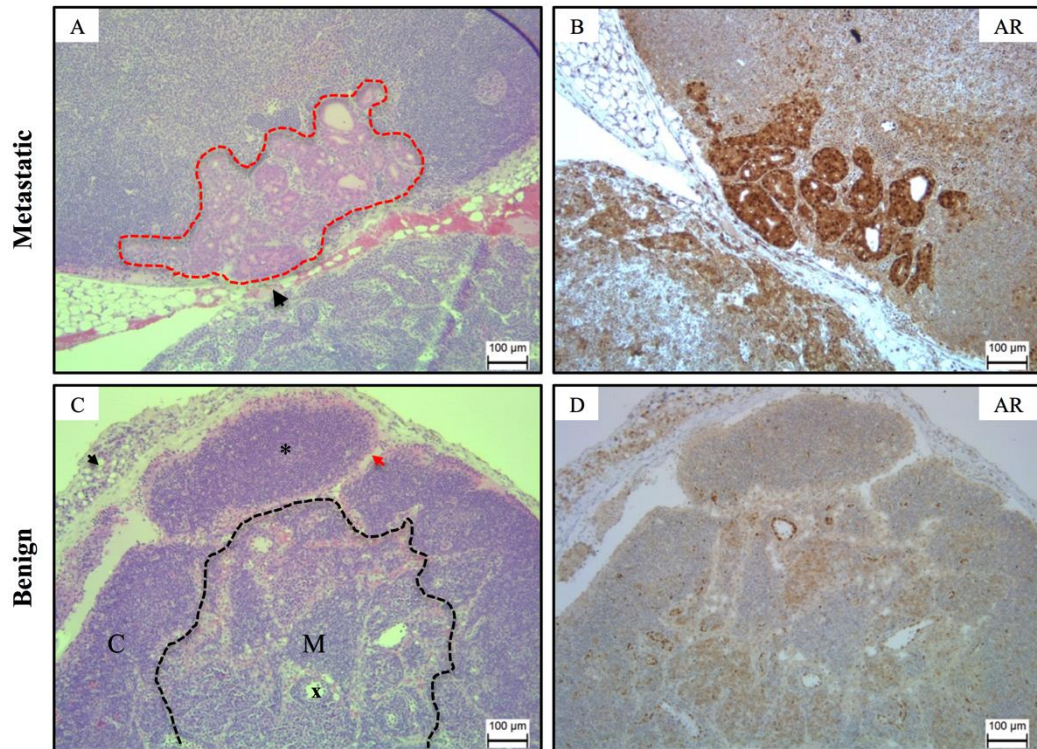
4.2.6 Both K-Ras and β -catenin mutations drive metastatic spread in the context of loss of Pten

In human PCa, metastasis usually spread to lymph nodes and bone. To assess metastatic potential in the mouse, at the time of sacrifice the retroperitoneal lymph nodes were harvested for each genotype and assessed histologically for metastasis (Figure 48).

In the presence of Pten loss, both additional mutations of either K-Ras or β -catenin developed lymph node metastasis (Figure 48E). This occurred at an incidence of 60% (n=6/10) in Pten/K-Ras and 10% (n=1/10) in β -catenin/Pten double mutant mice. β -catenin/K-Ras mutants did not develop any lymph node metastasis. Lymph fluid initially drains into the capsular region of the lymph gland and this is usually the first place where metastasis occurs. On H&E staining, metastatic lymph nodes have areas of prostatic epithelium located at the capsule of the node, with fusion of glands and a cribriform pattern, morphologically similar to that seen in the corresponding prostate tumour specimens (Figure 48A). They also stained strongly positive for AR (Figure 48B).

In contrast with other reports (S. Wang et al. 2003), Pten loss alone was insufficient to cause lymph node metastasis. Similar results were also seen for β -catenin and K-Ras single mutant mice. Interestingly, triple mutant mice did not have nodal metastasis, but reactive nodes with a nodular architecture with an abundance of immunoblasts draining an infective or toxic zone.

Lymph node characterisation



E Nodal Metastasis (n=10)	
Genotype	% Metastasis
WT	0
Catnb ^{+/ex3}	0
Pten ^{fl/fl}	0
K-Ras ^{+V12}	0
Catnb ^{+/ex3} Pten ^{fl/fl}	10
Catnb ^{+/ex3} K-Ras ^{+V12}	0
Pten ^{fl/fl} K-Ras ^{+V12}	60
Catnb ^{+/ex3} Pten ^{fl/fl} K-Ras ^{+V12}	0

Figure 48: Lymph node characterisation. (A) Metastatic prostate epithelium extending from the capsule (black arrow) and infiltrating into the node (red-dotted line). (B) Metastatic node staining avidly for AR. (C) Benign reactive node with the outer cortex (C) and inner medullar (M) separated by the dotted black line. The capsule and marginal sinus (black arrow) surrounds the node with the cortex separated by cortical sinuses (red arrow). Germinal center within the cortex of the node (*). (D) Minimal non-specific AR staining in a benign node. (E) Summary of % of metastatic nodes in each mouse model.

4.2.7 Pathway signalling analysis

To determine the activity of the PI3K, Wnt and MAPK pathway in each mouse cohort, the expression of different antibodies against downstream markers or target genes associated with each pathway was assessed and validated using both immunohistochemistry (IHC) and western-blot analysis.

4.2.7.1 Single mutants show variable pathway readouts

β -catenin single mutant tumours only demonstrated activation of the Wnt signalling pathway, with both increased nuclear β -catenin (Figure 49E) and positive membranous expression of the Wnt target gene, CD44 (Figure 49F) on IHC. In contrast, using western-blot analysis, there was no significant difference in protein level of total β -catenin when compared to WT (Figure 52). This model displayed low expression of both p-AKT^{Thr308} and p-AKT^{Ser473} (Figure 50 G-H) downstream markers of the PI3K pathway, consistent with WT and a reduced level of p-ERK1/2 compared to WT (Figure 51 and 52) suggesting possible compensatory negative feedback of the MAPK pathway. There was also widespread cytoplasmic and stromal staining for the downstream mTOR marker p-S6^{Ser240-244} (Figure 50I) similar to that seen in WT (Figure 50C).

K-Ras single mutant mice demonstrate very little activation of all three pathways: Wnt, PI3K and MAPK with low protein and expression levels of β -catenin, p-AKT^{Thr308}, p-AKT^{Ser473} and p-ERK1/2 (Figures 49-53). This is not surprising given the normal histological findings of these mice. In fact, the protein level of Pten is elevated in K-Ras single mutant mice (Figure 53B), which could represent a compensatory mechanism, preventing tumourigenesis in these mice. To explore this mechanism further, other markers could be analysed such as LKB1 or AMPK. Surprisingly, the protein level of p-ERK1/2, a downstream marker of the MAPK pathway, was significantly higher in WT mice (Figure 52 and 53D) when compared to K-Ras single mutant mice. This was consistent with nuclear positive p-ERK1/2 staining in WT mice (Figure 51B).

Pten null tumours demonstrated predominantly activity of the PI3K pathway with minor deregulation of Wnt and MAPK signalling. The tumours stained positive for p-AKT^{Thr308} and p-AKT^{Ser473} (Figure 50D-E) compared with no staining for WT controls (Figure 50A-B). Activation of the PI3K pathway was further confirmed using western-blot, with significantly elevated protein levels of p-AKT compared to WT (Figure 52 and 53A).

Pten null mice also demonstrate a degree of aberrant Wnt and MAPK signalling with evidence of nuclear expression of β -catenin (Figure 49C), cytoplasmic staining of p-MEK and heterogenous nuclear staining of p-ERK1/2 (Figure 51C-D). These findings indicates a degree of crosstalk between pathways even with single gene mutations.

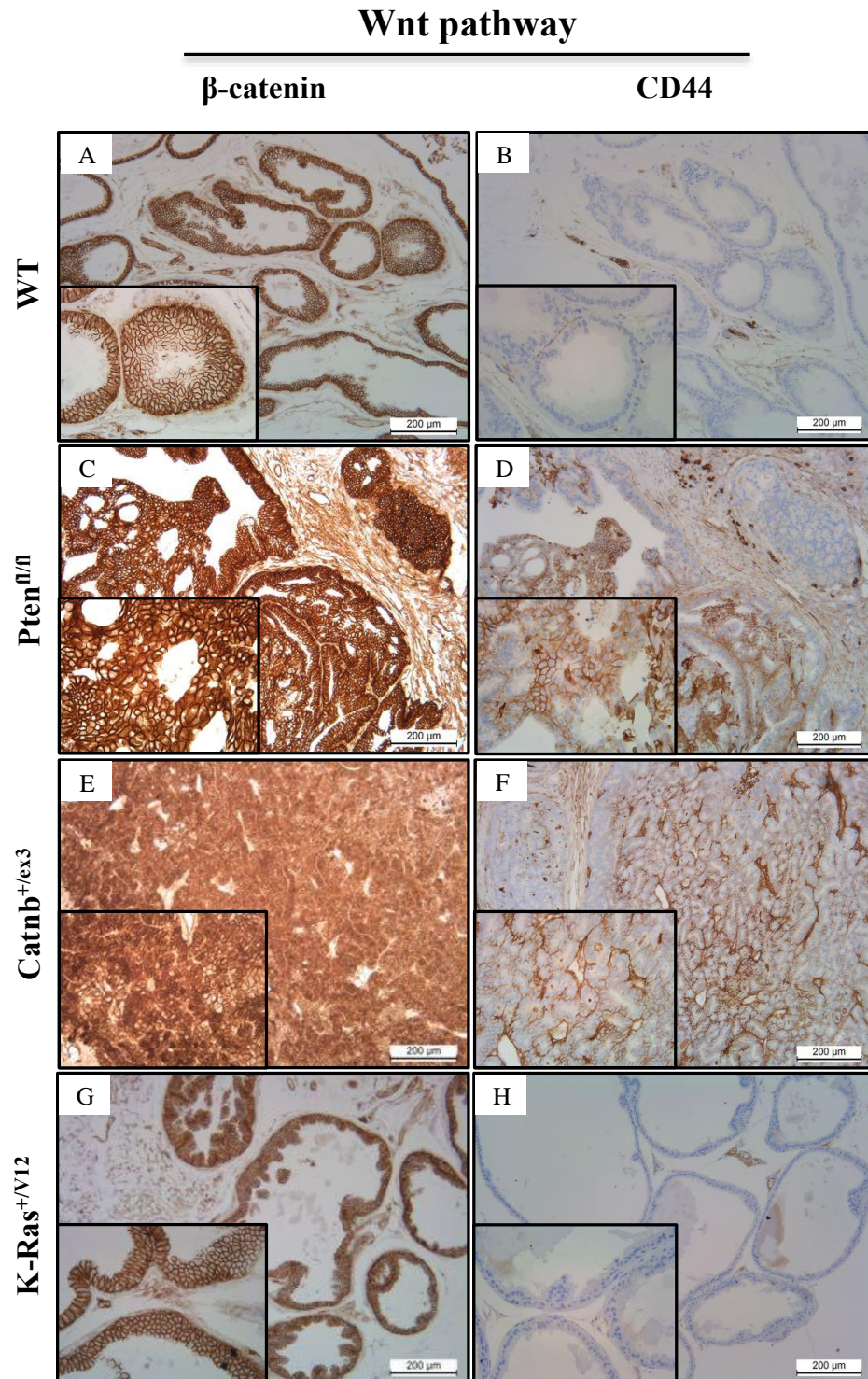


Figure 49: Immunohistochemistry of Wnt pathway markers for WT and single mutant mice. Immunohistochemistry was performed on cohorts of mice (n=4) at the endpoint of the experiment (500 days or when sick) using antibodies against β -catenin and the Wnt target gene CD44. WT and K-Ras^{+V12} mice had positive membranous staining for β -catenin (A+G) and no staining for CD44 (B+H). Pten^{f1/f1} demonstrated heterogeneous cytoplasmic and occasional nuclear staining for β -catenin (C) and membranous staining for CD44 (D). Catnb^{+ex3} had diffuse nuclear and cytoplasmic staining of β -catenin (E) and membranous staining of CD44 (F).

PI3-Kinase pathway

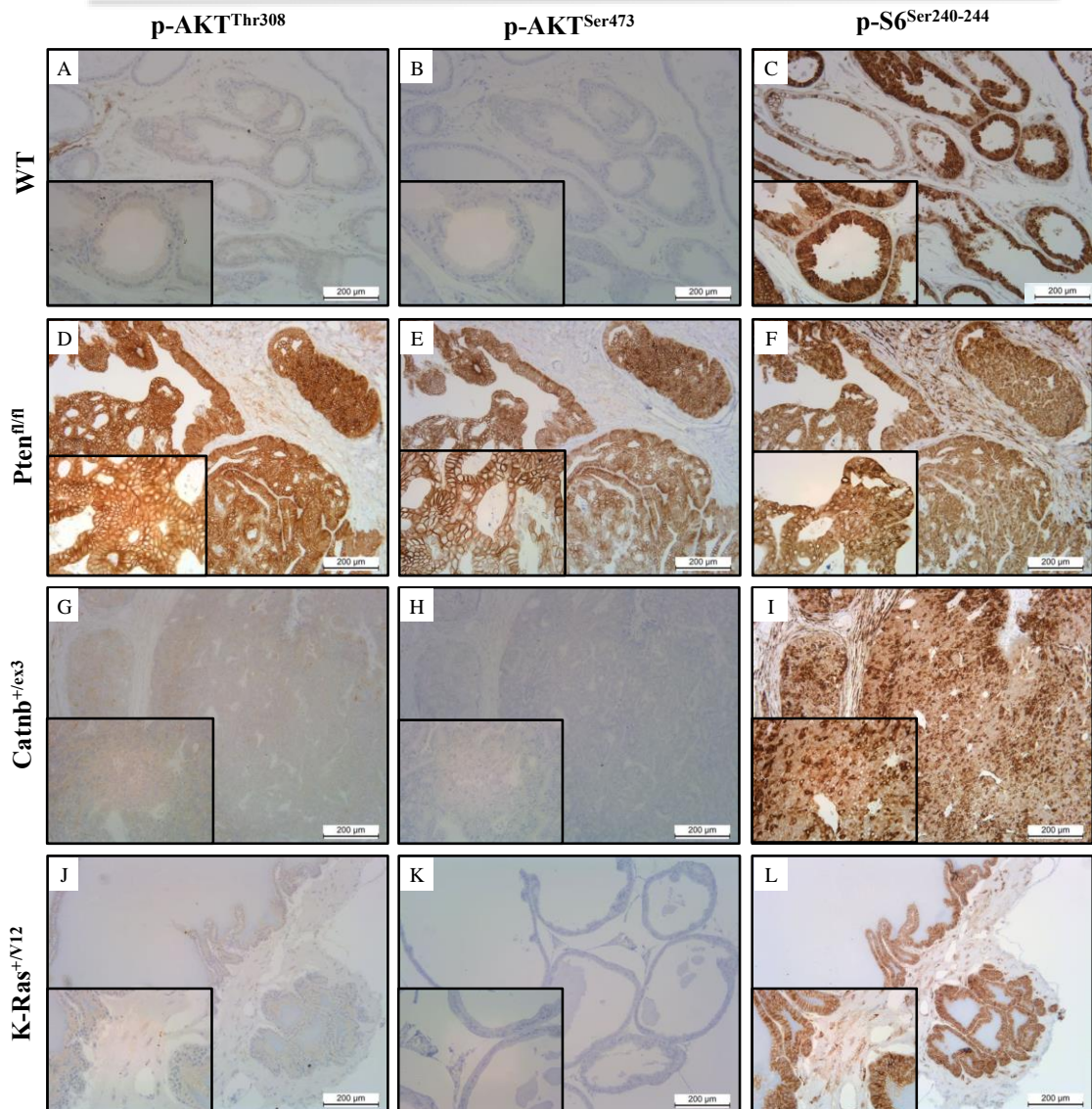


Figure 49: Immunohistochemistry for PI3-Kinase signalling pathway markers for WT and single mutant mice. Immunohistochemistry was performed on cohorts of mice (n=4) at the endpoint of the experiment (500 days or when sick) using antibodies against p-AKT^{Thr308}, AKT^{Ser473} and p-S6^{Ser240-244}. WT mice had negative staining for p-AKT^{Thr308} (A), AKT^{Ser473} (B) and heterogeneous positive nuclear and cytoplasmic staining for p-S6^{Ser240-244} (C). Pten^{fl/fl} stained avidly for all three markers (D-F). Catnb^{+/ex3} and K-Ras^{+/V12} had negative staining of p-AKT^{Thr308} (G+J), AKT^{Ser473} (H + K) and positive staining for p-S6^{Ser240-244} (I and L).

MAP-Kinase pathway

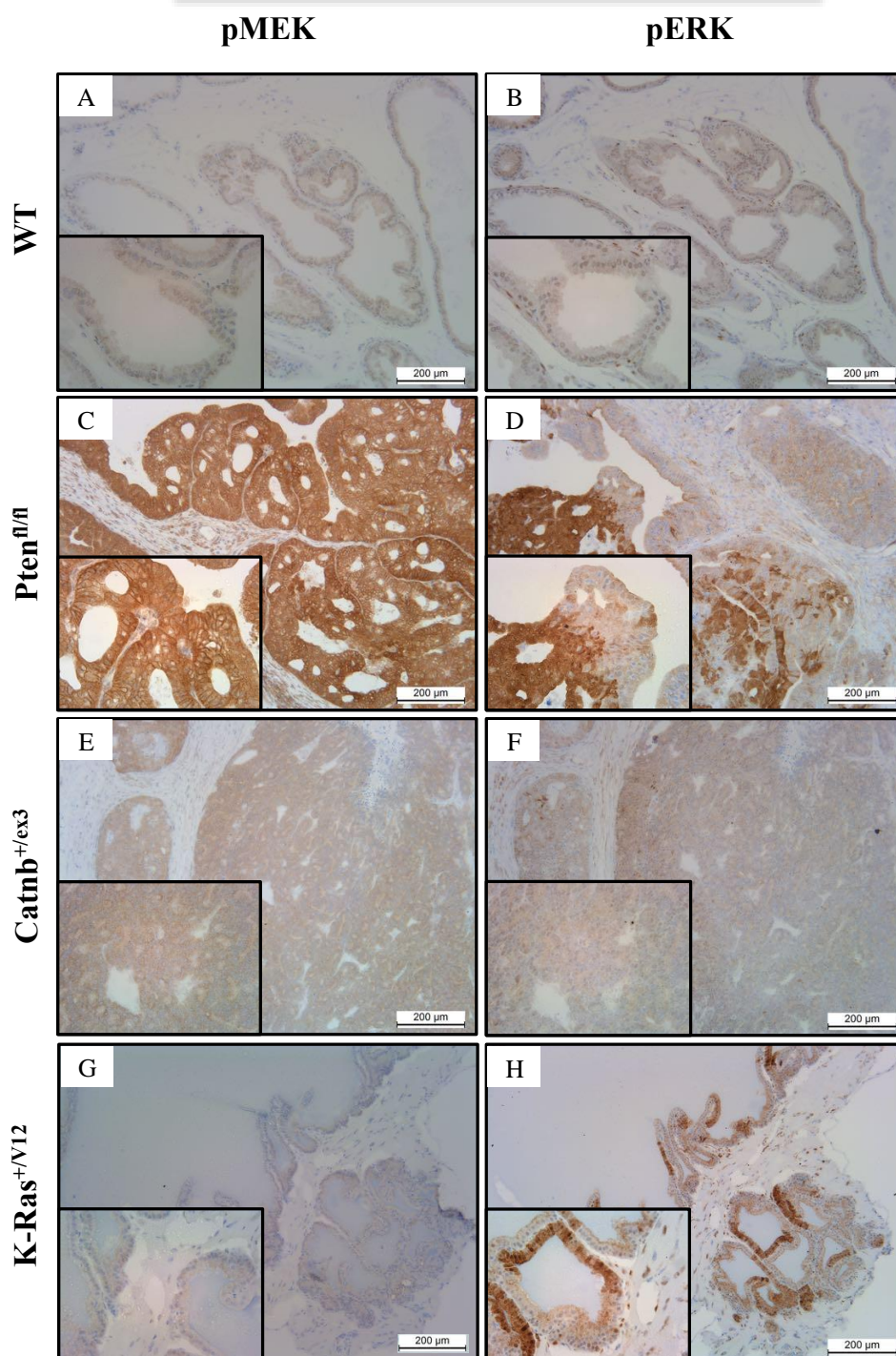


Figure 50: Immunohistochemistry of MAPK pathway markers for WT and single mutant mice. Immunohistochemistry was performed on cohorts of mice (n=4) at the endpoint of the experiment (500 days or when sick) using antibodies against the downstream markers pMEK and pERK. WT had no staining for pMEK (A) and occasional weak staining for pERK (B). Pten^{fl/fl} tumours had diffuse cytoplasmic pMEK staining and strong heterogeneous staining nuclear pERK positivity (D). Catnb^{+ex3} had no staining for either pMEK (E) or pERK (F). K-Ras^{+V12} samples had negative staining for pMEK (G) and strong focal positive staining for pERK (H).

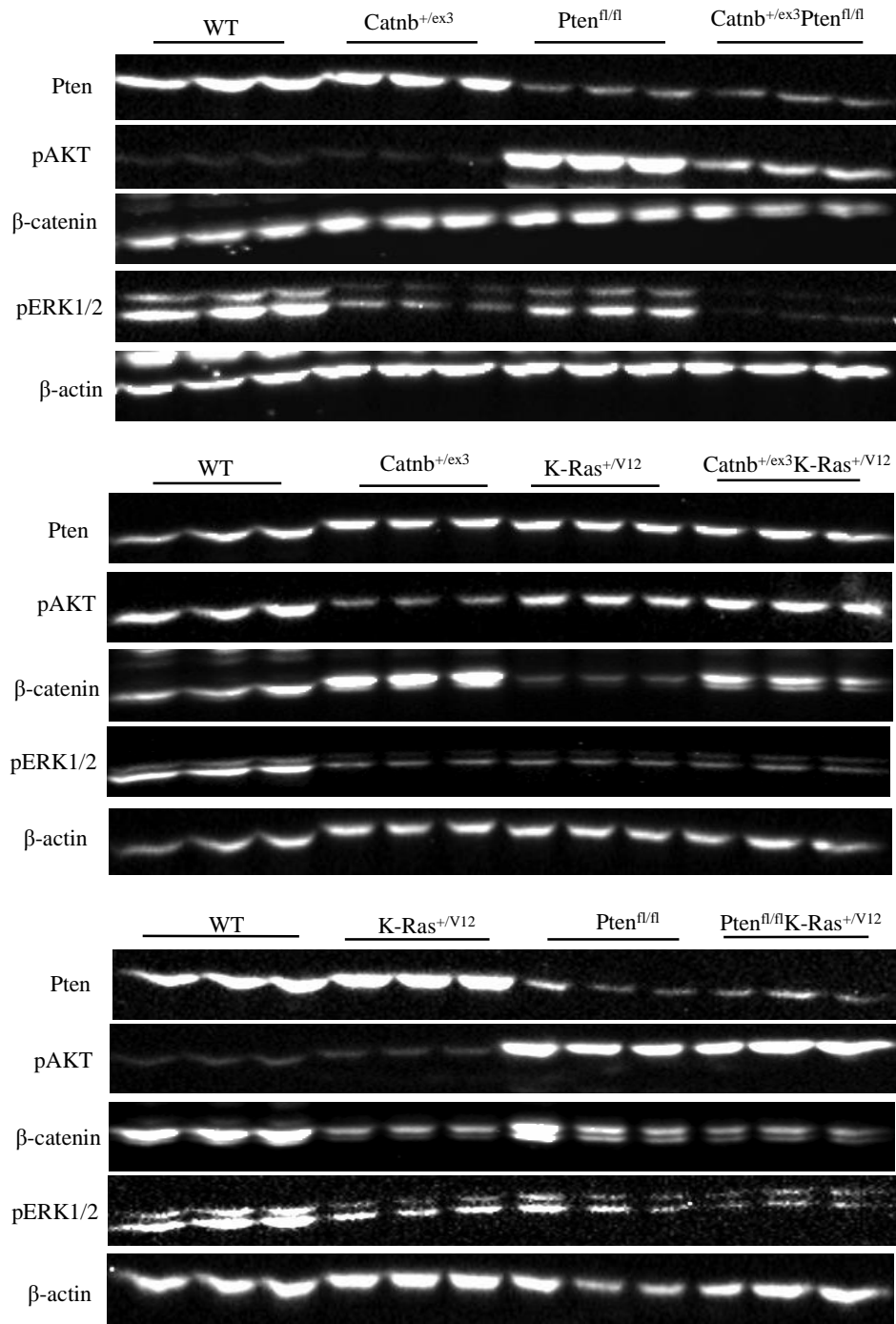


Figure 51: Western-blot analysis for markers of PI3K, Wnt and MAPK signalling pathways for wild-type (WT), single ($Catnb^{+/ex3}$, $K-Ras^{+/V12}$ and $Pten^{fl/fl}$) and double ($Catnb^{+/ex3} K-Ras^{+/V12}$, $Pten^{fl/fl} Catnb^{+/ex3}$ and $Pten^{fl/fl} K-Ras^{+/V12}$) mutant mice. Protein was extracted from fresh frozen prostate tissue from 100-day old mice for each cohort (n=3). Antibodies against each pathway were analysed: PI3K pathway markers; Pten and p-AKT, Wnt pathway marker; β -catenin and MAPK pathway marker; pERK1/2. β -actin was used as the reference-loading gene.

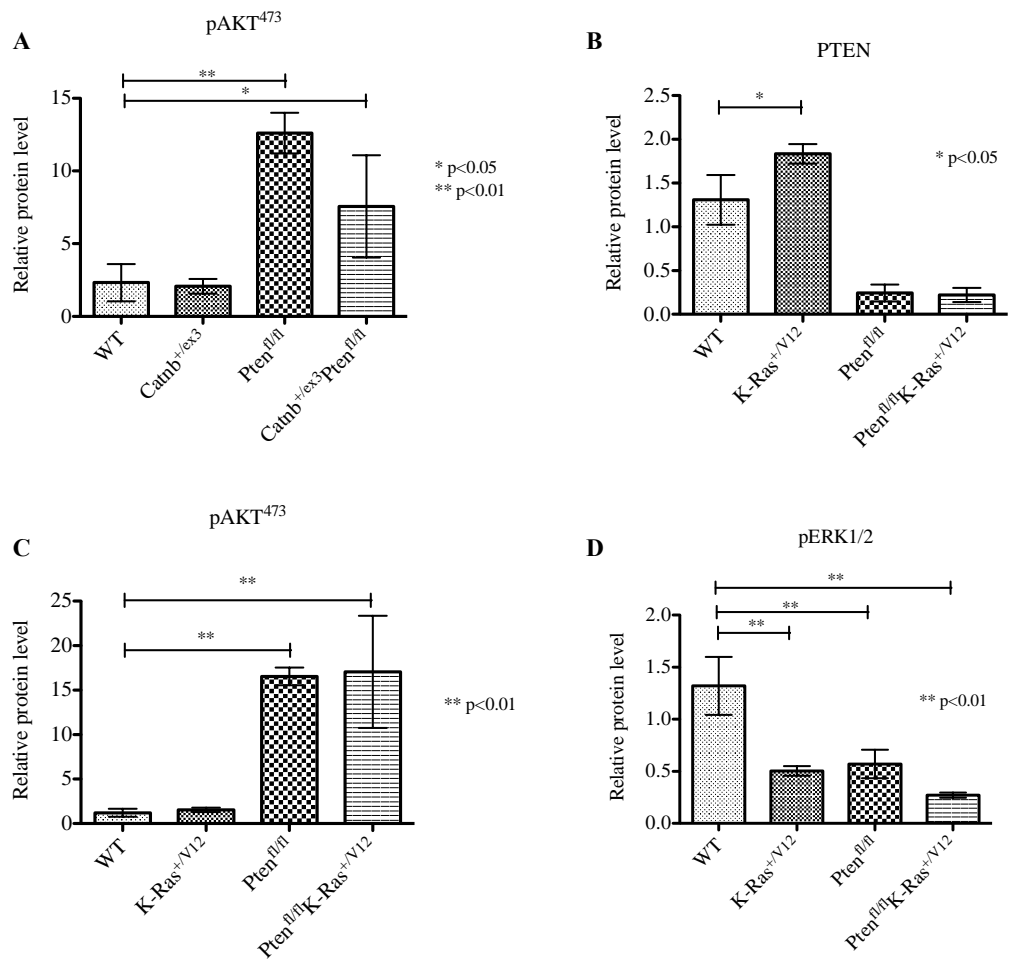


Figure 52: Western blot analysis comparing relative protein levels of wild-type (WT), single (Catnb^{+ex3}, K-Ras^{+V12} and Pten^{fl/fl}) and double (Catnb^{+ex3} K-Ras^{+V12}, Catnb^{+ex3} Pten^{fl/fl} and Pten^{fl/fl} K-Ras^{+V12}). (A) pAKT⁴⁷³ was significantly elevated in Pten^{fl/fl} and Catnb^{+ex3}Pten^{fl/fl} when compared to WT. (B) Pten protein level was significantly higher in K-Ras^{+V12} than WT mice. (C) pAKT⁴⁷³ was significantly elevated in Pten^{fl/fl} and Pten^{fl/fl} K-Ras^{+V12} when compared to WT. (D) pERK1/2 expression was lower in Pten^{fl/fl} and K-Ras^{+V12} single and Pten^{fl/fl} K-Ras^{+V12} double mutant mice when compared to WT. Each sample was normalised to β -actin and calculated as a relative upregulation or down regulation with respect to WT control. Mean with Error bars = 95% CI.

4.2.7.2 Double mutant mice show activation of multiple pathways

Compound mutations in β -catenin and K-Ras demonstrated Wnt and MAPK pathway activation. There was positive nuclear β -catenin staining and membranous CD44 activity (Figure 55A-B). Again, there was no significant difference in protein levels of total β -catenin (Figures 52 and 57). Consistent with previous work from our laboratory (Pearson et al. 2009), there was positive staining for both p-MEK and p-ERK1/2 (Figure 56A-B). Western blot analysis for p-ERK1/2 failed to confirm these findings however, with lower protein levels in β -catenin/K-Ras double mutant mice than when compared to WT. These inconsistencies on western blot for both total β -catenin and p-ERK 1/2 could be resolved with future analysis calculating protein levels of activated β -catenin and total ERK. Protein levels could then be normalised to total β -catenin or ERK as opposed to β -actin.

Loss of Pten in addition to β -catenin resulted in activation of both PI3K and Wnt pathways, with a significant increase in protein levels of p-AKT on western blot (Figure 57 and 58A) and IHC (Figure 54G-H) and positive nuclear β -catenin on IHC (Figure 55E). There was suppression of the MAPK pathway with reduced p-ERK1/2 levels compared with mice with Pten loss alone (Figure 52) and negative staining for p-MEK and p-ERK (Figure 56E and F).

Loss of Pten and activation of K-Ras resulted in activation of the PI3K pathway predominately, with minor aberration to the Wnt and MAPK pathways. There was an increased protein level and expression of p-AKT on western blot (Figures 52, 57 and 58A) and IHC (Figure 54D-E). There was concurrent mild staining for the Wnt markers; β -catenin and CD44 (Figure 55C-D), and the MAPK markers; p-MEK and p-ERK1/2 (Figure 56C-D). These findings on IHC were inconsistent to those seen on western-blot analysis, which showed no significant difference in total β -catenin and reduced p-ERK1/2 compared to WT (Figure 57 and 58C).

PI3-Kinase pathway

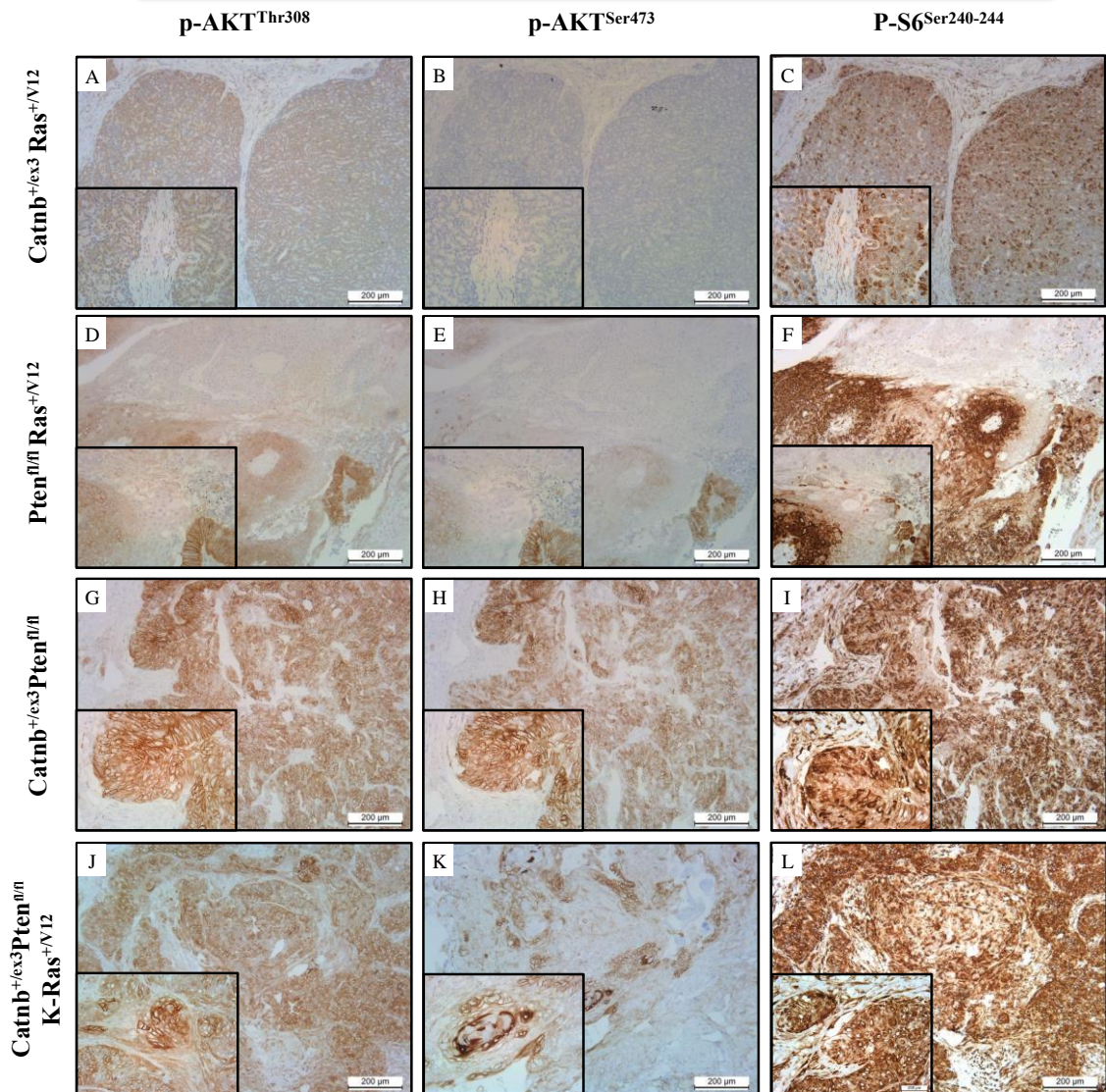


Figure 53: Immunohistochemical analysis of PI3-Kinase pathway markers for double (Catnb^{+/ex3}K-Ras^{+V12}, Catnb^{+/ex3}Pten^{fl/fl} and Pten^{fl/fl}K-Ras^{+V12}) and triple (Catnb^{+/ex3}Pten^{fl/fl}K-Ras^{+V12}) mutants tumours. Immunohistochemistry was performed on cohorts of mice (n=4) at the endpoint of the experiment (500 days or when sick) using antibodies against p-AKT^{Thr308}, p-AKT^{Ser473} and p-S6^{Ser240-244}. Catnb^{+/ex3}K-Ras^{+V12} had negative staining for both isotopes of AKT (A-B) with focal cytoplasmic staining for p-S6^{Ser240-244} (C). Pten^{fl/fl}K-Ras^{+V12} had focal positive staining for p-AKT^{Thr308} (D), AKT^{Ser473} (E) and p-S6^{Ser240-244} (F). Both Catnb^{+/ex3}Pten^{fl/fl} and Catnb^{+/ex3}Pten^{fl/fl}K-Ras^{+V12} tumours stained avidly for all PI3K pathway markers (G-L).

Wnt pathway

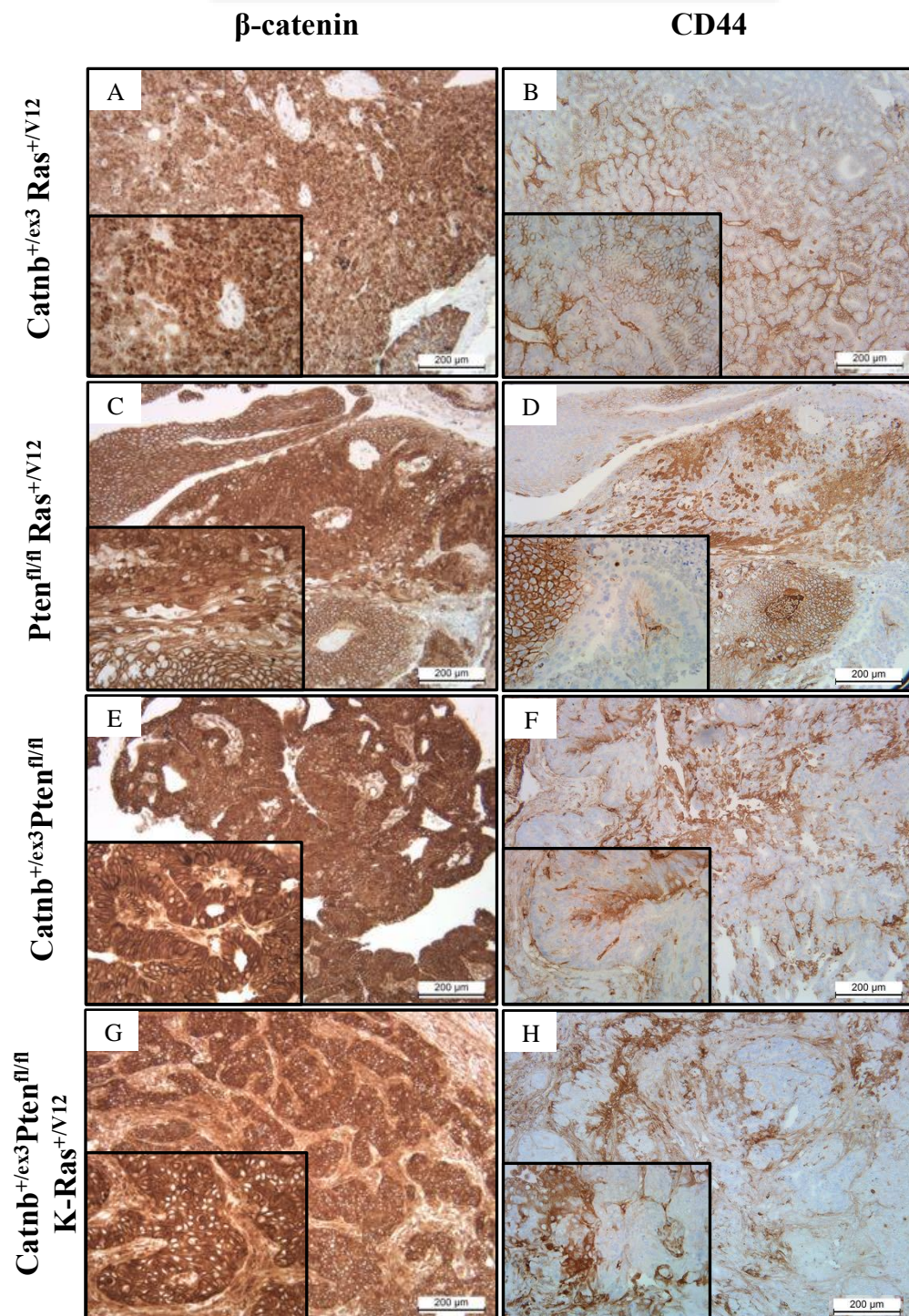


Figure 54: Immunohistochemical analysis of Wnt pathway markers for double (Catnb^{+/-ex3} K-Ras^{+/-V12}, Catnb^{+/-ex3} Pten^{fl/fl} and Pten^{fl/fl} K-Ras^{+/-V12}) and triple (Catnb^{+/-ex3} Pten^{fl/fl} K-Ras^{+/-V12}) mutant tumours. Immunohistochemistry was performed on cohorts of mice (n=4) at the endpoint of the experiment (500 days or when sick) using antibodies against β -catenin and the Wnt target gene CD44. Catnb^{+/-ex3} K-Ras^{+/-V12} had diffuse positive staining for both β -catenin (A) and CD44 (B). Pten^{fl/fl} K-Ras^{+/-V12} had focal nuclear β -catenin (C) and membranous CD44 (D) staining. Catnb^{+/-ex3} Pten^{fl/fl} and Catnb^{+/-ex3} Pten^{fl/fl} K-Ras^{+/-V12} had similar diffuse nuclear positive staining for β -catenin (E and G) and CD44 (F and H).

MAP-Kinase pathway

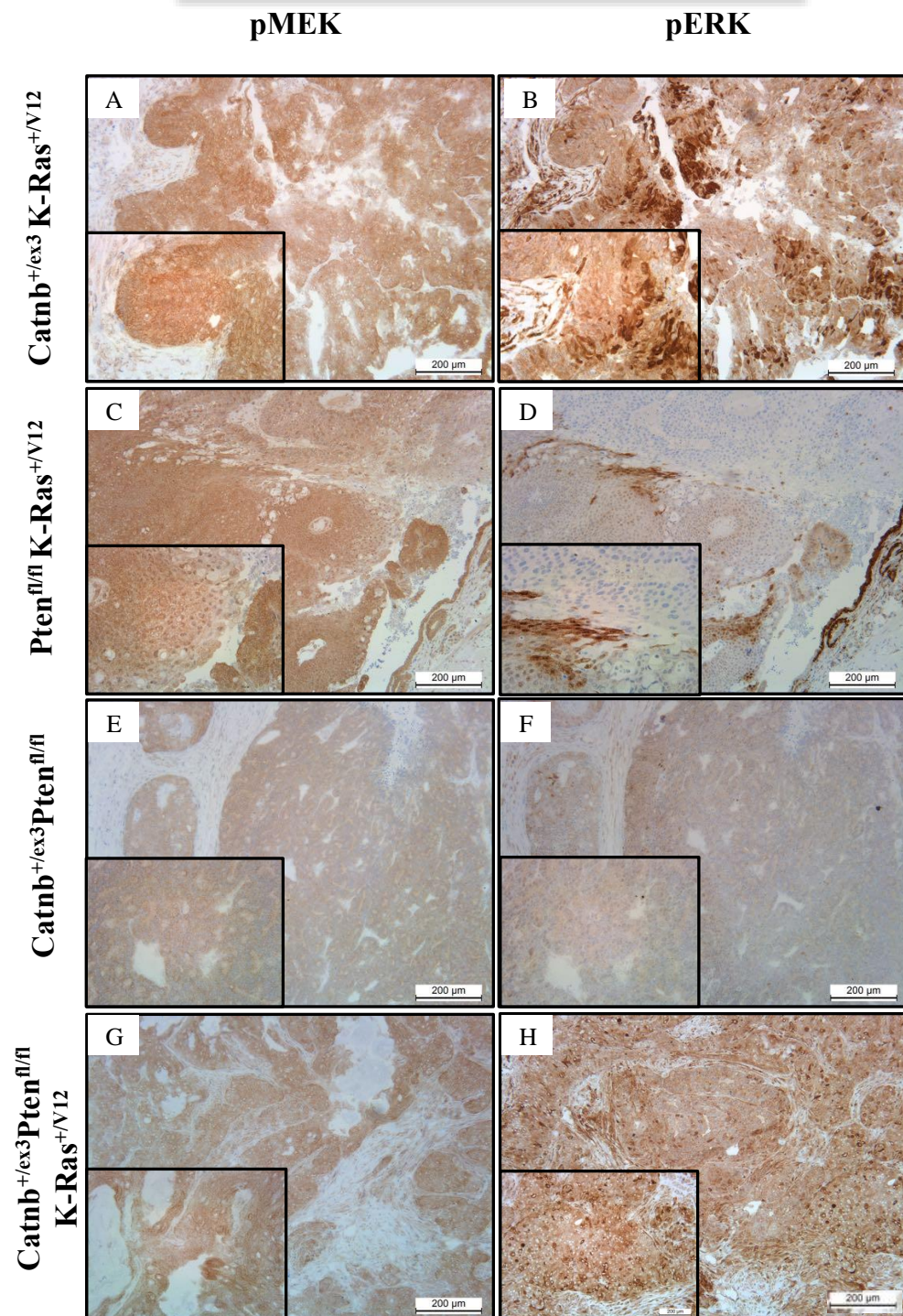


Figure 55: Immunohistochemical analysis of MAP-Kinase pathway markers for double (Catnb^{+/-ex3} K-Ras^{+V12}, Catnb^{+/-ex3} Pten^{fl/fl} and Pten^{fl/fl} K-Ras^{+V12}) and triple (Catnb^{+/-ex3} Pten^{fl/fl} K-Ras^{+V12}) mutants tumours. Catnb^{+/-ex3} K-Ras^{+V12} had positive staining of both pMEK and pERK (A-B). Pten^{fl/fl} K-Ras^{+V12} demonstrated widespread cytoplasmic pMEK staining (C) with focal nuclear p-ERK staining (D). Catnb^{+/-ex3} Pten^{fl/fl} had negative staining for pMEK (E) and pERK (F). Triple mutants displayed diffuse positive staining for both pMEK (G) and pERK (H). n=4.

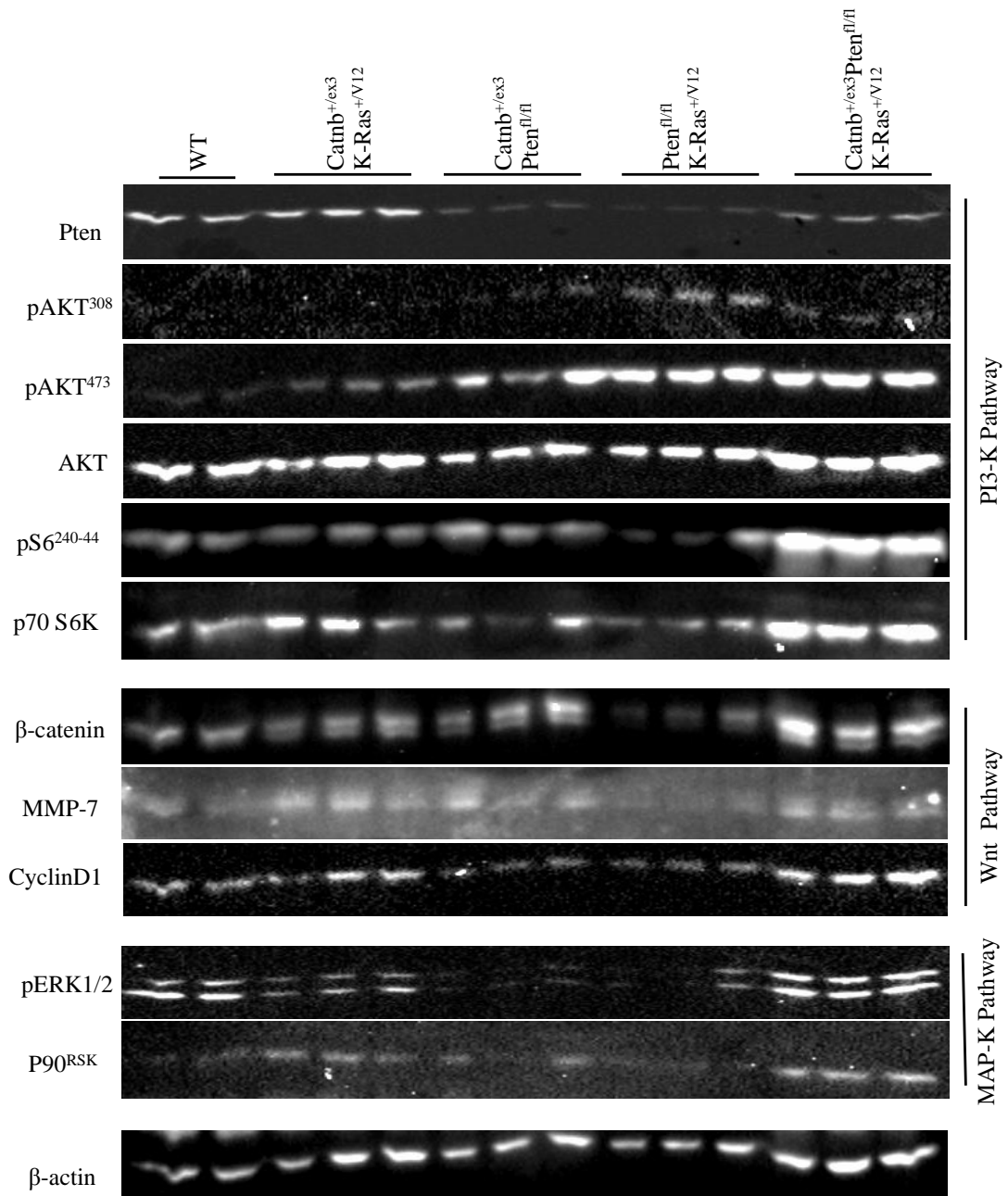


Figure 56: Western-blot analysis of markers of the PI3K, Wnt, MAPK and mTOR signalling pathways for Wild-type (WT), double ($Catnb^{+/ex3}$ K-Ras $^{+/V12}$, Pten $^{fl/fl}$ $Catnb^{+/ex3}$ and Pten $^{fl/fl}$ K-Ras $^{+/V12}$) and triple ($Catnb^{+/ex3}$ Pten $^{fl/fl}$ K-Ras $^{+/V12}$) mutants. Protein was extracted from fresh frozen prostate tissue from 100-day old mice for each cohort (n=3). Antibodies against each pathway were analysed: PI3K pathway markers; Pten and p-AKT, Wnt pathway marker; β -catenin, MAPK pathway marker; pERK1/2 and mTOR pathway markers; p70 S6K and pS6 $^{240-44}$. β -actin was used as the reference-loading gene.

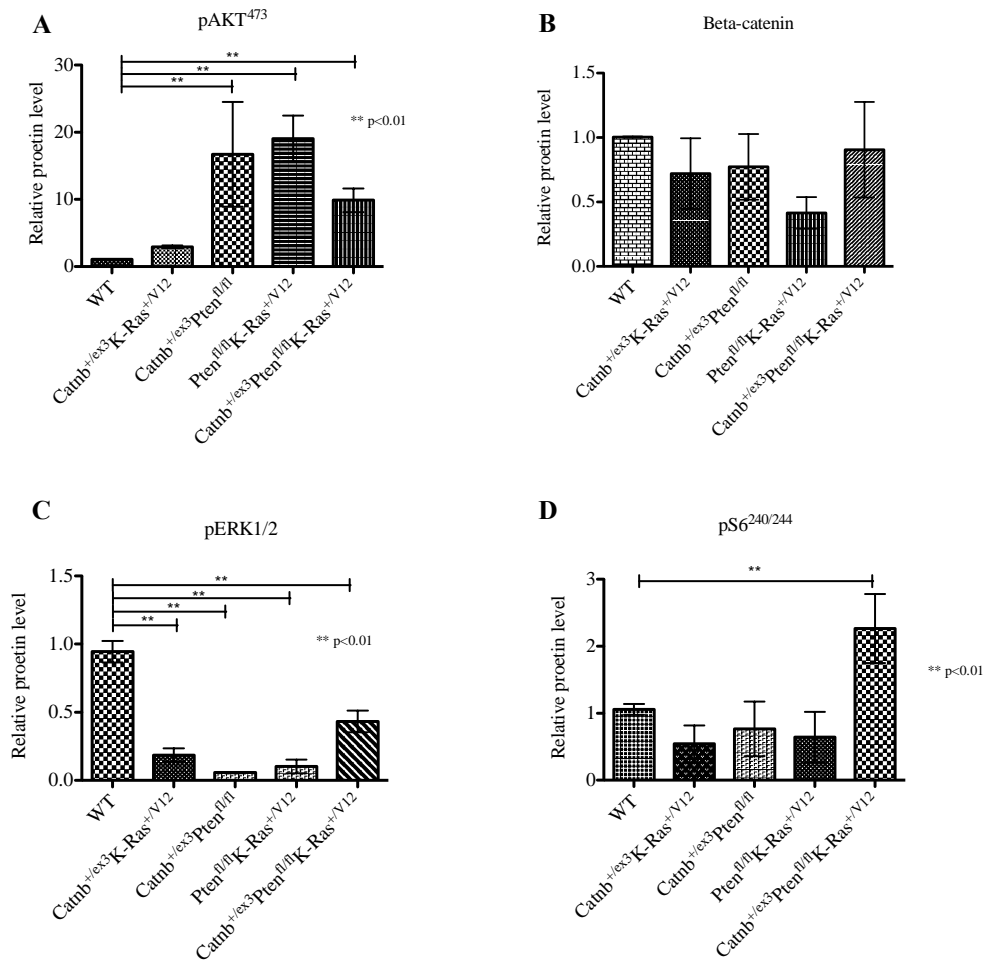


Figure 57: Western blot analysis comparing relative protein levels between WT and double (Catnb^{+/ex3}K-Ras^{+/V12}, Catnb^{+/ex3}Pten^{fl/fl} and Pten^{fl/fl}K-Ras^{+/V12}) and triple (Catnb^{+/ex3}Pten^{fl/fl}K-Ras^{+/V12}) mutants. (A) pAKT⁴⁷³ was significantly elevated in Catnb^{+/ex3}Pten^{fl/fl}, Pten^{fl/fl}K-Ras^{+/V12} and Catnb^{+/ex3}Pten^{fl/fl}K-Ras^{+/V12} compound mutant mice when compared to WT controls. (B) Total β -catenin expression was similar across all cohorts. (C) pERK1/2 was significantly lower in all compound mutant mice when compared to WT. (D) pS6^{240/244} was significantly elevated in triple mutant mice when compared to all double combinations and WT mice. Each sample was normalised to β -actin and calculated as a relative upregulation or down regulation with respect to WT control. Mean with Error bars = 95% CI.

4.2.7.3 Triple mutant mice cooperate displaying increased activation of the mTOR signalling pathway

Finally, Pten loss in addition to activation of mutated β -catenin and K-Ras resulted in activation of Wnt, PI3K and MAPK pathways with positive staining for β -catenin, p-AKT and p-MEK/p-ERK1/2 on IHC, respectively. There was a significantly increased protein level for p-AKT compared to WT, however this was less than Pten/K-Ras and β -

catenin/Pten double mutant mice (Figure 58A). Total β -catenin levels were similar for all double combination, triple mutant and WT mice (Figure 58B). To assess the Wnt pathway further, protein levels of two Wnt target genes were analysed: MMP-7 and Cyclin D1. There was a general trend for elevation of both markers in those mice with β -catenin mutations compared to WT, however this was not statistically significant (Figure 57). To further assess the Wnt pathway, the protein level of activated β -catenin could be calculated. The protein level of p-ERK1/2 was elevated compared to double mutant mice however it was less than that for WT (Figure 58C). There was also a further marked increase in the downstream markers, p-S6²⁴⁰⁻²⁴⁴ and p-70 S6K (Figure 52 and 58D), indicating significant mTOR signalling activity contributing to the aggressive nature of this model.

Interestingly, triple mutants also demonstrated marginally elevated Pten levels compared to other Pten null mice despite conditional knockout of the Pten gene using the probasin promoter (Figure 57). This could be secondary to upregulation of Pten in the surrounding stroma. This was illustrated by positive stromal staining but absent epithelial staining for Pten on IHC; suggesting compensatory upregulation of Pten in the stroma following loss in the epithelial compartment (Figure 59). To confirm this finding re-combination PCR could be performed following micro/laser-dissection of the stroma.

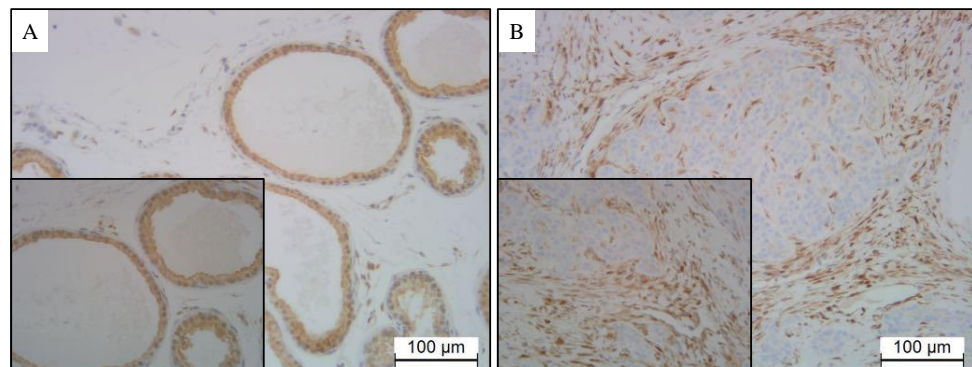


Figure 58: Pb-Cre4⁺ Catnb^{+ex3} Pten^{fl/fl} K-Ras^{+V12} (triple mutant) tumours display positive staining for Pten within the stromal but not epithelial compartment. (A) Diffuse cytoplasmic Pten staining in wild-type control mice. (B) Strong stromal positive staining for Pten with absent epithelial staining.

4.2.8 Summary of pathway readouts according to genotype

A summary of pathway status based on western and immunohistochemistry for each genotype and pathway is summarised in Figure 60.

Pathway status			
Genotype	PI3K	Wnt	MAPK
Pten^{fl/fl}	++	+	+
Catnb^{+/ex3}	-	++	-
K-Ras^{+V12}	-	-	+
Catnb^{+/ex3} K-Ras^{+V12}	-	++	+/-
Pten^{fl/fl} Catnb^{+/ex3}	++	++	-
Pten^{fl/fl} K-Ras^{+V12}	++	+/-	+/-
Catnb^{+/ex3} Pten^{fl/fl} K-Ras^{+V12}	++	++	++

Figure 59: PI3-Kinase, Wnt and MAP-Kinase signalling pathway status according to genotype. These were based on combined IHC and western analysis. No activation, +/- heterogeneous activity – whereby there was either heterogeneous IHC staining or the western and IHC data was inconsistent, + low activation – weak IHC staining or mildly elevated protein levels on western-blot analysis, ++ high activation – strong IHC staining with significantly elevated protein levels on western-blot.

4.3 Discussion

4.3.1 Pten loss alone causes significant PI3K pathway up-regulation with further mild aberrant Wnt and MAPK signalling resulting in prostate tumourigenesis

To attempt to deregulate the PI3K pathway, mice harbouring homozygous deletion of Pten were generated. Loss of Pten resulted in locally advanced adenocarcinoma of the prostate leading to death, with a reduced median survival of 373 days, consistent with reports from others (S. Wang et al. 2003). Pathway analysis using both IHC on tumour samples and western blot on 100-day-old mice demonstrated significant aberrant PI3K activity, with up-regulation of downstream markers p-AKT and p-S6. One would expect activation of the PI3K signalling given that Pten is the main player in regulating this pathway.

Interestingly, this research has further shown that mice models with Pten loss alone not only demonstrate up-regulation of the PI3K signalling pathway but also aberrant Wnt and MAPK signalling. The presence of nuclear β -catenin and its downstream transcriptional target CD44, albeit in heterogeneous fashion, on IHC analysis provided evidence for the activation of the Wnt pathway. One postulated mechanism to explain why Pten loss results in Wnt activity is through inhibitory signals on GSK3 β which is part of the axin complex (described in 1.5.2). Pten loss activates the PI3-Kinase pathway, which inactivates GSK3 β (Mulholland et al. 2006) resulting in destruction of the axin complex. Consequently, β -catenin accumulates in the cytoplasm and travels to the nucleus where it activates Wnt target gene expression such as c-MYC and MMP-7 (MacDonald et al. 2009; Kypta & Waxman 2012).

The presence on IHC of p-ERK1/2 activity in tumours with Pten loss infers aberrant activity of the MAPK pathway. Loss of Pten results in PI3K activation, which further activates and the MAPK pathway, this occurring at multiple levels as illustrated in Figure 61.

4.3.2 Activation of β -catenin alone causes activation of the Wnt pathway resulting in prostate tumourigenesis with squamous metaplasia

Activation of β -catenin alone also results in locally advanced prostate tumourigenesis with a reduced median survival of 383 days. Interestingly, histological analysis demonstrates adenocarcinoma with evidence of squamous metaplasia, a finding consistent with others (Bierie et al. 2003; Pearson et al. 2009; Francis et al. 2013). The significance of this is unclear; squamous metaplasia is uncommon in human PCa, with cases typically related to prior hormonal or radiation therapy, or associated with chronic prostatic inflammation or infarction (Arva & Das 2011). Squamous metaplasia, although a benign condition, is thought to be risk factor for developing squamous differentiation and later transformation to squamous cell carcinoma (SCC). This phenomenon is seen in the bladder where extensive keratinising squamous metaplasia can differentiate into a SCC. SCC of the prostate is an exceedingly rare entity. In the present study, squamous metaplasia was seen as early as 100 days and was associated with all models where a mutated allele for β -catenin was present. This observation has also been noted in other organs with Wnt activated tumours, such as murine mammary tumours (B. Liu et al. 2008). Persistent staining for basal markers CK5 or p63 may suggest that cells within this layer are able to differentiate aberrantly into the squamous cell lineage possible as a result of abnormal changes in stem cell function or pluripotent stem cells capable of multidirectional differentiation. This theory has not been well explored due to the small incidence of squamous metaplasia and SCC in the human prostate, thereby rendering any further research of limited clinical value.

4.3.3 Activation of K-Ras alone is insufficient to cause prostate tumourigenesis with elevated Pten levels

Mice harbouring an activated mutation of K-Ras alone are insufficient to result in tumourigenesis and have little effect on survival, with all mice surviving to the end of the experiment (500 days). This is somewhat surprising given that Taylor et al (2010) report alteration of the MAPK pathway in 43% of primary and 90% of metastatic samples. Clearly, further signals are required to permit tumourigenesis as demonstrated by compound mouse models involving K-Ras. Interestingly, the level of Pten is elevated in

K-Ras single mutant mice, thereby offering a protective role, through inhibition of the PI3K pathway, a mechanism that could explain the normal histology seen in these mice.

4.3.4 Double and triple mutant mice accelerate tumourigenesis through activation of multiple cell signalling pathways

Historically cell signalling pathways have been thought of as separate entities however there is great research enthusiasm in deciphering key links or crosstalk's between pathways in order to improve our understanding of the complexity of cancer and pave the way for future therapies. Our laboratory has previously shown cooperation between the Wnt and MAPK signalling pathway (Pearson et al. 2009) and others have shown cooperation between PI3K and Wnt signalling, and PI3K and MAPK in driving prostate tumourigenesis (Mulholland et al. 2012; Francis et al. 2013). The research presented here is consistent with these findings, whereby double mutant mice display a significant reduction in lifespan compared to single mutant mice through activation of one or both associated signalling pathways. For example, loss of Pten and activation of K-Ras results in predominant aberrant PI3K signalling with reduced median survival (238 days compared to 373 days for Pten single mutants with K-Ras single mutant mice all surviving to the end-point of the experiment [500 days]). These interactions are not PCa specific, with reports in other tissues such as intestine, bladder, biliary and ovary (Marsh et al. 2013; Davies et al. 2014; Ahmad et al. 2011; Laguë et al. 2008).

This study, for the first time, demonstrates cooperation between all three pathways: PI3K, Wnt and MAPK signalling. Pten loss in addition to our previously described mouse model (Catnb^{+/ex3}K-Ras^{+V12}, (Pearson et al. 2009) causes significant up-regulation of PI3K, Wnt and MAPK signalling highlighting important synergy between these pathways. This results in a significant reduction in survival of the mouse when compared to double and single mutant mice. Triple mutant mice develop very aggressive locally advanced prostate tumourigenesis with mortality resulting from urinary obstruction (bladder outflow or ureteric). Histological analysis of the tumours demonstrated a step-wise progression of disease similar to that seen in human disease, from mPIN to invasive adenocarcinoma. Triple mutants also display a more aggressive histological phenotype with a greater percentage of invasive adenocarcinoma at 100 days, when compared to double and single mutant tumours. As the tumour progresses the glandular architecture

becomes increasingly distorted with glands fusing together and areas of cribriform pattern forming, features pathognomonic of Gleason pattern 4 in human PCa. Furthermore, features of Gleason pattern 5 develop; with single PCa cells invading the stroma.

4.3.5 Triple mutant mice display further aberrant mammalian target of rapamycin (mTOR) signalling

In addition to upregulation of the PI3K, Wnt and MAPK signalling pathways, triple mutant mice also have significantly increased mTOR signalling, with increased levels of the downstream markers p-S6 and p70 S6K. The mTOR signalling pathway is a master growth regulator and integrates both intracellular and extracellular signals and serves as a central regulator of cell metabolism, growth, proliferation and survival. It has been implicated in many cancers (Motzer et al. 2008; Yao et al. 2011) through deregulation of these processes, particularly effecting tumour formation and angiogenesis.

Deregulation of all three pathways (PI3K, Wnt and MAPK) in the mouse results in significantly elevated mTOR signalling. A postulated mechanism to explain this is that the signals from all pathways converge and directly act on the same complex or protein. Figure 61 attempts to illustrate this hypothesis. PI3K is directly upstream of mTOR; therefore loss of Pten can result in aberrant mTOR signalling. In addition there are proposed mechanisms connecting the PI3K pathway with the MAPK and the Wnt pathways, both resulting in subsequent mTOR signalling. For example, Ras can directly bind and activate PI3K (Suire et al. 2002) and ERK has been shown to inhibit the TSC1/2 complex resulting in increased mTOR signaling (Carriere et al. 2011). Inoki et al (2006) has also shown that Wnt signaling increases mTOR signaling through the inactivation of the TSC1/2 complex. Stimulation of Wnt signaling inhibits GSK3, a kinase that promotes TSC1/2 activity by directly phosphorylating TSC2 (Inoki et al. 2006). Stimulation of ERK can result in up regulation of the Wnt pathway through activation of β -catenin by phosphorylating the β domain of GSK (Ding et al. 2005). These are examples of cross-activation or pathway convergence.

In addition, there are inhibitory signals (cross-inhibition) and negative feedback loops which act upon upstream activators (Mendoza et al. 2011) that occur not only in-between pathways but also within a single pathway. For example, AKT negatively regulates ERK

activation by phosphorylating inhibitory sites in the Raf N-terminus (Zimmermann & Moelling 1999). Also, there are negative feedback loops such as ERK phosphorylation inhibits Raf and MEK (Dhillon et al. 2007), and the phosphorylation of the downstream mTOR marker S6K inhibits AKT activity and mTORC1 signalling (Dibble et al. 2009). These mechanisms (illustrated in Figure 61) highlight the complexity and extent of crosstalk between these pathways making cancer therapeutics difficult.

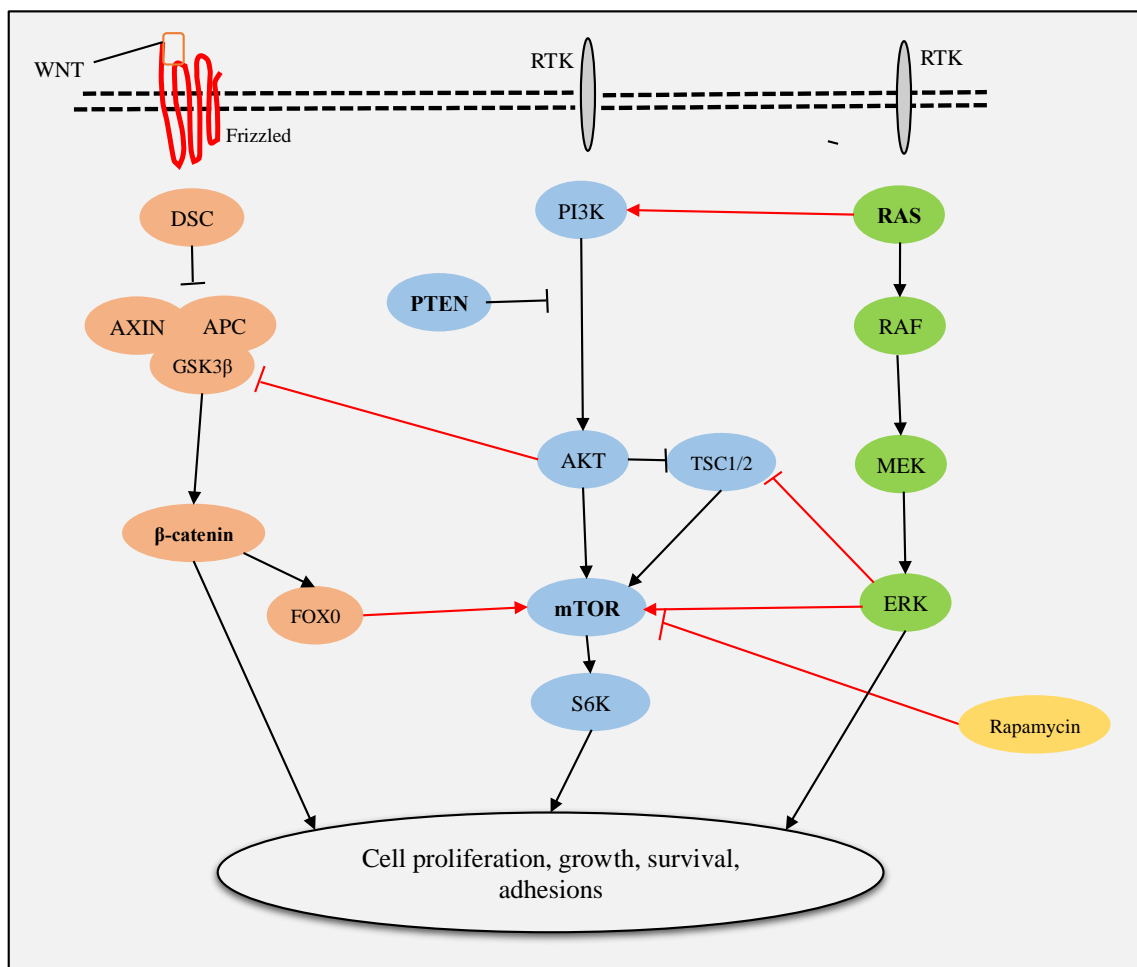


Figure 60: A schematic representation of cross reactivity between Wnt, PI3K and MAPK signalling pathway.

The importance of mTOR signalling has resulted in the development of inhibitors such as rapamycin and its analogues, including everolimus and temsirolimus. Early studies were promising demonstrating regression of PIN lesions in a mouse model overexpressing AKT (Majumder et al. 2004) and inhibition of growth of xenograft

models derived from human cells lines with Pten loss (L. Wu et al. 2005). Despite these promising preclinical results and the success of mTOR inhibitors in the treatment of patients with metastatic renal cell carcinoma (Motzer et al. 2008), the clinical use of mTOR inhibitors in men with metastatic PCa has been disappointing. Phase I/II trials using single agent such as rapamycin or everolimus, have failed to show anti-tumour effects with little response on PSA or clinical progression (Templeton et al. 2013; Amato et al. 2008).

Several explanations likely underlie the lack of clinical activity of rapamycin and its analogues in CRPC. Rapamycin binds to mammalian target of rapamycin complex 1 (mTORC1) and does not inhibit mTORC2, which results in increased AKT activity. Consequently, dual PI3K/mTOR1/2 drugs such as BEZ235 (Novartis) have been developed. Encouragingly, pre-clinical studies have shown that BEZ235 (Novartis) can overcome Docetaxel resistance in a human CRPC cell lines using a mouse xenograft model (Yasumizu et al. 2014).

More recently, PI3K signalling has been shown to inhibit androgen receptor (AR) activity via feedback inhibition on receptor tyrosine kinases (RTK) such as human epidermal growth factor 2/3 (HER2/3) (Carver et al. 2011). Following mTOR inhibition, the AR activity is reactivated in a RTK-dependent manner (Rathkopf et al. 2015), resulting in treatment failure. Conversely, AR signalling downregulates PI3K/mTOR activity through stabilisation of AKT (Carver et al. 2011). Activation of the mTOR pathway as a result of treatments targeting AR signalling or due to Pten loss may, therefore, enable prostate cancer cells to survive and proliferate in androgen-independent or reduced conditions. Consequently, Rathkopf et al (2015) conclude that future studies combining PI3K pathway inhibitors and second-generation AR inhibitors are required in CRPC. A recent trial of Abiraterone (inhibits androgen biosynthesis by blocking the CYP17 enzyme) in combination with either BEZ235 (a dual PI3K and mTOR inhibitor, Novartis) or BKM120 (a PI3K inhibitor, Novartis) will explore this. Recruitment completed in August 2014 and the results are awaited (CRUK).

Triple mutant mice explored in this thesis demonstrate upregulation of the mTOR pathway highlighting a possible treatment site for this aggressive model. What is evident is that cancer pathways, including mTOR, Wnt, PI3K and MAPK, are complex with the intensity and duration of pathway activation governed by the strengths of stimuli causing

cross-activation and cross-inhibition, and those resulting in negative feedback loops. This paradigm highlights the difficulty of future treatment strategies. Using these treatment methods single agents are certainly going to fail and a combinatory treatment approach is required.

4.3.6 Single gene mutations are insufficient to cause metastases

The development of a murine model for PCa metastasis is important, given the lack of models for advanced disease. Although, single mutations in Pten and β -catenin are sufficient to develop prostate tumourigenesis, the latency period is long (approx. 400 days) with insufficient ability to cause metastasis. This is however inconsistent with work by Wang et al (2003) which demonstrated lymph node and lung metastasis as early as 12 weeks in Pten homozygous mice. The reason for this discrepancy is unclear.

The pattern of disease observed in single mutant mice; a long latency period with no metastasis, may well be synchronous with that of Gleason 6 human PCa, which have little effect on survival and a low metastatic potential. It is hypothesised that further mutations or signals are required to transform these primary tumours to a metastatic state.

4.3.7 Both K-Ras and β -catenin mutations drive metastatic spread in the context of loss of Pten

Supporting the theory that more signals or mutations (“hits”) are required to produce metastases, this research has demonstrated that compound deletion of Pten and activation of K-Ras has a high preponderance to lymph node metastasis (60% incidence), consistent with others (Mulholland et al. 2012). To a lesser degree (10% incidence), mice with compound activation of β -catenin and loss of Pten also develop lymph node metastases. Interestingly despite a more aggressive phenotype, triple mutant mice did not develop metastatic lymph node deposits. The reason for this is likely due to the short life span of the mouse due to the aggressive nature of the tumours produced, not allowing enough time for the metastatic lesions to develop before the animal must be sacrificed owing to primary tumour burden.

The metastases observed in Pten loss and K-Ras activated compound model are small however, and mortality in these mice is almost certainly secondary to the local effects of the primary tumour, causing bladder outflow or ureteric obstruction, as oppose to the metastatic burden. Although similar local effects are seen in locally advanced human disease, the majority of men in the lethal phase of PCa, CRPC, have widespread soft-tissue and bony metastasis resulting in their death. Bony metastases have not formally been assessed in the mouse as it is notoriously difficult to detect small metastasis in the mouse skeleton and one would typically expect reciprocal lymph node metastasis if bone metastasis were to be present. Due to the small lymph node metastases seen, one could argue however, that the combinations of genetic mutations explored here are insufficient to initiate bone metastasis.

4.3.8 Rate of proliferation correlates positively with stage of disease and number of mutations/activated pathways

The rate of proliferation was assessed using immunohistochemistry, calculating the positivity of proliferation markers Ki67 and BRDU. The rate of proliferation not only increased with stage of disease (i.e. from normal to mPIN to invasive adenocarcinoma) but also with number of mutations or deregulated pathways present. For example, the rapid growth of triple mutants tumours correlated clearly with the higher proliferation rate when compared to double mutant mice. The same was apparent when comparing double mutant to single mutant mice.

Proliferation is arguable one of the most, if not the most important “hallmark” possessed by a cancer (Hanahan & Weinberg 2011). In addition to a greater proliferation rate seen in triple mutants, it can be postulated that as further mutations develop the cancer adopts further “hallmarks” to evade the body’s normal defences. For example, additional mutations in different genes such as the retinoblastoma (Rb) pathway would alter cell-cycle control and the p53 pathway affects apoptosis.

Proliferation markers, such as Ki67, have also been shown to be of prognostic value in human disease. Studies have shown Ki67 to be a powerful biomarker in predicting need for radical treatment in those undergoing conservative management (active surveillance) (Berney et al. 2009), time to biochemical relapse following radical prostatectomy

(Bettencourt et al. 1996), and is a strong marker of disease progression and distant metastasis in those undergoing external beam radiotherapy (Verhoven et al. 2013).

4.3.9 Tumours show signs of EMT with Triple mutants displaying additional stromal Pten activity

All mouse models explored (except for K-Ras single mutants) developed locally advanced disease with evidence of EMT. This thesis has not explored the degree of EMT between each model however, which could be performed using IHC or IF for antibodies against slug, snail and twist for example. Such markers have been shown to be of prognostic value in human disease by predicting biochemical relapse following radical prostatectomy for example (Behnsawy et al. 2013)

Triple mutant mice develop upregulation of Pten within the stromal compartment suggesting a compensatory protective role of this tumour suppressor in response to changes in the tumour microenvironment. The interaction between the stromal and epithelial compartment is complex and thought to be important for the progression of the tumour. It has been shown that loss of Pten in the stroma fibroblasts of mouse mammary glands resulted in accelerated initiation, progression and malignant transformation of mammary epithelial tumours. This was thought to be due to a massive remodelling of the extra-cellular matrix and tumour vasculature with recruitment of innate immune cells (Trimboli et al. 2009). Thus, as demonstrated by the triple mouse model, Pten may be involved in altering the epithelial-mesenchymal or tumour-stroma cross talk resulting in possible protective signals, however not significant enough to prevent prostate tumourigenesis. This could also explain the reactive stroma that is particular seen in Pten deficient mouse prostates.

4.3.10 Limitations

A limitation of this type of mouse model is exposing the prostate to three simultaneous mutations. Cancer is thought to develop as a result of multiple genetic “hits”, where the original clone or genetic mutation is exposed to another environmental factor such as smoking for example, resulting in multiple clones which can lead to cancer initiation, progression and metastasis. Some mouse models in other tissues, such as bladder have

used carcinogens to mimic these environmental exposures, which are known to give rise to bladder cancer in humans. The carcinogen typically used in bladder models is *N*-butyl-*N*-(4-hydroxybutyl) nitrosamine (BBN), which is delivered in drinking water. BBN is highly relevant to human bladder cancer because it is very similar to the major carcinogen associated with tobacco smoke (Vasconcelos-Nóbrega et al. 2012). A further advantage of using carcinogens is that they can also be combined with GEM models with different phenotypes (Kobayashi et al. 2015) in order to study the effects on carcinogens in different genetic background, for example those genetic lesions that are more likely to develop smoking related bladder cancer. Unfortunately, this approach cannot be adopted in PCa as there is limited evidence supporting any environmental risk factors for the initiation or development of PCa.

A further limitation of this study is the number of incorporated genetic mutations. As more mutations are incorporated into a mouse model it becomes more difficult to understand the biology behind the interactions, and to appreciate which might be the “driver” mutation in the model. Also, with increasing mutations, there would be both cross-inhibition and cross-activation between pathways resulting in a very complex array of signals. This complexity again makes it difficult to appreciate which mutation is responsible for each pathway signal.

Importantly however, mouse models can be manipulated to mimic virtually all disease stages seen in human cancer including lymph node metastasis, as demonstrated by this work. Some groups have also demonstrated positive recombination of genes in DNA from bone marrow flushing’s (Mulholland et al. 2012). Whether these cause the osteoblastic metastasis seen in human disease has yet to be established however.

4.3.11 Summary and future direction

To conclude, Pten loss and activation of β -catenin and K-Ras cooperate to accelerate prostate tumourigenesis through synchronous activation of the PI3-Kinase, Wnt and MAP-Kinase signalling pathways. It is evident that “hallmarks” of cancer such as proliferation are elevated when more pathways are activated. Furthermore, when all three mutations are present there is aberration of the mTOR pathway, a site where these signals may converge. To explore this mechanism further, these mouse models could be

challenged with mTOR inhibitors such as Rapamycin to assess effects on tumour growth, progression and metastasis.

Other mechanisms to explain why a more aggressive PCa phenotype develops when more pathways are activated will be explored in the next chapter. Although this will be a challenge, the next chapter will explore the effects of pathway deregulation on the cancer stem cell population.

Emerging evidence from next-generation sequencing is promising being able to subdivide tumours based on mutational profiles and categorising these to actionable aberrations (Robinson et al. 2015). What is apparent is that alterations to PI3K, Wnt and MAPK are commonplace in human PCa and understanding the complex interactions between them is paramount for future successful therapies. The future is to better understand mutational signatures for PCa and to discover different patterns of mutations that cause different cancer-causing events. In particular, distinguishing between lethal cancers that need aggressive treatment and non-lethal cancers that do not. These gene profiles could then be modelled in the mouse, which will not only improve our biological understanding of them, but also provide a platform for pre-clinical testing of novel therapeutic agents.

5 Assessment of putative cancer stem cells (CSC) in human prostate cancer and optimisation of tumour organoid culture in the mouse effected by deregulation of the Wnt, PI3-Kinase (PI3K) and MAP-Kinase (MAPK) signalling pathways

5.1 Introduction

Adult epithelial stem cells are able to facilitate organ homeostasis and have a potential role in tumourigenesis. Throughout the life span of an adult organ, stem cells operate to replace lost or damaged tissue to ensure proper function (Blanpain et al. 2007), such as

in the blood, skin, and intestine. Owing to their longevity and inherent self-renewal capacity, adult stem cells are potential cells of origin for certain cancers (Barker, 2009).

The stem cells within a tumour are often referred to as a cancer stem cell (CSC). The CSC theory has been described in detail in the main introduction of this thesis. Tumours are perceived to have a hierarchy of cells, with a small population of CSC residing at the top and their more differentiated progeny (transit-amplifying or progenitor cells) below. The CSC is then postulated to drive the growth of cancer resulting in metastasis. The CSC is also thought to be important in treatment failure and recurrence as most conventional primary treatments aim at reducing tumour bulk rather than targeting the ‘beating heart’ of the tumour, the CSC (Clevers 2011).

As the CSC may originate from oncogenic alteration of normal stem cells, many studies have focused on the identification of the normal stem cells in order to identify the cell of origin of PCa. The location of the prostate epithelial stem cell, whether basal or luminal has been a focus of great debate in PCa, with evidence supporting both locations (Table 8 of Introduction). The effect of oncogenic mutations on the CSC population has also been investigated but to a lesser degree.

5.1.1 Chapter Aims

1. To evaluate putative prostate CSC markers using a human tissue micro-array (TMA).
2. To optimise tumour organoid assay using fluorescence-activated cell sorting (FACS) and 3D culture using matrigel.
3. To evaluate the effect of Wnt, PI3-Kinase and MAP-Kinase deregulation on the stem cell population. Mouse tumours driven by single, double and triple mutations will be investigated to determine:
 - a) Stem cell population
 - b) Organoid forming capacity (OFC)
 - c) Self-renewal through serial passage

5.2 Results

5.2.1 Evaluation of putative CSC markers in human PCa

A number of markers have been postulated to represent the CSC in epithelial cancers. Examples of these include: CD49f (Lawson et al. 2007), Trop-2 (Goldstein et al. 2008), Notch 1 (Valdez et al. 2012) & 4 (Harrison 2010), Integrin- β 1 (Collins et al. 2001) and Forkhead box protein A1 (Foxa-1) (Zhang 2011a). IHC was performed using antibodies against these markers using a human PCa TMA. The clinicopathological data for the TMA is described in detail in chapter 3. Representative IHC staining is illustrated in Figure 62.

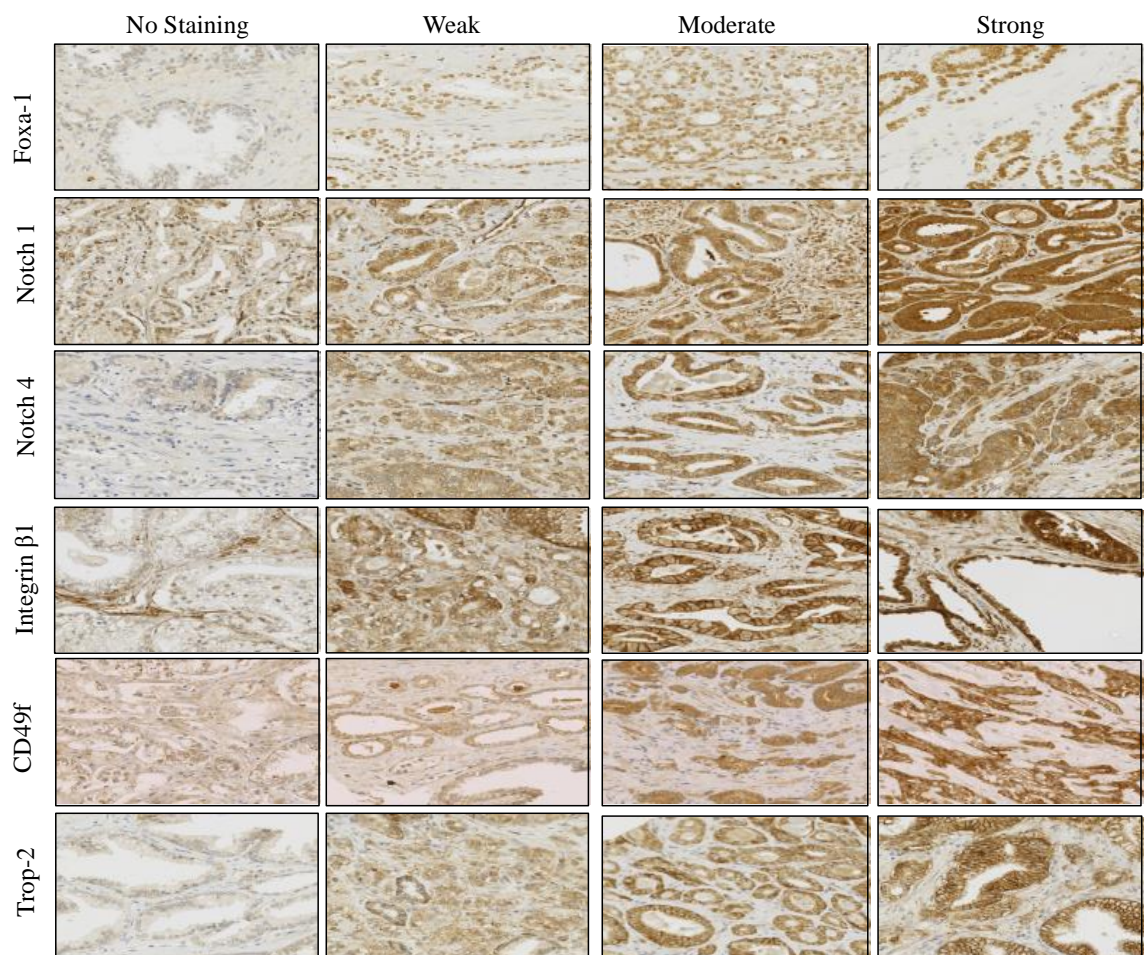


Figure 61: Examples of representative immunohistochemistry staining for putative stem cell markers: Foxa-1, Notch 1&4, Integrin- β 1, CD49f and Trop-2. Intensity scoring: No staining = 0, Weak = 1, Moderate = 2, Strong = 3. Proportion was also calculated formulating an overall quickscore (described in methods section).

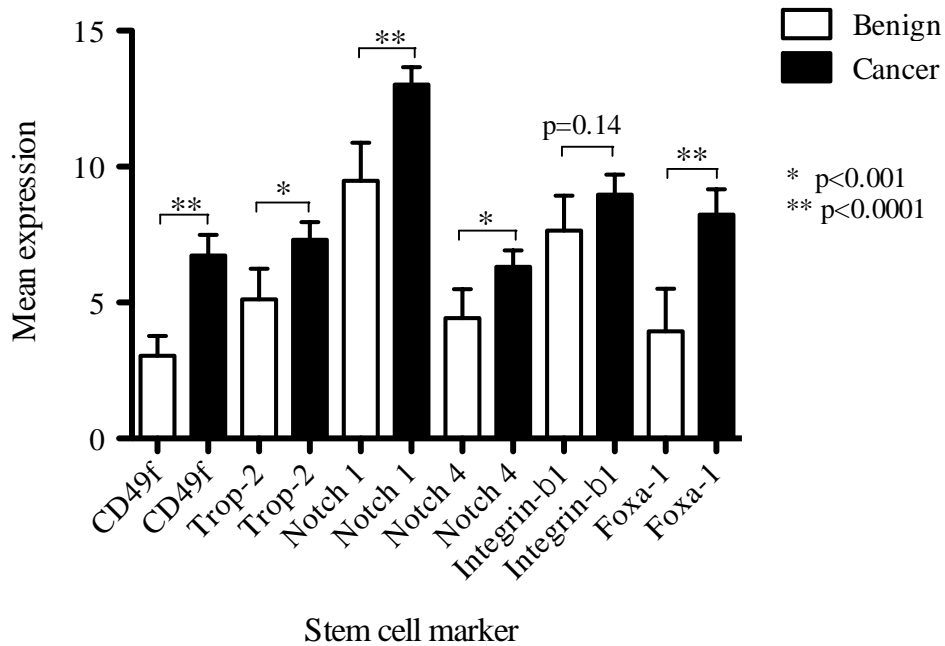


Figure 62: Summary of Stem cell marker expression (mean quickscore) between benign and cancer prostate samples. Error bars = 95% CI. There was significantly higher expression of all markers other than Intergrin-β1 in cancer specimens when compared to benign samples ($p < 0.001$ / $p < 0.0001$).

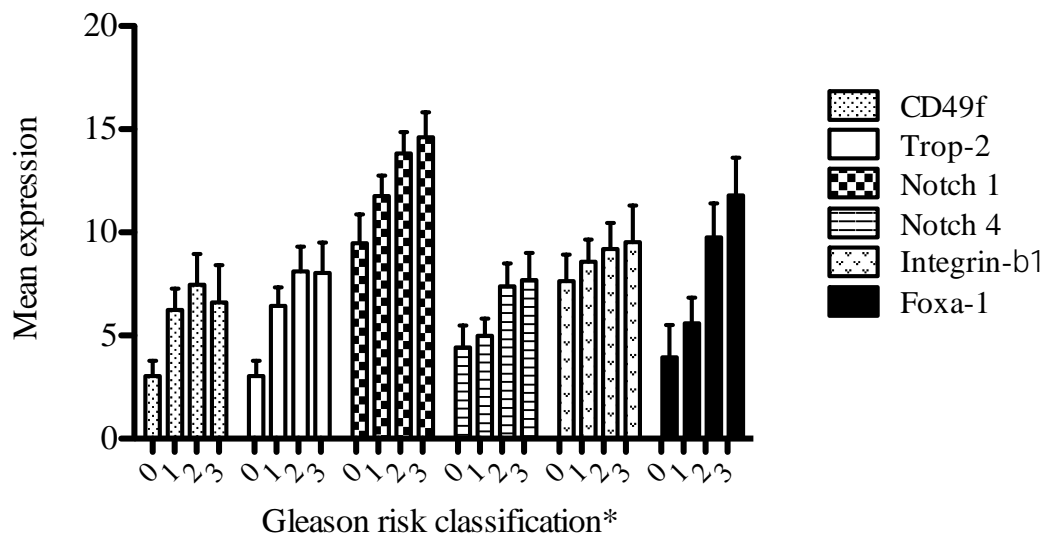


Figure 63: Summary of Stem cell marker expression (mean quickscore) categorised according to Gleason score (GS) risk classification as defined by D’Amico (*0 = normal, 1 = low-risk (GS=6), 2 = intermediate-risk (GS=7), 3 = high-risk (GS≥8)). Error bars = 95% CI.

There was significantly greater expression of all stem cell markers, other than for Intergrin- β , in human PCa samples when compared to benign samples (Figure 63). Furthermore, the mean expression increased as the Gleason risk group increased for many markers, in particular Notch 1 and Foxa-1 (Figure 64).

5.2.2 Optimisation of prostate organoid culture assay in the mouse

To enable the isolation and cultivation of prostate stem cells, a single cell suspension of prostate epithelial cells was selected using FACS, cultured using matrigel and PrEGM growth media to permit organoid formation, then passaged and re-plated to assess self-renewal capacity (as described in methods).

Our laboratory has experience in using FACS and the basal stem cell assay Lin⁻Sca1⁺CD49f⁺Trop-2^{HI} previously described by Goldstein et al (2008). We have shown in WT mice that the stem cell enriched population (Lin⁻Sca1⁺CD49f⁺Trop-2^{HI}) has the ability to self-renew with regeneration of organoids following serial passage to at least generation [G] 4. Unsorted WT cells were also able to form organoids but were less efficient, and only survived to G2. This work identified two areas of uncertainty:

1. Does the Probasin (Pb-Cre⁺) promoter cause recombination in both basal and luminal cells? As the Lin⁻Sca1⁺CD49f⁺Trop-2^{HI} adopts a basal stem cell assay it was vital to confirm genetic recombination within both cell compartments prior to further experiments.
2. A large number of mice (n=6-10) were needed for each experiment, as the yield of enriched cells was very low. In this study, in order to compare all genotypes (n=7) and replicate the experiment 3 times for each cohort, approximately 210 mice would be needed. This would be too costly.

5.2.2.1 Pb-Cre⁺ promoter causes recombination in both basal and luminal prostate cells

Mice modified with the Red Fluorescent Protein (RFP) reporter gene were used to confirm recombination in both basal and luminal prostate cells. The basal and luminal

cells can be characterised by their morphology and position. Basal cells are flatter and are located adjacent to the basement membrane whilst luminal cells are more cuboidal and located closer to the lumen of the glands. There was positive IHC staining in both cell types in Pb-Cre⁺RFP⁺ mice (Figure 65B&D) and absent in Pb-Cre⁻RFP⁺ mice (Figure 65A&C). Although not formally calculated, the recombination in both cells compartments appears to be similar. This differs from the original Pb-Cre study by X. Wu et al (2001), where recombination within the luminal compartment predominated. To further confirm cell specific recombination, co-staining with basal and luminal markers such as CK5 and CK8, respectively, could be used. A further observation was that there was more avid staining of RFP in the dorso-lateral lobes of Pb-Cre⁺RFP⁺ mice, an area of the mouse prostate that is thought to be more pathologically similar to that seen in human PCa.

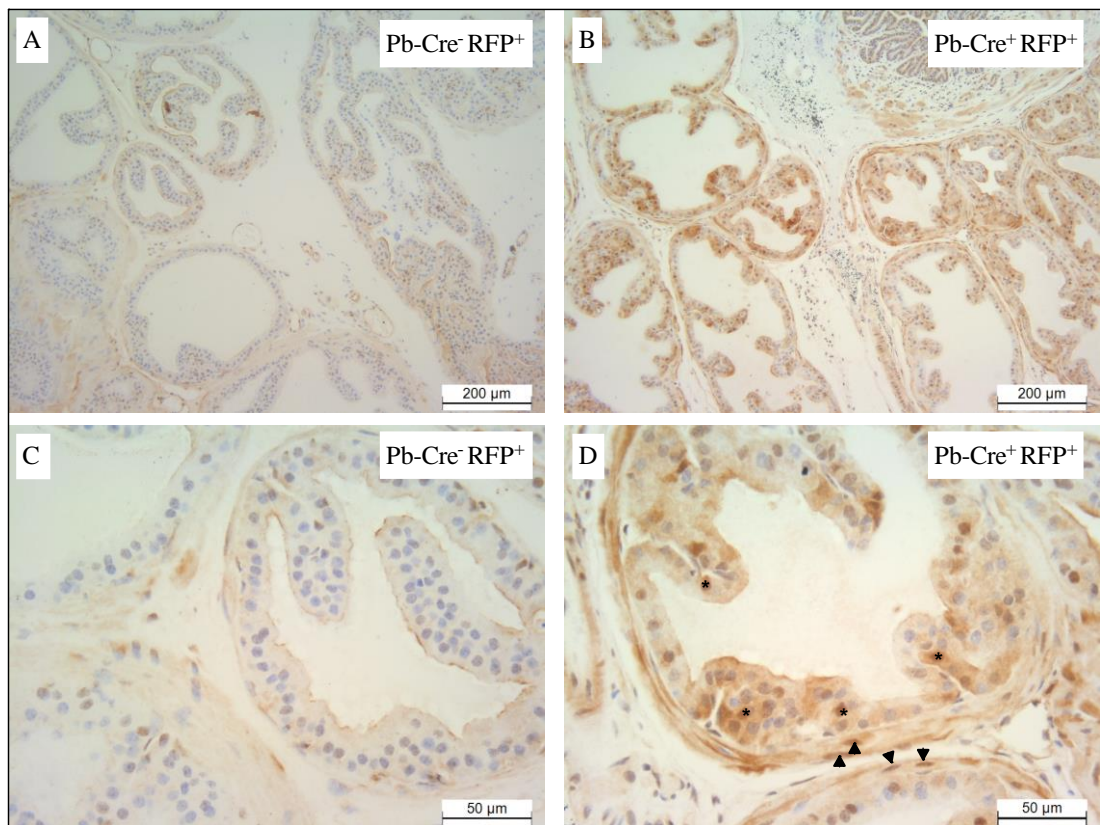


Figure 64: Anti-RFP Immunohistochemistry for Pb-Cre⁺ and Pb-Cre⁻ WT dorso-lateral lobes of the prostate at 100 days. Pb-Cre⁻ mice (A+C) demonstrated minimal staining, whereas Pb-Cre⁺ mice (B+D) stained both luminal (*) and basal cells (arrow head).

5.2.2.2 Optimising mouse numbers

Initially 100-day old mice were used. This time point was decided upon because it was before aggressive tumourigenesis had begun in most mouse cohorts, so the cell of origin theory could be investigated. Unfortunately, these experiments yielded very poor cell numbers at the expense of 6-10 mice per experiment. We could not afford to sacrifice 6-10 mutant mice for a single experiment and therefore a decision to use tumour tissue at endpoint (death) was made. At this time point only 1 mouse was required per experiment. Each experiment was repeated 3 times.

5.2.2.3 FACS assay

To aid further reduction in mouse numbers, the organoid forming capacity (OFC) and self-renewal capability through serial passage of the $\text{Lin}^- \text{Sca1}^+ \text{CD49f}^+$ assay (described by Lawson et al [2007]) without Trop-2 in WT mice was assessed. An example of this assay is shown in Figure 66. By excluding Trop-2, twice as many cells were enriched reducing the required mouse numbers by a half.

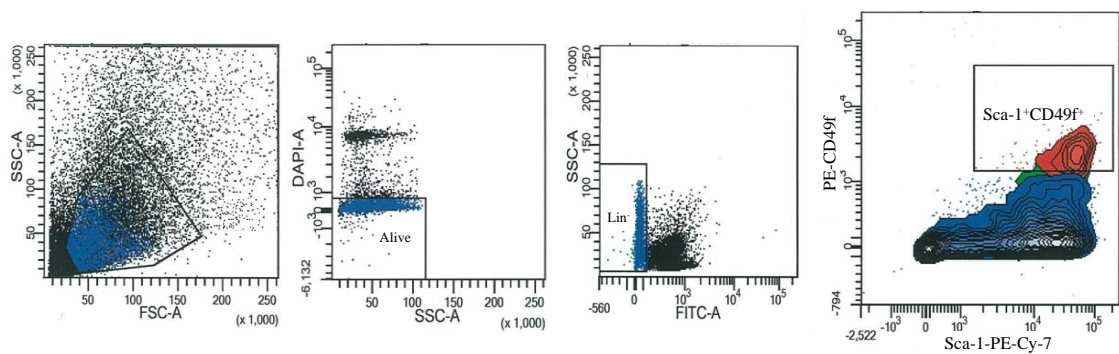


Figure 65: Fluorescence-activated cell sorting (FACS) using $\text{Lin}^- \text{Sca1}^+ \text{CD49f}^+$ stem cell/CSC enrichment assay. Single cells were initially selected using a combination of forward scatter (FSC) and side scatter (SSC). Alive cells were gated using 4', 6-diamidino-2-phenylindole (DAPI). Lineage negative (Lin^-) was used to select epithelial cells using a combination of antibodies CD31-FITC, CD45-FITC and Ter119-FITC. The stem cell/CSC enriched population was then gated using antibodies against CD49f and Sca-1 on the PE and PE-Cy-7 fluorochromes, respectively.

Similar to that observed in our laboratories previous work using the Lin⁻Sca1⁺CD49f⁺Trop-2^{HI} assay, the enriched cell population using the Lin⁻Sca1⁺CD49f⁺ (without Trop-2) assay in WT mice was able to passage to generation (G) 4 (Figure 67). There was an average of 340 (95% CI 299-380) organoids formed in G1, which equates to an OFC of 1 out of 29 Lin⁻Sca1⁺CD49f⁺ cells. This reduced to an average of 148 (95% CI 117-179) organoids in G2 (OFC 1 out of 67), 102 (95% CI 69-134) in G3 (OFC 1 out of 100) and 63 (95% CI 61-65) in G4 (OFC 1 out of 167) (Figure 67). Although the number of organoids decreased with each passage, there was still evidence of the stem cell property of self-renewal. The non-enriched population (Lin⁻Sca1⁺CD49f⁺ negative) formed very few organoids at G1 with no cells surviving for passage to G2.

As it was possible to obtain similar results using the Lin⁻Sca1⁺CD49f⁺ assay without the Trop-2 marker, this assay was used for future experiments using mutant mice.

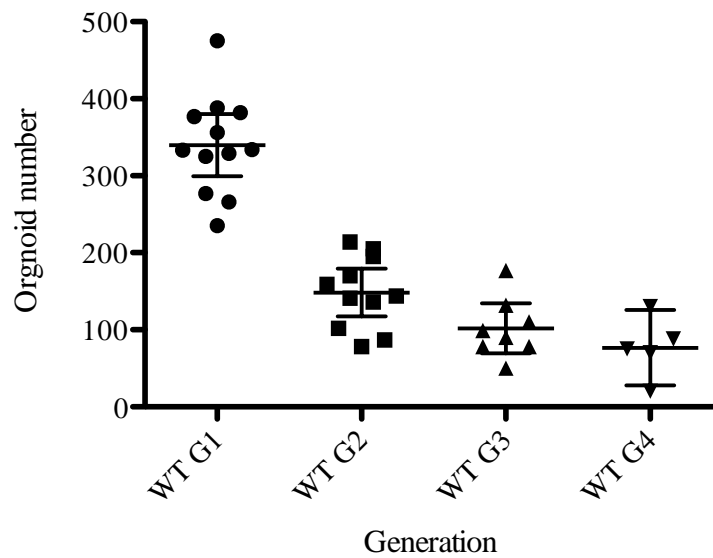


Figure 66: Lin⁻Sca1⁺CD49f⁺ enriched cells in wild-type (WT) mice were able to self-renew and passage to generation (G) 4. The mean number of organoids formed at day 7 was greatest in G1 (Mean=340, 95% CI 299-380). This reduced to a mean of 148 organoids (95% CI 117-179) for G2, 102 (95% CI 69-134) for G3 and 63 (95% CI 61-65) for G4. Error bars = Mean + 95% CI.

5.2.2.4 Optimising organoid culture conditions

Initially, a trial of single, double and triple mutant tumours were sorted on three separate days to assess the feasibility of the Lin⁻Sca1⁺CD49f⁺ assay in these mice. In addition, the usefulness of a selective Rho-associated kinase (ROCK) inhibitor added to the culture media was assessed. Activation of the ROCK-signalling pathway is associated with dissociation-induced apoptosis of stem cells, whereby cells are stressed during digestion and FACS sorting resulting in loss of stemness. Inhibition of this pathway using a ROCK inhibitor has been shown to improve cloning efficiency of prostate stem cells by 8 fold (Zhang et al. 2011). Our laboratory, using intestinal organoid culture, has also demonstrated an improvement in cell survival and organoid forming capacity when adopting this method. A ROCK inhibitor was therefore added to half of the wells for the first 72 hours following dissociation.

Figure 68 illustrates the OFC of three populations of cells for the 3 pilot tumours: unsorted, Lin⁻Sca1⁺CD49f⁺ and Lin⁻Sca1⁺CD49f⁺ negative. Across all three tumours the Lin⁻Sca1⁺CD49f⁺ cells consistently formed a greater number of organoids compared with unsorted cells and not Lin⁻Sca1⁺CD49f⁺ (Figure 68). The Lin⁻Sca1⁺CD49f⁺ assay was therefore feasible for murine prostate tumours. In contrast to Zhang et al (2011), the ROCK inhibitor did not show any strong trend towards improvement of OFC and therefore was not developed further.

Each experiment took 12-14 hours (Figure 16 in methods). Attempts were made to reduce this to a manageable time by splitting the experiment, including digesting the prostates overnight, and then dissociating into single cells, FACS and plate the following day. I also tried to leave the digested single cell preparation in the fridge at 4°C overnight prior to FACS and plating the following day. Unfortunately, the cell death adopting both these methods was too high and the illustrated method was used.

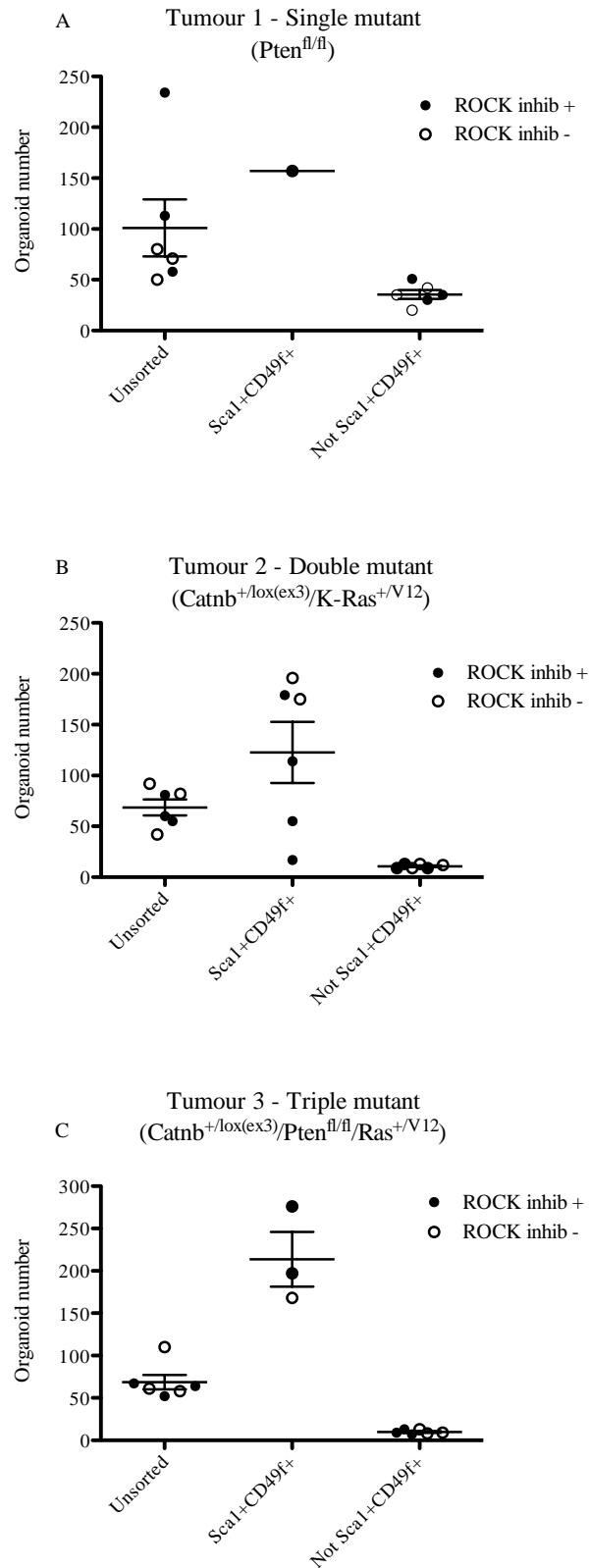


Figure 67: Organoid forming capacity (OFC) of 3 populations of cells: Unsorted, Lin⁻Sca1⁺CD49f⁺ and not Lin⁻Sca1⁺CD49f⁺ for 3 sample murine tumours and further separated by ROCK inhibitor treatment. A-C: The greatest OFC for all tumours was in the Lin⁻Sca1⁺CD49f⁺ cell population followed by the unsorted cells then the not Lin⁻Sca1⁺CD49f⁺ cells. ROCK inhibitor was added to half the wells and did not have any benefit to the OFC.

5.2.3 The percentage of the stem-cell/CSC enriched population (Lin⁻Sca1⁺CD49⁺) increases as genetic mutations increased

To assess the effect of genetic or pathway deregulation on the stem-cell/CSC population the Lin-Sca1⁺CD49⁺ assay (described by (Lawson et al. 2007) was used. The loss of Pten was incorporated as a means of activating the PI3K pathway and mutated β -catenin and K-Ras as means of aberrant Wnt and MAPK signalling. As the number of mutations increased the percentage of stem-cell/CSC enriched cells also increased (Figure 69).

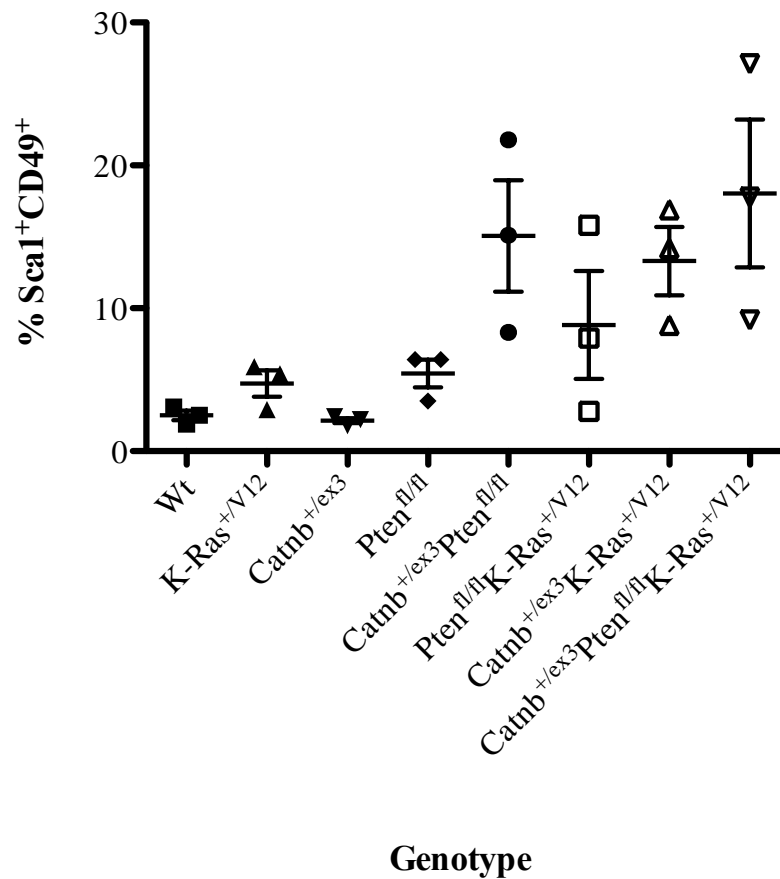


Figure 68: Percentage Sca1⁺CD49⁺ according to genotype. The percentage of Sca1⁺CD49⁺ increased with combinatory mutations when compared to single mutants and WT mice. Three individual sorts were performed for mice at endpoint of the experiment (death or 500 days). Error bars = mean + 95% CI.

5.2.4 WT enriched cells have the greatest organoid forming capacity with triple mutants demonstrating a greater OFC than single or double mutants

Stem-cell/CSC enriched cells were cultured in matrigel and number of organoids counted in each well at 7 days. WT cells had the greatest OFC with some recovery of function with increasing number of mutations (Figure 70). This finding was unexpected given the greater percentage of stem-cell/CSC enriched cells (Lin-Sca1⁺CD49⁺) in triple mutants (Figure 69). The reasons for this are unclear and are likely to be multi-factorial. The tumour organoids may require signals from its surrounding niche environment for significant growth or the media used may not have all the correct growth factors for efficient growth.

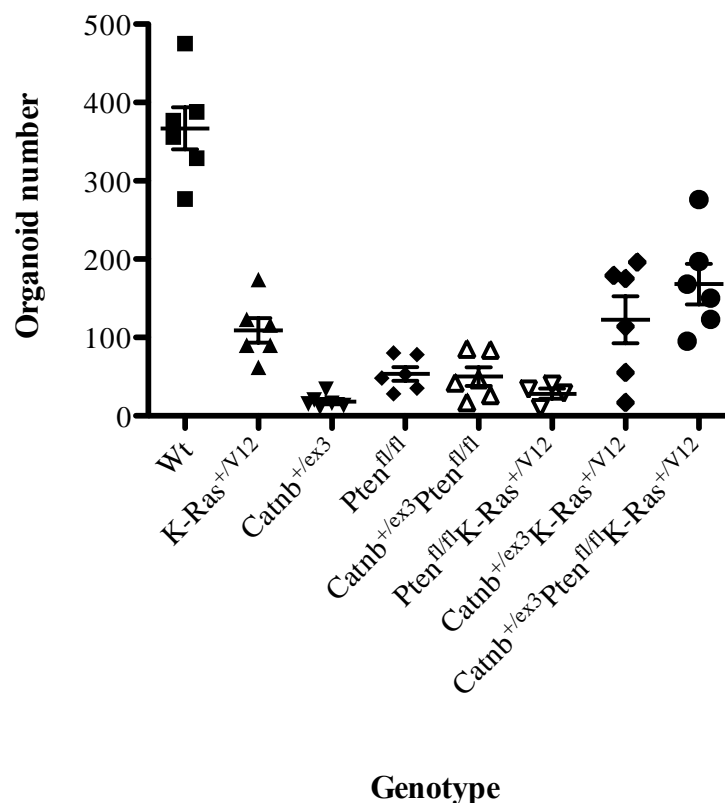


Figure 69: Number of organoids formed as function of genotype. WT enriched cells had the greatest organoid forming capacity. β -catenin/K-Ras double and triple mutant cells had some recovery in organoid forming capacity when compared to single mutant cells. Error bars = mean + 95% CI.

The capacity of organoids to undergo self-renewal through serial passage was assessed using WT mice, as discussed above (Figure 67). Unfortunately, due to the low number of enriched cells following FACS in the tumour models, there were only enough cells for 1 or 2 wells to be plated per experiment. There was therefore limited material available to passage and to demonstrate self-renewal of the tumour organoids.

5.2.5 All organoids had a similar morphological phenotype

A similar phenotype was seen across all genotypes including WT organoids. All were spherical, with some appearing more solid (Figure 71B), while others had a central core with signs of keratin deposition and squamous metaplasia (Figure 71C). In contrast to others (Mulholland et al. 2012) we did not observe any complex organoid formation. Where material was available, prostate organoids were formalin-fixed, paraffin-embedded and sectioned for H&E and IHC analysis. These organoids expressed a basal-phenotype with staining of CK5 and p63. These findings were inconsistent with other series (Lukacs et al. 2010; Goldstein et al. 2008), as they failed to show multi-potency with negative staining of the luminal marker CK8. It was observed that the most proliferative cells, resided at the periphery of the organoid with positive staining of Ki67.

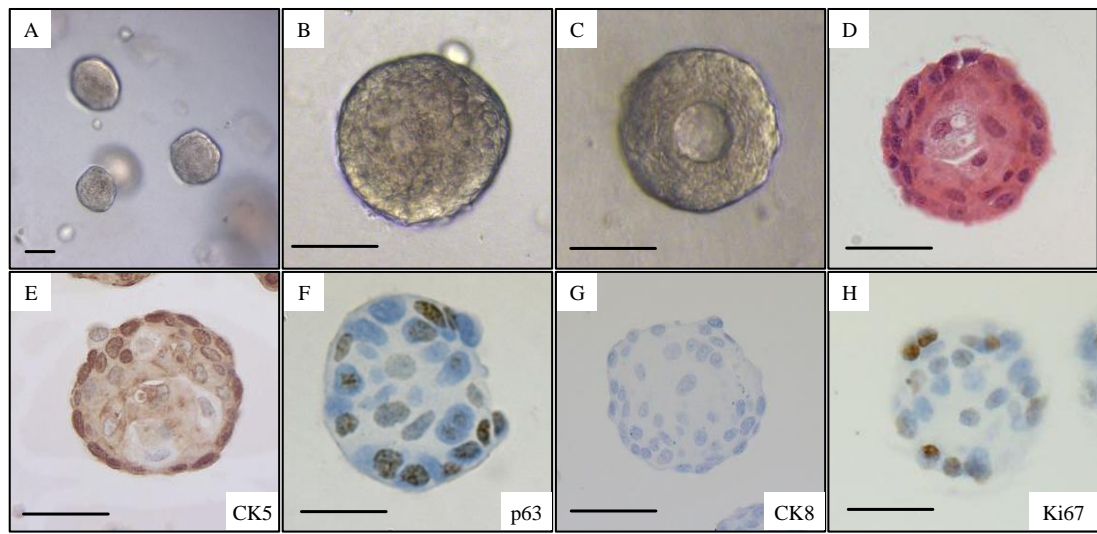


Figure 70: Prostate organoid characterisation. Bright-field images of solid organoids (A&B), with some demonstrating signs of squamous differentiation and keratin deposition centrally (C). H&E image of a solid organoid (D). The periphery of the organoids stained avidly for basal markers CK5 (E) and p63 (F), but failed to demonstrate multi-potency with negative staining of luminal marker CK8 (G). The proliferating cells, stained by Ki67, typically resided at the periphery (H). Error bars = 50 μ m.

5.3 Discussion

5.3.1 Putative CSC markers that are associated with many signalling processes or cell types, are elevated in human prostate cancer – is there more than one CSC?

All putative stem cells markers analysed appear to have a greater expression in human PCa and particularly in those with high-risk disease. The original CSC theory describes a small sub-population of cells within the tumour that largely drive growth and metastasis. The data presented here shows expansion of a pool of CSC but does not necessarily identify the sub-population of the driver cells or the “cell of origin”. There are two theories to explain this. There could be clonal expansion of the CSC or these markers could represent expansion of transit-amplifying or progenitor cells.

What is also evident is that these markers are associated with different cellular processes or cell types. CD49f and Trop-2 are basal markers and have been shown to possess many CSC characteristics such as a high potential for tumour growth, self-renewal, multi-differentiation, metastases and drug resistance (Lawson et al. 2007; Goldstein et al. 2008). Similarly, Collins et al (2001) have shown that a subset of basal cells expressing high levels of Intergrin- β 1 have the ability to generate prostate-like glands in vivo with morphologic and IHC evidence of prostate-specific differentiation (Collins et al. 2001). Foxa-1 also displays many features of a CSC: it is required for epithelial cell differentiation in the murine prostate (Gao et al. 2005) and promotes cell cycle progression in castration-resistant PCa (Zhang et al. 2011). Exon sequencing has also shown recurrence mutations of the Foxa-1 gene (Barbieri et al. 2012). Functionally, Foxa-1 is thought to modulate androgen receptor driven gene transcription (Gao et al, 2003). Unlike CD49f and Trop-2, Foxa-1 has recently been shown to affect the proliferating activity of luminal and not basal cells, albeit in breast cancer (Tachi et al. 2016). This is in contrast to the Notch pathway, which has been shown to be widely expressed in both the basal and luminal cell compartments of adult murine prostates (Valdez et al. 2012).

Two postulated theories have arisen from these data. Firstly, there is more than one CSC with different cell lineages or clones, which all represent properties that are common to stem cells. This plausible notion could explain the sub-types of cancers that are emerging

(Robinson et al. 2015) or explain the heterogeneity seen in PCa, with some patients getting aggressive disease and others indolent. Secondly, the high expression of multiple markers involving different cell types or signalling pathways, particularly seen here in aggressive disease, could simply confirm the complexity of signals and cross-talk present in aggressive PCa, as highlighted from the data presented in Chapters 3 and 4.

5.3.2 Increasing number of genetic mutations or pathway deregulation in the mouse causes expansion of the CSC population

To study the effects of deregulation of multiple molecular pathways or mutations, as seen in aggressive PCa, on the CSC population, the mouse models previously described in chapter 4 were used. It was hypothesised that deregulation of the PI3K, Wnt and MAPK pathways drive expansion of the CSC population, resulting in disease progression and metastasis.

Using the assay described here, following pathway deregulation there is an expansion of the pool of CSC. This is particularly seen in compound mutant mice (doubles and triples) whereby multiple cell signaling pathways have been affected. Despite this, stem-cell enriched WT cells demonstrate the greatest organoid forming capacity when compared to all other mutant cells. The reasons for the favored conditions seen in WT cells permitting organoid growth are unclear. These findings have also been reported in intestinal organoid culture (Sachs et al. 2014). Although, a basal stem cell media (PrEGM, Lonza) containing many growth factors was used other factor or conditions may be necessary to allow further growth, differentiation and passage of enriched mutant cells. What must also be remembered is that these media conditions have been optimised for WT cells and not tumour or mutant cells whose niche environment may be particular. Moreover, despite the use of matrigel (as a basement membrane substitute) and growth factors to aid signals from the stroma seen in vivo, there is potential loss of epithelial integrity (epithelial-mesenchymal transition-EMT) in tumour organoids studied ex-vivo. Further evidence for the suboptimal growth conditions is the presence of squamous metaplasia seen in organoids across all genotypes. This was also observed in the mouse prostates, however only in those harboring a mutated β -catenin allele (Chapter 4). Squamous metaplasia is a terminally differentiated cell and although not frequently seen

in human PCa is often associated with chronic injury or stress. Tumour organoids failed to successfully passage, which is partly explained by the loss of cells as a result of mechanically dissociating the organoids into single-cell and re-plating but the sub-optimal culture conditions may have also played a role.

Nevertheless, there does appear to be some recovery of stem cell activity with increasing number of mutations with double/triple mutant cells forming more organoids than single mutant cells. This could indicate that the hypothesis is correct in that with more pathway deregulation the pool of CSC increases. Further optimisation of growth conditions could prove this. Mullholland et al (2012) has shown similar results with significantly greater sphere formation in Pten/K-Ras compound mutant mice compared to single (Pten or K-Ras) mutants. Interestingly they did not compare to WT cells, which formed the most organoids in this study.

Since completing this work other groups have experimented with other types of media. For example, Clevers laboratory have used media that was initially tested in intestinal organoids, which contained other growth factors such as R-Spondin-1 and Noggin (Sato et al. 2011). These are thought to be indispensable stem cell maintenance factors necessary for intestinal organoid growth. The same group have since demonstrated successful growth of human PCa organoids using the same culture media (Gao et al. 2014).

The adopted assay used here enriches for basal-CSC. Although Probasin promotes recombination in both luminal and basal cells, more specific promoters are available. These include basal cell type specific promoters such as CK5-CreER (Rock et al. 2009) and p63 (Pignon et al. 2013), or luminal specific promoters such as PSA-CreER (Ratnacaram et al. 2008) and CK8-CreER (Van Keymeulen et al. 2011). For specific studies into the origin of the CSC future studies could adopt these.

Data from this chapter has shown that a population of cells with stem-cell-like properties expands with increasing deregulation of the PI3K, Wnt and MAPK pathways, through mutations of Pten, β -catenin and K-Ras. A further theory is that deregulation of these pathways drive initiation of PCa by altering the pool of 'cells of origin'. This theory has not been extensively studied here. Younger mice could be used prior to the onset of tumourigenesis or further organoid culture using a small sub-population of cells selected using FACS and xenotransplanting into immunodeficient (nude) mice could be

performed. The main draw back precluding mass uptake of both FACS and xenotransplant is the time, cost and the artificial microenvironment produced that does not accurately mimic the conditions seen in human PCa.

5.3.3 Chapter Summary

A number of putative CSC markers are increased in aggressive human PCa. Using mouse models of PCa, deregulation of the Wnt, PI3K and MAPK pathways result in expansion of the CSC population. Although, there is some recovery in organoid forming efficiency with increasing mutations, the growth conditions for tumour organoids is suboptimal and inferior to that of WT mice. This result was not expected given the contrasting results seen in the compound mouse models, with rapid tumour growth and proliferation. The reasons for this are unclear but are likely multifactorial; such as suboptimal growth conditions lacking key growth factors or the inability to grow in the current matrix (matrigel). If further optimisation is successful then one would expect similar results to that seen in the mouse models with a more proliferative phenotype and a great organoid forming efficiency. PCa organoids could then be used for drug screens and used in mechanistic studies of therapeutic response and resistance in PCa. Furthermore, primary human PCa organoids might be suitable for storing in a cryopreserved organoid library, and could be used for manufacturing targeted drugs.

6 Final Discussion

Mounting data suggests that epithelial cancers can be subdivided based on a molecular profile of genetic alteration known to affect certain cell signalling pathways such as Wnt, PI3K and MAPK, or genes associated with certain cellular mechanism such as DNA repair and cell cycle. This subdivision has been reported in bladder cancer, where FGFR3 mutations predominate in superficial papillary tumours and p53 and/or Rb pathway alterations predominate in muscle-invasive lesions (Goebell & Knowles 2010). Although the androgen signalling pathway and ADT are pivotal in the treatment of advanced PCa, men still relapse with CRPC where survival is poor. Alternative signalling pathways such as the Wnt, PI3K and MAPK are known to play important roles in PCa, but there is limited evidence supporting the communication between these pathways.

Data from this thesis has demonstrated activation of all three pathways in human PCa, which was most evident in high-risk disease. This was demonstrated using both IHC and targeted-NGS for markers or genes associated with these pathways. Based on readouts of these markers it was possible to cluster individual samples, in particular separating those with high- and low-risk disease. These data suggests that different grades of disease have different molecular or genetic signatures. This finding is important and may explain why some tumours have more aggressive features resulting in progression, metastasis and treatment failure.

To investigate this theory further, mouse models were used. Using Cre-LoxP technology and the Probasin promoter, the loss of Pten was incorporated as a means to activate the PI3K signalling pathway, and the β -catenin and K-Ras activated mouse model as means of aberrant Wnt and MAPK signalling. This study provides the first evidence of clear crosstalk between these signalling pathways, which has significant effects on prostate tumourigenesis. Mice with loss of Pten in addition to activation of β -catenin and K-Ras have significant up-regulation of the PI3K, Wnt and MAPK signalling as demonstrated by IHC and western-blot analysis for downstream markers and target genes of each pathway. Furthermore, they cooperate, resulting in a significantly shorter survival than double and single mutant mice. Tumourigenesis occurred in a step-wise fashion from mPIN to invasive adenocarcinoma. The aggressive phenotype seen in compound mutant mice was confirmed with a greater percentage of invasive adenocarcinoma at 100 days

and increased proliferation markers, Ki67 and BRDU. Specific combinations of gene mutations were also more prone to the development of lymph node metastasis.

Both human and mouse data presented here offer a glimpse into the molecular profile of individual PCa samples. This opens exciting future prospects, with the development of targeted assays or biomarker/genetic panels permitting personalised molecular profiles, thereby directing future therapies. Biomarker or genetic tests can help physicians to select the most effective therapy for a patient's condition and avoid treatments that could be ineffective or harmful. This type of approach, often referred to as precision medicine is rapidly expanding and has transformed the outlook of many epithelial cancers, in particular lung and melanoma (Ladanyi & Pao 2008; Flaherty et al. 2010; Chapman et al. 2011).

The results of targeted therapies in PCa clinical trials have on the whole been poor. The majority of these studies have been in the metastatic setting where there is a complex genetic profile making single agent targeted therapies ineffective. Historically, new treatments are tested first in the metastatic disease; however, is this too late? Future trials could aim to use drugs in a neo-adjuvant or adjuvant setting in primary cancer treatment (prostatectomy or radiotherapy) as opposed to waiting for the onset of metastatic disease where the molecular signature is more complicated.

Until recently, there has also been no selection criteria or personalisation of trial agents used in PCa, possibly contributing to the poor reported results. A recent study by Mateo et al (2015) has shown a three fold survival benefit by stratifying patients with a mutation in one or more DNA repair gene to the PARPi, Olaparib (Mateo et al. 2015). The incorporation of tumour molecular profiles (using both NGS and IHC) in future clinical trials is key for the success of these drugs. This thesis using IHC and the CHPv2 gene panel has shown the feasibility of obtaining molecular profiles for the WNT, PI3K and MAPK pathways. Future studies could stratify their targeted agents based on these profiles. The recently designed molecular stratified randomised control trial, FOCUS4 in metastatic colorectal cancer has adopted these ideas. Here, four molecular cohorts are identified: BRAF mutant tumours, PI3K mutant tumours, KRAS or NRAS mutant tumours and EGFR dependent tumours. Each cohort is given a specific agent, for example, dual pathway inhibition using an AKT inhibitor and MEK inhibitor in KRAS or NRAS mutant tumours. The primary outcome is effect on progression free survival

(further information is available at www.focus4trial.org). A similar trial could be set up for PCa.

To explain why more aggressive PCa phenotypes are seen in mice that harbour a greater number of mutations, the CSC theory was explored. If CSCs originate from malignant transformation of a normal stem cell, then it follows that they may share antigenic profiles. Here, using the basal assay: Lin⁻Sca⁺CD49f⁺ assay using FACS, as a marker of the CSC I hypothesised that the Wnt, PI3K and MAPK pathways synergise and drive expansion of this population. Also, compound mutations (doubles and triple) have a greater number of CSC or enriched cells compared to single mutants or WT mice. Although there is some recovery in organoid forming efficiency with increasing mutations, the growth conditions for tumour organoids is suboptimal and inferior to that of WT mice.

The difficulty experienced here with tumour organoid growth has been seen by others (Sachs et al. 2014). The reasons for this are unclear. The most likely explanation is due to suboptimal growth conditions. Although the media used in this thesis contained many growth factors, future experiments could use additional compounds such as R-Spondin-1 and Noggin, which have proved important in more recent studies in human prostate organoids (Gao et al. 2014). The microenvironment provided by Matrigel may also not provide the necessary support for tumour organoids to form efficiently and permit differentiation. If further optimisation is successful then PCa organoids could be used for drug screens and used in mechanistic studies of therapeutic response and resistance in PCa. Furthermore, primary human PCa organoids might be suitable for storing in a cryopreserved organoid library, and could be used for manufacturing targeted drugs. The main limitations of this technique that could prevent its widespread use are the duration of each experiment (often over 12 hours) and the cost, as experienced in this thesis. Attempts were made to improve these however these technical challenges remain.

The assay used here enriches for basal-CSC. There remains some doubt as to the origin of the CSC; whether in the basal or luminal cell compartment, or whether they originate from both lineages. Although, recombination of the targetted genes was evident in both basal and luminal cells using the Probasin promoter in the mouse, to explore the notion of multiple CSC or cells of origin, basal and luminal specific promoters could be used. This theory could also explain the mutli-focal and heterogenous nature of PCa.

7 References

- Aarnio, M. et al., 1999. Cancer risk in mutation carriers of DNA-mismatch-repair genes. *International journal of cancer. Journal international du cancer*, 81(2), pp.214–218.
- Ahmad, I. et al., 2011. Ras mutation cooperates with β -catenin activation to drive bladder tumourigenesis. *Cell death & disease*, 2(3), p.e124.
- Ahmed, M. & Rahman, N., 2006. ATM and breast cancer susceptibility. *Oncogene*, 25(43), pp.5906–5911.
- Albertsen, P.C., Hanley, J.A. & Fine, J., 2005. 20-year outcomes following conservative management of clinically localized prostate cancer. *JAMA*, 293(17), pp.2095–2101.
- Allred, D.C. et al., 1998. Prognostic and predictive factors in breast cancer by immunohistochemical analysis. *Modern pathology : an official journal of the United States and Canadian Academy of Pathology, Inc*, 11(2), pp.155–168.
- Amado, R.G. et al., 2008. Wild-type KRAS is required for panitumumab efficacy in patients with metastatic colorectal cancer. *Journal of clinical oncology : official journal of the American Society of Clinical Oncology*, 26(10), pp.1626–1634.
- Amaral, T. et al., 2013. Classification and immunohistochemical scoring of breast tissue microarray spots. *IEEE transactions on bio-medical engineering*, 60(10), pp.2806–2814.
- Amato, R.J. et al., 2008. Pilot study of rapamycin in patients with hormone-refractory prostate cancer. *Clinical genitourinary cancer*, 6(2), pp.97–102.
- Amory, J.K. & Bremner, W.J., 2003. Regulation of testicular function in men: implications for male hormonal contraceptive development. *The Journal of steroid biochemistry and molecular biology*, 85(2-5), pp.357–361.
- Andriole, G.L. et al., 2010. Effect of dutasteride on the risk of prostate cancer. *The New England journal of medicine*, 362(13), pp.1192–1202.
- Aparicio, A., Den, R.B. & Knudsen, K.E., 2011. Time to stratify? The retinoblastoma protein in castrate-resistant prostate cancer. *Nature reviews. Urology*, 8(10), pp.562–568.
- Arva, N.C. & Das, K., 2011. Diagnostic dilemmas of squamous differentiation in prostate carcinoma case report and review of the literature. *Diagnostic pathology*, 6(1), p.46.
- Aune, D. et al., 2015. Dairy products, calcium, and prostate cancer risk: a systematic review and meta-analysis of cohort studies. *The American journal of clinical nutrition*, 101(1), pp.87–117.
- Auprich, M. et al., 2011. Contemporary role of prostate cancer antigen 3 in the management of prostate cancer. *European urology*, 60(5), pp.1045–1054.

- Austin, C.P. et al., 2004. The knockout mouse project. *Nature genetics*, 36(9), pp.921–924.
- Ayala, G. et al., 2004. High levels of phosphorylated form of Akt-1 in prostate cancer and non-neoplastic prostate tissues are strong predictors of biochemical recurrence. *Clinical cancer research : an official journal of the American Association for Cancer Research*, 10(19), pp.6572–6578.
- Baca, S.C. et al., 2013. Punctuated evolution of prostate cancer genomes. *Cell*, 153(3), pp.666–677.
- Barbieri, C.E., 2013. Evolution of novel biomarkers for detection of prostate cancer. *The Journal of urology*, 190(6), pp.1970–1971.
- Barbieri, C.E., Demichelis, F. & Rubin, M.A., 2012. Molecular genetics of prostate cancer: emerging appreciation of genetic complexity. *Histopathology*, 60(1), pp.187–198.
- Barbieri et al. 2012. Exome sequencing identifies recurrent SPOP, FOXA1 and MED12 mutations in prostate cancer. 44(6), pp.685–689. Available at: <http://www.nature.com/doi/10.1038/ng.2279>.
- Barker, N. et al., 2007. Identification of stem cells in small intestine and colon by marker gene Lgr5. *Nature*, 449(7165), pp.1003–1007.
- Barker, N. et al., 2010. Lgr5(+ve) stem cells drive self-renewal in the stomach and build long-lived gastric units in vitro. *Cell stem cell*, 6(1), pp.25–36.
- Basu, S. & Tindall, D.J., 2010. Androgen action in prostate cancer. *Hormones & cancer*, 1(5), pp.223–228.
- Bedolla, R. et al., 2007. Determining risk of biochemical recurrence in prostate cancer by immunohistochemical detection of PTEN expression and Akt activation. *Clinical cancer research : an official journal of the American Association for Cancer Research*, 13(13), pp.3860–3867.
- Behnsawy, H.M. et al., 2013. Expression patterns of epithelial-mesenchymal transition markers in localized prostate cancer: significance in clinicopathological outcomes following radical prostatectomy. *BJU international*, 111(1), pp.30–37.
- Beltran, H. et al., 2013. Targeted next-generation sequencing of advanced prostate cancer identifies potential therapeutic targets and disease heterogeneity. *European urology*, 63(5), pp.920–926.
- Berg, K.D. et al., 2014. ERG protein expression in diagnostic specimens is associated with increased risk of progression during active surveillance for prostate cancer. *European urology*, 66(5), pp.851–860.
- Berger, M.F. et al., 2011. The genomic complexity of primary human prostate cancer. *Nature*, 470(7333), pp.214–220.
- Berney, D.M. et al., 2009. Ki-67 and outcome in clinically localised prostate cancer: analysis of conservatively treated prostate cancer patients from the Trans-Atlantic

- Prostate Group study. *British journal of cancer*, 100(6), pp.888–893.
- Beroukhi, R. et al., 2010. The landscape of somatic copy-number alteration across human cancers. *Nature*, 463(7283), pp.899–905.
- Bettencourt, M.C. et al., 1996. Ki-67 expression is a prognostic marker of prostate cancer recurrence after radical prostatectomy. *The Journal of urology*, 156(3), pp.1064–1068.
- Biankin, A.V. et al., 2012. Pancreatic cancer genomes reveal aberrations in axon guidance pathway genes. *Nature*, 491(7424), pp.399–405.
- Bierie, B. et al., 2003. Activation of beta-catenin in prostate epithelium induces hyperplasias and squamous transdifferentiation. *Oncogene*, 22(25), pp.3875–3887.
- Bill-Axelsson, A. et al., 2005. Radical prostatectomy versus watchful waiting in early prostate cancer. *The New England journal of medicine*, 352(19), pp.1977–1984.
- Bismar, T.A. et al., 2004. Expression of beta-catenin in prostatic adenocarcinomas: a comparison with colorectal adenocarcinomas. *American journal of clinical pathology*, 121(4), pp.557–563.
- Bisson, I. & Prowse, D.M., 2009. WNT signaling regulates self-renewal and differentiation of prostate cancer cells with stem cell characteristics. *Cell research*, 19(6), pp.683–697.
- Bitting, R.L. & Armstrong, A.J., 2013. Targeting the PI3K/Akt/mTOR pathway in castration-resistant prostate cancer. *Endocrine-related cancer*, 20(3), pp.R83–99.
- Blair, K., Wray, J. & Smith, A., 2011. The liberation of embryonic stem cells. D. R. Beier, ed. *PLoS genetics*, 7(4), p.e1002019.
- Blanpain, C et al. 2007. Epithelial stem cells: turning over new leaves. *Leading Edge Review*. 128(3), pp.445–458. Available at: <http://linkinghub.elsevier.com/retrieve/pii/S0092867407000700>.
- Bolla, M. et al., 2009. Duration of androgen suppression in the treatment of prostate cancer. *The New England journal of medicine*, 360(24), pp.2516–2527.
- Bonnet, D. & Dick, J.E., 1997. Human acute myeloid leukemia is organized as a hierarchy that originates from a primitive hematopoietic cell. *Nature medicine*, 3(7), pp.730–737.
- Bostwick, D.G. et al., 2004. Human prostate cancer risk factors. In *Cancer*. Wiley Subscription Services, Inc., A Wiley Company, pp. 2371–2490.
- Bratan, F. et al., 2013. Influence of imaging and histological factors on prostate cancer detection and localisation on multiparametric MRI: a prospective study. *European radiology*, 23(7), pp.2019–2029.
- Bray, F. et al., 2010. Prostate cancer incidence and mortality trends in 37 European countries: an overview. *European journal of cancer (Oxford, England : 1990)*, 46(17), pp.3040–3052.

- Breslow, N. et al., 1977. Latent carcinoma of prostate at autopsy in seven areas. The International Agency for Research on Cancer, Lyons, France. *International journal of cancer. Journal international du cancer*, 20(5), pp.680–688.
- Brewster, D.H. et al., 2000. Rising incidence of prostate cancer in Scotland: increased risk or increased detection? *BJU international*, 85(4), pp.463–72– discussion 472–3.
- Brioli, A. et al., 2014. The impact of intra-clonal heterogeneity on the treatment of multiple myeloma. *British journal of haematology*, 165(4), pp.441–454.
- Bruxvoort, K.J. et al., 2007. Inactivation of Apc in the mouse prostate causes prostate carcinoma. *Cancer research*, 67(6), pp.2490–2496.
- Burstein, H.J., 2005. The distinctive nature of HER2-positive breast cancers. *The New England journal of medicine*, 353(16), pp.1652–1654.
- Canil, C.M. et al., 2005. Randomized phase II study of two doses of gefitinib in hormone-refractory prostate cancer: a trial of the National Cancer Institute of Canada-Clinical Trials Group. *Journal of clinical oncology : official journal of the American Society of Clinical Oncology*, 23(3), pp.455–460.
- Cantley, L.C., 2002. The phosphoinositide 3-kinase pathway. *Science (New York, N.Y.)*, 296(5573), pp.1655–1657.
- Cao, Y. & Ma, J., 2011. Body Mass Index, Prostate Cancer–Specific Mortality, and Biochemical Recurrence: a Systematic Review and Meta-analysis. *Cancer Prevention Research*.
- Carriere, A. et al., 2011. ERK1/2 phosphorylate Raptor to promote Ras-dependent activation of mTOR complex 1 (mTORC1). *The Journal of biological chemistry*, 286(1), pp.567–577.
- Carter, B.S. et al., 1992. Mendelian inheritance of familial prostate cancer. *Proceedings of the National Academy of Sciences of the United States of America*, 89(8), pp.3367–3371. Available at: <http://eutils.ncbi.nlm.nih.gov/entrez/eutils/elink.fcgi?dbfrom=pubmed&id=1565627&retmode=ref&cmd=prlinks>.
- Carver, B.S. et al., 2011. Reciprocal feedback regulation of PI3K and androgen receptor signaling in PTEN-deficient prostate cancer. *Cancer cell*, 19(5), pp.575–586.
- Castellano, E. & Downward, J., 2011. RAS Interaction with PI3K: More Than Just Another Effector Pathway. *Genes & cancer*, 2(3), pp.261–274.
- Castro, E. et al., 2013. Germline BRCA mutations are associated with higher risk of nodal involvement, distant metastasis, and poor survival outcomes in prostate cancer. *Journal of clinical oncology : official journal of the American Society of Clinical Oncology*, 31(14), pp.1748–1757.
- Chan, J.M. et al., 2001. Dairy products, calcium, and prostate cancer risk in the Physicians' Health Study. *The American journal of clinical nutrition*, 74(4), pp.549–

554.

- Chapman, P.B. et al., 2011. Improved survival with vemurafenib in melanoma with BRAF V600E mutation. *The New England journal of medicine*, 364(26), pp.2507–2516.
- Chen, C. et al., 2003. Endogenous sex hormones and prostate cancer risk: a case-control study nested within the Carotene and Retinol Efficacy Trial. *Cancer epidemiology, biomarkers & prevention : a publication of the American Association for Cancer Research, cosponsored by the American Society of Preventive Oncology*, 12(12), pp.1410–1416.
- Chen, G. et al., 2004. Up-regulation of Wnt-1 and beta-catenin production in patients with advanced metastatic prostate carcinoma: potential pathogenetic and prognostic implications. *Cancer*, 101(6), pp.1345–1356.
- Chen, M.-L. et al., 2006. The deficiency of Akt1 is sufficient to suppress tumor development in Pten^{+/-} mice. *Genes & development*, 20(12), pp.1569–1574.
- Clevers, H., 2011. The cancer stem cell: premises, promises and challenges. *Nature medicine*, 17(3), pp.313–319.
- Clevers, H., 2006. Wnt/beta-catenin signaling in development and disease. *Cell*, 127(3), pp.469–480.
- Clinton, S.K. et al., 1988. Growth of Dunning transplantable prostate adenocarcinomas in rats fed diets with various fat contents. *The Journal of nutrition*, 118(7), pp.908–914.
- Clouston, D. & Bolton, D., 2012. In situ and intraductal epithelial proliferations of prostate: definitions and treatment implications. Part 1: Prostatic intraepithelial neoplasia. *BJU international*, 109 Suppl 3(s3), pp.22–26.
- Collins, A.T. et al., 2001. Identification and isolation of human prostate epithelial stem cells based on alpha(2)beta(1)-integrin expression. *Journal of cell science*, 114(Pt 21), pp.3865–3872.
- Collins, A.T. et al., 2005. Prospective identification of tumorigenic prostate cancer stem cells. *Cancer research*, 65(23), pp.10946–10951.
- Cox, A.D. & Der, C.J., 2003. The dark side of Ras: regulation of apoptosis. *Oncogene*, 22(56), pp.8999–9006.
- Crowe, F.L. et al., 2008. Dietary fat intake and risk of prostate cancer in the European Prospective Investigation into Cancer and Nutrition. *The American journal of clinical nutrition*, 87(5), pp.1405–1413.
- D'Amico, A.V. et al., 1998. Biochemical outcome after radical prostatectomy, external beam radiation therapy, or interstitial radiation therapy for clinically localized prostate cancer. *JAMA*, 280(11), pp.969–974.
- Dalerba, P. et al., 2007. Phenotypic characterization of human colorectal cancer stem cells. *Proceedings of the National Academy of Sciences of the United States of*

- America*, 104(24), pp.10158–10163.
- Dall'Era, M.A. et al., 2012. Active surveillance for prostate cancer: a systematic review of the literature. *European urology*, 62(6), pp.976–983.
- Davies, E.J. et al., 2014. PTEN loss and KRAS activation leads to the formation of serrated adenomas and metastatic carcinoma in the mouse intestine. *The Journal of pathology*, 233(1), pp.27–38.
- de Bono, J.S. et al., 2007. Open-label phase II study evaluating the efficacy and safety of two doses of pertuzumab in castrate chemotherapy-naive patients with hormone-refractory prostate cancer. *Journal of clinical oncology : official journal of the American Society of Clinical Oncology*, 25(3), pp.257–262.
- de Carvalho, H.F. & Line, S.R., 1996. Basement membrane associated changes in the rat ventral prostate following castration. *Cell biology international*, 20(12), pp.809–819.
- De Sousa E Melo, F. et al., 2013. Cancer heterogeneity--a multifaceted view. *EMBO reports*, 14(8), pp.686–695.
- Dehm, S.M. & Tindall, D.J., 2006. Molecular regulation of androgen action in prostate cancer. *Journal of cellular biochemistry*, 99(2), pp.333–344.
- Deslypere, J.P. et al., 1992. Testosterone and 5 alpha-dihydrotestosterone interact differently with the androgen receptor to enhance transcription of the MMTV-CAT reporter gene. *Molecular and cellular endocrinology*, 88(1-3), pp.15–22.
- Detre, S., Saclani Jotti, G. & Dowsett, M., 1995. A “quickscore” method for immunohistochemical semiquantitation: validation for oestrogen receptor in breast carcinomas. *Journal of clinical pathology*, 48(9), pp.876–878.
- Dhillon, A.S. et al., 2007. MAP kinase signalling pathways in cancer. *Oncogene*, 26(22), pp.3279–3290.
- Dibble, C.C., Asara, J.M. & Manning, B.D., 2009. Characterization of Rictor phosphorylation sites reveals direct regulation of mTOR complex 2 by S6K1. *Molecular and cellular biology*, 29(21), pp.5657–5670.
- Ding, Q. et al., 2005. Erk associates with and primes GSK-3beta for its inactivation resulting in upregulation of beta-catenin. *Molecular cell*, 19(2), pp.159–170.
- Discacciati, A. et al., 2011. Body mass index in early and middle-late adulthood and risk of localised, advanced and fatal prostate cancer: a population-based prospective study. *British journal of cancer*, 105(7), pp.1061–1068.
- Dontu, G. et al., 2003. Stem cells in normal breast development and breast cancer. *Cell proliferation*, 36 Suppl 1, pp.59–72.
- Epstein, J.I., 2010. An update of the Gleason grading system. *The Journal of urology*, 183(2), pp.433–440.
- Epstein, J.I. et al., 2016. A Contemporary Prostate Cancer Grading System: A Validated

- Alternative to the Gleason Score. *European urology*, 69(3), pp.428–435.
- Epstein, J.I. et al., 2006. Update on the Gleason grading system for prostate cancer: results of an international consensus conference of urologic pathologists. In *Advances in anatomic pathology*. pp. 57–59.
- Epstein, J.I., Pizov, G. & Walsh, P.C., 1993. Correlation of pathologic findings with progression after radical retropubic prostatectomy. *Cancer*, 71(11), pp.3582–3593.
- Etzioni, R., Durand-Zaleski, I. & Lansdorp-Vogelaar, I., 2013. Evaluation of new technologies for cancer control based on population trends in disease incidence and mortality. *Journal of the National Cancer Institute. Monographs*, 2013(46), pp.117–123.
- Evans, G.S. & Chandler, J.A., 1987. Cell proliferation studies in the rat prostate: II. The effects of castration and androgen-induced regeneration upon basal and secretory cell proliferation. *The Prostate*, 11(4), pp.339–351.
- Faderl, S. et al., 1999. The biology of chronic myeloid leukemia. *The New England journal of medicine*, 341(3), pp.164–172.
- Figuroa-Magalhães, M.C. et al., 2014. Treatment of HER2-positive breast cancer. *Breast (Edinburgh, Scotland)*, 23(2), pp.128–136.
- Fizazi, K et al., 2012. Abiraterone acetate for treatment of metastatic castration-resistant prostate cancer: final overall survival analysis of the COU-AA-301 randomised, double-blind, placebo-controlled phase 3 study. *The Lancet Oncology*, 13 (10), p983-992.
- Flaherty, K.T. et al., 2010. Inhibition of mutated, activated BRAF in metastatic melanoma. *The New England journal of medicine*, 363(9), pp.809–819.
- Forbes, S.A. et al., 2015. COSMIC: exploring the world's knowledge of somatic mutations in human cancer. *Nucleic acids research*, 43(Database issue), pp.D805–11.
- FOULDS, L., 1954. The experimental study of tumor progression: a review. *Cancer research*, 14(5), pp.327–339.
- Foulkes, W.D. et al., 1997. The CDKN2A (p16) gene and human cancer. *Molecular medicine (Cambridge, Mass.)*, 3(1), pp.5–20.
- Fox, E.J. et al., 2014. Accuracy of Next Generation Sequencing Platforms. *Next generation, sequencing & applications*, 1.
- Francis, J.C. et al., 2013. β -catenin is required for prostate development and cooperates with Pten loss to drive invasive carcinoma. B. E. Clurman, ed. *PLoS genetics*, 9(1), p.e1003180.
- Freedland, S.J. et al., 2004. Impact of obesity on biochemical control after radical prostatectomy for clinically localized prostate cancer: a report by the Shared Equal Access Regional Cancer Hospital database study group. *Journal of clinical oncology : official journal of the American Society of Clinical Oncology*, 22(3),

pp.446–453.

- Friedlander, T.W. et al., 2012. Common structural and epigenetic changes in the genome of castration-resistant prostate cancer. *Cancer research*, 72(3), pp.616–625.
- Furuya, Y. et al., 2002. Low serum testosterone level predicts worse response to endocrine therapy in Japanese patients with metastatic prostate cancer. *Endocrine journal*, 49(1), pp.85–90.
- Futreal, P.A. et al., 2004. A census of human cancer genes. *Nature reviews. Cancer*, 4(3), pp.177–183.
- Galletti, G. et al., 2014. ERG induces taxane resistance in castration-resistant prostate cancer. *Nature communications*, 5, p.5548.
- Gao D et al. 2014. Organoid Cultures Derived from Patients with Advanced Prostate Cancer. *Cell*: 159(1), pp.176–187. Available at: <http://linkinghub.elsevier.com/retrieve/pii/S0092867414010472>.
- Gao, N et al. 2005. Forkhead box A1 regulates prostate ductal morphogenesis and promotes epithelial cell maturation. *Development*: 132(15), pp.3431–3443. Available at: <http://dev.biologists.org/cgi/doi/10.1242/dev.01917>.
- Gao, N et al. 2003. The role of hepatocyte nuclear factor-3 alpha (Forkhead Box A1) and androgen receptor in transcriptional regulation of prostatic genes. 17(8), pp.1484–1507. Available at: <http://press.endocrine.org/doi/abs/10.1210/me.2003-0020>.
- Gathirua-Mwangi, W.G. & Zhang, J., 2014. Dietary factors and risk for advanced prostate cancer. *European journal of cancer prevention : the official journal of the European Cancer Prevention Organisation (ECP)*, 23(2), pp.96–109.
- Giles, R.H., van Es, J.H. & Clevers, H., 2003. Caught up in a Wnt storm: Wnt signaling in cancer. *Biochimica et biophysica acta*, 1653(1), pp.1–24.
- Gill, J.K. et al., 2010. Androgens, growth factors, and risk of prostate cancer: the Multiethnic Cohort. *The Prostate*, 70(8), pp.906–915.
- Gleason, D.F., 1966. Classification of prostatic carcinomas. *Cancer chemotherapy reports. Part 1*, 50(3), pp.125–128.
- Goebell, P.J. & Knowles, M.A., 2010. Bladder cancer or bladder cancers? Genetically distinct malignant conditions of the urothelium. *Urologic oncology*, 28(4), pp.409–428.
- Goldstein, A.S. & Witte, O.N., 2013. Does the microenvironment influence the cell types of origin for prostate cancer? *Genes & development*, 27(14), pp.1539–1544.
- Goldstein, A.S. et al., 2010. Identification of a cell of origin for human prostate cancer. *Science (New York, N.Y.)*, 329(5991), pp.568–571.
- Goldstein, A.S. et al., 2008. Trop2 identifies a subpopulation of murine and human prostate basal cells with stem cell characteristics. *Proceedings of the National*

- Academy of Sciences of the United States of America*, 105(52), pp.20882–20887.
- Grada, A. & Weinbrecht, K., 2013. Next-generation sequencing: methodology and application. *The Journal of investigative dermatology*, 133(8), p.e11.
- Grasso, C.S. et al., 2012. The mutational landscape of lethal castration-resistant prostate cancer. *Nature*, 487(7406), pp.239–243.
- Grönberg, H., 2003. Prostate cancer epidemiology. *Lancet*, 361(9360), pp.859–864.
- Grubb, R.L. et al., 2009. Serum prostate-specific antigen hemodilution among obese men undergoing screening in the Prostate, Lung, Colorectal, and Ovarian Cancer Screening Trial. *Cancer epidemiology, biomarkers & prevention : a publication of the American Association for Cancer Research, cosponsored by the American Society of Preventive Oncology*, 18(3), pp.748–751.
- Grünwald, V. et al., 2002. Inhibitors of mTOR reverse doxorubicin resistance conferred by PTEN status in prostate cancer cells. *Cancer research*, 62(21), pp.6141–6145.
- Guerra, C. et al., 2003. Tumor induction by an endogenous K-ras oncogene is highly dependent on cellular context. *Cancer cell*, 4(2), pp.111–120.
- Guo, C. et al., 2012. Epcam, CD44, and CD49f distinguish sphere-forming human prostate basal cells from a subpopulation with predominant tubule initiation capability. A. Androutsellis-Theotokis, ed. *PloS one*, 7(4), p.e34219.
- Haffner, M.C. et al., 2013. Tracking the clonal origin of lethal prostate cancer. *The Journal of clinical investigation*, 123(11), pp.4918–4922.
- Hamdy, F.C., 2001. Prognostic and predictive factors in prostate cancer. *Cancer treatment reviews*, 27(3), pp.143–151.
- Hamdy, F.C. et al., 2016. 10-Year Outcomes after Monitoring, Surgery, or Radiotherapy for Localized Prostate Cancer. *The New England journal of medicine*, 375(15), pp.1415–1424.
- Hammond, G.L., Avvakumov, G.V. & Muller, Y.A., 2003. Structure/function analyses of human sex hormone-binding globulin: effects of zinc on steroid-binding specificity. *The Journal of steroid biochemistry and molecular biology*, 85(2-5), pp.195–200.
- Hanahan, D. & Weinberg, R.A., 2011. Hallmarks of cancer: the next generation. *Cell*, 144(5), pp.646–674.
- Hanahan, D. & Weinberg, R.A., 2000. The hallmarks of cancer. *Cell*, 100(1), pp.57–70.
- Hanchanale, V.S., McCabe, J.E. & Javlé, P., 2010. Radical prostatectomy practice in England. *Urology journal*, 7(4), pp.243–248.
- Hansen, J. et al., 2013. Initial prostate biopsy: development and internal validation of a biopsy-specific nomogram based on the prostate cancer antigen 3 assay. *European urology*, 63(2), pp.201–209.

- Harada, N. et al., 1999. Intestinal polyposis in mice with a dominant stable mutation of the beta-catenin gene. *The EMBO journal*, 18(21), pp.5931–5942.
- Haraldsdottir, S. et al., 2014. Prostate cancer incidence in males with Lynch syndrome. *Genetics in medicine : official journal of the American College of Medical Genetics*, 16(7), pp.553–557.
- Harrison, H et al., 2010. Regulation of breast cancer stem cell activity by signaling through the Notch4 receptor. *Tumour and Stem Cell Biology*: 70(2), pp.709–718. Available at: <http://cancerres.aacrjournals.org/cgi/doi/10.1158/0008-5472.CAN-09-1681>.
- Hägglöf, C. et al., 2014. TMPRSS2-ERG expression predicts prostate cancer survival and associates with stromal biomarkers. Z. Culig, ed. *PloS one*, 9(2), p.e86824.
- Hedegaard, J. et al., 2014. Next-generation sequencing of RNA and DNA isolated from paired fresh-frozen and formalin-fixed paraffin-embedded samples of human cancer and normal tissue. Z. Zuo, ed. *PloS one*, 9(5), p.e98187.
- Heidenreich, A. et al., 2014. EAU guidelines on prostate cancer. part 1: screening, diagnosis, and local treatment with curative intent-update 2013. *European urology*, 65(1), pp.124–137.
- Heuberger, J. & Birchmeier, W., 2010. Interplay of cadherin-mediated cell adhesion and canonical Wnt signaling. *Cold Spring Harbor perspectives in biology*, 2(2), pp.a002915–a002915.
- Horvath, L.G. et al., 2005. Lower levels of nuclear beta-catenin predict for a poorer prognosis in localized prostate cancer. *International journal of cancer. Journal international du cancer*, 113(3), pp.415–422.
- Huber, A.H. & Weis, W.I., 2001. The structure of the beta-catenin/E-cadherin complex and the molecular basis of diverse ligand recognition by beta-catenin. *Cell*, 105(3), pp.391–402.
- Huch, M. et al., 2013. In vitro expansion of single Lgr5+ liver stem cells induced by Wnt-driven regeneration. *Nature*, 494(7436), pp.247–250.
- Huncharek, M. et al., 2010. Smoking as a risk factor for prostate cancer: a meta-analysis of 24 prospective cohort studies. *American journal of public health*, 100(4), pp.693–701.
- Ilic, D. et al., 2013. Screening for prostate cancer. D. Ilic, ed. *The Cochrane database of systematic reviews*, 1, p.CD004720.
- Imamoto, T. et al., 2005. Pretreatment serum testosterone level as a predictive factor of pathological stage in localized prostate cancer patients treated with radical prostatectomy. *European urology*, 47(3), pp.308–312.
- Indovina, P. et al., 2015. RB1 dual role in proliferation and apoptosis: cell fate control and implications for cancer therapy. *Oncotarget*, 6(20), pp.17873–17890.
- Inoki, K. et al., 2006. TSC2 integrates Wnt and energy signals via a coordinated

- phosphorylation by AMPK and GSK3 to regulate cell growth. *Cell*, 126(5), pp.955–968.
- James, N.D. et al., 2015. Survival with Newly Diagnosed Metastatic Prostate Cancer in the “Docetaxel Era”: Data from 917 Patients in the Control Arm of the STAMPEDE Trial (MRC PR08, CRUK/06/019). *European urology*, 67(6), pp.1028–1038.
- Jung, S.J. et al., 2013. Clinical Significance of Wnt/ β -Catenin Signalling and Androgen Receptor Expression in Prostate Cancer. *The world journal of men's health*, 31(1), pp.36–46.
- Kallakury, B.V. et al., 2001. Decreased expression of catenins (alpha and beta), p120 CTN, and E-cadherin cell adhesion proteins and E-cadherin gene promoter methylation in prostatic adenocarcinomas. *Cancer*, 92(11), pp.2786–2795.
- Karakas, B., Bachman, K.E. & Park, B.H., 2006. Mutation of the PIK3CA oncogene in human cancers. *British journal of cancer*, 94(4), pp.455–459.
- Karthaus, W.R. et al., 2014. Identification of multipotent luminal progenitor cells in human prostate organoid cultures. *Cell*, 159(1), pp.163–175.
- Kenfield, S.A. et al., 2011. Smoking and prostate cancer survival and recurrence. *JAMA*, 305(24), pp.2548–2555.
- Khan, M.A. et al., 2003. Probability of biochemical recurrence by analysis of pathologic stage, Gleason score, and margin status for localized prostate cancer. *Urology*, 62(5), pp.866–871.
- Kiciński, M., Vangronsveld, J. & Nawrot, T.S., 2011. An Epidemiological Reappraisal of the Familial Aggregation of Prostate Cancer: A Meta-Analysis J. Little, ed. *PLoS one*, 6(10), p.e27130.
- Klotz, L., O'Callaghan, C., et al., 2015. Nadir testosterone within first year of androgen-deprivation therapy (ADT) predicts for time to castration-resistant progression: a secondary analysis of the PR-7 trial of intermittent versus continuous ADT. *Journal of clinical oncology : official journal of the American Society of Clinical Oncology*, 33(10), pp.1151–1156.
- Klotz, L., Vesprini, D., et al., 2015. Long-term follow-up of a large active surveillance cohort of patients with prostate cancer. *Journal of clinical oncology : official journal of the American Society of Clinical Oncology*, 33(3), pp.272–277.
- Kobayashi, T. et al., 2015. Modelling bladder cancer in mice: opportunities and challenges. *Nature reviews. Cancer*, 15(1), pp.42–54.
- Kolonel, L.N., Altshuler, D. & Henderson, B.E., 2004. The multiethnic cohort study: exploring genes, lifestyle and cancer risk. *Nature reviews. Cancer*, 4(7), pp.519–527.
- Korsten, H. et al., 2009. Accumulating progenitor cells in the luminal epithelial cell layer are candidate tumor initiating cells in a Pten knockout mouse prostate cancer

- model. S. Wöfl, ed. *PloS one*, 4(5), p.e5662.
- Kote-Jarai, Z. et al., 2011. BRCA2 is a moderate penetrance gene contributing to young-onset prostate cancer: implications for genetic testing in prostate cancer patients. *British journal of cancer*, 105(8), pp.1230–1234.
- Kryvenko, O.N. et al., 2014. Biopsy criteria for determining appropriateness for active surveillance in the modern era. *Urology*, 83(4), pp.869–874.
- Kumar, A. et al., 2011. Exome sequencing identifies a spectrum of mutation frequencies in advanced and lethal prostate cancers. *Proceedings of the National Academy of Sciences of the United States of America*, 108(41), pp.17087–17092.
- Kurita, T. et al., 2004. Role of p63 and basal cells in the prostate. *Development (Cambridge, England)*, 131(20), pp.4955–4964.
- Kvåle, R. et al., 2007. Interpreting trends in prostate cancer incidence and mortality in the five Nordic countries. *Journal of the National Cancer Institute*, 99(24), pp.1881–1887.
- Kypta, R.M. & Waxman, J., 2012. Wnt/ β -catenin signalling in prostate cancer. *Nature reviews. Urology*, 9(8), pp.418–428.
- la Taille, de, A. et al., 2003. Beta-catenin-related anomalies in apoptosis-resistant and hormone-refractory prostate cancer cells. *Clinical cancer research : an official journal of the American Association for Cancer Research*, 9(5), pp.1801–1807.
- Ladanyi, M. & Pao, W., 2008. Lung adenocarcinoma: guiding EGFR-targeted therapy and beyond. *Modern pathology : an official journal of the United States and Canadian Academy of Pathology, Inc*, 21 Suppl 2, pp.S16–22.
- Laguë, M.-N. et al., 2008. Synergistic effects of Pten loss and WNT/CTNNB1 signaling pathway activation in ovarian granulosa cell tumor development and progression. *Carcinogenesis*, 29(11), pp.2062–2072.
- Lang, S.H. et al., 1997. Primary prostatic epithelial cell binding to human bone marrow stroma and the role of alpha2beta1 integrin. *Clinical & experimental metastasis*, 15(3), pp.218–227.
- Lawson, D.A. et al., 2010. Basal epithelial stem cells are efficient targets for prostate cancer initiation. *Proceedings of the National Academy of Sciences of the United States of America*, 107(6), pp.2610–2615.
- Lawson, D.A. et al., 2007. Isolation and functional characterization of murine prostate stem cells. *Proceedings of the National Academy of Sciences of the United States of America*, 104(1), pp.181–186.
- Lee, M.C. et al., 2010. Multifocal high grade prostatic intraepithelial neoplasia is a risk factor for subsequent prostate cancer. *The Journal of urology*, 184(5), pp.1958–1962.
- Leongamornlert, D. et al., 2012. Germline BRCA1 mutations increase prostate cancer risk. *British journal of cancer*, 106(10), pp.1697–1701.

- Li, C. et al., 2007. Identification of pancreatic cancer stem cells. *Cancer research*, 67(3), pp.1030–1037.
- Lilja, H. et al., 1987. Seminal vesicle-secreted proteins and their reactions during gelation and liquefaction of human semen. *The Journal of clinical investigation*, 80(2), pp.281–285.
- Liu, B. et al., 2008. Co-opted JNK/SAPK signaling in Wnt/beta-catenin-induced tumorigenesis. *Neoplasia (New York, N.Y.)*, 10(9), pp.1004–1013.
- Liu, J. et al., 2013. Targeting Wnt-driven cancer through the inhibition of Porcupine by LGK974. *Proceedings of the National Academy of Sciences of the United States of America*, 110(50), pp.20224–20229.
- Logan, C.Y. & Nusse, R., 2004. The Wnt signaling pathway in development and disease. *Annual review of cell and developmental biology*, 20(1), pp.781–810.
- Lotan, T.L. et al., 2011. PTEN protein loss by immunostaining: analytic validation and prognostic indicator for a high risk surgical cohort of prostate cancer patients. *Clinical cancer research : an official journal of the American Association for Cancer Research*, 17(20), pp.6563–6573.
- Lukacs, R.U. et al., 2010. Isolation, cultivation and characterization of adult murine prostate stem cells. *Nature protocols*, 5(4), pp.702–713.
- MacDonald, B.T., Tamai, K. & He, X., 2009. Wnt/beta-catenin signaling: components, mechanisms, and diseases. *Developmental cell*, 17(1), pp.9–26.
- MacInnis, R.J. & English, D.R., 2006. Body size and composition and prostate cancer risk: systematic review and meta-regression analysis. *Cancer causes & control : CCC*, 17(8), pp.989–1003.
- Majumder, P.K. et al., 2004. mTOR inhibition reverses Akt-dependent prostate intraepithelial neoplasia through regulation of apoptotic and HIF-1-dependent pathways. *Nature medicine*, 10(6), pp.594–601.
- Manning, B.D. & Cantley, L.C., 2007. AKT/PKB signaling: navigating downstream. *Cell*, 129(7), pp.1261–1274.
- Marsh, V. et al., 2013. PTEN loss and KRAS activation cooperate in murine biliary tract malignancies. *The Journal of pathology*, 230(2), pp.165–173.
- Martin, P. et al., 2011. Prostate epithelial Pten/TP53 loss leads to transformation of multipotential progenitors and epithelial to mesenchymal transition. *The American journal of pathology*, 179(1), pp.422–435.
- Massengill, J.C. et al., 2003. Pretreatment total testosterone level predicts pathological stage in patients with localized prostate cancer treated with radical prostatectomy. *The Journal of urology*, 169(5), pp.1670–1675.
- Mateo, J. et al., 2015. DNA-Repair Defects and Olaparib in Metastatic Prostate Cancer. *The New England journal of medicine*, 373(18), pp.1697–1708.

- McCormick, F., 1999. Signalling networks that cause cancer. *Trends in cell biology*, 9(12), pp.M53–6.
- McNeal, J.E., 1981a. Normal and pathologic anatomy of prostate. *Urology*, 17(Suppl 3), pp.11–16.
- McNeal, J.E., 1988. Normal histology of the prostate. *The American journal of surgical pathology*, 12(8), pp.619–633.
- McNeal, J.E., 1981b. The zonal anatomy of the prostate. *The Prostate*, 2(1), pp.35–49.
- McNeal, J.E. et al., 1990. Histologic differentiation, cancer volume, and pelvic lymph node metastasis in adenocarcinoma of the prostate. *Cancer*, 66(6), pp.1225–1233.
- Melia, J. & Moss, S., 2001. Survey of the rate of PSA testing in general practice. *British journal of cancer*, 85(5), pp.656–657.
- Mendoza, M.C., Er, E.E. & Blenis, J., 2011. The Ras-ERK and PI3K-mTOR pathways: cross-talk and compensation. *Trends in biochemical sciences*, 36(6), pp.320–328.
- Merola, R. et al., 2015. PCA3 in prostate cancer and tumor aggressiveness detection on 407 high-risk patients: a National Cancer Institute experience. *Journal of experimental & clinical cancer research : CR*, 34(1), p.15.
- Merrimen, J.L., Jones, G. & Srigley, J.R., 2010. Is high grade prostatic intraepithelial neoplasia still a risk factor for adenocarcinoma in the era of extended biopsy sampling? *Pathology*, 42(4), pp.325–329.
- Millender, L.E. et al., 2004. Daily electronic portal imaging for morbidly obese men undergoing radiotherapy for localized prostate cancer. *International journal of radiation oncology, biology, physics*, 59(1), pp.6–10.
- Miller, L.S. et al., 1985. Estrogen receptor analyses. Correlation of biochemical and immunohistochemical methods using monoclonal antireceptor antibodies. *Archives of pathology & laboratory medicine*, 109(8), pp.716–721.
- Mistry, M. et al., 2011. Cancer incidence in the United Kingdom: projections to the year 2030. *British journal of cancer*, 105(11), pp.1795–1803.
- Morote, J. et al., 1999. Prognostic value of immunohistochemical expression of the c-erbB-2 oncoprotein in metastatic prostate cancer. *International journal of cancer. Journal international du cancer*, 84(4), pp.421–425.
- Motzer, R.J. et al., 2008. Efficacy of everolimus in advanced renal cell carcinoma: a double-blind, randomised, placebo-controlled phase III trial. *Lancet*, 372(9637), pp.449–456.
- Mukherjee, R. et al., 2011. Upregulation of MAPK pathway is associated with survival in castrate-resistant prostate cancer. *British journal of cancer*, 104(12), pp.1920–1928.
- Mulholland, D.J. et al., 2011. Cell autonomous role of PTEN in regulating castration-resistant prostate cancer growth. *Cancer cell*, 19(6), pp.792–804.

- Mulholland, D.J. et al., 2009. Lin-Sca-1+CD49^{high} stem/progenitors are tumor-initiating cells in the Pten-null prostate cancer model. *Cancer research*, 69(22), pp.8555–8562.
- Mulholland, D.J. et al., 2006. PTEN and GSK3beta: key regulators of progression to androgen-independent prostate cancer. *Oncogene*, 25(3), pp.329–337.
- Mulholland, D.J. et al., 2012. Pten loss and RAS/MAPK activation cooperate to promote EMT and metastasis initiated from prostate cancer stem/progenitor cells. *Cancer research*, 72(7), pp.1878–1889.
- Mundy, G.R., 2002. Metastasis to bone: causes, consequences and therapeutic opportunities. *Nature reviews. Cancer*, 2(8), pp.584–593.
- Narod, S.A. et al., 2008. Rapid progression of prostate cancer in men with a BRCA2 mutation. *British journal of cancer*, 99(2), pp.371–374.
- Ni, J. et al., 2014. Cancer stem cells in prostate cancer chemoresistance. *Current cancer drug targets*, 14(3), pp.225–240.
- Ni, J. et al., 2012. Role of the EpCAM (CD326) in prostate cancer metastasis and progression. *Cancer metastasis reviews*, 31(3-4), pp.779–791.
- Parker, C. et al., 2013. Alpha emitter radium-223 and survival in metastatic prostate cancer. *The New England journal of medicine*, 369(3), pp.213–223.
- Parker, C. et al., 2007. Radiotherapy and androgen deprivation in combination after local surgery (RADICALS): a new Medical Research Council/National Cancer Institute of Canada phase III trial of adjuvant treatment after radical prostatectomy. *BJU international*, 99(6), pp.1376–1379.
- Pashayan, N. et al., 2006. Incidence trends of prostate cancer in East Anglia, before and during the era of PSA diagnostic testing. *British journal of cancer*, 95(3), pp.398–400.
- Pearson, H.B., Pheasant, T.J. & Clarke, A.R., 2009. K-ras and Wnt signaling synergize to accelerate prostate tumorigenesis in the mouse. *Cancer research*, 69(1), pp.94–101.
- Pignon, J.-C. et al., 2013. p63-expressing cells are the stem cells of developing prostate, bladder, and colorectal epithelia. *Proceedings of the National Academy of Sciences of the United States of America*, 110(20), pp.8105–8110.
- Podsypanina, K. et al., 1999. Mutation of Pten/Mmac1 in mice causes neoplasia in multiple organ systems. *Proceedings of the National Academy of Sciences of the United States of America*, 96(4), pp.1563–1568.
- Popiolek, M. et al., 2013. Natural history of early, localized prostate cancer: a final report from three decades of follow-up. *European urology*, 63(3), pp.428–435.
- Potten, C.S. & Loeffler, M., 1990. Stem cells: attributes, cycles, spirals, pitfalls and uncertainties. Lessons for and from the crypt. *Development (Cambridge, England)*, 110(4), pp.1001–1020.

- PRICE, D., 1963. COMPARATIVE ASPECTS OF DEVELOPMENT AND STRUCTURE IN THE PROSTATE. *National Cancer Institute monograph*, 12, pp.1–27.
- Prior, I.A., Lewis, P.D. & Mattos, C., 2012. A comprehensive survey of Ras mutations in cancer. *Cancer research*, 72(10), pp.2457–2467.
- Pylyayeva-Gupta, Y., Grabocka, E. & Bar-Sagi, D., 2011. RAS oncogenes: weaving a tumorigenic web. *Nature reviews. Cancer*, 11(11), pp.761–774.
- Rajan, P. et al., 2014. Next-generation sequencing of advanced prostate cancer treated with androgen-deprivation therapy. *European urology*, 66(1), pp.32–39.
- Rathkopf, D.E. et al., 2015. Everolimus combined with gefitinib in patients with metastatic castration-resistant prostate cancer: Phase 1/2 results and signaling pathway implications. *Cancer*, 121(21), pp.3853–3861.
- Ratnacaram, C.K. et al., 2008. Temporally controlled ablation of PTEN in adult mouse prostate epithelium generates a model of invasive prostatic adenocarcinoma. *Proceedings of the National Academy of Sciences of the United States of America*, 105(7), pp.2521–2526.
- Reid, A.H.M. et al., 2010. Molecular characterisation of ERG, ETV1 and PTEN gene loci identifies patients at low and high risk of death from prostate cancer. *British journal of cancer*, 102(4), pp.678–684.
- Reig, Ò. et al., 2016. TMPRSS2-ERG in Blood and Docetaxel Resistance in Metastatic Castration-resistant Prostate Cancer. *European urology*, 70(5), pp.709–713.
- Renan, M.J., 1993. How many mutations are required for tumorigenesis? Implications from human cancer data. *Molecular carcinogenesis*, 7(3), pp.139–146.
- Rittenhouse, H.G. et al., 1998. Human Kallikrein 2 (hK2) and prostate-specific antigen (PSA): two closely related, but distinct, kallikreins in the prostate. *Critical reviews in clinical laboratory sciences*, 35(4), pp.275–368.
- Robinson, D. et al., 2015. Integrative clinical genomics of advanced prostate cancer. *Cell*, 161(5), pp.1215–1228.
- Rock, J.R. et al., 2009. Basal cells as stem cells of the mouse trachea and human airway epithelium. *Proceedings of the National Academy of Sciences of the United States of America*, 106(31), pp.12771–12775.
- Ross-Adams, H. et al., 2015. Integration of copy number and transcriptomics provides risk stratification in prostate cancer: A discovery and validation cohort study. *EBioMedicine*, 2(9), pp.1133–1144.
- Rökman, A. et al., 2002. Germline alterations of the RNASEL gene, a candidate HPC1 gene at 1q25, in patients and families with prostate cancer. *American journal of human genetics*, 70(5), pp.1299–1304.
- Sachs et al. 2014. Organoid cultures for the analysis of cancer phenotypes. *Current opinion in genetics and development*: 24, pp.68–73. Available at:

<http://linkinghub.elsevier.com/retrieve/pii/S0959437X13001615>.

- Sakr, W.A. et al., 1993. The frequency of carcinoma and intraepithelial neoplasia of the prostate in young male patients. *The Journal of urology*, 150(2 Pt 1), pp.379–385.
- Sanger, F., 1975. The Croonian Lecture, 1975. Nucleotide sequences in DNA. *Proceedings of the Royal Society of London. Series B, Biological sciences*, 191(1104), pp.317–333.
- Sasieni, P.D. et al., 2011. What is the lifetime risk of developing cancer?: the effect of adjusting for multiple primaries. *British journal of cancer*, 105(3), pp.460–465.
- Sato, T. et al., 2011. Long-term expansion of epithelial organoids from human colon, adenoma, adenocarcinoma, and Barrett's epithelium. *Gastroenterology*, 141(5), pp.1762–1772.
- Sato, T. et al., 2009. Single Lgr5 stem cells build crypt-villus structures in vitro without a mesenchymal niche. *Nature*, 459(7244), pp.262–265.
- Savinainen, K.J. et al., 2002. Expression and gene copy number analysis of ERBB2 oncogene in prostate cancer. *The American journal of pathology*, 160(1), pp.339–345.
- Schatzl, G. et al., 2003. Associations of serum testosterone with microvessel density, androgen receptor density and androgen receptor gene polymorphism in prostate cancer. *The Journal of urology*, 169(4), pp.1312–1315.
- Scher, H et al., 2012. Increased survival with enzalutamide in prostate cancer after chemotherapy. *New England journal of medicine* 367 (12), pp1187-1197.
- Scherl, A. et al., 2004. Prostatic intraepithelial neoplasia and intestinal metaplasia in prostates of probasin-RAS transgenic mice. *The Prostate*, 59(4), pp.448–459.
- Schröder, F.H. et al., 2014. Screening and prostate cancer mortality: results of the European Randomised Study of Screening for Prostate Cancer (ERSPC) at 13 years of follow-up. *Lancet*, 384(9959), pp.2027–2035.
- SEER 1973-2011, Surveillance, Epidemiology, and End Results Program.
- Selley, S. et al., 1997. Diagnosis, management and screening of early localised prostate cancer. *Health technology assessment (Winchester, England)*, 1(2), pp.i–1–96.
- Severi, G. et al., 2006. Circulating steroid hormones and the risk of prostate cancer. *Cancer epidemiology, biomarkers & prevention : a publication of the American Association for Cancer Research, cosponsored by the American Society of Preventive Oncology*, 15(1), pp.86–91.
- Shaneyfelt, T. et al., 2000. Hormonal predictors of prostate cancer: a meta-analysis. *Journal of clinical oncology : official journal of the American Society of Clinical Oncology*, 18(4), pp.847–853.
- Shappell, S.B. et al., 2004. Prostate pathology of genetically engineered mice: definitions and classification. The consensus report from the Bar Harbor meeting of

- the Mouse Models of Human Cancer Consortium Prostate Pathology Committee. In *Cancer research*. pp. 2270–2305.
- Shendure, J. & Ji, H., 2008. Next-generation DNA sequencing. *Nature biotechnology*, 26(10), pp.1135–1145.
- Sidransky, D. & Hollstein, M., 1996. Clinical implications of the p53 gene. *Annual review of medicine*, 47(1), pp.285–301.
- Signoretti, S. et al., 2000. p63 is a prostate basal cell marker and is required for prostate development. *The American journal of pathology*, 157(6), pp.1769–1775.
- Skvortsova, I. et al., 2008. Intracellular signaling pathways regulating radioresistance of human prostate carcinoma cells. L. A. Huber, ed. *Proteomics*, 8(21), pp.4521–4533.
- Song, M.S., Salmena, L. & Pandolfi, P.P., 2012. The functions and regulation of the PTEN tumour suppressor. *Nature reviews. Molecular cell biology*, 13(5), pp.283–296.
- Suire, S., Hawkins, P. & Stephens, L., 2002. Activation of phosphoinositide 3-kinase gamma by Ras. *Current biology : CB*, 12(13), pp.1068–1075.
- Sun, X. et al., 2009. Genetic alterations in the PI3K pathway in prostate cancer. *Anticancer research*, 29(5), pp.1739–1743.
- Suzuki, A. et al., 2001. T cell-specific loss of Pten leads to defects in central and peripheral tolerance. *Immunity*, 14(5), pp.523–534.
- Tachi, K et al., 2016. FOXA1 expression affects the proliferation activity of luminal breast cancer stem cell populations. *Cancer Science*: 107(3), pp.281–289. Available at: <http://doi.wiley.com/10.1111/cas.12870>.
- Tavtigian, S.V. et al., 2001. *Nature genetics*, 27(2), pp.172–180.
- Taylor, B.S. et al., 2010. Integrative genomic profiling of human prostate cancer. *Cancer cell*, 18(1), pp.11–22.
- Templeton, A.J. et al., 2013. Phase 2 trial of single-agent everolimus in chemotherapy-naive patients with castration-resistant prostate cancer (SAKK 08/08). *European urology*, 64(1), pp.150–158.
- Thompson, I.M. et al., 2003. Prevention of prostate cancer with finasteride: US/European perspective. *European urology*, 44(6), pp.650–655.
- Tolis, G. et al., 1982. Tumor growth inhibition in patients with prostatic carcinoma treated with luteinizing hormone-releasing hormone agonists. *Proceedings of the National Academy of Sciences of the United States of America*, 79(5), pp.1658–1662.
- Tomlins, S.A. et al., 2005. Recurrent fusion of TMPRSS2 and ETS transcription factor genes in prostate cancer. *Science (New York, N.Y.)*, 310(5748), pp.644–648.
- Tomlins, S.A. et al., 2008. Role of the TMPRSS2-ERG gene fusion in prostate cancer.

- Neoplasia (New York, N.Y.)*, 10(2), pp.177–188.
- Tomlins, S.A. et al., 2015. Urine TMPRSS2:ERG Plus PCA3 for Individualized Prostate Cancer Risk Assessment. *European urology*.
- Trimboli, A.J. et al., 2009. Pten in stromal fibroblasts suppresses mammary epithelial tumours. *Nature*, 461(7267), pp.1084–1091.
- Valdez, J et al 2012. Notch and TGF β form a reciprocal positive regulatory loop that suppresses murine prostate basal stem/progenitor cell activity. *Cell*: 11(5), pp.676–688. Available at: <http://linkinghub.elsevier.com/retrieve/pii/S1934590912004183>.
- Valkenburg, K.C. & Williams, B.O., 2011. Mouse models of prostate cancer. *Prostate cancer*, 2011(3), pp.895238–22.
- Van Keymeulen, A. et al., 2011. Distinct stem cells contribute to mammary gland development and maintenance. *Nature*, 479(7372), pp.189–193.
- Vasconcelos-Nóbrega, C. et al., 2012. Review: BBN as an urothelial carcinogen. *In vivo (Athens, Greece)*, 26(4), pp.727–739.
- Verhoven, B. et al., 2013. Ki-67 is an independent predictor of metastasis and cause-specific mortality for prostate cancer patients treated on Radiation Therapy Oncology Group (RTOG) 94-08. *International journal of radiation oncology, biology, physics*, 86(2), pp.317–323.
- Verras, M. et al., 2004. Wnt3a growth factor induces androgen receptor-mediated transcription and enhances cell growth in human prostate cancer cells. *Cancer research*, 64(24), pp.8860–8866.
- Visvader, J.E., 2009. Keeping abreast of the mammary epithelial hierarchy and breast tumorigenesis. *Genes & development*, 23(22), pp.2563–2577.
- Wagers, A.J. & Weissman, I.L., 2004. Plasticity of adult stem cells. *Cell*, 116(5), pp.639–648.
- Wang, G., Wang, J. & Sadar, M.D., 2008. Crosstalk between the androgen receptor and beta-catenin in castrate-resistant prostate cancer. *Cancer research*, 68(23), pp.9918–9927.
- Wang, S. et al., 2003. Prostate-specific deletion of the murine Pten tumor suppressor gene leads to metastatic prostate cancer. *Cancer cell*, 4(3), pp.209–221.
- Wang, X. et al., 2009. A luminal epithelial stem cell that is a cell of origin for prostate cancer. *Nature*, 461(7263), pp.495–500.
- Wang, Z.A. & Shen, M.M., 2011. Revisiting the concept of cancer stem cells in prostate cancer. *Oncogene*, 30(11), pp.1261–1271.
- Wang, Z.A. et al., 2014. Luminal cells are favored as the cell of origin for prostate cancer. *Cell reports*, 8(5), pp.1339–1346.
- Warde, P. et al., 2011. Combined androgen deprivation therapy and radiation therapy

- for locally advanced prostate cancer: a randomised, phase 3 trial. *Lancet*, 378(9809), pp.2104–2111.
- Weiss, J.M. et al., 2007. IGF-1 and IGFBP-3: Risk of prostate cancer among men in the Prostate, Lung, Colorectal and Ovarian Cancer Screening Trial. *International journal of cancer. Journal international du cancer*, 121(10), pp.2267–2273.
- Welte, Y. et al., 2010. Cancer stem cells in solid tumors: elusive or illusive? *Cell communication and signaling : CCS*, 8(1), p.6.
- Whitaker, H.C. et al., 2008. Alterations in beta-catenin expression and localization in prostate cancer. *The Prostate*, 68(11), pp.1196–1205.
- Widmark, A. et al., 2009. Endocrine treatment, with or without radiotherapy, in locally advanced prostate cancer (SPCG-7/SFUO-3): an open randomised phase III trial. *Lancet*, 373(9660), pp.301–308.
- Williams, N. et al., 2011. Prostate-specific antigen testing rates remain low in UK general practice: a cross-sectional study in six English cities. *BJU international*, 108(9), pp.1402–1408.
- Wilson, J.D., 2001. The role of 5alpha-reduction in steroid hormone physiology. *Reproduction, fertility, and development*, 13(7-8), pp.673–678.
- Wilt, T.J. et al., 2012. Radical prostatectomy versus observation for localized prostate cancer. *The New England journal of medicine*, 367(3), pp.203–213.
- Wolk, A., 2005. Diet, lifestyle and risk of prostate cancer. *Acta oncologica (Stockholm, Sweden)*, 44(3), pp.277–281.
- Wu, L., Birle, D.C. & Tannock, I.F., 2005. Effects of the mammalian target of rapamycin inhibitor CCI-779 used alone or with chemotherapy on human prostate cancer cells and xenografts. *Cancer research*, 65(7), pp.2825–2831.
- Wu, X. et al., 2001. Generation of a prostate epithelial cell-specific Cre transgenic mouse model for tissue-specific gene ablation. *Mechanisms of development*, 101(1-2), pp.61–69.
- Yao, J.C. et al., 2011. Everolimus for advanced pancreatic neuroendocrine tumors. *The New England journal of medicine*, 364(6), pp.514–523.
- Yasumizu, Y. et al., 2014. Dual PI3K/mTOR inhibitor NVP-BEZ235 sensitizes docetaxel in castration resistant prostate cancer. *The Journal of urology*, 191(1), pp.227–234.
- Zack, T.I. et al., 2013. Pan-cancer patterns of somatic copy number alteration. *Nature genetics*, 45(10), pp.1134–1140.
- Zhang, J. et al., 2012. Trends in mortality from cancers of the breast, colon, prostate, esophagus, and stomach in East Asia: role of nutrition transition. *European journal of cancer prevention : the official journal of the European Cancer Prevention Organisation (ECP)*, 21(5), pp.480–489.

- Zhang, C et al., 2011. Definition of a FoxA1 Cistrome that is crucial for G1 to S-phase cell-cycle transit in castration-resistant prostate cancer., 71(21), pp.6738–6748. *Molecular and cellular pathology*. Available at: <http://cancerres.aacrjournals.org/cgi/doi/10.1158/0008-5472.CAN-11-1882>.
- Zhang, L et al., 2011. ROCK inhibitor Y-27632 suppresses dissociation-induced apoptosis of murine prostate stem/progenitor cells and increases their cloning efficiency. *PloS one*: 6(3), p.e18271. Available at: <http://dx.plos.org/10.1371/journal.pone.0018271>.
- Zimmermann, S. & Moelling, K., 1999. Phosphorylation and regulation of Raf by Akt (protein kinase B). *Science (New York, N.Y.)*, 286(5445), pp.1741–1744.
- Zoncu, R., Efeyan, A. & Sabatini, D.M., 2011. mTOR: from growth signal integration to cancer, diabetes and ageing. *Nature reviews. Molecular cell biology*, 12(1), pp.21–35.